frontiers | Research Topics

Endothelial activation and microcirculatory disorders in sepsis and critical illness

Edited by
Jeremie Joffre and W. Conrad Liles

Published in
Frontiers in Medicine
Frontiers in Physiology

ISSN 1664-8714
ISBN 978-2-83251-438-2
DOI 10.3389/978-2-83251-438-2

About Frontiers

Frontiers is more than just an open access publisher of scholarly articles: it is a pioneering approach to the world of academia, radically improving the way scholarly research is managed. The grand vision of Frontiers is a world where all people have an equal opportunity to seek, share and generate knowledge. Frontiers provides immediate and permanent online open access to all its publications, but this alone is not enough to realize our grand goals.

Frontiers journal series

The Frontiers journal series is a multi-tier and interdisciplinary set of open-access, online journals, promising a paradigm shift from the current review, selection and dissemination processes in academic publishing. All Frontiers journals are driven by researchers for researchers; therefore, they constitute a service to the scholarly community. At the same time, the *Frontiers journal series* operates on a revolutionary invention, the tiered publishing system, initially addressing specific communities of scholars, and gradually climbing up to broader public understanding, thus serving the interests of the lay society, too.

Dedication to quality

Each Frontiers article is a landmark of the highest quality, thanks to genuinely collaborative interactions between authors and review editors, who include some of the world's best academicians. Research must be certified by peers before entering a stream of knowledge that may eventually reach the public - and shape society; therefore, Frontiers only applies the most rigorous and unbiased reviews. Frontiers revolutionizes research publishing by freely delivering the most outstanding research, evaluated with no bias from both the academic and social point of view. By applying the most advanced information technologies, Frontiers is catapulting scholarly publishing into a new generation.

What are Frontiers Research Topics?

Frontiers Research Topics are very popular trademarks of the *Frontiers journals series*: they are collections of at least ten articles, all centered on a particular subject. With their unique mix of varied contributions from Original Research to Review Articles, Frontiers Research Topics unify the most influential researchers, the latest key findings and historical advances in a hot research area.

Find out more on how to host your own Frontiers Research Topic or contribute to one as an author by contacting the Frontiers editorial office: frontiersin.org/about/contact

Endothelial activation and microcirculatory disorders in sepsis and critical illness

Topic editors

Jeremie Joffre — University of California, San Francisco, United States

W. Conrad Liles — University of Washington, United States

Citation

Joffre, J., Liles, W. C., eds. (2023). *Endothelial activation and microcirculatory disorders in sepsis and critical illness*. Lausanne: Frontiers Media SA.

doi: 10.3389/978-2-83251-438-2

Table of contents

frontiers | Frontiers in Medicine

TYPE Editorial
PUBLISHED 11 January 2023
DOI 10.3389/fmed.2022.1133408

OPEN ACCESS

EDITED AND REVIEWED BY
Ata Murat Kaynar,
University of Pittsburgh, United States

*CORRESPONDENCE
Jérémie Joffre
✉ Jeremie.joffre@aphp.fr

SPECIALTY SECTION
This article was submitted to Intensive Care Medicine and Anesthesiology, a section of the journal Frontiers in Medicine

RECEIVED 28 December 2022
ACCEPTED 29 December 2022
PUBLISHED 11 January 2023

CITATION
Joffre J and Liles WC (2023) Editorial: Endothelial activation and microcirculatory disorders in sepsis and critical illness. *Front. Med.* 9:1133408. doi: 10.3389/fmed.2022.1133408

Editorial: Endothelial activation and microcirculatory disorders in sepsis and critical illness

Jérémie Joffre[1,2]* and W. Conrad Liles[3,4,5,6]

[1]Medical Intensive Care Unit, Hôpital Saint Antoine, Sorbonne University, Assistance Publique-Hôpitaux de Paris, Paris, France, [2]Centre de Recherche Saint-Antoine (CRSA), INSERM UMR_S938, Paris, France, [3]Department of Medicine (Primary), Laboratory Medicine, Pharmacology, and Global Health, University of Washington, Seattle, WA, United States, [4]Department of Pathology, Laboratory Medicine, Pharmacology, and Global Health, University of Washington, Seattle, WA, United States, [5]Sepsis Center of Research Excellence-UW (SCORE-UW), University of Washington, Seattle, WA, United States, [6]Center for Lung Biology, University of Washington, Seattle, WA, United States

KEYWORDS

endothelium, microcirculation, critical illness, sepsis, glycocalyx (glycocalix)

Editorial on the Research Topic
Endothelial activation and microcirculatory disorders in sepsis and critical illness

Over the past two decades, clinical and experimental studies have shown that endothelial and microvascular dysfunction are key drivers of organ failure in critical illnesses, such as sepsis, cardiogenic shock, and trauma. From the basic mechanisms of endothelial activation and signaling under inflammatory conditions to clinical trials targeting microcirculation, this field of research is one of the most dynamic and promising in the critical care community.

Therefore, we, as co-guest editors, are pleased to present the first volume of the topic collection "*Endothelium and Microvascular Dysfunction in Critical Illness*" in *Frontiers in medicine*. This first volume, broad in scope, aimed to cover the multiple facets of endothelial biology and its translational opportunities. It starts with a general review by Raia and Zafrani. and a narrative review specifically focused on glycocalyx (GCX) biology (Patterson et al.) and the potential pharmacological strategies to protect or restore it during critical illness and injury. Nevertheless, assessing GCX integrity is challenging in daily practice. To do so, Bol et al. reported a remarkable study about multimodal assessment of GCX degradation during CABG combining SDF GCX thickness assessment by sublingual capillaroscopy and biomarkers of GCX degradation and EC activation. They highlighted a significant correlation between GCX thinning during CABG and elevation of GCX shedding biomarkers, but not associated with biomarkers of permeability such as Tie-2 and Ang-2 (Bol et al.).

Several original research articles accepted in the collection are remarkable and complementary: the study by Amunugama et al. provides new insight into the microvascular biology during sepsis by showing that endothelial cell lipidomics is differentially altered depending on *Escherichia coli* strain infection and interactions with neutrophils, suggesting that despite a pleiotropic and redundant system, the endothelial response to bacterial pathogens varies differentially in terms of the pro-adhesive and/or pro-coagulant phenotype induced by a specific pathogen. This result is supported by the study of Dechamps et al. that performed a differential analysis of the coagulopathy present in patients with sepsis vs. severe COVID-19, suggesting that inflammation-induced endothelial activation and coagulopathy differs substantially from sepsis-induced coagulopathy.

Among the articles with a primary focus on COVID-19, Gao et al. reported that COVID-19 patients may experience long-lasting endothelial dysfunction up to 10 months after recovery, characterized by an altered flow-mediated vasodilation response and associated with low-grade persisting inflammation. Such findings are significant regarding the potentially delayed cardiovascular adverse events experienced by ICU survivors as part of the post-ICU syndrome (1, 2).

Despite accumulated evidence that endothelial dysfunction and microcirculatory failure are key factors in determining clinical outcome and recent advances in microcirculation monitoring, integrating the microcirculation or the endothelium into resuscitation strategies or adjuvant therapy algorithms remains highly challenging. In this Research Topic, van Lier et al. performed a *post-hoc* analysis of the AdrenOSS-2 study (3). The AdrenOSS-2 study was a phase 2a, randomized placebo-controlled clinical trial using a non-neutralizing anti-adrenomedullin antibody in early septic shock patients with serum adrenomedullin at admission $>$ 70 pg/ml. This work was a proof of concept and dose-finding study, documenting feasibility of biomarker-guided therapy and the safety of adrecizumab. The authors reported that a cDPP3-based enrichment strategy may help to identify a sub-group of patients with sepsis in which the effect of adrecizumab is more pronounced. Specifically, in the sub-group of patients with admission cDPP3 $<$ 50 ng/ml that received early treatment, the impact of adrecizumab on decreasing organ failure at 24 h (delta SOFA) was significant ($p = 0.045$), and the increase in survival was close to significant (HR:0.49 [0.2–1.18]; $p = 0.094$) (van Lier et al.). The study illustrates that innovative precision medicine strategies based on endothelial-related biomarkers may improve clinical outcomes in septic shock.

Building on the success of *Endothelial Activation and Microcirculatory Disorders in Sepsis and Critical Illness*, volume I collection, we are pleased to launch the volume II of this Research Topic. Therefore, we welcome submissions of Original Research, Review, and Correspondence focusing on the following areas of research:

- Basic endothelial biology focusing on the immune role of the endothelium, coagulation/fibrinolysis, oxidative stress, leukocytes/ platelets adhesion, rheology, vasoreactivity or endothelial heterogeneity;
- Biomarker and translational studies;
- Assessment and monitoring of microcirculatory disorders in critical illness or major surgery;
- Bioinformatic and digital solutions for real-time multiparametric hemodynamic assessment and/or outcome prediction.

Author contributions

All authors listed have made a substantial, direct, and intellectual contribution to the work and approved it for publication.

Conflict of interest

The authors declare that the research was conducted in the absence of any commercial or financial relationships that could be construed as a potential conflict of interest.

Publisher's note

References

1. Voiriot G, Oualha M, Pierre A, Salmon-Gandonniere C, Gaudet A, Jouan Y, et al. Chronic critical illness and post-intensive care syndrome: from pathophysiology to clinical challenges. *Ann Intensive Care*. (2022) 12:58. doi: 10.1186/s13613-022-01038-0

2. Merdji H, Schini-Kerth V, Meziani F, Toti F. Long-term cardiovascular complications following sepsis: is senescence the missing link? *Ann Intensive Care*. (2021) 11:166. doi: 10.1186/s13613-021-00937-y

3. Laterre PF, Pickkers P, Marx G, Wittebole X, Meziani F, Dugernier T, et al. Safety and tolerability of non-neutralizing adrenomedullin antibody adrecizumab (HAM8101) in septic shock patients: the AdrenOSS-2 phase 2a biomarker-guided trial. *Intensive Care Med*. (2021) 47:1284–94. doi: 10.1007/s00134-021-06537-5

frontiers in Medicine

ORIGINAL RESEARCH
published: 17 January 2022
doi: 10.3389/fmed.2021.780750

Inflammation-Induced Coagulopathy Substantially Differs Between COVID-19 and Septic Shock: A Prospective Observational Study

Mélanie Dechamps[1,2†], Julien De Poortere[1†], Manon Martin[3], Laurent Gatto[3], Aurélie Daumerie[4], Caroline Bouzin[4], Marie Octave[1], Audrey Ginion[1], Valentine Robaux[1], Laurence Pirotton[1], Julie Bodart[1], Ludovic Gerard[5,6], Virginie Montiel[5], Alessandro Campion[1], Damien Gruson[7], Marie-Astrid Van Dievoet[7], Jonathan Douxfils[8,9], Hélène Haguet[8,9], Laure Morimont[8,9], Marc Derive[10], Lucie Jolly[10], Luc Bertrand[1], Laure Dumoutier[11], Diego Castanares-Zapatero[1,5], Pierre-François Laterre[5], Sandrine Horman[1‡] and Christophe Beauloye[1,12‡]*

[1] Pôle de Recherche Cardiovasculaire, Institut de Recherche Expérimentale et Clinique, Université Catholique de Louvain, Brussels, Belgium, [2] Department of Cardiovascular Intensive Care, Cliniques Universitaires Saint-Luc, Brussels, Belgium, [3] Computational Biology and Bioinformatics Unit, de Duve Institute, Université Catholique de Louvain, Brussels, Belgium, [4] IREC Imaging Platform, Institut de Recherche Expérimentale et Clinique, Université Catholique de Louvain, Brussels, Belgium, [5] Department of Intensive Care, Cliniques Universitaires Saint-Luc, Brussels, Belgium, [6] Pôle de Pneumologie, Institut de Recherche Expérimentale et Clinique, Université Catholique de Louvain, Brussels, Belgium, [7] Department of Clinical Biology, Cliniques Universitaires Saint-Luc, Brussels, Belgium, [8] Department of Pharmacy, Namur Research Institute for Life Sciences, Namur, Belgium, [9] Qualiblood, s.a., Namur, Belgium, [10] Inotrem s.a., Vandoeuvre-les-Nancy, France, [11] Experimental Medicine Unit, de Duve Institute, Université Catholique de Louvain, Brussels, Belgium, [12] Division of Cardiology, Cliniques Universitaires Saint-Luc, Brussels, Belgium

Critical COVID-19, like septic shock, is related to a dysregulated systemic inflammatory reaction and is associated with a high incidence of thrombosis and microthrombosis. Improving the understanding of the underlying pathophysiology of critical COVID-19 could help in finding new therapeutic targets already explored in the treatment of septic shock. The current study prospectively compared 48 patients with septic shock and 22 patients with critical COVID-19 regarding their clinical characteristics and outcomes, as well as key plasmatic soluble biomarkers of inflammation, coagulation, endothelial activation, platelet activation, and NETosis. Forty-eight patients with matched age, gender, and co-morbidities were used as controls. Critical COVID-19 patients exhibited less organ failure but a prolonged ICU length-of-stay due to a prolonged respiratory failure. Inflammatory reaction of critical COVID-19 was distinguished by very high levels of interleukin (IL)-1β and T lymphocyte activation (including IL-7 and CD40L), whereas septic shock displays higher levels of IL-6, IL-8, and a more significant elevation of myeloid response biomarkers, including Triggering Receptor Expressed on Myeloid cells-1 (TREM-1) and IL-1ra. Subsequent inflammation-induced coagulopathy of COVID-19 also differed from sepsis-induced coagulopathy (SIC) and was characterized by a marked increase in soluble tissue factor (TF) but less platelets, antithrombin, and fibrinogen

OPEN ACCESS

Edited by:
W. Conrad Liles, University of Washington, United States

Reviewed by:
Francesco Forfori, University of Pisa, Italy
Jeremie Joffre, University of California, San Francisco, United States

***Correspondence:**
Christophe Beauloye
christophe.beauloye@uclouvain.be

[†] These authors have contributed equally to this work and share first authorship
[‡] These authors have contributed equally to this work and share last authorship

Specialty section:
This article was submitted to Intensive Care Medicine and Anesthesiology, a section of the journal Frontiers in Medicine

Received: *21 September 2021*
Accepted: *24 December 2021*
Published: *17 January 2022*

Citation:
Dechamps M, De Poortere J, Martin M, Gatto L, Daumerie A, Bouzin C, Octave M, Ginion A, Robaux V, Pirotton L, Bodart J, Gerard L, Montiel V, Campion A, Gruson D, Van Dievoet M-A, Douxfils J, Haguet H, Morimont L, Derive M, Jolly L, Bertrand L, Dumoutier L, Castanares-Zapatero D, Laterre P-F, Horman S and Beauloye C (2022) Inflammation-Induced Coagulopathy Substantially Differs Between COVID-19 and Septic Shock: A Prospective Observational Study. Front. Med. 8:780750. doi: 10.3389/fmed.2021.780750

consumption, and less fibrinolysis alteration. In conclusion, COVID-19 inflammation-induced coagulopathy substantially differs from SIC. Modulating TF release and activity should be evaluated in critical COVID-19 patients.

Keywords: COVID-19, septic shock, inflammation, coagulopathy, platelet, NETosis, endothelium

INTRODUCTION

The coronavirus disease 2019 (COVID-19) varies from asymptomatic to a severe form with acute respiratory distress syndrome (ARDS) and the pathophysiology of the severe form has yet to be fully elucidated. The variability of host immune responses suggests that dysregulated systemic inflammation, classically called a "cytokine storm," could contribute to the pathogenesis of severe cases (1, 2). In addition, COVID-19 is associated with a high incidence of arterial and deep venous thrombosis leading to pulmonary embolism (3, 4) and pulmonary microthrombosis (5).

Several mechanisms underlying the pathophysiology of COVID-19 have been proposed. First, ribonucleic acid (RNA) viruses like SARS-CoV-2 usually initiate innate immunity through their detection by pattern recognition receptors (PRRs), triggering subsequent inflammatory and immune responses via the secretion of various cytokines (6). Supporting this hypothesis, critical COVID-19 has been associated with high levels of interferon-γ (IFN-γ), tumor necrosis factor-α (TNF-α), numerous interleukins (ILs), macrophage inflammatory proteins (MIPs), and IFN γ-induced protein 10 (IP-10) (1, 7, 8). Second, internalization of SARS-CoV-2 within endothelial cells after binding to angiotensin-converting enzyme 2 (ACE2) contributes to endotheliitis (9). Both direct injury and activation of the endothelium by dysregulated inflammation may lead to loss of endothelial barrier integrity and to the occurrence of a prothrombotic phenotype (10). Indeed, plasmatic level of vascular cell adhesion molecule-1 (VCAM-1), intercellular adhesion molecule 1 (ICAM-1) (11), plasminogen activator inhibitor-1 (PAI-1) (12), tissue factor (TF) (13), and von Willebrand factor (vWF) (4, 14) antigens and activities are all elevated in severe COVID-19 cases. However, a simultaneous increase in tissue plasminogen activator (tPA) or tissue factor pathway inhibitor (TFPI) could mitigate thrombosis formation (15).

Critical COVID-19-associated coagulopathy is characterized by high D-dimers due to increased thrombin generation and increased fibrinolysis (14, 16). In addition, platelets are hyperactivated (8, 17) and cooperate with the endothelium and immune cells to promote pulmonary microthrombosis through neutrophil extracellular trap (NET) formation. Dysregulated NETosis contributes to hypercoagulability and thrombosis (18). Accordingly, NET-containing microthrombi have been detected in COVID-19 pulmonary autopsies, and increased NET formation correlates with COVID-19-related ARDS and disease severity (19). Moreover, the interaction of platelets with monocytes triggers TF expression in severe COVID-19 patients, further exacerbating the hypercoagulable state (20).

Interestingly, sepsis and septic shock are well-known models of cytokine storms and coagulopathy (21). Like infection by RNA viruses, sepsis is initiated by activation of the innate immune system through recognition of pathogen-associated molecular patterns and damage-associated molecular patterns by PRRs. This inflammatory reaction enhances endothelial dysfunction and contributes to the procoagulant state with microvascular thrombi formation and, eventually, organ damage (22). The procoagulant state of sepsis is further amplified by NETs (23). Sepsis-induced coagulopathy (SIC) occurs as a continuum, progressing to disseminated intravascular coagulopathy (DIC) if the underlying etiology of the sepsis is not resolved. The clinical characteristics of critical COVID-19 and septic shock patients are extensively discussed in the literature although the entities have never been systematically compared in a prospective clinical setting including control patients with matched age, gender, and co-morbidities (24–26).

The current study prospectively compared patients with septic shock and those with critical COVID-19 on admission to the ICU regarding their clinical characteristics and outcomes, as well as key plasmatic soluble biomarkers of inflammation, coagulation, endothelial activation, platelet activation, and NETosis. Here, we show both coagulopathy and inflammatory pattern substantially differ between patients with septic shock and critical COVID-19, highlighting the specific actors involved in their respective pathogenesis.

METHODS

Aim, Design, and Setting of the Study

This study comparing clinical outcomes, inflammatory reaction, and coagulopathy between critical COVID-19 and septic shock was a monocenter, prospective, translational observational study. Adult patients were systematically included between February 1, 2019, and June 1, 2020. The ethics committee approved the study protocol, and all patients signed their informed consent (B403201938590, NCT04107402). Protocol amendment was done to include COVID-19 patients in the ongoing study. All authors had full access to primary clinical data.

Population

Patients with critical COVID-19 were those admitted to the ICU for moderate or severe ARDS due to SARS-Cov-2 infection; they were included within 5 days of admission. Acute respiratory distress syndrome was diagnosed according to the Berlin definition (27), and SARS-Cov-2 infection was demonstrated by real-time reverse transcription PCR on nasopharyngeal swabs. Septic shock was defined according to the Sepsis-3 definition as sepsis with vasopressor therapy needed to elevate the mean arterial pressure ≥65 mmHg and lactate levels >2 mmol/L

despite adequate fluid resuscitation of 30 ml/kg of intravenous crystalloid within 6 h (28). A similar protective ventilation strategy (including positive end expiratory pressure above 5 cmH_2O, maximum tidal volume of 6 ml/kg, and maximal plateau pressure of 30 cmH_2O) was applied in both COVID-19 and septic shock patients with ARDS. Prone positioning and inhaled nitric oxide were used for severe ARDS, and venovenous extracorporeal membrane oxygenation (VV-ECMO) for refractory hypoxemia despite optimal treatment (29). Venovenous extracorporeal membrane oxygenation was never used in septic shock patients. Patients with septic shock admitted to the ICU were included within 2 days of admission. Control patients with matched age, gender, and co-morbidities were recruited at a central laboratory consultation. Similar exclusion criteria were applied to all groups: therapeutic anticoagulation (oral or parenteral, including heparins, fondaparinux, vitamin K antagonists, and direct oral anticoagulants), recent (within <1 month) chemotherapy, active inflammatory disease, hemophilia and other coagulopathies, previous history of thrombocytopenia (<100,000 platelets/mm^3), cirrhosis (Child–Pugh >A), recent (within <48 h) major surgery (behalf, for septic shock, for infection source control), cardiac arrest during ICU stay, and decision of care limitation. All septic and COVID-19 cases received thromboprophylaxis using low-molecular-weight heparin (LMWH; nadroparin 3,800 IU/days subcutaneously). Sampling was performed at least 6 h after LMWH injection. For the patients with COVID-19, patients on antibiotics for any suspected or confirmed bacterial coinfections were formally excluded.

Clinical Outcomes

Patient baseline characteristics and clinical outcomes were compared. Patient prognosis was assessed using acute physiologic assessment and chronic health evaluation II (APACHE II) (30) and sequential organ failure assessment (SOFA) (31) scores. Moreover, disseminated intravascular coagulation (DIC) and SIC were diagnosed using the International Society of Thrombosis and Hemostasis scoring at inclusion (32, 33). Data were collected from central medical records, including biological datasets that were routinely performed in patients admitted in ICU such as platelet count, CRP (C-reactive protein) level, coagulation assessment, renal function, and liver enzymology. Clinical outcomes were assessed 30 days after ICU admission. Bleeding complications were assessed with Thrombolysis in Myocardial Infarction (TIMI) bleeding criteria, frequently used for cardiovascular trials (34). A major bleeding is defined by the following criteria: any intracranial bleeding, clinically overt signs of hemorrhage associated with a drop in hemoglobin of ≥5 g/dl or a ≥15% absolute decrease in haematocrit and fatal bleeding.

Sampling

Blood samples were collected through the central venous catheter in all ICU patients and by venous puncture in the control group. Venous blood was collected using vacutainer tubes containing CPDA. After two centrifugation runs enabling platelet isolation, plasma was collected, apportioned into 1 ml aliquots and stored at −80°C until use.

Measurement of Biomarkers

Soluble biomarkers of inflammation, coagulation, endothelial and platelet activation, and NETosis were measured using enzyme-linked immunosorbent assay (ELISA) or suspension array sandwich immunoassays according to regulatory requirements for commercially available research use only ELISA assays. Frozen platelet poor plasma was thawed at room temperature the day of the experiment. The details of each markers analyzed are listed in the **Supplementary Table 1**. Each analytical run was performed in duplicate. Methods respected their respective validated lower limit of quantification and upper limit of quantification. Cytokines and chemokines were measured using Bio-Plex Pro Human Cytokine 27-Plex Panel (27-Plex) and Bio-Plex Human ICAM-VCAM (hICAM-hVCAM) following the manufacturer's protocol.

Lung Biopsies and Autopsies

Lung biopsies and autopsies were obtained from the biolibrary of Cliniques Universitaires Saint-Luc. A "Human Material Transfer Agreement for research purpose" was elaborated between CUSL and UCLouvain. Use of Residual Human Body Material was approved by the local Ethic committee (B403201938590). Control patients, patients with ARDS from septic shock, and COVID-19 were compared. COVID-19 specimens were lung autopsies obtained from patients who died from respiratory failure at intensive care unit (ICU). Septic shock samples were biopsies taken owing to ARDS due to bacterial pulmonary or extra-pulmonary infection. Control specimens were archived tissues from patients who underwent lung surgery. Details about the methods and analyses are provided in the **Supplementary Material** (**Supplementary Methods**).

Statistical Analyses

The analyses were conducted using GraphPad Prism Version 9 (GraphPad Software, San Diego, California). Continuous variables were expressed as mean ± standard deviation (SD) and categorical variables were expressed as number and percentage. The data were subjected to the Kolmogorov–Smirnov normality test and Bartlett's test for homogeneity of variance. Log transformations were performed when appropriate. The categorical variables were analyzed using the Chi-squared test or Fisher's exact test, and the continuous variables using Tukey's ordinary one-way ANOVA or an unpaired Student's *t*-test, as appropriate. A log-rank test was applied to compare ICU length of stay and ventilation duration. All *p*-values were two-sided, and $p < 0.05$ was considered statistically significant.

A principal component analysis (PCA) was conducted in R (35), based on the patients with COVID-19 or septic shock and study outcomes. As an exploratory multivariate analysis, PCA provides a condensed overview of the main sources of variability in a dataset composed of individuals (here, the patients) with a large number of variables measured (here, the study outcomes). The core idea is to reduce data dimensionality by building new latent variables—called the principal components (PCs)—from the measured ones. The PCs, which are orthogonal between each other, capture the main sources of data variability in a decreasing manner (PC1 captures more variability than PC2,

etc.). Each original variable contributes with a certain weight (called a loading) to the construction of these PCs. Thereafter, the individuals are projected onto these PCs, with these projections called the scores. From this graphical representation, one can inspect the data structure with respect to the main sources of variability. This technique enables to explore the variables that seek to recover the grouped structure of the patients from the measured variables that are segregating the patients and the relationship between the variables of interest. Prior to PCA, the data were standardized, then imputed with the missMDA package (36), so that imputed values would not impact the factorial analysis results.

RESULTS

Baseline Characteristics and Clinical Outcomes of Critical COVID-19 and Septic Shock

Overall, 118 patients were enrolled, including 48 with septic shock, 22 with COVID-19, and 48 controls matched for age, gender, and main co-morbidities (flowchart, **Figure 1**). Type of infection and culture in septic shock patients are detailed in **Supplementary Table 2**. The baseline characteristics of all groups, as well as the clinical outcomes of septic shock and COVID-19 patients are detailed in **Table 1**.

The demographic characteristics and past medical history were similar among the three groups, except that the COVID-19 group included less smokers and oncologic patients. Before inclusion into the study, most COVID-19 patients had been treated with hydroxychloroquine ($n = 18$, 82%) but only one had received corticosteroids (methylprednisolone) as compared with five septic shock patients receiving low-dose hydrocortisone. At the end of the ICU stay, five COVID-19 patients (19%) and 22 septic shock patients (46%) had been treated with corticosteroids. The time delay between symptom onset and ICU admission was longer for COVID-19 compared with septic shock (2.6 ± 2.4 days and 7.3 ± 3.2 days, respectively, $p < 0.01$). The patients with septic shock displayed worse severity scores due to multiple organ failure. By contrast, the COVID-19 patients presented with more severe respiratory failure, as indicated by a lower PaO_2/FiO_2 (arterial oxygen partial pressure/fractional inspired oxygen) ratio, a higher rate of mechanically ventilated patients, longer ventilation duration and ICU length of stay. The 30-day mortality did not differ between both groups.

Coagulopathies in Critical COVID-19 and Septic Shock Patients

The critical COVID-19 and septic shock cases were compared with the matched controls considered as a reference. Circulating levels of ICAM-1, reflecting endothelial dysfunction, were similarly increased in both COVID-19 and septic shock patients, compared to matched controls (**Figure 2A**). Other endothelial biomarkers differed between COVID-19 and septic shock. Circulating TF was higher in COVID-19 patients than septic shock patients, while TFPI was similarly elevated in both groups (**Figures 2B,C**). By contrast, vWF, PAI-1, and tPA were predominant in septic shock (**Figures 2D–F**). The difference in TF levels did not impact thrombin generation, as reflected by the thrombin–antithrombin complex (TAT), which was similarly increased in critical COVID-19 and septic shock, compared to matched controls (**Figure 2G**). Both critical conditions led to increased international normalized ratio (INR) and antithrombin consumption, while these changes were more pronounced in septic shock (**Figures 2H,I**). Interestingly, platelet and fibrinogen consumption mainly occurred in septic shock (**Figures 2J,K**). Accordingly, SIC and DIC were diagnosed in 24 and 16% of septic shock cases, respectively, but in none of the critical COVID-19 cases ($p < 0.05$). D-dimers were significantly elevated in both COVID-19 and septic shock patients compared with matched controls, but further in septic shock compared with COVID-19 patients (**Figure 2L**). Of interest, the levels of TAT and D-dimers that were measured in several control patients with co-morbidities were like those found in some critically ill patients, whether they had COVID-19 or not.

Platelet Activation and NETosis in Critical COVID-19 and Septic Shock Patients

Platelet activation soluble biomarkers P-selectin (sCD62P) and triggering receptor expressed on myeloid cells (TREM)-like transcript-1 (sTLT-1) were significantly increased in septic shock, but not in COVID-19 (**Figures 3A,B**). Levels of circulating NE and Cit-H3, reflecting neutrophil activation and NETosis, respectively, were increased in both diseases compared to matched controls but there were no differences between septic shock and COVID-19 (**Figures 3C,D**). This result was supported by the histopathological analysis of lung sections from control patients and patients with critical COVID-19- and septic shock-induced ARDS (**Figure 3E**). The baseline characteristics of patients included in the histopathological analysis are described in the **Supplementary Table 3**. As already described (37–39), vascular immunothrombosis containing platelets and neutrophils was observed in the lungs of patients with COVID-19 and septic shock, but not in the controls.

Inflammation and Immune Response in Critical COVID-19 and Septic Shock Patients

The inflammation and immune response substantially differed between COVID-19 and septic shock cases. The CRP elevation and peak were similar in both groups (**Figure 4A**; **Table 1**). The septic shock group exhibited a higher neutrophil count, whereas the lymphocyte count at inclusion or nadir during follow-up was similar in both groups (**Table 1**). Ubiquitous proinflammatory cytokines like TNF-α, IL-1β, IL-6, and IL-8 were discrepantly increased in both groups (**Figures 4B–E**). Septic shock was characterized by a higher level of myeloid-derived cytokines including IL-1 receptor antagonists (IL-1ra), monocyte chemoattractant protein 1 (MCP-1), macrophage inflammatory protein-1α (MIP-1α), and the soluble form of TREM-1 (**Figures 4F–I**). In contrast, COVID-19 was distinguished by a lymphocyte T cytokine response (40), as reflected by an increase in IL-2, IL-4, IL-5, IL-7, IL-13, IL-17, and

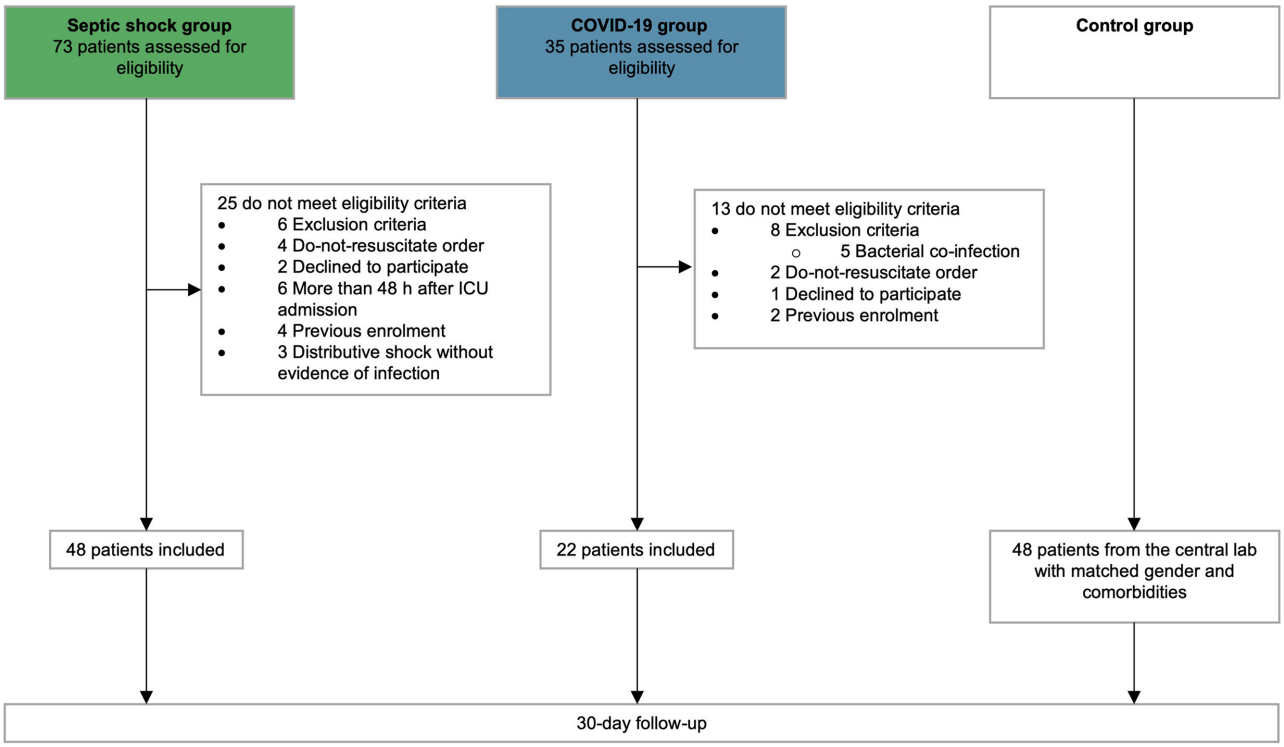

FIGURE 1 | Flow chart. Flow chart of patients screening and inclusion.

soluble CD40L (sCD40L) (**Figures 4J–P**). Of note, IFN-γ, IL-10, and IP-10, although elevated, did not differ between COVID-19 and sepsis (**Figures 4Q–S**).

Exploratory Multivariate Analysis

A PCA was done on the basis of 53 variables to assess the main relations between study outcomes (correlations), patients (similarities among patients from the same group), and between the outcomes and patients. The first two PCs of the PCA captured 39.65% of the total data variability and inflammatory and immune response biomarkers as well as SOFA, PAI-1, NE, and antithrombin ranked among their main contributors (**Supplementary Figures 1A–C**). The first two PCs allowed the discrimination of COVID-19 and septic shock patients (**Figure 5A**), consolidating results of the univariate analysis. COVID-19 patients were characterized by an increased IL1β, increased lymphoid activation biomarkers, increased TF, and higher fibrinogen, antithrombin, and platelet count. Septic shock patients were characterized by an increased IL-6 and IL-8, increased myeloid activation biomarkers, endothelial activation biomarkers (except TF), a prolonged coagulation, increased D-Dimers, and platelets activation biomarkers (**Figures 5B–G**).

DISCUSSION

For the first time, the inflammation-related coagulopathy of critical COVID-19 and septic shock was prospectively and extensively compared. This study overcame two major limitations of the literature, given that bacterial coinfections were formally excluded from the COVID-19 cohort, while pathological changes were assessed using a control group matched for age, gender, and comorbidities instead of healthy volunteers.

This study highlighted essential clinical differences between critical COVID-19 and septic shock cases. The patients with COVID-19 displayed a longer time delay between symptom onset and ICU admission, and a much longer ICU length of stay, reflecting an extended disease course. Critical COVID-19 patients, in the absence of any bacterial coinfection, rarely presented with hypotension or organ failure. These results contrast with previous observational studies that did not exclude coinfection, demonstrating a higher rate of vasopressor use (41, 42).

Inflammation-induced coagulopathy remarkably differed between COVID-19 and septic shock patients. For instance, COVID-19 was characterized by high circulating TF levels, no platelet or fibrinogen consumption, and lower levels of PAI-1, tPA, and D-dimers, suggesting less fibrinolysis activation. Although TF is recognized as one of the main actors in the inflammatory response during sepsis (43), an increase in circulating TF has never been described outside the DIC context (44). However, an increase in extracellular vesicle TF activity has been shown in COVID-19 (13, 45) and moreover, other viral diseases including human dengue infection and HIV

TABLE 1 | Baseline characteristics of prospective cohort of patients.

	Control $n = 48$	COVID-19 $n = 22$	Septic shock $n = 48$	*p*-Value
Demographics				
Men	26 (54)	15 (68)	24 (50)	0.36
Women	22 (46)	7 (32)	24 (50)	
Age (years)	61.9 ± 14.5	59.9 ± 10.3	65.0 ± 14.2	0.53
Medical history				
Hypertension	20 (42)	12 (56)	25 (52)	0.48
BMI >25	26 (58)	14 (74)	26 (54)	0.34
Diabetes	11 (23)	8 (36)	5 (10)	0.71
History of smoking	10 (21)	1 (5)	15 (31)	0.04
COPD	4 (8)	3 (14)	5 (10)	0.75
CKD	9 (19)	0 (0)	10 (21)	0.07
Cancer	15 (31)	0 (0)	9 (19)	0.01
Delay symptoms-ICU admission (days)		7.3 ± 3.2	2.6 ± 2.4	<0.01
Routine laboratory testing				
Highest CRP (mg/dl)		323 ± 119	313 ± 122	0.75
Creatinine (mg/dl)		0.91 ± 0.59	2.19 ± 1.91	<0.01
Hemoglobin (g/dl)		11.62 ± 1.90	10.34 ± 2.05	0.02
Neutrophils ($10^3/\mu l$)		8.0 ± 3.0	15.5 ± 10.2	<0.01
Lymphocytes ($/\mu l$)		893 ± 319	779 ± 521	0.33
Lowest lymphocytes ($10^3/\mu l$)		484 ± 335	469 ± 310	0.86
Platelet count ($10^3/\mu l$)		271 ± 117	203 ± 143	0.04
Organ failure, severity scores, and complications				
PaO_2/FiO_2		103 ± 37	225 ± 119	<0.01
Mechanical ventilation		17 (77)	25 (52)	0.06
VV ECMO		5 (23)	0 (0)	<0.01
Norepinephrine ($\mu g/kg/min$)		0.049 ± 0.105	0.330 ± 0.350	<0.01
Norepinephrine duration (days)		1.2 ± 3.4	4.8 ± 6.1	<0.01
Renal replacement therapy		1 (5)	13 (27)	0.04
Apache II score		15 ± 4	20 ± 7	<0.01
SOFA score		4 ± 1	9 ± 3	<0.01
SIC		0 (0)	11 (24)	0.01
DIC		0 (0)	7 (16)	0.09
Thromboembolic events		6 (27)	4 (8)	0.06
TIMI major bleeding events		5 (23)	1 (2)	0.01
Outcome				
30-day mortality		6 (27)	22 (46)	0.45
Ventilation duration (days)		27 ± 24	4 ± 7	<0.01
ICU length of stay (days)		29 ± 30	8 ± 9	<0.01

Values are numbers (percentages) or mean ± standard deviation. Major bleeding complications have been defined according to the TIMI definition. All bleeding complications in COVID-19 group occurred in ECMO-treated patients. APACHE, acute physiology and chronic health evaluation, BMI, body mass index; COPD, chronic obstructive pulmonary disease; CKD, chronic kidney disease; CRP, C-reactive protein; DIC, disseminated intravascular coagulopathy; ICU, intensive care unit; PaO_2/FiO_2, arterial oxygen partial pressure/fractional inspired oxygen; SIC, sepsis-induced coagulopathy; SOFA, sepsis-related organ failure assessment; VV ECMO, venovenous extracorporeal membrane oxygenation.

are characterized by an increased soluble TF release (46, 47). Altogether, these results indicate that coagulation abnormalities of COVID-19-associated coagulopathy promote a procoagulant state. In contrast, SIC and DIC are septic shock features, in which the coagulation imbalance can be either pro- or anti-coagulant (48). Therefore, the current study formally supports that COVID-19-associated coagulopathy should not be assimilated to SIC or DIC (49). Given the prolonged disease course, a procoagulant state may explain the high rate of thrombotic complications observed in COVID-19 patients (3, 4).

The histopathological data on COVID-19- and septic-shock-induced ARDS confirmed the presence of lung microthrombi in both diseases. These microthrombi contain numerous Cit-$H3^+$-NE^+ neutrophils at early stages of NET formation, as reported by others (37–39). Neutrophil extracellular traps represent a mechanism by which neutrophils

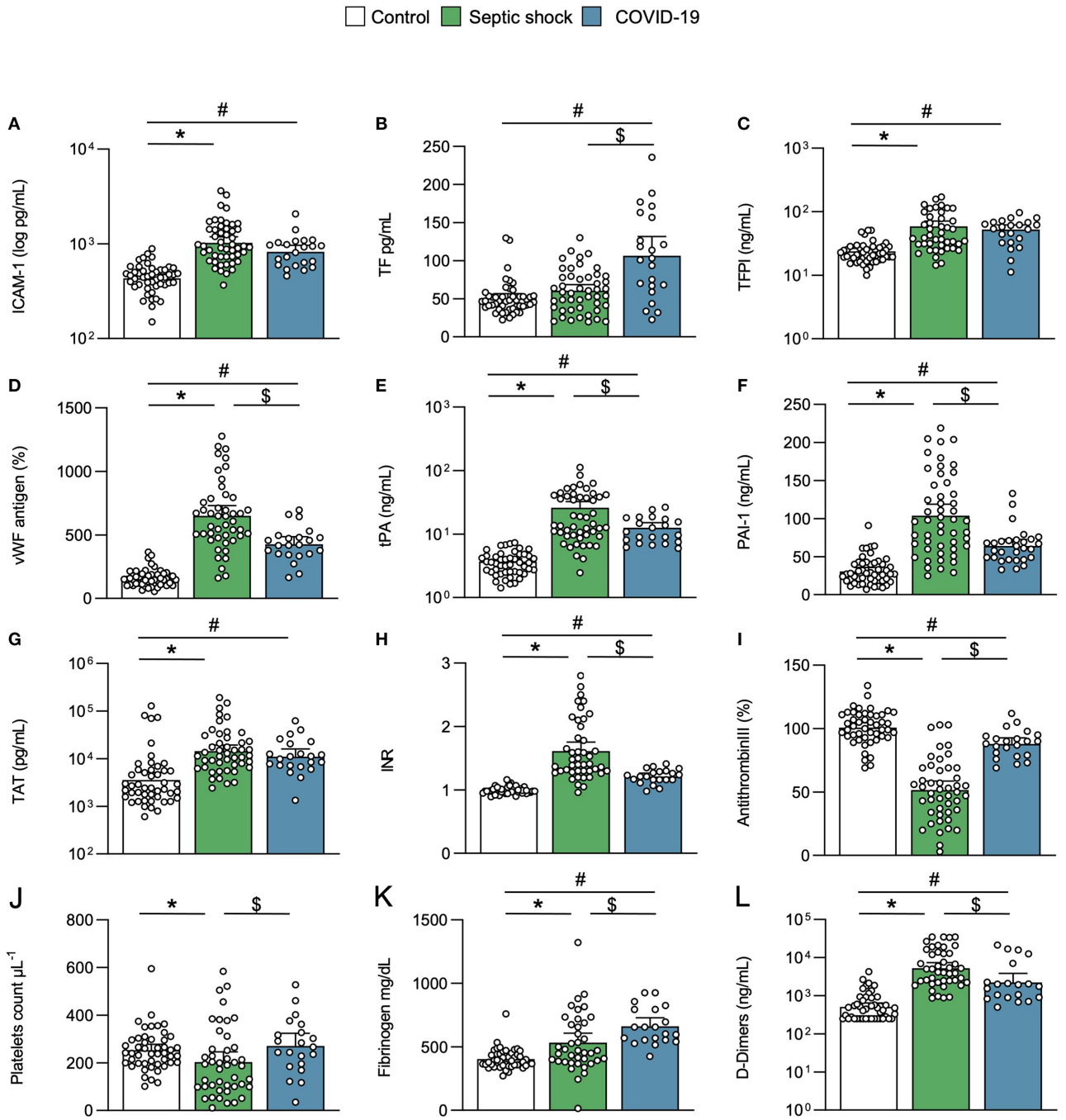

FIGURE 2 | Endothelial activation and coagulation. Scatter graphs of soluble biomarkers of **(A–F)** endothelial activation and **(G–L)** coagulation. Individual values (open circle), mean (colored rectangle), and standard deviation are presented on the graphs. $^{*}p < 0.05$ between septic shock and control patients. $^{\#}p < 0.05$ between COVID-19 and control patients. $^{\$}p < 0.05$ between septic shock and COVID-19 patients. ICAM-1, intercellular adhesion molecule-1; INR, international normalized ratio; PAI-1, plasminogen activator inhibitor-1; TAT, thrombin–antithrombin complex; TF, tissue factor; TFPI, tissue factor pathway inhibitor; tPA, tissue plasminogen activator; vWF, von Willebrand factor.

participate to thrombus formation in COVID-19 (19), possibly leading to organ dysfunction (50) and lung injury (51). The similar level of NETosis formation in ARDS due to COVID-19 vs. septic shock suggests that this parameter could be equally involved in the pathophysiology of both diseases. This hypothesis was reinforced by the plasmatic measurements in this clinical cohort revealing identical levels of circulating Cit-H3.

The secretion of soluble markers of platelet activation, namely CD62P and TLT1, was increased in septic shock but unaltered in

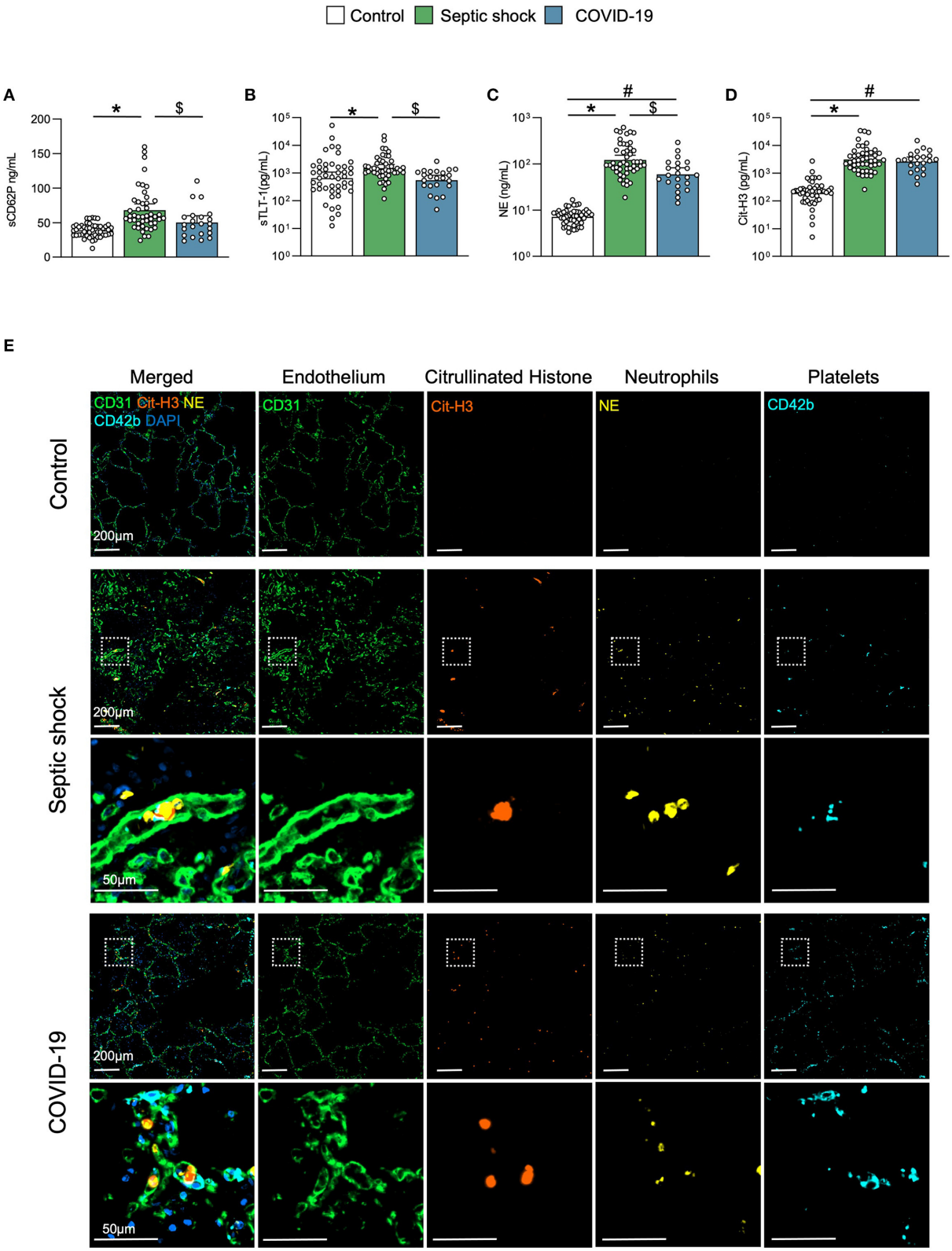

FIGURE 3 | Platelet activation and NETosis. Scatter graphs of soluble biomarkers of **(A,B)** platelet activation and **(C,D)** NETosis. Individual values (open circle), mean (colored rectangle), and standard deviation are presented on the graphs. $^{*}p < 0.05$ between septic shock and control patients. $^{\#}p < 0.05$ between COVID-19 and control patients. $^{\$}p < 0.05$ between septic shock and COVID-19 patients. **(E)** Representative microscopy pictures of endothelial cells (CD31, green), Cit-H3 (orange),

(Continued)

FIGURE 3 | neutrophils (NE, yellow), platelets (CD42b, light blue), nucleus (DAPI, dark blue), and merged staining, from control, septic shock, and COVID-19 lungs. sCD62P, soluble p-selectin; Cit-H3, citrullinated histone 3; NE, neutrophil elastase; NET, neutrophil extracellular traps; MPO, myeloperoxidase; sTLT-1, soluble triggering receptor expressed on myeloid cells (TREM) like transcript-1.

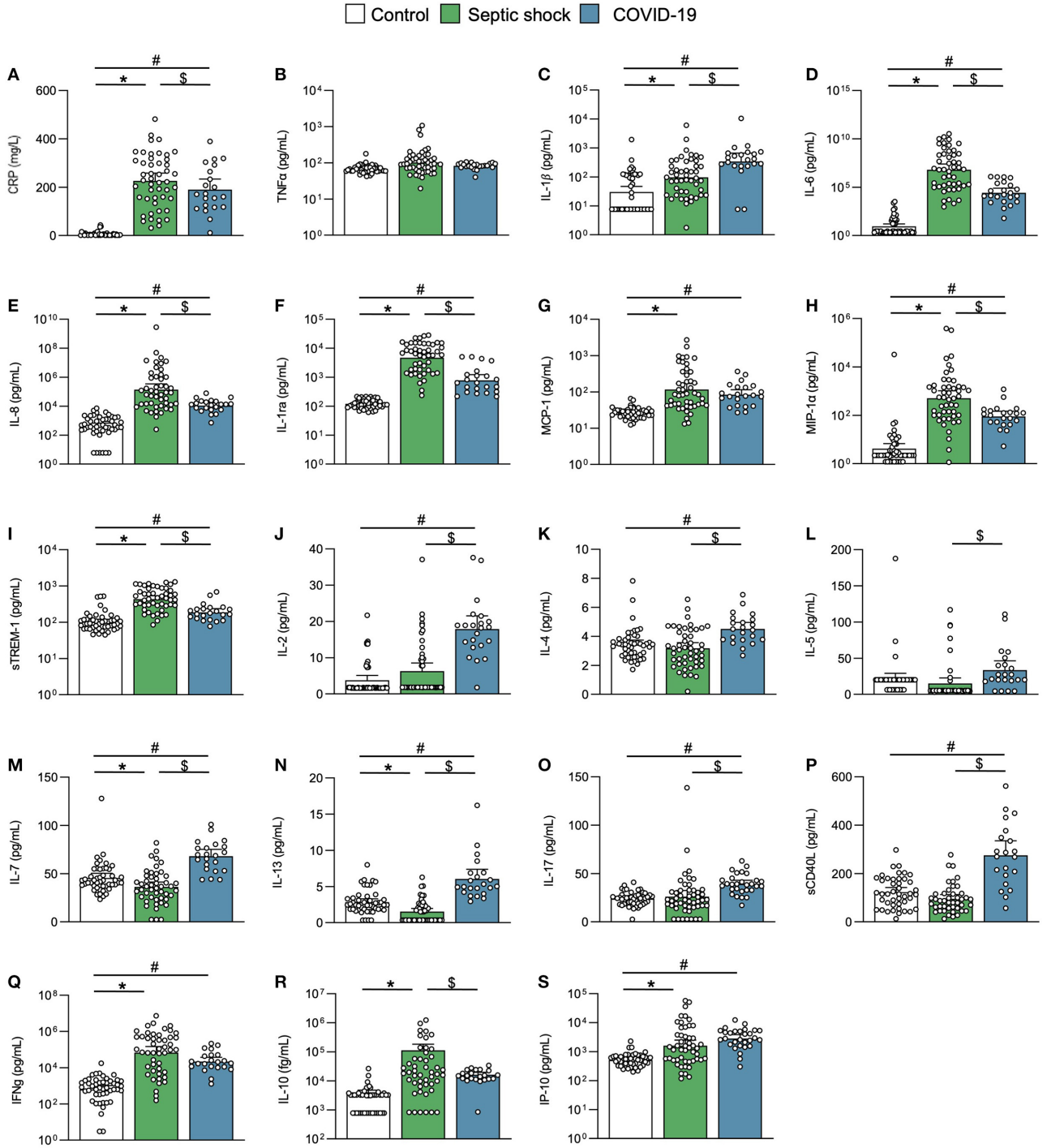

FIGURE 4 | Inflammation and immune response. Scatter graphs of **(A–E)** ubiquitous proinflammatory cytokines, **(F–I)** myeloid inflammatory cytokines, and **(J–S)** lymphoid inflammatory cytokines. Individual values (open circle), mean (colored rectangle), and standard deviation are presented on the graphs. $^{*}p < 0.05$ between septic shock and control patients. $^{\#}p < 0.05$ between COVID-19 and control patients. $^{\$}p < 0.05$ between septic shock and COVID-19 patients. CD40L, CD40 ligand; CRP, C-reactive protein; IFNγ, interferon gamma; IL, interleukin; IL-1ra, IL-1 receptor antagonist; IP-10, interferon gamma-induced protein 10; MCP-1, monocyte chemoattractant protein 1; MIP-1α, Macrophage inflammatory protein-1α; sTREM-1, soluble triggering receptor expressed on myeloid cells 1.

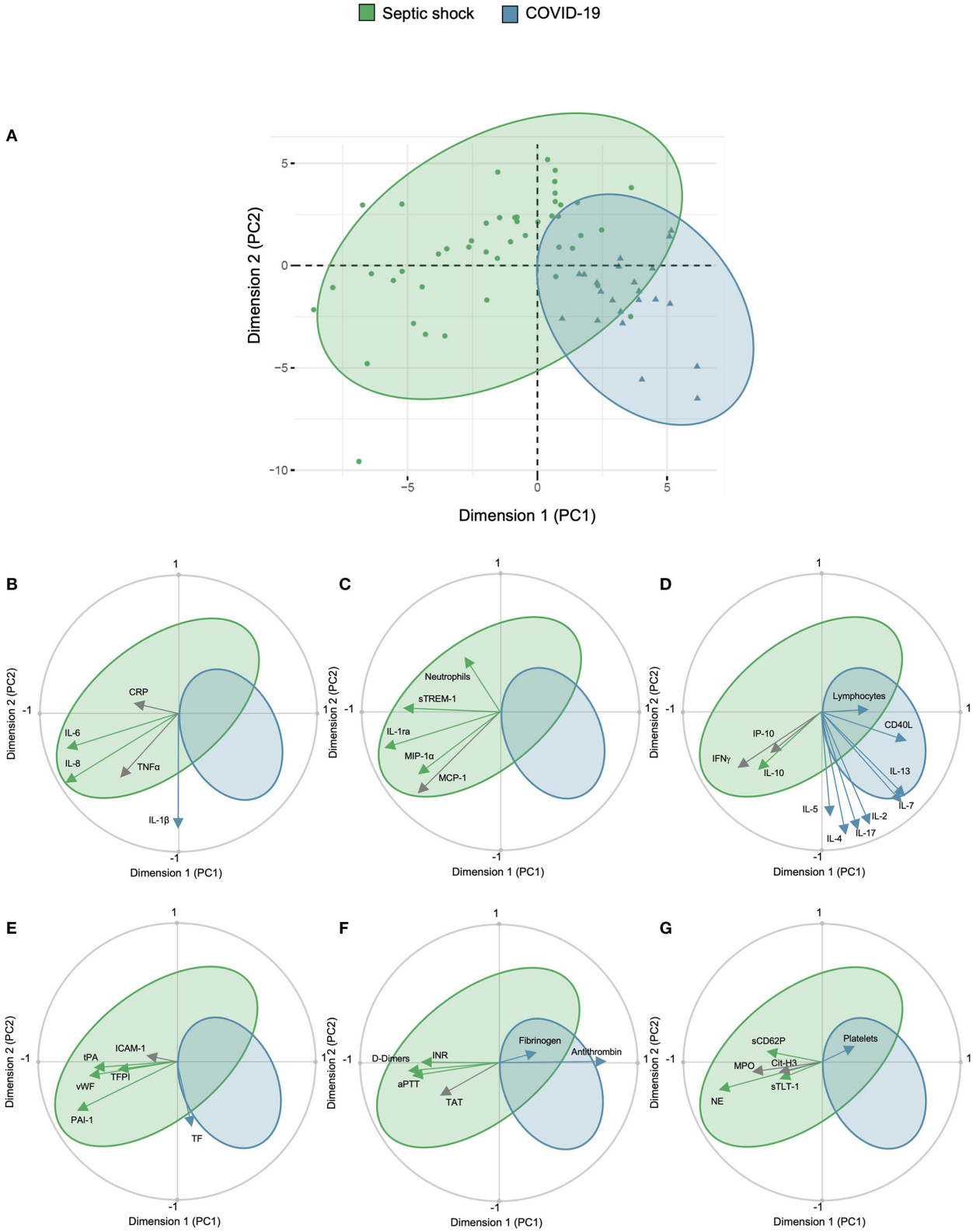

FIGURE 5 | Principal component analysis of study cohort. Principal component analysis showing **(A)** representation of COVID-19 and septic shock population in the two dimensions (score plot). Variables are separated in biplots of **(B)** ubiquitous, **(C)** myeloid, **(D)** lymphoid biomarkers, **(E)** endothelial activation, **(F)** coagulation activation, and **(G)** platelet and NETosis activation with correlation. Scores and loadings are presented in a scatterplot of one principal component (PC) against

(Continued)

FIGURE 5 | another. The loadings are represented in a circle of correlations: the closer the arrow of a loading is to the circle, the more the variable is well-represented in the space of the two plotted PCs and contributed to the building of these PCs. This graph also indicates the positive or negative links between the variables and groupings of variables. Arrow colors correspond to the between-group comparison as mentioned in the scatter graphs. CD40L, CD40 ligand; 1Cit-H3, citrullinated histone H3; CRP, C-reactive protein; ICAM-1, intercellular adhesion molecule-1; IFNγ, interferon gamma; IL, interleukin; IL-1ra, IL-1 receptor antagonist; INR, international normalized ration; IP-10, interferon gamma-induced protein 10; MCP-1, monocyte chemoattractant protein 1; MIP-1α, macrophage inflammatory protein-1α; PCA, principal component analysis; MPO, myeloperoxidase; NE, neutrophil elastase; PAI-1, plasminogen activator inhibitor-1; TAT, thrombin–antithrombin complex; TF, tissue factor; TFPI, tissue factor pathway inhibitor; sTLT-1, soluble TREM like transcript-1; tPA, tissue plasminogen activator; sTREM-1, soluble triggering receptor expressed on myeloid cells 1; TT, thrombin time; VCAM-1, vascular cell adhesion protein 1; vWF, von Willebrand factor; WBC, white blood cells.

COVID-19 cases, thereby corroborating previous findings (17). However, this observation remains controversial in the literature (52, 53). The discrepancies could be explained by a small sample size or the possible presence of bacterial coinfections in the critical COVID-19 cohort. Nevertheless, platelets from COVID-19 patients have been reported to display a hyperactive phenotype upon agonist stimulation (8, 17) and it must be noted that soluble CD62P does not inform on the presence of the protein on platelet surface neither on platelet reactivity.

The immune response was characterized by lymphocyte T activation in critical COVID-19 cases, whereas those with septic shock exhibited a greater activation of myeloid cells. Variables related to the immune and inflammatory responses were the most discriminating in distinguishing COVID-19 from septic shock at ICU admission. It has already been shown for patients infected with SARS-CoV-1 that elevation of T helper Type 2 (Th2) cytokines (IL-4, IL-5, IL-10) is correlated with disease severity (54). Interestingly, here, sCD40L also differentiated critical COVID-19 from septic shock patients. sCD40L is expressed by cells of the immune system, especially by activated $CD4^+$ T lymphocytes and activated platelets (55). In COVID-19, the elevation of sCD40L was dissociated from the raise of the other platelet activation biomarkers sCD62P and sTLT1, suggesting that its source could be the T lymphocytes. A similar result was recently found in another study (56) and corroborates the elevation of other lymphocyte T-derived ILs. Finally, sCD40L–CD40 interaction promoted endothelial cell and monocyte TF expression (57, 58), linking these two COVID-19 specific observations.

The study had limitations. First, the COVID-19 group was relatively small, so the results must probably be validated in a larger confirmation cohort. However, prospective and systematic enrollment of patients with either COVID-19 or septic shock within a closed time period has limited inclusion bias. Second, the patients with COVID-19 were included during the first wave of the pandemic, when the systematic use of corticosteroids was not yet recommended. It is therefore possible that the study findings would differ in patients that were systematically treated with dexamethasone. Finally, the observations were based on a single time point, namely early after ICU admission. A longitudinal assessment of these specific biomarkers could better define the dynamic changes in inflammatory and coagulation processes over time, which remain to be clarified, particularly in the COVID-19 context.

In conclusion, coagulopathy and inflammation patterns of critical COVID-19 substantially differ from septic shock at ICU admission. Critical COVID-19 is distinguished by very high levels of IL-1β and T lymphocyte activation (including IL-7), whereas septic shock displays higher levels of IL-6, IL-8 and a more significant myeloid response (including TREM-1 and IL-1ra). Moreover, COVID-19-associated coagulopathy is formally different from SIC and DIC, with a marked increase in soluble TF, yet less platelet, antithrombin, and fibrinogen consumption, and less fibrinolysis alteration. Hence, coagulation imbalance of severe COVID-19 almost exclusively tends toward a procoagulant state, and in the context of a prolonged disease course, this could explain the very high rate of thrombo-embolic complications of the disease. A better understanding of critical COVID-19 pathophysiology suggests potential therapeutic strategies, in particular recombinant IL-1ra and recombinant TFPI could modulate these two over-expressed pathways.

DATA AVAILABILITY STATEMENT

The raw data supporting the conclusions of this article will be made available by the authors, without undue reservation.

ETHICS STATEMENT

The studies involving human participants were reviewed and approved by Comité d'Ethique Hospitalo-Facultaire Saint-Luc-UCLouvain. The patients/participants provided their written informed consent to participate in this study.

AUTHOR CONTRIBUTIONS

SH and CBe: had full access to all of the study data and takes responsibility for the data integrity and the accuracy of data analysis. MDec, DC-Z, P-FL, SH, and CBe: concept and design. CBo, AD, SH, LGe, MDec, JDP, MO, LP, VR, AG, JB, DG, M-AVD, JD, HH, LM, MDer, and LJ: acquisition, analysis, or interpretation of data. MDec, JDP, P-FL, SH, and CBe: drafting of the manuscript. VM, LD, and LB: critical revision of the manuscript for important intellectual content. MDec, JDP, MM, and LGa: statistical analysis. MDec, P-FL, LB, SH, and CBe: obtained funding. P-FL and CBe: administrative, technical, or material support. P-FL, SH, and CBe: supervision. MDec, JDP, P-FL, AC, and VM: other—monitoring of the study progress, supporting patient recruitment, data clarifications, and data

entry. All authors contributed to the article and approved the submitted version.

FUNDING

This work was supported by grants from the *Fondation Saint-Luc* (Brussels, Belgium). The Division of Cardiology at Cliniques Universitaires Saint-Luc, Belgium, has received unrestricted research grants from AstraZeneca (Belgium). MDec is Clinical Master Specialist Applicant to a Ph.D. at the *Fonds National de la Recherche Scientifique et Médicale* (FNRS, Belgium). JDP was supported by a grant from the Salus Sanguinis Foundation (UCLouvain, Belgium). MO, LP, and JB are supported by Fund for Research Training in Industry and Agriculture (FRIA, FNRS). VM is post-doctorate Clinical Master Specialist at the FNRS. LD and SH are senior research associates at FNRS. QUALIblood s.a. offered the analyses for determining the cytokinic profile.

ACKNOWLEDGMENTS

The authors would like to thank all the patients for their participation in this study, as well as Fatima Laarbaui, Olivier Van Caenegem, Sophie Pierard, Luc Jaquet, Xavier Wittebole, Philippe Hantson, Christine Collienne, and Mathieu Luyckx for their help to enroll patients, Suzanne Renard, Caroline Berghe, Marie-France Dujardin, Leslie Gieslen, Florence Sinnaeve, Brice Lambert, all ICU nurses, and central lab nurses for their help at collecting samples.

SUPPLEMENTARY MATERIAL

The Supplementary Material for this article can be found online at: https://www.frontiersin.org/articles/10.3389/fmed.2021.780750/full#supplementary-material

REFERENCES

1. Huang C, Wang Y, Li X, Ren L, Zhao J, Hu Y, et al. Clinical features of patients infected with 2019 novel coronavirus in Wuhan, China. *Lancet.* (2020) 395:497–506. doi: 10.1016/S0140-6736(20)30183-5
2. Fajgenbaum DC, June CH. Cytokine storm. *N Engl J Med.* (2020) 383:2255–73. doi: 10.1056/NEJMra2026131
3. Klok FA, Kruip M, van der Meer NJM, Arbous MS, Gommers D, Kant KM, et al. Incidence of thrombotic complications in critically ill ICU patients with COVID-19. *Thromb Res.* (2020) 191:145–7. doi: 10.1016/j.thromres.2020.04.013
4. Helms J, Tacquard C, Severac F, Leonard-Lorant I, Ohana M, Delabranche X, et al. High risk of thrombosis in patients with severe SARS-CoV-2 infection: a multicenter prospective cohort study. *Intens Care Med.* (2020) 46:1089–98. doi: 10.1007/s00134-020-06062-x
5. Ackermann M, Verleden SE, Kuehnel M, Haverich A, Welte T, Laenger F, et al. Pulmonary vascular endothelialitis, thrombosis, and angiogenesis in Covid-19. *N Engl J Med.* (2020) 383:120–8. doi: 10.1056/NEJMoa2015432
6. Vabret N, Britton GJ, Gruber C, Hegde S, Kim J, Kuksin M, et al. Immunology of COVID-19: current State of the Science. *Immunity.* (2020) 52:910–41. doi: 10.1016/j.immuni.2020.05.002
7. Zhu Z, Cai T, Fan L, Lou K, Hua X, Huang Z, et al. Clinical value of immune-inflammatory parameters to assess the severity of coronavirus disease 2019. *Int J Infect Dis.* (2020) 95:332–9. doi: 10.1016/j.ijid.2020.04.041
8. Zaid Y, Puhm F, Allaeys I, Naya A, Oudghiri M, Khalki L, et al. Platelets can associate with SARS-Cov-2 RNA and are hyperactivated in COVID-19. *Circ Res.* (2020) 127:1404–18. doi: 10.1161/CIRCRESAHA.120.317703
9. Varga Z, Flammer AJ, Steiger P, Haberecker M, Andermatt R, Zinkernagel AS, et al. Endothelial cell infection and endotheliitis in COVID-19. *Lancet.* (2020) 395:1417–8. doi: 10.1016/S0140-6736(20)30937-5
10. Lowenstein CJ, Solomon SD. Severe COVID-19 is a microvascular disease. *Circulation.* (2020) 142:1609–11. doi: 10.1161/CIRCULATIONAHA.120.050354
11. Tong M, Jiang Y, Xia D, Xiong Y, Zheng Q, Chen F, et al. Elevated expression of serum endothelial cell adhesion molecules in COVID-19 patients. *J Infect Dis.* (2020) 222:894–8. doi: 10.1093/infdis/jiaa349
12. Nougier C, Benoit R, Simon M, Desmurs-Clavel H, Marcotte G, Argaud L, et al. Hypofibrinolytic state and high thrombin generation may play a major role in SARS-COV2 associated thrombosis. *J Thromb Haemost.* (2020) 18:2215–9. doi: 10.1111/jth.15016
13. Guervilly C, Bonifay A, Burtey S, Sabatier F, Cauchois R, Abdili E, et al. Dissemination of extreme levels of extracellular vesicles: tissue factor activity in patients with severe COVID-19. *Blood Adv.* (2021) 5:628–34. doi: 10.1182/bloodadvances.2020003308
14. Masi P, Hékimian G, Lejeune M, Chommeloux J, Desnos C, Pineton De Chambrun M, et al. Systemic inflammatory response syndrome is a major contributor to COVID-19-associated coagulopathy: insights from a prospective, single-center cohort study. *Circulation.* (2020) 142:611–4. doi: 10.1161/CIRCULATIONAHA.120.048925
15. Dupont A, Rauch A, Staessens S, Moussa M, Rosa M, Corseaux D, et al. Vascular endothelial damage in the pathogenesis of organ injury in severe COVID-19. *Arterioscler Thromb Vasc Biol.* (2021) 41:1760–73. doi: 10.1161/ATVBAHA.120.315595
16. Zuo Y, Warnock M, Harbaugh A, Yalavarthi S, Gockman K, Zuo M, et al. Plasma tissue plasminogen activator and plasminogen activator inhibitor-1 in hospitalized COVID-19 patients. *Sci Rep.* (2021) 11:1580. doi: 10.1038/s41598-020-80010-z
17. Leopold V, Pereverzeva L, Schuurman AR, Reijnders TDY, Saris A, de Brabander J, et al. Platelets are hyperactivated but show reduced glycoprotein VI reactivity in COVID-19 patients. *Thromb Haemost.* (2021). doi: 10.1055/a-1347-5555
18. Papayannopoulos V. Neutrophil extracellular traps in immunity and disease. *Nat Rev Immunol.* (2018) 18:134–47. doi: 10.1038/nri.2017.105
19. Middleton EA, He XY, Denorme F, Campbell RA, Ng D, Salvatore SP, et al. Neutrophil extracellular traps contribute to immunothrombosis in COVID-19 acute respiratory distress syndrome. *Blood.* (2020) 136:1169–79. doi: 10.1182/blood.2020007008
20. Hottz ED, Azevedo-Quintanilha IG, Palhinha L, Teixeira L, Barreto EA, Pao CRR, et al. Platelet activation and platelet-monocyte aggregate formation trigger tissue factor expression in patients with severe COVID-19. *Blood.* (2020) 136:1330–41. doi: 10.1182/blood.2020007252
21. Rhodes A, Evans LE, Alhazzani W, Levy MM, Antonelli M, Ferrer R, et al. Surviving sepsis campaign: international guidelines for management of sepsis and septic shock: 2016. *Crit Care Med.* (2017) 45:486–552. doi: 10.1097/CCM.0000000000002255
22. Hotchkiss RS, Moldawer LL, Opal SM, Reinhart K, Turnbull IR, Vincent JL. Sepsis and septic shock. *Nat Rev Dis Primers.* (2016) 2:16045. doi: 10.1038/nrdp.2016.45
23. Engelmann B, Massberg S. Thrombosis as an intravascular effector of innate immunity. *Nat Rev Immunol.* (2013) 13:34–45. doi: 10.1038/nri3345
24. Connors JM, Levy JH. COVID-19 and its implications for thrombosis and anticoagulation. *Blood.* (2020) 135:2033–40. doi: 10.1182/blood.2020006000
25. Kox M, Waalders NJB, Kooistra EJ, Gerretsen J, Pickkers P. Cytokine levels in critically ill patients with COVID-19 and other conditions. *JAMA.* (2020) 324:1565–7. doi: 10.1001/jama.2020.17052

26. Olwal CO, Nganyewo NN, Tapela K, Djomkam Zune AL, Owoicho O, Bediako Y, et al. Parallels in sepsis and COVID-19 conditions: implications for managing severe COVID-19. *Front Immunol.* (2021). 12:602848. doi: 10.3389/fimmu.2021.602848
27. Force ADT, Ranieri VM, Rubenfeld GD, Thompson BT, Ferguson ND, Caldwell E, et al. Acute respiratory distress syndrome: the Berlin Definition. *JAMA*. (2012) 307:2526–33. doi: 10.1001/jama.2012.5669
28. Singer M, Deutschman CS, Seymour CW, Shankar-Hari M, Annane D, Bauer M, et al. The Third International Consensus Definitions for Sepsis and Septic Shock (Sepsis-3). *JAMA.* (2016) 315:801–10. doi: 10.1001/jama.2016.0287
29. Papazian L, Aubron C, Brochard L, Chiche J-D, Combes A, Dreyfuss D, et al. Formal guidelines: management of acute respiratory distress syndrome. *Ann Intensive Care.* (2019) 9:69. doi: 10.1186/s13613-019-0540-9
30. Knaus WA, Draper EA, Wagner DP, Zimmerman JE, APACHE II. a severity of disease classification system. *Crit Care Med.* (1985) 13:818–29. doi: 10.1097/00003246-198510000-00009
31. Jones AE, Trzeciak S, Kline JA. The Sequential Organ Failure Assessment score for predicting outcome in patients with severe sepsis and evidence of hypoperfusion at the time of emergency department presentation. *Crit Care Med.* (2009) 37:1649–54. doi: 10.1097/CCM.0b013e31819def97
32. Iba T, Nisio MD, Levy JH, Kitamura N, Thachil J. New criteria for sepsis-induced coagulopathy (SIC) following the revised sepsis definition: a retrospective analysis of a nationwide survey. *BMJ Open.* (2017) 7:e017046. doi: 10.1136/bmjopen-2017-017046
33. Taylor FB Jr, Toh CH, Hoots WK, Wada H, Levi M, Scientific Subcommittee on Disseminated Intravascular Coagulation of the International Society on Thrombosis and Haemostasis (ISTH). Towards definition, clinical and laboratory criteria, and a scoring system for disseminated intravascular coagulation. *Thromb Haemost.* (2001) 86:1327–30. doi: 10.1055/s-0037-1616068
34. Bovill EG, Terrin ML, Stump DC, Berke AD, Frederick M, Collen D, et al. Hemorrhagic events during therapy with recombinant tissue-type plasminogen activator, heparin, and aspirin for acute myocardial infarction. Results of the Thrombolysis in Myocardial Infarction (TIMI), phase II trial. *Ann Intern Med.* (1991) 115:256–65. doi: 10.7326/0003-4819-115-4-256
35. R-Core-Team. *R: A Language and Environment for Statistical Computing 2020.* Available online at: http://www.r-project.org/
36. Josse J, Husson F. missMDA: a package for handling missing values in multivariate data analysis. (2016). *J Stat Softw.* 70:31. doi: 10.18637/jss.v070.i01
37. Carsana L, Sonzogni A, Nasr A, Rossi RS, Pellegrinelli A, Zerbi P, et al. Pulmonary post-mortem findings in a series of COVID-19 cases from northern Italy: a two-centre descriptive study. *Lancet Infect Dis.* (2020) 20:1135–40. doi: 10.1016/S1473-3099(20)30434-5
38. Nicolai L, Leunig A, Brambs S, Kaiser R, Joppich M, Hoffknecht ML, et al. Vascular neutrophilic inflammation and immunothrombosis distinguish severe COVID-19 from influenza pneumonia. *J Thromb Haemost.* (2021) 19:574–81. doi: 10.1111/jth.15179
39. Radermecker C, Detrembleur N, Guiot J, Cavalier E, Henket M, d'Emal C, et al. Neutrophil extracellular traps infiltrate the lung airway, interstitial, and vascular compartments in severe COVID-19. *J Exp Med.* (2020). 217 :e20201012. doi: 10.1084/jem.20201012
40. Akdis M, Burgler S, Crameri R, Eiwegger T, Fujita H, Gomez E, et al. Interleukins, from 1 to 37, and interferon-γ: receptors, functions, and roles in diseases. *J Allergy Clin Immunol.* (2011). 127:701–21.e1–70. doi: 10.1016/j.jaci.2010.11.050
41. Azoulay E, Fartoukh M, Darmon M, Geri G, Voiriot G, Dupont T, et al. Increased mortality in patients with severe SARS-CoV-2 infection admitted within seven days of disease onset. *Intensive Care Med.* (2020) 46:1714–22. doi: 10.1007/s00134-020-06202-3
42. Argenziano MG, Bruce SL, Slater CL, Tiao JR, Baldwin MR, Barr RG, et al. Characterization and clinical course of 1000 patients with coronavirus disease 2019 in New York: retrospective case series. *BMJ.* (2020) 369:m1996. doi: 10.1136/bmj.m1996
43. Witkowski M, Landmesser U, Rauch U. Tissue factor as a link between inflammation and coagulation. *Trends Cardiovasc Med.* (2016) 26:297–303. doi: 10.1016/j.tcm.2015.12.001
44. Wegrzyn G, Walborn A, Rondina M, Fareed J, Hoppensteadt D. Biomarkers of platelet activation and their prognostic value in patients with sepsis-associated disseminated intravascular coagulopathy. *Clin Appl Thromb Hemost.* (2021) 27:1076029620943300. doi: 10.1177/1076029620943300
45. Campbell RA, Hisada Y, Denorme F, Grover SP, Bouck EG, Middleton EA, et al. Comparison of the coagulopathies associated with COVID-19 and sepsis. *Res Pract Thromb Haemost.* (2021) 5:e12525. doi: 10.1002/rth2.12525
46. Leal de Azeredo E, Solórzano VE, de Oliveira DB, Marinho CF, de Souza LJ, da Cunha RV, et al. Increased circulating procoagulant and anticoagulant factors as TF and TFPI according to severity or infecting serotypes in human dengue infection. *Microbes Infect.* (2017) 19:62–8. doi: 10.1016/j.micinf.2016.08.005
47. Ford ES, Greenwald JH, Richterman AG, Rupert A, Dutcher L, Badralmaa Y, et al. Traditional risk factors and D-dimer predict incident cardiovascular disease events in chronic HIV infection. *Aids.* (2010) 24:1509–17. doi: 10.1097/QAD.0b013e32833ad914
48. Levi M, van der Poll T. Coagulation and sepsis. *Thromb Res.* (2017) 149:38–44. doi: 10.1016/j.thromres.2016.11.007
49. Uaprasert N, Moonla C, Sosothikul D, Rojnuckarin P, Chiasakul T. Systemic coagulopathy in hospitalized patients with coronavirus disease 2019: a systematic review and meta-analysis. *Clin Appl Thromb Hemost.* (2021) 27:1076029620987629. doi: 10.1177/1076029620987629
50. Kaplan MJ, Radic M. Neutrophil extracellular traps: double-edged swords of innate immunity. *J Immunol.* (2012) 189:2689–95. doi: 10.4049/jimmunol.1201719
51. Caudrillier A, Kessenbrock K, Gilliss BM, Nguyen JX, Marques MB, Monestier M, et al. Platelets induce neutrophil extracellular traps in transfusion-related acute lung injury. *J Clin Invest.* (2012) 122:2661–71. doi: 10.1172/JCI61303
52. Goshua G, Pine AB, Meizlish ML, Chang CH, Zhang H, Bahel P, et al. Endotheliopathy in COVID-19-associated coagulopathy: evidence from a single-centre, cross-sectional study. *Lancet Haematol.* (2020) 7:e575–e82. doi: 10.1016/S2352-3026(20)30216-7
53. Comer SP, Cullivan S, Szklanna PB, Weiss L, Cullen S, Kelliher S, et al. COVID-19 induces a hyperactive phenotype in circulating platelets. *PLoS Biol.* (2021) 19:e3001109. doi: 10.1371/journal.pbio.3001109
54. Li CK, Wu H, Yan H, Ma S, Wang L, Zhang M, et al. T cell responses to whole SARS coronavirus in humans. *J Immunol.* (2008) 181:5490–500. doi: 10.4049/jimmunol.181.8.5490
55. Henn V, Slupsky JR, Grafe M, Anagnostopoulos I, Forster R, Muller-Berghaus G, et al. CD40 ligand on activated platelets triggers an inflammatory reaction of endothelial cells. *Nature.* (1998) 391:591–4. doi: 10.1038/35393
56. Campo G, Contoli M, Fogagnolo A, Vieceli Dalla Sega F, Zucchetti O, Ronzoni L, et al. Over time relationship between platelet reactivity, myocardial injury and mortality in patients with SARS-CoV-2-associated respiratory failure. *Platelets.* (2021). 32:560–7. doi: 10.1080/09537104.2020.1852543
57. Miller DL, Yaron R, Yellin MJ. CD40L-CD40 interactions regulate endothelial cell surface tissue factor and thrombomodulin expression. *J Leukoc Biol.* (1998) 63:373–9. doi: 10.1002/jlb.63.3.373
58. Mach F, Schönbeck U, Bonnefoy JY, Pober JS, Libby P. Activation of monocyte/macrophage functions related to acute atheroma complication by ligation of CD40: induction of collagenase, stromelysin, and tissue factor. *Circulation.* (1997) 96:396–9. doi: 10.1161/01.CIR.96.2.396

Conflict of Interest: JD is the CEO and founder of QUALIblood s.a., a Belgian Contract Research Organization. LM and HH were employed by the company QUALIblood s.a. and authors MDer and LJ were employed by the company Inotrem s.a.

The remaining authors declare that the research was conducted in the absence of any commercial or financial relationships that could be construed as a potential conflict of interest.

The authors declare that this study received funding from Foundation Saint-Luc.

The funder was not involved in the study design, collection, analysis, interpretation of data, the writing of this article or the decision to submit it for publication.

Publisher's Note: All claims expressed in this article are solely those of the authors and do not necessarily represent those of their affiliated organizations, or those of the publisher, the editors and the reviewers. Any product that may be evaluated in this article, or claim that may be made by its manufacturer, is not guaranteed or endorsed by the publisher.

frontiers in Medicine

ORIGINAL RESEARCH
published: 14 February 2022
doi: 10.3389/fmed.2022.809033

Persistent Endothelial Dysfunction in Coronavirus Disease-2019 Survivors Late After Recovery

*Yi-Ping Gao†, Wei Zhou†, Pei-Na Huang, Hong-Yun Liu, Xiao-Jun Bi, Ying Zhu, Jie Sun, Qiao-Ying Tang, Li Li, Jun Zhang, Wei-Hong Zhu, Xue-Qing Cheng, Ya-Ni Liu and You-Bin Deng**

Department of Medical Ultrasound, Tongji Medical College, Tongji Hospital, Huazhong University of Science and Technology, Wuhan, China

OPEN ACCESS

Edited by:
Renee W. Y. Chan, The Chinese University of Hong Kong, China

Reviewed by:
Christine Cheung, Nanyang Technological University, Singapore
Takamichi Ishikawa, Hamamatsu University School of Medicine, Japan

***Correspondence:**
You-Bin Deng
ybdeng2007@hotmail.com

†These authors have contributed equally to this work and share first authorship

Specialty section:
This article was submitted to Infectious Diseases – Surveillance, Prevention and Treatment, a section of the journal Frontiers in Medicine

Received: *04 November 2021*
Accepted: *10 January 2022*
Published: *14 February 2022*

Citation:
Gao Y-P, Zhou W, Huang P-N, Liu H-Y, Bi X-J, Zhu Y, Sun J, Tang Q-Y, Li L, Zhang J, Zhu W-H, Cheng X-Q, Liu Y-N and Deng Y-B (2022) Persistent Endothelial Dysfunction in Coronavirus Disease-2019 Survivors Late After Recovery. Front. Med. 9:809033. doi: 10.3389/fmed.2022.809033

Background: Coronavirus disease 2019 (COVID-19) can result in an endothelial dysfunction in acute phase. However, information on the late vascular consequences of COVID-19 is limited.

Methods: Brachial artery flow-mediated dilation (FMD) examination were performed, and inflammatory biomarkers were assessed in 86 survivors of COVID-19 for 327 days (IQR 318–337 days) after recovery. Comparisons were made with 28 age-matched and sex-matched healthy controls and 30 risk factor-matched patients.

Results: Brachial artery FMD was significantly lower in the survivors of COVID-19 than in the healthy controls and risk factor-matched controls [median (IQR) 7.7 (5.1–10.7)% for healthy controls, 6.9 (5.5–9.4)% for risk factor-matched controls, and 3.5(2.2–4.6)% for COVID-19, respectively, $p < 0.001$]. The FMD was lower in 25 patients with elevated tumor necrosis factor (TNF)-α [2.7(1.2–3.9)] than in 61 patients without elevated TNF-α [3.8(2.6–5.3), $p = 0.012$]. Furthermore, FMD was inversely correlated with serum concentration of TNF-α ($r = -0.237$, $p = 0.007$).

Conclusion: Survivors of COVID-19 have a reduced brachial artery FMD, which is inversely correlated with increased serum concentration of TNF-α. Prospective studies on the association of endothelial dysfunction with long-term cardiovascular outcomes, especially the early onset of atherosclerosis, are warranted in survivors of COVID-19.

Keywords: COVID-19, endothelial function, flow-mediated dilation, inflammation, TNF-α

INTRODUCTION

The coronavirus disease 2019 (COVID-19) pandemic caused by severe acute respiratory syndrome coronavirus 2 (SARS-CoV-2) has become a significant challenge to healthcare systems worldwide (1). Though primarily known as a respiratory disease, manifestations from head to toe have been reported in patients with COVID-19 (2). The SARS-CoV-2 attacks the host through angiotensin converting enzyme 2 (ACE2) receptors, which are present in nearly every human organ, including the lungs, heart, kidney, and intestines. Endothelial cells also express ACE2 receptors, representing a potential target for SARS-CoV-2 infection (3). Indeed, previous investigations have confirmed a direct viral infection of endothelial cells and diffuse a vascular inflammation in multiple organs of patients with COVID-19 (4–6). A high prevalence of thrombotic events, including venous

thrombosis, pulmonary embolism, and disseminated intravascular coagulation in patients with severe COVID-19 also indicates a dysregulated coagulation system induced by endothelial damage and inflammation during severe SARS-CoV-2 infection (6–8). The endothelial cells participate in the regulation of local and systemic inflammation by generating or responding to cytokines that characterize the cytokine storm in COVID-19, including interleukin (IL)-1, IL-6, IL-8, and tumor necrosis factor (TNF)-α (9), which finally leads to a pro-thrombotic phenotype in patients with severe COVID-19. With increasing evidence of the crucial role of vascular endothelium in the pathophysiology of COVID-19, it has been proposed that endothelial biomarkers and tests of function should be developed and evaluated for their value in risk stratification in patients with COVID-19 and for early detection of long-term cardiovascular complications in convalescent survivors (10).

Recent studies have reported endothelial dysfunction in patients with COVID-19 and convalescent survivors reflected by reduced brachial artery flow-mediated dilation (FMD) in response to hyperemia, which is a non-invasive method to assess systemic vascular endothelial function (11–15). However, these studies have been limited by their short interval between diagnosis and follow-up ranging from 23 to 120 days. Data on endothelial function in survivors of COVID-19 late after recovery are not available. Therefore, the purpose of this study was to examine brachial artery FMD in response to hyperemia with high-resolution ultrasonography in survivors of COVID-19 late after recovery and to explore the potential mechanism underlying the endothelial dysfunction.

METHODS

Study Design and Participants

This prospective observational study was conducted in Tongji Hospital of Huazhong University of Science and Technology, a tertiary medical center and a designated institute for treating patients with COVID-19. The COVID-19 was diagnosed on the basis of SARS-CoV-2 nucleic acid detection *via* upper respiratory tract swab by a reverse transcriptase-polymerase chain reaction (rt-PCR). Adult patients with confirmed COVID-19 after hospital discharge were invited to participate in the study. Patients were excluded if they had acute conditions such as infection, organ dysfunction, active autoimmune disease, were required hospitalization for other disease, and/or were unwilling to participate. Finally, 86 survivors were recruited between December 2020 and January 2021. Twenty-eight healthy subjects matched for age and sex were recruited as healthy controls. Thirty subjects matched for age, sex, hypertension, diabetes mellitus, smoking, hypercholesterolemia, and coronary artery disease were also recruited as the risk factor-matched controls. All procedures were performed in concordance with the Declaration of Helsinki and International Conference on Harmonization of Good Clinical Practice. The study was approved by the Tongji Hospital Ethics Committee (TJ-C20200156) and informed consent was obtained from each participant before their enrollment in the study.

Clinical characteristics, laboratory results, and medication for acute phase of illness were recorded from the electronic medical system or patient discharge summary of Tongji Hospital. Classification of COVID-19 clinical type was based on the Diagnosis and Treatment Protocol of Novel Coronavirus issued by the National Health Commission of the People's Republic of China (16).

Patients who had fever and respiratory symptoms and had radiologic assessments that showed signs of pneumonia were classifed as Moderate type, while patients who met any of the following criteria were classified as Severe type: (1) shortness of breath, respiratory rate $\geq$30 times/min; (2) oxygen saturation $\leq$93% at rest; (3) alveolar oxygen partial pressure/fraction of inspiration O_2 (PaO_2/FiO_2) $\leq$300 mmHg; and (4) pulmonary imaging showed significant progression of lesion of $>$50% within 24–48 h. Lastly, patients who met any of the following criteria were classified as Critical type: (1) respiratory failure requiring mechanical ventilation; (2) shock; and (3) had organ failure and needed intensive care unit monitoring and treatment.

Assessment of Brachial Artery FMD

Systemic endothelial function was evaluated by measuring brachial artery response to endothelium-dependent stimulus according to the recommendations of European Society of Cardiology (17). All subjects were told to fast and to abstain from drinking coffee or tea before examination. Brachial ultrasound examinations were performed with a subject supine in a quiet, temperature-controlled (22-−24^0C) environment using a Vivid E95 ultrasound system (GE Medial System, Horten, Norway), equipped with 4–8 MHz 9 L linear array transducer operated by the same examiner throughout the study. The right brachial artery was scanned longitudinally, 5 cm above the antecubital fossa with great care to obtain the maximal vessel diameter and optimal lumen-to-vessel wall interface. When a satisfactory transducer position was found, the skin and the matching position on the probe were marked for reference for later examinations, while the arm was kept in the same position throughout the study. At the same time, anatomical landmarks, like bifurcation of the artery, were also identified and recorded for reference for later examination and measurements. After a resting baseline scan was recorded, the blood pressure cuff placed around the forearm was inflated to a pressure of 200 mm Hg or exceeding $>$50 mm Hg above systolic pressure if the systolic pressure of the patient was $>$150 mm Hg for 5 min. Reactive hyperemia was then induced by sudden cuff deflation. The second recording of brachial artery was performed 30 s before the release of the cuff and was continued for a further 3 min after cuff deflation. All recordings were stored in a machine hard disk. The offline analysis was performed by a single observer blinded to the clinical details, time, and intervention. The brachial artery images were input to the computer-assisted analysis platform and the diameter was measured using an automatic echo tracking algorithm. Mean artery diameter was calculated over pre-selected segments at end-diastole and averaged from three consecutive cardiac cycles. The percent change in diameter caused by reactive hyperemia was calculated by dividing the difference from baseline diameter by the baseline value. The Bland-Altman

analyses of intra-observer and inter-observer reproducibility for measurements of FMD were previously reported in our laboratory. The mean (95% confidence interval) of FMD difference for intra-observer reproducibility was −0.3(−2.8–2.1) %. The mean (95% confidence interval) of FMD difference for interobserver reproducibility was −0.4(−3.3–2.4) % (18).

Serum Inflammatory Biomarkers

Peripheral venous blood samples were drawn at least 30 min before vascular ultrasound examination. Blood samples were processed using standardized commercially available test kits for high-sensitivity C-reactive protein (hsCRP), IL-1β, IL-2R, IL-6, IL-8, IL-10, and TNF-α. The hsCRP was detected by immunoturbidimetry method according to the instruction of SEKISUI CHEMICAL CO., LTD (Tokyo, Japan). The IL-1β, IL-2R, IL-6, IL-8, IL-10, and TNF-α were assessed by chemiluminescence immunoassay (CLIA) performed on a fully automated analyzer (Siemens Immulite 1000, DiaSorin Liaison, Vercelli, Italy, or Roche Diagnostics Cobas e602, Basel, Switzerland) according to the instructions of the manufacturers. The CLIA kits for IL-1β (LKL11), IL-2R (LKIP1), IL-8 (LK8P1), IL-10 (LKXP1), and TNF-α (LKNF1) were purchased from DiaSorin (Vercelli, Italy). An IL-6 kit (#05109442 190) was purchased from Roche Diagnostics (Basel, Switzerland). Cut-off values were set according to the kit instructions and were also clinically validated by Laboratory Department of Tongji Hospital. The cut-off values were 10 mg/L, 5 pg/ml, 710 U/ml, 7 pg/ml, 62 pg/ml, 9.1 pg/ml, 8.1 pg/ml for hsCRP, IL-1β, IL-2R, IL-6, IL-8, IL-10, and TNF-α, respectively. The lower limits of detection (LLOD) of hsCRP, IL-1β, IL-2R, IL-6, IL-8, IL-10, and TNF-α were 0.1 mg/L, 5 pg/ml, 5 U/ml, 1.5 pg/ml, 5 pg/ml, 5 pg/ml, and 4 pg/ml, respectively. Values below LLOD were substituted with LLOD for statistical analysis. Participants with TNF-α >8.1 pg/ml were considered to have an elevated TNF-α.

Statistical Analysis

Categorical variables were expressed as counts and percentage, and continuous variables as mean ± SD or median [interquartile range (IQR)]. Normality was evaluated using the Shapiro-Wilk test. Comparisons among healthy control, risk-factor matched control, and COVID-19 survivor groups were performed using one-way ANOVA with Bonferroni-corrected *post-hoc* tests for normally distributed parameters including body mass index, body surface area, and systolic blood pressure. Kruskal-Wallis test was used among three groups for non-normally distributed parameters, including age, heart rate, diastolic blood pressure, brachial flow-mediated dilation parameters, and inflammatory biomarkers, with Bonferroni-corrected *post-hoc* tests for pairwise comparisons. Mann-Whitney *U*-test was utilized for comparison between TNF-α normal and elevated groups. Comparison of FMD among three clinical types was performed using Kruskal-Wallis test. Wilcoxon test was utilized for comparisons of the data obtained at acute phase and recovery of the illness. Chi-square test or Fisher's exact test was used to compare categorical variables. Associations between FMD and inflammatory biomarkers were analyzed using Pearson or Spearman correlation. A $p < 0.05$ was considered to indicate statistical significance. All statistical analysis was performed using SPSS version 21.0 software (IBM, Armonk, NY, USA).

RESULTS

Patient Characteristics

Patient characteristics, brachial artery FMD, and serum inflammatory biomarkers on the day of follow-up are shown in **Table 1**. A total of 86 patients were enrolled in this study. The median (IQR) age of the COVID-19 group was 58 (39–70) years and 32 patients (37%) were male. According to the Diagnosis and Treatment Protocol of Novel Coronavirus issued by the National Health Commission of the People's Republic of China (16), 45 of 86 patients (52%) were classified as Moderate type of illness, 27 (31%) as Severe type and 14 (17%) as Critical type. The most common chronic cardiovascular conditions in these survivors were hypertension (37%), hypercholesterolemia (19%), diabetes mellitus (16%), and coronary heart disease (15%). Seventy-eight (91%) patients required hospitalization. Among them, 1 patient (1%) underwent an extra-corporeal membrane oxygenation, 6 (8%) underwent mechanical ventilation, and 10 (13%) underwent non-invasive ventilation with positive airway pressure. Inflammatory biomarkers were available in a proportion of patients during hospitalization (**Table 2**). The IQR interval between the COVID-19 diagnosis and follow-up was 327 (318–337) days. Exertional shortness of breath and chest discomfort were reported in 25 (29%) and 33 (38%) patients, respectively, on the day of follow-up.

Endothelial Function

No significant differences were found in baseline artery diameter among three groups. During reactive hyperemia, the diameter of the brachial artery increased significantly in the control group ($p < 0.001$), survivors of COVID-19 ($p < 0.001$), and risk factor-matched group ($p < 0.001$, **Table 1**), but FMD was significantly lower in the survivors of COVID-19 than in the healthy controls and the risk factor-matched controls (**Table 1**). Although no significant differences in FMD existed among groups with different severity of the illness [3.8 (2.2–5.4)% for Moderate, 3.3 (2.3–4.4)% for Severe and 3.2 (0.5–4.1)% for Critical type, respectively, $p = 0.262$, **Figure 1A**], it was lower in 25 patients with an elevated TNF-α [2.7(1.2–3.9)%] than in 61 patients without an elevated TNF-α [3.8(2.6–5.3)%, $p = 0.012$, **Figure 1A**]. Furthermore, FMD was inversely correlated with IL-1β, IL-2R, and TNF-α (**Table 3** and **Figure 1B**).

Serum Inflammatory Biomarkers

There were no significant differences among three groups with respect to serum concentrations of IL-1β, IL-2R, IL-6, IL-8, IL-10, and TNF-α. The serum concentration of hsCRP in survivors of COVID-19 was significantly higher than in healthy controls ($p < 0.01$, **Table 1**). The proportion of participants with elevated TNF-α in survivors of COVID-19 was significantly higher than that of healthy controls ($p < 0.01$, **Table 1**) and higher than that of risk factor-matched controls ($p < 0.01$, **Table 1**). **Table 2** shows the changes in serum inflammatory biomarkers found between the acute phase and the follow-up 327 days after diagnosis in

TABLE 1 | Clinical characteristics, brachial artery flow-mediated dilation, and inflammatory biomarkers of survivors of COVID-19 327 days after diagnosis.

	Healthy control ($n = 28$)	Risk Factor-Matched control ($n = 30$)	COVID-19 ($n = 86$)	*p*-value
Patient characteristics				
Age, years	56 (37–65)	62 (39–67)	58 (39–70)	0.392
Male, *n*%	10 (36%)	11 (37%)	32 (37%)	0.990
Body mass index, kg/m^2	23 ± 3	24 ± 3	24 ±3	0.304
Body surface area, m^2	1.7 ± 0.2	1.7 ± 0.2	1.7 ± 0.2	0.561
Heart rate, bpm	67 (61–81)	69 (63–73)	73 (65–79)	0.119
Systolic blood pressure, mmHg	125 ± 12	126 ± 16	131 ± 18	0.132
Diastolic blood pressure, mmHg	73 (67–82)	72 (67–79)	77 (70–82)	0.228
Oxygen saturation, %	NA	NA	98 (97–99)	NA
Hypertension, *n*%	0 (0%)	10 (33%)*	32 (37%)*	0.001
Diabetes mellitus, *n*%	0 (0%)	2 (7%)	14 (16%)*	0.032
Coronary heart disease, *n*%	0 (0%)	3 (10%)	13 (15%)	0.076
Hypercholesterolemia, *n*%	0 (0%)	9 (30%)*	16 (19%)*	0.003
Brachial flow-mediated dilation				
Baseline diameter, mm	3.6 (3.2–3.9)	3.5 (3.3–4.0)	3.8 (3.2–4.3)	0.266
Diameter during reactive hyperemia, mm	3.8 (3.5–4.2)	3.8 (3.6–4.3)	3.9 (3.4–4.4)	0.940
Percent change in diameter, %	7.7 (5.1–10.7)	6.9 (5.5–9.4)	3.5 (2.2–4.6)*†	<0.001
Inflammatory biomarkers				
High-sensitivity CRP, mg/L	0.7 (0.3–1.6)	0.7 (0.3–1.8)	1.1 (0.6–2.2)*	0.039
Interleukin-1β, pg/mL	5.0 (5.0–5.0)	5.0 (5.0–5.0)	5.0 (5.0–5.5)	0.282
Interleukin-2R, U/mL	366 (294–444)	385 (297–482)	370 (282–473)	0.800
Interleukin-6, pg/mL	1.5 (1.5–3.4)	1.5 (1.5–2.8)	1.5 (1.5–2.4)	0.572
Interleukin-8, pg/mL	9.2 (7.0–11.1)	8.1(6.7–10.7)	8.8 (6.8–13.0)	0.482
Interleukin-10, pg/mL	5.0 (5.0–5.0)	5.0 (5.0–5.0)	5.0 (5.0–5.0)	0.371
TNF-α, pg/mL	6.3 (5.5–7.1)	6.2 (5.8–6.8)	6.3 (5.1–8.5)	0.863
Elevated TNF-α, n%	4 (14%)	2 (7%)	25 (29%)*†	0.027

Numbers are given as median (interquartile range) or mean ± standard deviation or as case number with percentage in parentheses.
NA, not applicable; CRP, C-reactive protein; TNF, tumor necrosis factor.
$^*p < 0.01$, vs. healthy control. $^\dagger p < 0.01$, vs. risk factor-matched control.

TABLE 2 | Comparisons of inflammatory biomarkers obtained at an acute phase and after recovery.

	Number of cases	Acute Phase	Recovery	*p*-value
High-sensitivity CRP, mg/L	$n = 48$	45.1 (6.6–110.7)	1.4 (0.6–2.3)	<0.001
Interleukin-1β, pg/mL	$n = 47$	5.0 (5.0–8.8)	5.0 (5.0–8.3)	0.666
Interleukin-2R, pg/mL	$n = 47$	714 (481–1,154)	410 (336–508)	<0.001
Interleukin-6, pg/mL	$n = 47$	15.9 (4.8–50.8)	1.5 (1.5–2.6)	<0.001
Interleukin-8, pg/mL	$n = 47$	20.4 (10.9–43.5)	9.9 (7.5–14.4)	<0.001
Interleukin-10, pg/mL	$n = 47$	6.7 (5.0–12.5)	5.0 (5.0–5.0)	<0.001
Tumor necrosis factor -α, pg/mL	$n = 47$	10.8 (7.7–15.4)	7.7 (5.8–9.3)	<0.001

Numbers are given as median (interquartile range).
NA, not applicable; CRP, C-reactive protein; TNF, tumor necrosis factor.

a proportion of survivors with obtainable biomarker data in acute phase. Of the 47 survivors with cytokine data, 29 (62%) survivors had an undetectable IL-1β and the other 18 (38%) had slightly increased IL-1β in acute phase. In addition, there was no significant difference in median concentrations of IL-1β in acute phase and after recovery ($p = 0.666$, **Table 2**). Other cytokines and hsCRP, however, decreased significantly ($p < 0.001$, **Table 2**). The median age (65 years) in this subgroup of 47 survivors was significantly higher than in the overall age of 86 survivors (58 years, $p = 0.012$). However, the clinical type which indicated the severity of the disease at the acute phase of illness showed no significant difference between the two groups ($p = 0.101$). One explanation for the age difference was that seniors were more likely to get tested for cytokine storms in

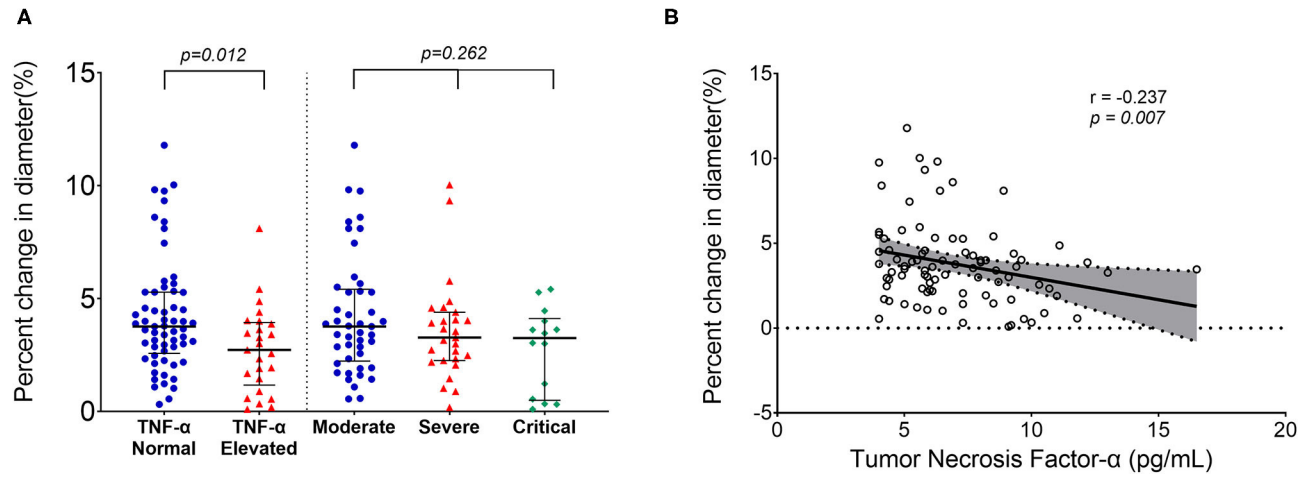

FIGURE 1 | Reduced endothelial function in survivors of COVID-19 late after recovery. No significant differences in brachial artery percent change in diameter existed among groups with different severity of the illness, but it was lower in patients with elevated tumor necrosis factor (TNF)-α than in patients without elevated TNF-α **(A)**. Correlation plots showing the inverse correlation between percent change in diameter and the serum TNF-α level **(B)**. Longer black lines indicate the median and shorter black lines indicate interquartile range in **(A)**. Each dot represents a value. Correlation plots display results from spearman correlation tests and a linear regression line with 95% confidence interval shading in **(B)**.

the acute phase of illness since they were more vulnerable to the infection.

DISCUSSION

Our study showed that survivors of COVID-19 had reduced brachial artery FMD compared with healthy control and risk factor-matched control, which is independent of severity of the illness, but inversely correlated with serum concentration of TNF-α after a median of 327 days from diagnosis. Although concentrations of most inflammatory biomarkers were resolved in survivors of COVID-19, the concentration of hsCRP and percentage of elevated TNF-α in survivors of COVID-19 were still greater than those in healthy and risk factor-matched controls, indicating that a chronic low-grade inflammation could persist late after recovery from COVID-19.

The SARS-CoV-2 attacks the host through the ACE2 receptor, which is also expressed in endothelial cells (3). Previous studies showed that COVID-19 can result in systemic endotheliitis and in widespread endothelial dysfunction *via* direct viral infection of the endothelium or immune-mediated recruitment of immune cells (4, 10). The systemic endotheliitis and endothelial dysfunction in different vascular beds explain the prevalent macro- and micro-vasculopathy in multiple organs in patients with COVID-19. Endothelial dysfunction is characterized by a reduction of the bioavailability of the endothelium-derived vasoactive mediator (mainly nitric oxide) and arterial flow-mediated dilation depends on the ability of the endothelium to release nitric oxide in response to reactive hyperemia or shear stress. Therefore, the brachial artery FMD during reactive hyperemia reflects an endothelial nitric oxide activity and is the marker of endothelial function (19). Unexpectedly, there are only few reports published on FMD measures in patients suffering from COVID-19, so far (11–15, 20, 21). Oliveira et al. reported an endothelial vascular dysfunction assessed by FMD at early stage of illness in patients hospitalized for COVID-19 (20), and Ambrosino et al. documented a significant improvement in FMD in patients with convalescent COVID-19 after a stay of 23 days in hospital (11). A recent study showed reduced brachial artery FMD in 11 young patients with COVID-19 after 3–4 weeks from symptom onset (12), while another study presented lower FMD in survivors of COVID-19 when compared with a control group 4 months after diagnosis (15). In the present study, we demonstrated that brachial artery FMD was reduced in survivors of COVID-19 even 327 days after diagnosis. Furthermore, we also found elevated concentrations of hsCRP, increased percentage of elevated TNF-α, and an inverse correlation between reduced FMD and inflammatory biomarkers in survivors of COVID-19. Although the correlation between FMD and cytokines is not strong, our findings bring new insights into the underlying mechanism of impaired endothelial function in survivors of COVID-19 late after recovery. Previous studies have reported no significant change of IL-1β concentration during the progression of illness in nearly all the patients with either severe or moderate COVID-19 (22). Our study also found that there was no up or downregulation of IL-1β in survivors late after recovery, which further demonstrated the disengagement of IL-1β in the pathogenesis of the disease. On the contrary, TNF-α seems to have participated in the whole course of COVID-19 illness. In acute phase of COVID-19, TNF-α is widely present in blood and infected tissues and acts as an amplifier of inflammation (23). Inflammation is an important factor of endothelial dysfunction, and it has been demonstrated that TNF-α impairs the endothelium-dependent relaxation by affecting nitric oxide production and inducing reactive oxygen species (24–26). It is speculated that during

TABLE 3 | Correlation analysis between the percent change in brachial artery diameter caused by reactive hyperemia and inflammatory biomarkers in survivors of COVID-19.

	correlation coefficient	*p*-value
High-sensitivity CRP	r = −0.152	0.086
Interleukin-1β	r = −0.186	0.036
Interleukin-2R	r = −0.177	0.046
Interleukin-6	r = −0.167	0.060
Interleukin-8	r = −0.159	0.074
Interleukin-10	r = −0.075	0.399
Tumor necrosis factor -α	r = −0.237	0.007

NA, not applicable; CRP, C-reactive protein; TNF, tumor necrosis factor.

acute SARS-CoV-2 infection, the overwhelming inflammation mediated by TNF-α leads to the systematic injury of endothelial cells, and subsequent endothelial dysfunction remains even after the inflammation subsides (27, 28). The chronic low-grade inflammation indicated by the increased percentage of elevated TNF-α and the elevated concentration of hsCRP in survivors of COVID-19 might partially explain the reduced FMD even nearly 1year after diagnosis. Our findings are consistent with data from previous long-term follow-up studies of Kawasaki disease. Kawasaki disease is characterized by an acute systemic vasculitis that affects infants and young children. Japanese researchers found that the adult patients with history of Kawasaki disease had reduced brachial artery FMD even 24 years after the acute phase of the disease (29). The long-term clinical implication of endothelial dysfunction found in our study is unclear. However, it is well-known that functional arterial changes precede structural abnormalities in atherosclerosis, and endothelial dysfunction is an early event in the pathogenesis of atherosclerosis (30, 31). Thus, the endothelial dysfunction observed in patients with COVID-19 from our cohort and previous studies raises a concern for an increased risk for atherosclerosis in convalescents. Except for the traditional established risk factors for atherosclerosis, such as age, smoking, hyperlipidemia, and hypertension, viral infection has been supposed to be a potential implication in atherosclerosis (32). Endothelial dysfunction emerges as a common mechanism underlying the increased risk of atherosclerosis in people infected with human immunodeficiency virus, hepatitis C virus, and influenza A virus (33–35). Based on the above findings, endothelial dysfunction caused by SARS-CoV-2 becomes a reasonable risk factor in the development of atherosclerosis in survivors of COVID-19. Therefore, prospective longitudinal studies on the association of endothelial dysfunction with long-term cardiovascular outcomes, especially the early onset of atherosclerosis, are warranted in survivors of COVID-19.

There are some limitations in this study. First, no data on FMD values before infection and values at the acute stage of illness were available, which makes the longitudinal comparison of FMD impossible. Second, our study comprised a small sample size of survivors of COVID-19, which limited the generalization of the study conclusion. Third, endothelial function is influenced by multiple factors and, sometimes, it is difficult to distinguish the physiological and pathological arteriosclerosis before any atherosclerotic plaque forms. In our study, COVID-19 was indicated as a potential risk factor rather than an identified pathogenic factor of atherosclerosis. Fourth, hsCRP and cytokines tested in our study could not fully delineate the systemic inflammation. Therefore, a comprehensive long-term follow-up study with larger population is necessary to confirm the impairment of endothelial function and to elucidate its association with SARS-CoV-2 infection.

CONCLUSION

This study shows that survivors of COVID-19 have reduced brachial artery FMD that is inversely correlated with concentration of TNF-α after 327 days from diagnosis. Considering the fact that endothelial dysfunction is an early event in the pathogenesis of atherosclerosis, prospective studies on the association of endothelial dysfunction with long-term cardiovascular outcomes, especially the early onset of atherosclerosis, are warranted in survivors of COVID-19.

DATA AVAILABILITY STATEMENT

The raw data supporting the conclusions of this article will be made available by the authors, without undue reservation.

ETHICS STATEMENT

The studies involving human participants were reviewed and approved by Tongji Hospital Ethics Committee. The patients/participants provided their written informed consent to participate in this study.

AUTHOR CONTRIBUTIONS

Y-BD, Y-NL, X-JB, H-YL, and YZ conceived and designed the study. Y-PG, WZ, P-NH, X-QC, W-HZ, Y-NL, and Y-BD collected clinical and ultrasonographical data. Y-PG, WZ, LL, Q-YT, JZ, and JS performed statistical analysis and interpretation of data for the work. Y-PG, WZ, and Y-BD wrote the manuscript. All authors approved the manuscript.

ACKNOWLEDGMENTS

The authors would like to thank clinical staffs of the Department of Laboratory Medicine, Tongji Hospital, Huazhong University of Science and Technology for their help in laboratory tests. We also appreciate the dedicated efforts of our colleagues in COVID-19 treatment.

REFERENCES

1. Fauci AS, Lane HC, Redfield RR. COVID-19 - navigating the uncharted. *N Engl J Med.* (2020) 382:1268–9. doi: 10.1056/NEJMe2002387
2. Wang D, Hu B, Hu C, Zhu F, Liu X, Zhang J, et al. Clinical characteristics of 138 hospitalized patients with 2019 novel coronavirus-infected pneumonia in Wuhan, China. *JAMA.* (2020) 323:1061–9. doi: 10.1001/jama.2020.1585
3. Ferrario CM, Jessup J, Chappell MC, Averill DB, Brosnihan KB, Tallant EA, et al. Effect of angiotensin-converting enzyme inhibition and angiotensin II receptor blockers on cardiac angiotensin-converting enzyme 2. *Circulation.* (2005) 111:2605–10. doi: 10.1161/CIRCULATIONAHA.104.510461
4. Varga Z, Flammer AJ, Steiger P, Haberecker M, Andermatt R, Zinkernagel AS, et al. Endothelial cell infection and endotheliitis in COVID-19. *Lancet.* (2020) 395:1417–8. doi: 10.1016/S0140-6736(20)30937-5
5. Colmenero I, Santonja C, Alonso-Riano M, Noguera-Morel L, Hernandez-Martin A, Andina D, et al. SARS-CoV-2 endothelial infection causes COVID-19 chilblains: histopathological, immunohistochemical and ultrastructural study of seven paediatric cases. *Br J Dermatol.* (2020) 183:729–37. doi: 10.1111/bjd.19327
6. Ackermann M, Verleden SE, Kuehnel M, Haverich A, Welte T, Laenger F, et al. Pulmonary vascular endothelialitis, thrombosis, and angiogenesis in COVID-19. *N Engl J Med.* (2020) 383:120–8. doi: 10.1056/NEJMoa2015432
7. Escher R, Breakey N, Lammle B. Severe COVID-19 infection associated with endothelial activation. *Thromb Res.* (2020) 190:62. doi: 10.1016/j.thromres.2020.04.014
8. Zhang J, Tecson KM, McCullough PA. Endothelial dysfunction contributes to COVID-19-associated vascular inflammation and coagulopathy. *Rev Cardiovasc Med.* (2020) 21:315–9. doi: 10.31083/j.rcm.2020.03.126
9. Pons S, Fodil S, Azoulay E, Zafrani L. The vascular endothelium: the cornerstone of organ dysfunction in severe SARS-CoV-2 infection. *Crit Care.* (2020) 24:353. doi: 10.1186/s13054-020-03062-7
10. Evans PC, Rainger GE, Mason JC, Guzik TJ, Osto E, Stamataki Z, et al. Endothelial dysfunction in COVID-19: a position paper of the ESC working group for atherosclerosis and vascular biology, and the ESC council of basic cardiovascular science. *Cardiovasc Res.* (2020) 116:2177–84. doi: 10.1093/cvr/cvaa230
11. Ambrosino P, Molino A, Calcaterra I, Formisano R, Stufano S, Spedicato GA, et al. Clinical assessment of endothelial function in convalescent COVID-19 patients undergoing multidisciplinary pulmonary rehabilitation. *Biomedicines.* (2021) 9:614. doi: 10.3390/biomedicines9060614
12. Ratchford SM, Stickford JL, Province VM, Stute N, Augenreich MA, Koontz LK, et al. Vascular alterations among young adults with SARS-CoV-2. *Am J Physiol Heart Circ Physiol.* (2021) 320:H404–10. doi: 10.1152/ajpheart.00897.2020
13. Riou M, Oulehri W, Momas C, Rouyer O, Lebourg F, Meyer A, et al. Reduced flow-mediated dilatation is not related to COVID-19 severity three months after hospitalization for SARS-CoV-2 infection. *J Clin Med.* (2021) 10:1318. doi: 10.3390/jcm10061318
14. Ergul E, Yilmaz AS, Ogutveren MM, Emlek N, Kostakoglu U, Cetin M, et al. 19 Disease independently predicted endothelial dysfunction measured by flow-mediated dilatation. *Int J Cardiovasc Imaging.* (2021). doi: 10.21203/rs.3.rs-438168/v1
15. Lambadiari V, Mitrakou A, Kountouri A, Thymis J, Katogiannis K, Korakas E, et al. Association of COVID-19 with impaired endothelial glycocalyx, vascular function and myocardial deformation 4 months after infection. *Eur J Heart Fail.* (2021) 23:1916–26. doi: 10.1002/ejhf.2326
16. National Health Commission of the People's Republic of China. *Diagnosis and Treatment Protocol of Novel Coronavirus (Trial Version 7th).* (2020). Available online at: http://www.nhc.gov.cn/yzygj/s7653p/202003/46c9294a7dfe4cef80dc7f5912eb1989.shtml (accessed March 4, 2020).
17. Thijssen DHJ, Bruno RM, van Mil A, Holder SM, Faita F, Greyling A, et al. Expert consensus and evidence-based recommendations for the assessment of flow-mediated dilation in humans. *Eur Heart J.* (2019) 40:2534–47. doi: 10.1093/eurheartj/ehz350
18. Wang YB, Li Y, Deng YB, Liu YN, Zhang J, Sun J, et al. Enlarged size and impaired elastic properties of the ascending aorta are associated with endothelial dysfunction and elevated plasma matrix metalloproteinase-2 level in patients with bicuspid aortic valve. *Ultrasound Med Biol.* (2018) 44:955–62. doi: 10.1016/j.ultrasmedbio.2018.01.012
19. Deng YB, Xiang HJ, Chang Q, Li CL. Evaluation by high-resolution ultrasonography of endothelial function in brachial artery after Kawasaki disease and the effects of intravenous administration of vitamin C. *Circ J.* (2002) 66:908–12. doi: 10.1253/circj.66.908
20. Oliveira MR, Back GD, da Luz Goulart C, Domingos BC, Arena R, Borghi-Silva A. Endothelial function provides early prognostic information in patients with COVID-19: A cohort study. *Respir Med.* (2021) 185:106469. doi: 10.1016/j.rmed.2021.106469
21. Ambrosino P, Calcaterra I, Molino A, Moretta P, Lupoli R, Spedicato GA, et al. Persistent endothelial dysfunction in post-acute COVID-19 syndrome: a case-control study. *Biomedicines.* (2021) 9:957. doi: 10.3390/biomedicines9080957
22. Chen G, Wu D, Guo W, Cao Y, Huang D, Wang H, et al. Clinical and immunological features of severe and moderate coronavirus disease 2019. *J Clin Invest.* (2020) 130:2620–9. doi: 10.1172/JCI137244
23. Del Valle DM, Kim-Schulze S, Huang HH, Beckmann ND, Nirenberg S, Wang B, et al. An inflammatory cytokine signature predicts COVID-19 severity and survival. *Nat Med.* (2020) 26:1636–43. doi: 10.1038/s41591-020-1051-9
24. Spillmann F, Van Linthout S, Miteva K, Lorenz M, Stangl V, Schultheiss HP, et al. LXR agonism improves TNF-alpha-induced endothelial dysfunction in the absence of its cholesterol-modulating effects. *Atherosclerosis.* (2014) 232:1–9. doi: 10.1016/j.atherosclerosis.2013.10.001
25. Katz SD, Rao R, Berman JW, Schwarz M, Demopoulos L, Bijou R, et al. Pathophysiological correlates of increased serum tumor necrosis factor in patients with congestive heart failure. Relation to nitric oxide-dependent vasodilation in the forearm circulation. *Circulation.* (1994) 90:12–6. doi: 10.1161/01.CIR.90.1.12
26. Yan G, You B, Chen SP, Liao JK, Sun J. Tumor necrosis factor-alpha downregulates endothelial nitric oxide synthase mRNA stability via translation elongation factor 1-alpha 1. *Circ Res.* (2008) 103:591–7. doi: 10.1161/CIRCRESAHA.108.173963
27. Zeng Z, Yu H, Chen H, Qi W, Chen L, Chen G, et al. Longitudinal changes of inflammatory parameters and their correlation with disease severity and outcomes in patients with COVID-19 from Wuhan, China. *Crit Care.* (2020) 24:525. doi: 10.1186/s13054-020-03255-0
28. Feldmann M, Maini RN, Woody JN, Holgate ST, Winter G, Rowland M, et al. Trials of anti-tumour necrosis factor therapy for COVID-19 are urgently needed. *Lancet.* (2020) 395:1407–9. doi: 10.1016/S0140-6736(20)30858-8
29. Niboshi A, Hamaoka K, Sakata K, Yamaguchi N. Endothelial dysfunction in adult patients with a history of Kawasaki disease. *Eur J Pediatr.* (2008) 167:189–96. doi: 10.1007/s00431-007-0452-9
30. Ross R. Atherosclerosis–an inflammatory disease. *N Engl J Med.* (1999) 340:115–26. doi: 10.1056/NEJM199901143400207
31. Davignon J, Ganz P. Role of endothelial dysfunction in atherosclerosis. *Circulation.* (2004) 109:III27–32. doi: 10.1161/01.CIR.0000131515.03336.f8
32. Liu Y, Zhang HG. Vigilance on new-onset atherosclerosis following SARS-CoV-2 infection. *Front Med.* (2020) 7:629413. doi: 10.3389/fmed.2020.629413
33. Anand AR, Rachel G, Parthasarathy D. HIV proteins and endothelial dysfunction: Implications in cardiovascular disease. *Front Cardiovasc Med.* (2018) 5:185. doi: 10.3389/fcvm.2018.00185
34. Adinolfi LE, Restivo L, Zampino R, Guerrera B, Lonardo A, Ruggiero L, et al. Chronic HCV infection is a risk of atherosclerosis. Role of hcv and hcv-related steatosis. *Atherosclerosis.* (2012) 221:496–502. doi: 10.1016/j.atherosclerosis.2012.01.051
35. Campbell LA, Rosenfeld ME. Infection and atherosclerosis development. *Arch Med Res.* (2015) 46:339–50. doi: 10.1016/j.arcmed.2015.05.006

Conflict of Interest: The authors declare that the research was conducted in the absence of any commercial or financial relationships that could be construed as a potential conflict of interest.

frontiers | Frontiers in Medicine

REVIEW
published: 03 June 2022
doi: 10.3389/fmed.2022.907992

Endothelial Activation and Microcirculatory Disorders in Sepsis

Lisa Raia[1] *and Lara Zafrani*[1,2]*

[1] Medical Intensive Care Unit, Hôpital Saint-Louis, Assistance Publique des Hôpitaux de Paris, Paris, France, [2] INSERM UMR 976, University of Paris Cité, Paris, France

The vascular endothelium is crucial for the maintenance of vascular homeostasis. Moreover, in sepsis, endothelial cells can acquire new properties and actively participate in the host's response. If endothelial activation is mostly necessary and efficient in eliminating a pathogen, an exaggerated and maladaptive reaction leads to severe microcirculatory damage. The microcirculatory disorders in sepsis are well known to be associated with poor outcome. Better recognition of microcirculatory alteration is therefore essential to identify patients with the worse outcomes and to guide therapeutic interventions. In this review, we will discuss the main features of endothelial activation and dysfunction in sepsis, its assessment at the bedside, and the main advances in microcirculatory resuscitation.

Keywords: endothelial dysfunction, sepsis, microcirculation, organ failure, peripheral perfusion, endothelium

OPEN ACCESS

Edited by:
W. Conrad Liles, University of Washington, United States

Reviewed by:
Takashi Ito, Kumamoto University, Japan
Sakir Akin, Haga Hospital, Netherlands

***Correspondence:**
Lara Zafrani
lara.zafrani@aphp.fr

Specialty section:
This article was submitted to Intensive Care Medicine and Anesthesiology, a section of the journal Frontiers in Medicine

Received: *30 March 2022*
Accepted: *16 May 2022*
Published: *03 June 2022*

Citation:
Raia L and Zafrani L (2022) Endothelial Activation and Microcirculatory Disorders in Sepsis. Front. Med. 9:907992. doi: 10.3389/fmed.2022.907992

INTRODUCTION

Sepsis is a life-threatening condition defined by multi-organ dysfunction secondary to a dysregulated host response to infection (1). Incidence of sepsis represents one of the leading causes of hospitalization in the Intensive Care Unit (ICU) and mortality remains high despite several improvements in early resuscitation (2).

The vascular endothelium consists of a single cell layer at the interface of the circulating blood and vessel wall. Composed of about 10^{13} cells representing 1.5 kg, the endothelium maintains microvascular homeostasis, regulating vascular tone, primary hemostasis, and cellular traffic. By its privileged localization, the vascular endothelium plays a crucial role in the response to infection. However, the exaggerated host response can cause structural and functional endothelial damage. Thus, most endothelial functions are disrupted in sepsis, leading to microthrombi, tissue edema, interstitial leakage, and dysregulated vascular tone.

Experimental and clinical studies have evidenced microcirculatory abnormalities in sepsis, which are strongly associated with organ dysfunction and mortality (3). The correction of systemic hemodynamic variables fails to restore microcirculatory perfusion and suggests a need for new axes and new therapeutics.

In this review we will discuss the key role of the endothelium in the microvascular response to sepsis.

VASCULAR ENDOTHELIUM

Structure

The vascular endothelium, comprising a cell monolayer, covers the interior surface of blood vessels all along the vasculature. About 10^13 endothelial cells (ECs), covering 1000 m^2, provide a direct interface between the circulating blood cells and the vessel wall. ECs share common properties

but are also heterogeneous according to specific organs and vascular beds, both concerning their structure and their function (4). This also implies distinct responses to pathological conditions with various structural and functional modifications.

At their surface, ECs are covered by a multicomponent layer, the glycocalyx, consisting of proteoglycans, glycoprotein, and glycosaminoglycans (5).The glycocalyx constitutes a first-line barrier which provides the regulation of cellular and molecular traffic. In addition, because of its negative electrical charge, the glycocalyx acts as an anticoagulant layer. The glycocalyx participates in vascular homeostasis as a vascular barrier, powerful antioxidant, and transducer of shear stress to the endothelium (6).

Regarding its weight and its numerous functions, the endothelium should be considered as a fully-fledged organ.

Resting Endothelium

The integrity of ECs is a chief regulator of vascular homeostasis. The vascular endothelium has a fundamental role in several physiologic processes such as vasomotor tone regulation, primary hemostasis, osmotic balance, and vascular barrier function. ECs also perform important immunologic functions. By sensing pathogen components present in blood, ECs can initiate the immune response. ECs are also conditional antigen-presenting cells (APCs) and, in some specific situations, allow the initiation of adaptive immunity (7). In normal conditions, ECs do not interact with circulation leukocytes, mainly because of the glycocalyx barrier and internalized membrane adhesion molecules.

Primary hemostasis is the process in which platelets adhere, activate, and aggregate to restore vascular integrity after an aggression. The endothelium synthesizes and expresses key hemostasis regulating factors, such as the von Willebrand factor (vWF) and tissue factor (TF). When the endothelium is damaged, the vWF is exposed to the circulation and can initiate platelet recruitment to the lesion. Then, binding to glycoproteins GPIa, GPVI, GPIb-IX-V, platelets activate and can enhance recruitment and activation of circulating platelets in order to form a clot.

At rest, the endothelium has anticoagulant and profibrinolytic properties. While the endothelium is one of the main producers of TF, it also negatively regulates the TF pathway, producing the TF pathway inhibitor (TFPI). TFPI limits thrombin generation, binding to activated factor X and inhibiting aFVII complex. In addition, ECs are responsible for thrombomodulin (TM) production and release. TM, combined with endothelial protein C receptor (EPCR), regulates activated protein C, which inhibits factor V, factor VIII, and Plasminogen activation inhibitor (PAI-1). Beside its role of co-factor, TM has its own anticoagulant properties. ECs also express and release tissue plasminogen activator (t-PA), the main initiator of fibrinolysis.

The endothelium is the main regulator of the vasomotor tone *via* its capacity to produce and release vasoactive substances in response to several environment signals. Nitric oxide (NO) is the most important vasodilator agent and is constitutively produced by ECs. NO is generated by the endothelial nitric oxide synthase (eNOS) and derived from L-arginine. NO is constitutively released by ECs and eNOS is induced by chemical (ADP, bradykinin) or physical (shear stress) factors to adapt blood flow to various conditions. Then, NO applies its vasodilatory function, diffusing in vascular smooth cells to activate cyclic GMP production by guanylate cyclase. Moreover, besides its vasoactive action, NO possesses many other biological properties (e.g., anti-agregant, endothelial cell growth) contributing to vascular homeostasis.

ENDOTHELIUM IN SEPSIS

Because of their privileged contact with circulating blood, ECs are the first to interact with the microbial component and act as a "sentinel" for circulating micro-organisms. Moreover, the vascular endothelium is very sensitive to various stimulating factors that induce different phenotypes and initiate the immune response to infection.

ECs express Toll-like receptors (TLRs), surface receptors recognizing a pathogen antigen, such as Pathogen-Associated Molecular Patterns (PAMPs) and Damage-Associated Molecular Patterns (DAMPs). Some TLRs are ubiquitous whereas others depend on organs or are expressed under specific circumstances. Moreover, TLR expression and signalization can be modulated by inflammatory cytokines (8). ECs predominantly express TLR4, which is the main receptor for lipopolysaccharide (LPS), a Gram-negative bacteria molecule. However, TLR2 expression might also be triggered by inflammatory conditions. This recognition initiates intracellular signalization, resulting in expression of proinflammatory transcription factors such as Nuclear factor of the k-chain in B cells (NF-kB) (9).

Endothelial Activation

During sepsis, activated ECs recruit immune cells (leukocytes) at the site of infection to eliminate the micro-organism and limit the spread of infection.

Proinflammatory Phenotype

NF-kB is a ubiquitous transcription factor involved in all major inflammatory reactions. It is implicated in cytokine production, molecule expression, cell survival, and differentiation (10). NF-kB activity can be induced in ECs by several stimuli,

Abbreviations: Ang/Tie2, Angiopoietin-1/Tie2 receptor; APC, Antigen-presenting cell; AT, Antithrombin; CLP, Cecal ligation and puncture; CRT, Capillary refill time; DAMPs, Damage-Associated Molecular Patterns; ECs, Endothelial cells; EPCR, Endothelial protein C receptor; GLUT 1, Glucose transporter; HIF, Hypoxia inducible factor; ICU, Intensive Care Unit; IDF, Incident dark field imaging; IL-1, Interleukin; iNOS, Inducible NO synthase; LPS, Lipopolysaccharide; MPs, Microparticles; NF-kB, Nuclear factor of the k-chain in B-cells; NIRS, Near infrared spectroscopy; NO, Nitric oxide; eNOS, Endothelial nitric oxide synthase; OPS, Orthogonal polarization spectral imaging; O2, Oxygen; PAI-1, Plasminogen activation inhibitor 1; PAMPs, Pathogen-Associated Molecular Patterns; PECAM, Platelet endothelial cell adhesion molecule; PI, Pulsatility index; PO2, Partial oxygen pressure; SDF, Sidestream dark field; SOFA, Sequential Organ Failure Assessment; StO2, Tissular oxygen saturation; t-PA, Tissue plasminogen activator; TF, Tissue factor; TFPI, Tissue factor pathway inhibitor; TLR, Toll-like receptor; TM, Thrombomodulin; TNF-α, Tumor necrosis factor; VCAM, Vascular adhesion molecule; vWF, Von Willebrand factor.

including inflammatory cytokines [Tumor necrosis factor (TNFα), Interleukin (IL-1)], and microbial components (LPS). Moreover, inhibiting NF-kB activity in mice stimulated by LPS led to decreased tissue neutrophilic infiltration and damage, suggesting its central role in sepsis (11).

During infection, ECs reprogram toward a proinflammatory and secretory phenotype. Numerous proteins produced by ECs are stocked in intracellular vesicles, the Weibel-Palade bodies. Under stimulation, ECs degranulate and release the content of these bodies (TF, P-selectin, vWF, angiopoietin-2) into the vasculature. ECs may then produce and release proinflammatory cytokines (IL-6) in the circulation, amplifying and spreading the inflammatory response in order to recruit immune cells at the infected site.

Pro-adhesive Phenotype

Activated endothelium and shedding of the glycocalyx in septic conditions lead to increased membrane expression of adhesion molecules that mediate leukocyte trafficking and recruitment to the area of infection. First, the selectins (E- and L-selectin) orchestrate the first phase of contact, rolling between circulating leukocytes and the endothelium. Then, prolonged and firm adhesion depends on immunoglobulin molecules, intercellular adhesion molecules (ICAM-1, ICAM-2), and the vascular adhesion molecule (VCAM). Finally, trans endothelial migration involves disruption of the tight junction and platelet endothelial cell adhesion molecule (PECAM). The final goal of this process is the diapedesis of leukocytes and extravasation into the tissues. The infiltration of immune cells in infected tissues is crucial to eliminate the pathogen. In experimental studies, LPS-exposed ECs expressed ICAM-1 and E-selectin mRNA, and blocking proinflammatory cytokines resulted in inhibition of mRNA transcription of adhesion molecules (12). Moreover, ECs release adhesion molecules in the circulation. E-selectin (13) and ICAM1 (14) plasma levels have been found to be increased in septic patients. The soluble circulating form of the adhesion molecules are increased in septic patients compared to patients admitted for a trauma (15), and the plasma levels of these adhesion molecules are closely related to sepsis severity (16).

Procoagulant Phenotype

In sepsis, ECs acquire procoagulant and antifibrinolytic properties which help to prevent dissemination of infection. Either expressed by activated immune cells or released from Webel-Palade bodies, TF level is increased in septic conditions. TF then initiates the coagulation cascade. In parallel, anticoagulant proteins [protein C, TFPI (17), TM] are downregulated by increased consumption and decreased production. Endothelial TM expression is decreased in sepsis and inactivated by leukocyte elastase release, limiting protein C activation. Skin biopsies of patients with purpura fulminans revealed a decreased expression of endothelial TM and ECPR in parallel with low blood levels of protein C, protein S and antithrombin (AT) (18). Moreover, decreased circulating activated protein C in neutropenic septic patients was associated with disease severity (19). In addition, the endothelium releases large amounts of PAI-1 when stimulated by IL-1 and TNF-α, resulting in an antifibrinolytic condition (20).

In addition, degradation of glycocalyx and EC apoptosis induce the release of large amounts of vWF. This permits the recruitment and aggregation of platelets at the infected site.

Endothelium activation is therefore an appropriate and necessary response of the host to an acute infection. Thus, this microcirculatory response (leukocyte recruitment, coagulation) is adaptive and often successful in localizing and eliminating infectious insults (21). However, in extreme cases of overwhelming infection, these processes may contribute to overall morbidity, organ failure, and death. The challenge is in the balance between the adaptative immune response and endothelial activation to control the infectious process and excessive and maladaptive response. Moreover, this is a dynamic process and an adaptative response at one timepoint can become deleterious at another (**Figure 1**).

Microvascular Endothelial Dysfunction

Endothelial dysfunction is defined by the loss of or exaggerated endothelial function.

The uncontrolled amplification of the host's proinflammatory response can lead to septic shock and the failure of distant, non-infected organs.

Structural Damage/Increased Permeability

In animal models of sepsis, ECs experienced morphological changes, including nuclear and cytoplasm lesion, rupture of cells, and even apoptosis. These kinds of damage have been confirmed in septic patients who demonstrate an increased number of circulating ECs and apoptotic bodies (22).

During sepsis, the damaged glycocalyx exposes a denuded endothelium. In an endotoxemic mouse model, the authors revealed pulmonary microvascular glycocalyx degradation related to TNF-alpha and heparinase. Interestingly, in this experimental study, inhibiting heparinase maintained glycocalyx integrity and reduced neutrophil adhesion and tissue damage (23). There are several consequences for the microcirculation following glycocalyx degradation, including decreased capillary density and increased permeability of macromolecules, although there are no macrohemodynamic changes (24).

In septic patients, glycocalyx impairment can be evidenced by the presence of glycocalyx shedding components in the circulation. The levels of circulating serum hyaluronan and syndecan are associated with the prognosis of septic patients (25). Moreover, new techniques can evaluate glycocalyx thickness in sublingual microcirculation. The decreased microvascular glycocalyx thickness in sepsis is correlated to microcirculation perfusion (26) and is an early predictor of mortality (27).

In addition, several pathways, like the Angiopoietin/Tie-2 (Ang/Tie2) axis, are altered during sepsis. Ang/Tie2 signaling is critical for maintaining vascular barrier integrity. During sepsis, the Ang/Tie2 system is disrupted, leading to increased microvascular permeability which contributes to organ failure and death (28). Moreover, the neutrophilic accumulation may enhance tissue and cell damage by generating inflammatory cytokines, reactive oxygen, and proteases (29).

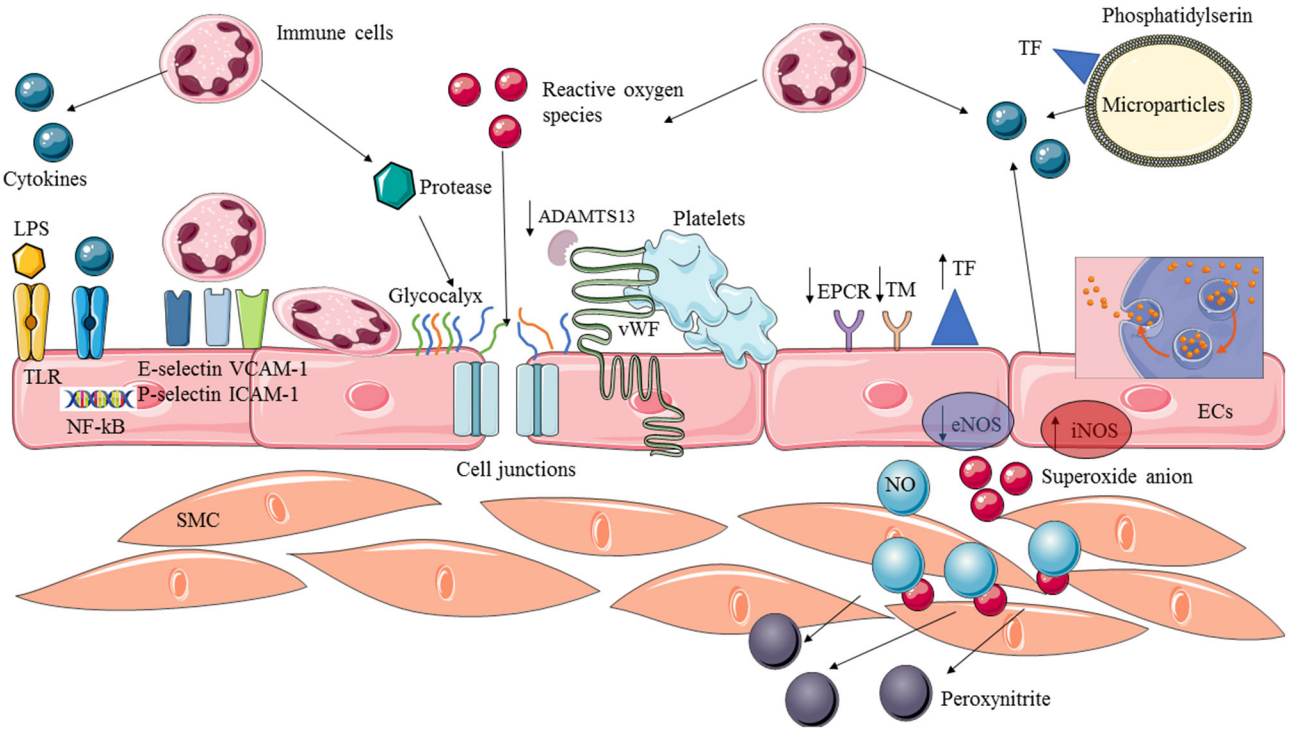

FIGURE 1 | Endothelial activation and dysfunction in sepsis. Endothelial cells are provided with membrane receptors (ex:TLRs) and can be activated by various stimuli factors such as microbial components (LPS) or pro-inflammatory cytokines. The recognition of circulating stimuli leads to the activation of NF-kB transcription factor allowing expression of adhesion molecules and switch to a pro-inflammatory and pro-coagulant phenotype. Circulating leukocytes are recruited, adhere to the endothelium and extravasate into the tissue. Pro-coagulant protein are overexpressed whereas anticoagulant and profibrinolytic proteins are downregulated. Cytokines, ROS and protease released by activated immune cells can cause structural damage, leading to an increased permeability and exposition of endothelial-derived proteins. Vasoreactivity is impaired by (1) decreased production of NO by the eNOS, and (2) complexed available NO with superoxide anion to produce peroxynitrite. Moreover, ECs play a crucial role in spreading the inflammatory reaction which, in turn, produces cytokines and free radicals, and the release of microparticles. ADAMTS13, A disintegrin and metalloprotease with thrombospondin type I repeats-13; ECs, Endothelial cells; SMC, Smooth muscular cells; TF, Tissue factor; TM, Thrombomodulin; EPCR, Endothelial protein C receptor; vWF, Von Willebrand factor; LPS, Lipopolysaccharide; TLR, Toll like receptor; eNOS, Endothelial nitric oxide synthase; iNOS, Inducible nitric oxide synthase; NO, Nitric oxide; ICAM, Intercellular adhesion molecules; VCAM, Vascular cells adhesion molecules; NF-kB, Nuclear factor of k-chain of B.

All together, these structural damages imply disrupted barrier function and increased permeability, leading to interstitial leakage and edema. Moreover, the denuded endothelium and apoptotic ECs display a proinflammatory and procoagulant phenotype, enhancing the systemic response to infection. Furthermore, leukocyte adherence to the endothelium may participate in microvascular blood flow alterations (30).

Impaired Vasoreactivity

Microvascular endothelium is the chief regulator of vascular tone, mainly through the production of NO, a vasoactive soluble gas. During sepsis, NO production is dysregulated, with various changes depending on the course of the disease, leading to an impaired endothelium-dependent vasorelaxation and ultimately an alteration of microvascular blood flow.

First, there is a decreased production of NO by endothelial NO synthase, precipitating so-called "nitrosopenia". The causes are multifactorial, with the downregulated expression of eNOS mRNA (31), a modified membrane receptor, and impaired signal transduction (32). Moreover, septic ECs are depleted of tetrahydrobiopterin, the limiting substrate for eNOS, uncoupling the enzyme and resulting in production of superoxide anion instead of NO.

The inducible NO synthase (iNOS) is also increased during sepsis (33). iNOS produces large amounts of NO, about 1,000-fold more than eNOS, and is responsible for intense and diffuse microvascular vasodilatation. This effect can cause an impaired response to norepinephrine. Moreover, the overproduced NO can complex with oxygen reactive species (superoxide anion) to generate peroxynitrite, a highly cytotoxic oxidant product. The rapid formation of peroxynitrite in an oxidative environment leads to reduced NO availability.

Overall, sepsis is characterized by a decrease of NO bioavailability and impaired vasoreactivity. Moreover, besides its effects on vascular tone, the lack of NO also results in dysregulated platelet adhesion and endothelium integrity. However, the pathophysiology of NO in sepsis is not fully understood as showed by the controversial therapeutic interventions targeting NO.

Oxidative Stress

Large amounts of reactive species are produced during sepsis, causing structural and cellular damage (41). There is an imbalance in the production of reactive species and a decrease in antioxidant agents. Firstly, oxidative species are produced in large amounts by inflammatory cells (42) and play a role in cell adhesion and inflammatory reaction (43). Besides being a target, ECs also produce and release reactive species (superoxide anion, hydrogen peroxide, radical hydroxyl) in sepsis through the NADPH pathway (44).

Inside cells, the accumulation of reactive species in the form of hydrogen peroxide and peroxynitrite causes protein and DNA damage, contributing to endothelial dysfunction (45). Moreover, besides complexing the NO to generate highly unstable peroxynitrite, oxidant agents induce uncoupling of eNOS (46), thus creating a vicious circle and amplifying oxidative stress (47). Overall, this results in decreased NO bioavailability. On the other hand, reactive oxygen and nitrogen species can enhance NF-kB activation and thus endothelial activation (48).

Microthrombi

Dysfunctional endothelium activates primary hemostasis and coagulation in a supra-physiologic way by decreased anticoagulant signaling. Generalized activation of coagulation during sepsis may enhance widespread microvascular injury (49, 50).

Autopsy studies of patients who died from *Streptococcus suis* infection found multiple microthrombi in the capillaries of the lung, kidney, and intestine (51). Several post-mortem studies have confirmed disseminated microthrombosis in the kidney, liver, brain, and gut microcirculation of septic patients (52).

Therefore, a new pathogenic entity in sepsis was defined as "endotheliopathy-associated vascular microthrombotic disease" involving microthrombosis mainly through unusually large vWF multimers (53). Indeed, sepsis may lead to acquired a disintegrin and metalloprotease with thrombospondin type I repeats-13 (ADAMTS13) deficiency since inflammatory mediators can inactivate ADAMTS13. ADAMTS13 is a metalloproteinase that cleaves the multimers of vWF in order to limit platelet activation in physiological conditions. Sepsis results in overexpressed vWF from ECs and a decreased availability of ADAMTS13. Then, large multimers of vWF recruit circulating platelets, thereby contributing to platelet-endothelium interactions (54, 55).

In parallel to leukocyte adherence to the endothelium (30), the presence of disseminated microthrombosis may participate in alterations to the microvascular blood flow (56). Platelet-to-endothelium adhesion is associated with stopped-flow capillaries and the inhibiting adhesion process may lead to an improved microvascular blood flow (57).

Microparticles

Microparticles (MPs) are small vesicles derived from activated or apoptotic cells which are released into the circulation with the detachment of cell membrane. MPs are embedded with various surface antigens. In physiological conditions, microparticles are essential to intercellular traffic and act as messengers. In response to an inflammatory environment, ECs release microparticles that can activate coagulation, amplifying the inflammatory and procoagulant response and dispersing it away from the initial site of infection. In sepsis, MPs express proinflammatory and procoagulant mediators. Endothelium-derived MPs expose phosphatidylserine at their surface, providing a privileged site to initiate coagulation cascade (58). Moreover, MPs express high levels of TF, which contribute to coagulation activation (59).

Delabranche and co-authors have suggested that circulating levels of endothelium-derived MPs in the plasma of septic patients may be a good predicting factor of outcome (60).

MICROCIRCULATION IN SEPSIS

The microcirculation, composed of a series of <100 micron-diameter arterioles, venules and capillaries, is the terminus of the vascular tree (61). Arterioles mostly guarantee vascular tone because of their muscular surface, whereas capillaries provide oxygen delivery, nutriments, and solute exchange depending on the tissue need (61).

Sepsis is associated with profound changes in microcirculation (62).

Microcirculatory Disorders

Microcirculatory alterations in sepsis mainly consist of a decreased capillary density and an increased heterogeneity of blood flow. As compared to hemorrhagic shock, endotoxemic shock leads to considerably greater impaired gut microvascular perfusion (63). During sepsis, microcirculation suffers from quantitative and qualitative alterations.

Firstly, sepsis is associated with a decrease in functional capillary density and a reduction in the proportion of perfused small vessels, whereas stopped and intermittently perfused capillaries are increased (64, 65). Altered capillary density has been observed in gut (64), brain (65), skin, and tongue (66) microcirculation in various septic animal models.

Sepsis-associated microcirculatory dysfunction is responsible for suboptimal capillary perfusion, resulting in impaired oxygen extraction by tissues, a finding which is not explained by impaired delivery of oxygen by systemic circulation (67). It has been shown that muscular microcirculation in a cecal ligation and puncture (CLP) rat model heterogeneously delivers oxygen to capillaries (68). Heterogeneous perfusion is defined by the presence of intermittently or non-perfused capillaries close to well perfused capillaries, and this process is dynamic over time. Minimal under physiological conditions, the heterogeneity of perfusion is highly increased in sepsis. Thus, heterogeneous perfusion exists between organs, with redistribution of blood flow to vital organs at the expense of other tissues, but it is also present within the same organ. Experimental studies evidenced microvascular shunting in sepsis, especially in the gut, creating local zones of hypoxia (69, 70). One of the main features of microvascular shunting can be attributed to the heterogeneity of perfusion (71).

The gut and splanchnic circulation represents an elective measurement site because of its early impairment in sepsis. Experimental studies provided evidence that the disturbance in oxygen extraction was related to the heterogeneity of microcirculatory perfusion. Heterogeneous perfusion is

therefore considerably more deleterious than uniformly perfused capillaries regarding tissue oxygen extraction (72).

This heterogeneous perfusion also implies different expression of key proteins, enzymes, and molecules, which are increased during sepsis. For example, in endotoxemia rats, iNOS is differently expressed along the gut tractus, suggesting that the vasomotor tone within the gut is different (73). This observation has been confirmed in a sheep sepsis model in which animals were treated with iNOS inhibitors resulting in various microvascular blood flow responses in the gut, pancreas, and spleen (74).

Together, the decreased capillary density and heterogeneous alterations in microcirculation contribute to an increased diffusion distance for oxygen and an impaired extraction capacity, thus creating hypoxic zones. Heterogeneous expression of hypoxic genes within myocardial microcirculation has been demonstrated in a murine model of sepsis. Indeed, during entoxemia, Hypoxia inducible factor (HIF)-1a and Glucose transporter (GLUT)1 expression co-existed with ICAM-1 expression in malfunctioning capillaries, suggesting that microcirculatory alterations were associated with hypoxic zones (75).

ASSOCIATION BETWEEN MICROVASCULAR DYSFUNCTION AND OUTCOME

Hemodynamic coherence is the hypothesis that normalization of systemic variables will be accompanied by improvement of microcirculatory perfusion in resuscitated patients (76). In experimental studies, microcirculatory disorders poorly correlate with systemic variables. Several authors have highlighted the loss of hemodynamic coherence in critically ill patients, especially in sepsis. The resulting consequences are: (1) conventional systemic parameters fail to reflect the state of microcirculation; (2) therapeutic strategies which aim to correct macrohemodynamic parameters are probably ineffective in improving microcirculation.

Knowing that microcirculatory disorders are central to the pathophysiology of sepsis, it is essential to assess their clinical relevance in the course of the disease and in patient outcome. Although macrohemodynamic parameters can be improved with conventional resuscitation interventions, the persistence of microcirculation abnormalities may explain unfavorable outcomes. Several experimental studies have found a correlation between survival and microcirculatory perfusion (77). Moreover, Zhang et al. provided strong evidence that micro- and macrocirculation are dissociated in endotoxemic shock, and that microcirculatory disorders precede the alterations in macrocirculation (78). Sakr and colleagues (3) demonstrated that, with equal baseline alterations, sublingual capillary density increased over the time course of septic shock in survivors, whereas this did not occur in non-survival patients. These microvascular alterations could predict ICU mortality contrary to global hemodynamic parameters. In a pilot observational study, the authors assessed sublingual microvascular perfusion by Sidestream Dark Field (SDF) in the early course of sepsis, with repeated measures during the early goal-directed therapy. They found that an improvement in microcirculatory perfusion during resuscitation was associated with less organ failure (79). Finally, De Backer et al. (80) confirmed the independence of micro- and macrovascular parameters and the strong association of sublingual microcirculatory parameters with outcome.

Although it is difficult to assess a causal relationship in the absence of randomized controlled trials, the development of more accurate techniques allows better identification of prognostic factors. Concordant data found several microcirculatory variables to be independent prognostic factors in sepsis and septic shock. Thus, the loss of hemodynamic coherence, and the association of microcirculatory disorders with outcome, support the extension of microcirculatory assessments and the use of microvascular variables to guide resuscitation.

MICROCIRCULATORY DYSFUNCTION ASSESSMENT

Microcirculatory dysfunction plays a crucial role in the pathophysiology of sepsis. Early recognition of critical illness severity, leading to an early appropriate resuscitation, is essential to improve outcome (1). For a long time, management of critically ill patients has focused on restoring systemic hemodynamic parameters. Indeed, patient monitoring has comprised assessment of macrohemodynamic parameters such as arterial pressure, and both urine and cardiac output. However, in the past few years, it has been shown that classic hemodynamic parameters fail to identify microcirculatory disorders. Beyond classic systemic monitoring, we need specific tools to assess microcirculation dysfunction (**Table 1**).

Microcirculatory Perfusion

Evidence for microcirculatory dysfunction was first found in experimental studies using intravital microscopy, allowing direct visualization of microcirculation with large microscopes on fixed tissues. Bedside assessment of microcirculation in critically ill patients is challenging, as intravital microscopy cannot be used in humans. The main concerns are the site of measurement, the timing (80), and the availability of validated tools. In the past decade, several techniques have been examined in the study of microcirculation.

Microvascular Blood Flow

The Laser Doppler flowmetry technique applies the Doppler effect, in which laser light shifts its frequency after reflecting from red blood cells. Laser Doppler provides a measure of relative microcirculatory blood flow defined by the average of the velocities in vessels in the area of interest. Thus, this technique does not give an absolute value of blood flow but a quantitative index of flux (81).

Laser Doppler flowmetry can be performed in skin, muscle, and mucosal microcirculation. Interestingly, gut mucosal perfusion is accessible to Laser Doppler using specific probes, and is of particular interest in critically ill patients to assess visceral organ perfusion (97).

TABLE 1 | Assessment of microcirculatory disorders in critically ill patients.

Technique	Principle	Site of measure	Variable	Modifications in sepsis	References
Microvascular blood flow					
Laser Doppler	Doppler effect Relative blood flow analysis	Skin, muscle, digestive mucosa	Blood flow (relative units)	Decreased blood flow Decreased reactivity	Eun et al. (81) Neviere et al. (82)
Pulsatility index	Doppler ultrasonography	Visceral organs (kidney, spleen, liver)	PI= (systolic blood flow velocity-minimum diastolic blood flow velocity)/mean blood flow velocity)	PI is increased in septic shock	Brunauer et al. (83)
Videomicroscopy					
Nailfold videomicroscopy	Transillumination Microscope with reflected light	Finger ungual microcirculation	Vascular density	*NA*	Freedlander et al. (84) Weinberg et al. (85)
OPS and SDF Cytocam incident dark field	Direct microvascular visualization Absorption of a selected wavelength by hemoglobin	Sublingual microcirculation	Capillary density, perfused capillary density, functional capillary density, microvascular flow index	Decreased capillary density Increased heterogeneity of perfusion	De Backer et al. (86) Dilken et al. (87) Aykut et al. (88)
Tissue oxygenation					
Near Infrared Spectrometry	Transmitted and reflected light at several wavelengths Different absorption properties of oxy- and deoxyhemoglobin	Muscle Thenar eminence	Tissue oxygen saturation: $StO_2 = (HbO_2)/(HbO_2+Hb)$	Decreased StO_2 Decreased reactivity	Mancini et al. (89) Creteur et al. (90)
PO_2 electrodes	Transcutaneous electrodes that detect oxygen and carbon dioxide	Skin	Tissue PO_2	*NA*	Vesterager (91)
Peripheral tissue perfusion					
Capillary refill time (CRT)	Return to baseline color of a soft tissue after applying a pressure for 15s	Fingertip or knee	Time (in seconds) to baseline return after releasing the pressure	Increased CRT	Ait-Oufella et al. (92) Lima et al. (93)
Mottling	Discoloration of the skin	Knee	Mottling extension	Increased mottling score	Ait-Oufella et al. (94) Ait-Oufella et al. (95)
Temperature gradient	Cutaneous probes to evaluate skin temperature	Skin, toe, finger	Central-to-skin temperature gradient Skin-to-room temperature gradient	High central-to-skin temperature gradient Reduced skin-to-room temperature gradient	Bourcier et al. (96)

NA, not available; OPS, orthogonal polarization spectral imaging technique; O_2, oxygen; PI, Pulsatility index; PO_2, Partial oxygen pressure; SDF, sidestream dark field imaging technique; StO_2, tissue oxygen saturation.

This technique allows continuous microcirculatory blood flow recording and measurement of microvascular blood flow reactivity to various interventions (vascular occlusion test, pharmacologic products) (98). The method is advantageous in critically ill patients as it can be applied to the skin, an easily accessible site. It has been observed that basal blood flow is decreased in critically ill patients as compared to healthy volunteers. Moreover, vascular reactivity is impaired during sepsis (82).

The main limitation of this technique is the relatively large sample volume of analysis (0.5–1 mm^3) in which arterioles, capillaries, and venules of diverse size and perfusion are analyzed within the same timeframe. In sepsis, where perfusion is particularly heterogeneous, even in the same area, this method may miss some perfusion abnormalities.

Pulsatility Index

The pulsatility index (PI) is used to estimate the organ vascular tone rather than to directly assess blood flow. The PI is assessed using a Doppler sonography technique which can explore visceral organs [kidney (99), spleen, liver (100)]. Using color Doppler, an artery of interest is identified and pulse wave Doppler is performed. The resulting blood flow signal is recorded, and PI is calculated as the ratio of systolic blood flow velocity-minimum diastolic blood flow velocity/mean blood flow velocity.

Brunauer and colleagues (83) reported alteration of the PI of the liver, spleen, intestine, and kidney in septic shock patients, which were correlated to peripheral perfusion alterations.

Tissue Oxygenation

Near infrared spectroscopy (NIRS) is a procedure which measures tissue oxygenation. It can reach vessels at 0 to 25 mm from the applied area. Limited to vessels of <1 mm diameter, NIRS focuses on microcirculation oxygenation (89).

In critically ill patients, the thenar eminence is the preferential site of measure, limiting confounding factors such as edema. Using transmitted and reflected light at different wavelengths, tissue oxygenation is estimated by the different absorption properties of oxy- and deoxyhemoglobin. Septic patients had a reduced tissular oxygen saturation (StO_2) whose value correlated with organ failure and which was associated with poor outcome (101). This technique does not assess microvascular blood flow directly; however, it can be used to evaluate vascular reactivity. Septic patients evidenced reduced vascular reactivity, defined by a decreased slope in StO_2 changes after occlusion challenge (90).

Microvascular partial oxygen pressure (PO_2) electrodes can be used for direct tissue oxygenation assessment. This provides a reliable tissue PO_2 in conditions of homogenous microcirculation (91). However, in the context of heterogeneous microcirculation, its accuracy decreases, limiting its use in critically ill patients.

Videomicroscopy

Nailfold videomicroscopy is historically the first procedure used in the clinical setting. It relies on the principle that organs can become translucent using reflecting light (84). The nailfold area provides an easily accessible, non-invasive site for direct visualization of the microcirculation under an ordinary microscope. Ungual microvascular blood flow undergoes severe impairment under various conditions (85). However, this technique has not been studied specifically in septic patients and is limited by its sensitivity to room temperature and local vasoconstriction.

Orthogonal polarization spectral imaging (OPS) and SDF are both techniques that rely on the principle of transillumination, which permits direct visualization of the microcirculation (86). The OPS light source emits polarized light which is reflected as: (1) (still) polarized light by the superficial layers, and (2) scattered depolarized light by the deeper layers of tissue which is absorbed by red blood cells. SDF uses green light and, like OPS, the superficial layer reflected light is not analyzed by the apparatus whereas reflected light from deep tissue reaches the center of the device. Red blood cells are seen as black bodies because of absorption of the light as a selected wavelength.

These two techniques allow direct visualization of the microcirculation with high contrast images provided by the reflected light from deeper layers. However, the visualization of microcirculation can be biased by the presence of red blood cells from the vessels.

Visualization has been mainly tested and validated in sublingual microcirculation because of the thin epithelial layer providing better images (87). The analyzed variables comprise vascular density, heterogeneity of perfusion, and capillary density (102).

In septic patients, De Backer et al. evidenced a decrease in the proportion of perfused small vessels (mainly capillaries) in addition to an increase in non or intermittently perfused capillaries (30).

These alterations are depicted even in the very early stages of sepsis. In addition, there are more severe sublingual microcirculatory alterations in non-survivor patients when compared to survivors (79).

One could question whether there is a correlation between sublingual microcirculation and vital organ perfusion. In pigs, sublingual and gut perfusion were similar during sepsis (103). Boerma and co-workers showed that sublingual microcirculation alterations are related to intestinal perfusion in septic patients (104). However, sublingual assessment presents some limitations (secretion, movement artifact), and cannot be used in patients with non-invasive ventilation.

These techniques use semi-quantitative analysis to perform microcirculatory evaluations and can only be used reliably by trained investigators (105). More recently, a third generation of handheld videomicroscope has been developed based on incident dark field imaging (IDF). Illuminating the vessel on all sides, IDF provides a three-dimensional effect and allows better optical resolution compared to SDF imaging (88). The last generation, Cytocam-IDF videomicroscope is a fully digitalized device computer-controlled, with a lower weight, high resolution sensor and a shortened pulse time. Therefore, IDF overcomes many of handheld microscopy previous limitations (106). Compared to SDF, Cytocam IDF provides superior image quality and better microcirculatory analysis (107) and in a preterm neonate's population, IDF imaging allowed visualization of 20 % more vessels than SDF (108).

The development of a bedside assessment of microcirculatory blood flow and oxygenation should provide a better and earlier recognition of microcirculatory dysfunction and guide resuscitation.

However, despite recent improvements, the application of these techniques is mainly confined to the field of research and rarely available in routine practice.

Peripheral Tissue Perfusion Assessment

In critically ill patients, systemic hemodynamic parameters and biomarkers are not always an accurate reflection of microcirculatory disorders. The primary marker at the bedside is arterial lactate, which recognizes circulatory failure and guides resuscitation. However, hyperlactatemia is not specific to hypoperfusion and, in many cases, persistent hyperlactatemia is not related to circulatory dysfunction and can thus lead to over-resuscitation (92).

During septic shock, sympathetic activation redistributes blood flow toward the "noble organ" at the expense of less important tissue, such as the skin, which is deprived of autoregulation. Evaluation of perfusion of those tissues with non-invasive parameters can therefore provide a good estimation of microcirculatory disorders. Skin provides an easily accessible site at the bedside of critically ill patients.

Capillary Refill Time

The capillary refill time (CRT) is assessed by applying a pressure of 3 to 7 Newtons on the knee or on the fingertip for at least 2 s (93). There is agreement in the literature that "good" pressure is that needed to produce a "thin white distal crescent" under the physician's nail. After releasing the pressure, the time in seconds necessary to return the skin color to baseline defines CRT. It provides an easy-to-use clinical tool to assess skin perfusion and microcirculatory dysfunction. In trained physicians using standardized pressure and chronometer time recording, CRT has a good reproducibility (109).

This quantitative tool can reliably provide information on critical illness severity. Lima et al. demonstrated that a prolonged fingertip CRT longer than 4.5 s is associated with high arterial lactate level and organ failure in critically ill patients (110). In septic patients, Brunauer and colleagues showed that CRT is related to the PI (83). Moreover, the persistence of prolonged CRT (>2.4 s at the fingertip and >4.9 s at the knee) after resuscitation of septic shock patients is a reliable predictive factor of 14-day mortality (109).

Recently, it has been suggested that CRT could guide resuscitation therapeutics. The ANDROMEDA-SHOCK study (111) compared a fluid resuscitation initiation and cessation guided by arterial lactate or by CRT. The authors found no significant difference in primary outcome between the groups. However, this study suggests that a resuscitation strategy based on CRT can decrease fluid and vasopressor administration. Moreover, the latest guidelines from the Surviving Sepsis Campaign recommends taking into account CRT measurement in the management of septic shock patients (96).

Skin Temperature

The aspect of the skin in circulatory failure circumstances has historically been described as "pale and cold" (94). Using probes, skin temperature is easily accessible in critically ill patients. Septic shock patients experience increased central-to-skin and decreased skin-to-room temperature gradients. This provides quantitative information which is related to ICU mortality (95).

Mottling

Mottling is described as a purple discoloration of the skin, primarily localized in the knee area. Although the pathophysiology of mottling is not completely understood, it is related to alterations of skin perfusion (112). Ait-Oufella et al. provided a semi-quantitative evaluation score of mottling which depended on skin extension of mottling around the knee area. This score can reliably predict sepsis severity and mortality (113).

Mottling provides an excellent risk stratification tool. This is a non-invasive and easily used bedside tool, with excellent reproducibility even in non-trained clinicians. In septic shock patients, the mottling score is correlated to organ failure and is a strong predictor of 14-day mortality (114). De Moura et al. confirmed the excellent positive predictive value of a mottling score of 4 or more to predict 28-day mortality (115).

A multimodal approach taking into account these markers should be recommended for personalized management of septic patients. Lavelligrand et al. showed in a retrospective observational study that daily clinical evaluation, including the mottling score, oliguria, lactatemia, and neurological exam, may allow physicians to tolerate a mild arterial hypotension in septic patients (116).

Peripheral perfusion assessment suffers from several limitations. First, CRT and mottling are difficult to assess in patients with dark skin. Second, due to the high heterogeneity of microcirculation in organs during sepsis, these markers may not accurately reflect visceral organ perfusion.

THERAPEUTIC AXES

Sepsis and septic shock represent one of the leading causes of critically ill mortality despite improvement in management (early antibiotic therapy, fluid resuscitation, vasopressors). Alterations in microcirculatory perfusion play a key role in the pathophysiology of sepsis and are associated with organ failure. Resuscitating the microcirculation should be considered a major therapeutic goal in septic patients (117). Considering the loss of hemodynamic coherence, *one* of the foremost questions is whether the most common therapeutics used to resuscitate macrohemodynamic parameters impact the microcirculation.

Fluid Resuscitation

Fluid resuscitation is the administration of fluids (crystalloids, colloids) in hypotensive patients to restore organ perfusion. However, there is some debate about the microcirculatory consequences. In an experimental study, fluid resuscitation worsened shock severity and impaired the microcirculation (118). Conversely, Santos et al. found an improvement of capillary density and blood flow following fluid resuscitation in a rodent model (77). In humans, Ospina-Tascon and team (119) found that fluid administration might improve sublingual microvascular perfusion for patients in the early sepsis phase. However, this effect was not confirmed in later phases of sepsis. Interestingly, the authors demonstrated a dissociation between micro- and macrohemodynamic response to fluid resuscitation in some patients with no microvascular response despite improvement of cardiac output. Moreover, the type of fluid used, whether colloids or crystalloids, had no impact on sublingual microcirculation in this study (120). Recently, in a pilot study of 35 septic shock patients, Hariri et al. (121) found an improvement in skin microvascular endothelial function in patients receiving albumin compared to crystalloids.

Inotropes/Vasopressors

Vasopressive and inotropic agents are used in sepsis to maintain organ perfusion pressure. However, their effects on microcirculation may vary among patients and between different organs (122). Experimental studies have suggested that dobutamine might improve hepatic (123) and mesenteric (124) but not renal perfusion (125). Using the OPS imaging technique, De Backer et al. additionally showed that administration of dobutamine partially recruited the microcirculation independently of systemic hemodynamic parameters in the early phase of sepsis. However, this effect was not maintained in the later phases of the disease (126). In a randomized

TABLE 2 | Human randomized controlled trials targeting endothelium and microcirculation in sepsis and septic shock.

Tested intervention	Study	Study design	Microcirculatory assessment	Primary outcome	Results/status
Oxidative stress					
Vitamin C	The Vitamin C, Hydrocortisone and Thiamine in Patients With Septic Shock Trial (VITAMINS) (34)	*216 patients* High dose Vitamin C (6 g/d), Thiamine (400 mg/d) and Hydrocortisone (200 mg/d) vs. Hydrocortisone alone	NA	Vasopressor-free days	Not significant
	Hydrocortisone, vitamin C, and thiamine for the treatment of sepsis and septic shock (HYVCTTSSS) [NCT03258684]	*80 patients* Vitamin C 1.5 g/6 h, hydrocortisone 50 mg/6 h and thiamine 200 mg/12 h vs. saline	NA	Hospital mortality	Completed Awaiting results
	Metabolic Resuscitation Using Ascorbic Acid, Thiamine, and Glucocorticoids in Sepsis (ORANGES) [NCT03422159]	*140 patients* Vitamin C (4 g/d), Hydrocortisone (200 mg/d), thiamine (400 mg/d) for 4 days vs. placebo	NA	– Time to vasopressor independence – Change in SOFA score at day 4	Completed Awaiting results
	Vitamin C and Thiamine in Sepsis [NCT03592277]	*120 patients* Vitamin C (4 g/d) and Thiamine (400 mg/d) vs. placebo	NA	60-day mortality	Recruiting
	Ascorbic acid, Corticosteroids, and thiamine in sepsis (ACTS) trial [NCT03389555]	*205 patients* Vitamin C 1.5 g/6h, Thiamine 100 mg/6 h and Hydrocortisone 50 mg/6 h for 4 days vs. placebo	NA	SOFA score at 72 h	Completed, not published
	Clinical trial of antioxidant therapy in patients with septic shock [NCT03557229]	*131 patients* Vitamin C 4g/d, vitamin E 1,200 UNT/d, N-acetyl cysteine 2,400 mg/d and melatonin 50 mg/d for 5 days vs. placebo	Oxidative stress and inflammatory biomarker	SOFA score at day 7	Not yet recruiting
	Evaluation of Hydrocortisone, Vitamin C and Thiamine for the Treatment of Septic Shock (HYVITS) [NCT03380507]	*106 patients* Vitamin C 6 g/d, hydrocortisone 200 mg/d and thiamine 400mg/d vs. placebo	NA	60-day mortality	Terminated due to futility
	Ascorbic acid and thiamine effect in septic shock (ATESS) [NCT03756220]	*116 patients* Vitamin C 100 mg/kg/d, Thiamine 400 mg/d vs. placebo	NA	Change in SOFA score at 72 h	Completed Awaiting results
Para-tyrosine	Efficacy of Para-Tyrosine Supplementation on the Survival and Clinical Outcome in Patients With Sepsis [NCT03278730]	*296 patients* Para-tyrosine 2 g x 3/d oral or enteral for 7 days vs. placebo	NA	30-day mortality	Not yet recruiting
Melatonin	Efficacy of Melatonin in Patients With Severe Sepsis or Septic Shock [NCT01858909]	*110 patients* 30 mg/12 h 28 days vs. placebo	Oxidative stress and inflammatory biomarkers	28-day mortality and organ dysfunction	Unknown status
	Effects of Melatonin as a Novel Antioxidant and Free Radicals Scavenger in Neonatal Sepsis [NCT03295162]	*55 patients* Melatonin 10 mg x 2/days vs. placebo	NA	Free radicals scavenge	Awaiting results
Inflammation					
Evolocumab (anti-PSCK9)	Evolocumab for PCSK9 Lowering in Early Acute Sepsis (The PLEASe Study) [NCT03869073]	*36 patients* Low dose (420 mg) vs. high dose (840 mg) vs. placebo in 3 SC injections	NA	Decrease bacteria LPS levels	Recruiting
Atorvastatin	Study the Impact of Statins in Septic Shock [NCT02681653]	*80 patients* Atorvastatin 40 mg/d or placebo for 7 days	Cytokines	28-day mortality	Awaiting results
Nitric oxide/Vasoreactivity					
NOS inhibitor	Nitric oxide synthase inhibitor 54C88 in patients with septic shock (35)	*797 patients* NOS inhibitor vs. placebo for 7 or 14 days	NA	Mortality	Increased mortality in intervention group

(Continued)

TABLE 2 | Continued

Tested intervention	Study	Study design	Microcirculatory assessment	Primary outcome	Results/status
NO	Randomized controlled trial of inhaled nitric oxide for the treatment of microcirculatory dysfunction in patients with sepsis (36)	*49 patients* Inhaled NO 40 parts per million for 6 h vs. placebo	Sublingual microcirculation using sidestream dark field videomicroscopy	– Change in SOFA score – Change in sublingual microcirculation flow index	Not significant
Nitroglycerin	Effects of nitroglycerin on sublingual microcirculatory blood flow in patients with severe sepsis/septic shock after a strict resuscitation protocol: a double-blind randomized placebo controlled trial (37)	*70 patients* Nitroglycerin at 4 mg/h for 30 min then 2 mg/h for 24 h or placebo	Sublingual microcirculatory blood flow using SDF imaging	Sublingual microcirculatory flow index	No significant differences
Methylene blue	Effect of methylene blue on hemodynamic and metabolic response in septic shock patients (38)	*64 patients* Methylene blue vs. placebo	NA	Septic shock resolution	Unknown status
	Methylene Blue in Early Septic Shock (SHOCKEM-Blue) [NCT04446871]	*91 patients* I.V. infusion of 100mg of methylene blue for 6 hours x3 doses a day vs. placebo	NA	Vasopressor requirement	Awaiting results
	Methylene Blue and Microcirculation in Septic Shock [NCT04295993]	*32 patients* Methylene blue 2 mg/kg over 10 min vs. standard of care	Sublingual microcirculation	Microvascular flow index at 6 hours	Not yet recruiting
Ilomedin	Ilomedin in Septic Shock With Persistent Microperfusion Defects (I-MICRO) [NCT03788837]	*235 patients* I.V. ilomedin at 0.5 ng/kg/min with increments of 0.5 ng/kg/min every 30 min up to a maximum of 1.5 ng/kg/min for 48 h vs. placebo	Mottling, cutaneous laser Doppler, NIRS, videomicroscopy, tissular PCO_2, perfusion index	Change in SOFA score at day 7	Recruiting
	Co-administration of Iloprost and Eptifibatide in Septic Shock Patients (CO-ILEPSS) [NCT02204852]	*18 patients* Iloprost 1 ng/kg/min + Eptifibatide 0.5 ug/kg/min for 48 h continuously vs. placebo	Biomarkers of inflammation, coagulation, adhesion molecules	Biomarkers of endothelial activation and dysfunction	Awaiting results
	Infusion of Prostacyclin (Iloprost) vs. Placebo for 72-hours in Patients With Septic Shock Suffering From Organ Failure (COMBAT-SHINE) [NCT04123444]	*380 patients* Continuous infusion of 1 ng/kg/min for 72 h vs. placebo	NA	Change in SOFA score	Recruiting
Citrulline	Citrulline in Severe Sepsis [NCT01474863]	*72 patients* Low dose vs. high dose vs. placebo	NA	Vasopressor dependency index	Not published
	Effect of Citrulline on the Clinical and Biochemical Evolution of Patients With Sepsis. (CITRUSEP) [NCT02370030]	*176 patients* Citrulline malate 10g/day for 7 days vs. placebo	NA	Multiple organ failure	Unknown status
Coagulation/hemostasis					
Thrombomodulin	Effect of a recombinant human soluble thrombomodulin on mortality in patients with sepsis-associated coagulopathy (SCARLET study)	*800 patients* I.V. thrombomodulin at 0.06 mg/kg/d vs. placebo for 6 days	Biomarkers	28-day mortality	Not significant

(Continued)

TABLE 2 | Continued

Tested intervention	Study	Study design	Microcirculatory assessment	Primary outcome	Results/status
Protein C	Drotrecogin Alfa (Activated) in Adults with Septic Shock (39)	*1,697 patients* Drotrecogin alfa or placebo for 96 hours	NA	28-day mortality	Not significant
	Human protein C concentrates in patients with sepsis and septic shock [NCT01411670]	*60 patients* with protein C activity <60% Human Protein C concentrate of activated protein C vs. placebo	Sublingual microcirculatory blood flow	Sublingual microcirculatory blood flow assessed by SDF	Awaiting results
	Modulation of vasoreactivity in septic shock: impact of recombinant protein C [NCT02885168]	*30 patients* Recombinant activated protein C during 96 h vs. placebo	Near-infrared spectroscopy with reactive hyperemia	Vascular reactivity	Awaiting results
Recombinant antithrombin	Recombinant human Antithrombin (ATryn) in the treatment of patients with DIC associated with severe sepsis [NCT00506519]	*25 patients* High dose or low dose of I.V. antithrombin vs. placebo for 5 days	Inflammatory markers	Improvement in the DIC score by 2 points at day 28	Awaiting results
Antithrombin + recombinant human thrombomodulin	The efficacy and safety of antithrombin and recombinant human thrombomodulin combination therapy in patients with severe sepsis and disseminated intravascular coagulation (40)	*129 patients* Antithrombin + thrombomodulin vs. antithrombin alone	NA	Platelet count and D-dimer levels at day 7	Intervention group had significant improvement of platelet count and D-dimer levels at day 7
Heparin	Efficacy and Safety of Unfractionated Heparin on Severe sepsis With Suspected Disseminated Intravascular Coagulation [NCT02654561]	*700 patients* Heparin 12,500 units/d for 7 days	NA	ICU mortality	Recruiting
	Heparin Anticoagulation to Improve Outcomes in Septic shock: The HALO Pilot [NCT01648036]	*76 patients* Unfractionated heparin 18 UI/kg/h continuous I.V. for 7 days vs. Dalteparin 5000IU subcutaneous daily	Biomarkers	Unknown	Not published
Annexin 5	SY-005(Recombinant Human Annexin A5)in Patients With Sepsis [NCT04898322]	*96 patients* Annexin 5 vs. placebo for 5 days	Biomarkers	Safety and tolerability	Not yet recruiting
Aspirin	ASpirin for Patients With SEPsis and SeptIc Shock (ASP-SEPSIS) [NCT01784159]	*240 patients* 200 mg/day of placebo for 7 days	NA	Change in SOFA score at day 7	Recruiting
Heart rate control					
Landiolol	LANdiolol MIcrocirculatory Effects During Septic shOck (MILANOS) [NCT04931225]	Landiolol (Rapibloc) perfusion will be started at T0 at 0.5 mcg/kg/min and increased by 0.5 mcg/kg/min every 30 min in order to achieve a 15% (T1) decrease in heart rate	Laser Doppler coupled with iontophoresis of acetylcholine	Microcirculatory reactivity	Not yet recruiting
Ivabradine	Ivabradine for Heart Rate Control In Septic Shock (IRISS) [NCT04031573]	*429 patients* Ivabradine 2.5 to 7.5 mg/12 h *via* enteral administration, to achieve a heart rate of 80–94 bpm vs. placebo	NA	– Succeed in heart rate control – 28-day mortality	Recruiting

d, day; DIC, Disseminated intravascular coagulation; h, hours; ICU, Intensive care unit; I.V., intravenous; LPS, Lipopolysaccharide; NIRS, Near Infrared Spectrometry; NA, not available;NO, Nitric Oxide; NOS, Nitric oxide synthase; PCO2, partial pressure of carbon dioxide; SDF, Sidestream Dark Field; SOFA, Sequential Organ Failure Assessment; SC, subcutaneous.

controlled trial, dobutamine failed to improve sublingual, peripheral, and splanchnic perfusion in septic shock patients, when compared to placebo (127). Conversely, Morelli and team (128) found that, due to its vasodilatory effects, levosimendan significantly improved microcirculatory blood flow and increased perfused capillary density in septic shock patients, as compared to dobutamine.

Similarly, data focusing on the microvascular effects of vasopressor agents are controversial. While norepinephrine improved both hepatic (129) and renal blood flow (130) in endotoxemic shock, this observation was not confirmed in another study focusing on the liver (131) and gut (132) microcirculations. In septic shock patients, norepinephrine failed to improve sublingual microvascular blood flow despite restoring macrohemodynamic parameters (mean arterial pressure) (133). Indeed, increasing blood pressure in septic patients did not affect various microcirculatory and perfusion parameters (134). Due to the complex pathophysiology of sepsis, which implies an imbalance between vasodilatation and vasoconstriction, it is reasonable to expect that the microvascular response might be highly unpredictable.

Microhemodynamic parameter assessment is required to evaluate the effects of the main drugs used during sepsis, as well as to select the patients for randomized trials in a tailored strategy, taking into account both macro- and microhemodynamic parameters.

Many strategies targeting endothelial and microvascular dysfunction have been proposed. Therapeutic drugs focus on endothelial vasoreactivity, inflammation, oxidative stress, and coagulation/anticoagulation balance. **Table 2** (34–40) presents the major recent trials focusing on microcirculation during sepsis. Overall, while some studies showed an improvement in microcirculatory parameters, very few interventions succeeded in reducing mortality in critically ill septic patients. As endothelial activation is part of the host's required response during sepsis, its inhibition may be deleterious. Conversely, targeting one pathway may not be sufficient to improve outcome, and combination therapy should be discussed for future trials.

Given the encouraging results in recent studies and incoming trials, new therapeutic targets deserve attention.

In the past few years, many authors have evidenced a decrease of antioxidant defense in septic patients (135). Vitamin C, or ascorbic acid, is a well-known antioxidant molecule, easily accessible and safe to use at the bedside (136). Several trials have studied the combination of vitamin C, thiamine, and hydrocortisone in septic shock patients. A meta-analysis of nine randomized controlled trials confirmed that this combination therapy could improve Sequential Organ Failure Assessment (SOFA) score and vasopressor-free days. However its benefit for survival is still under debate (137). Recently, Lavillegrand et al. found that supplementation of vitamin C in septic shock patients with persistent peripheral tissue impairment improved skin microvascular reactivity and peripheral perfusion in patients with or without vitamin C deficiency (138).

Other studies have focused on the adrenergic system. Indeed, the deleterious effects of sympathetic overstimulation in septic shock led several authors to study beta blockers. Morelli and co-workers (139) studied esmolol in order to reduce heart rate in septic shock patients. The authors found that the use of esmolol was safe, and improved outcomes of septic shock patients, and that it also improved microvascular blood flow (140). These results led to other trials that aimed to reduce heart rate and adrenergic stress in septic patients (**Table 2**).

CONCLUSION

In the past two decades, the endothelium has been the focus of particular interest, especially in sepsis. As the major regulator of vascular homeostasis, the endothelium is one of the leading actors in response to aggression. In sepsis, the exaggerated and systemic endothelial activation leads to microcirculatory alterations which thus participate in organ failure and death. Recent advances in the assessment of the microcirculation promote a better understanding of microcirculatory impairments in sepsis. However, their use in clinical practice is limited by their availability and difficulty of use in critically ill patients with multiple confusing factors. New technical devices and clinical tools can be useful at the bedside to recognize microcirculatory impairments.

Despite improvements in patient care, sepsis and septic shock lead to high morbidity and mortality in critical care. Testing the prognostic value of microcirculatory disorders in sepsis, several trials have studied new molecules targeting endothelial functions and dysfunctions. However, despite some promising leads, the foremost studies have shown unfavorable results for outcomes of mortality or organ failure. We believe that microcirculatory resuscitation should be one of the goals in the management of septic patients. It is therefore crucial to identify microvascular endothelial dysfunction more effectively to better select patients for future trials.

AUTHOR CONTRIBUTIONS

LR and LZ both performed the review of the literature and wrote the study. All authors contributed to the article and approved the submitted version.

REFERENCES

1. S, Seymour CW, Shankar-Hari M, Annane D, Bauer M, et al. The Third International Consensus Definitions for Sepsis and Septic Shock (Sepsis-3). *JAMA*. (2016) 315:801–10. doi: 10.1001/jama.2016.0287
2. Dupuis C, Bouadma L, Ruckly S, Perozziello A, Van-Gysel D, Mageau A, et al. Sepsis and septic shock in France: incidences, outcomes and costs of care. *Ann Intensive Care*. (2020) 10:145. doi: 10.1186/s13613-020-00760-x
3. Sakr Y, Dubois M-J, De Backer D, Creteur J, Vincent J-L. Persistent microcirculatory alterations are associated with organ failure and death in patients with septic shock. *Crit Care Med*. (2004) 32:1825–31. doi: 10.1097/01.CCM.0000138558.16257.3F
4. Aird WC. Phenotypic heterogeneity of the endothelium: I. Structure, function, and mechanisms. *Circ Res*. (2007) 100:158–73. doi: 10.1161/01.RES.0000255691.76142.4a

5. Reitsma S, Slaaf DW, Vink H, van Zandvoort MAMJ. oude Egbrink MGA. The endothelial glycocalyx: composition, functions, and visualization. *Pflugers Arch.* (2007) 454:345–59. doi: 10.1007/s00424-007-0212-8
6. Weinbaum S, Tarbell JM, Damiano ER. The structure and function of the endothelial glycocalyx layer. *Annu Rev Biomed Eng.* (2007) 9:121–67. doi: 10.1146/annurev.bioeng.9.060906.151959
7. Pons S, Arnaud M, Loiselle M, Arrii E, Azoulay E, Zafrani L. Immune Consequences of Endothelial Cells' Activation and Dysfunction During Sepsis. *Crit Care Clin.* (2020) 36:401–13. doi: 10.1016/j.ccc.2019.12.001
8. Faure E, Thomas L, Xu H, Medvedev A, Equils O, Arditi M. Bacterial lipopolysaccharide and IFN-gamma induce Toll-like receptor 2 and Toll-like receptor 4 expression in human endothelial cells: role of NF-kappa B activation. *J Immunol.* (2001) 166:2018–24. doi: 10.4049/jimmunol.166.3.2018
9. Faure E, Equils O, Sieling PA, Thomas L, Zhang FX, Kirschning CJ, et al. Bacterial lipopolysaccharide activates NF-kappaB through toll-like receptor 4 (TLR-4) in cultured human dermal endothelial cells. Differential expression of TLR-4 and TLR-2 in endothelial cells. *J Biol Chem.* (2000) 275:11058–63. doi: 10.1074/jbc.275.15.11058
10. Mitchell S, Vargas J, Hoffmann A. Signaling *via* the NFκB system. *Wiley Interdiscip Rev Syst Biol Med.* (2016) 8:227–41. doi: 10.1002/wsbm.1331
11. Ye X, Ding J, Zhou X, Chen G, Liu SF. Divergent roles of endothelial NF-kappaB in multiple organ injury and bacterial clearance in mouse models of sepsis. *J Exp Med.* (2008) 205:1303–15. doi: 10.1084/jem.20071393
12. Nooteboom A, van der Linden CJ, Hendriks T. Modulation of adhesion molecule expression on endothelial cells after induction by lipopolysaccharide-stimulated whole blood. *Scand J Immunol.* (2004) 59:440–8. doi: 10.1111/j.0300-9475.2004.01413.x
13. Kuhns DB, Alvord WG, Gallin JI. Increased circulating cytokines, cytokine antagonists, and E-selectin after intravenous administration of endotoxin in humans. *J Infect Dis.* (1995) 171:145–52. doi: 10.1093/infdis/171.1.145
14. Kayal S, Jaïs JP, Aguini N, Chaudière J, Labrousse J. Elevated circulating E-selectin, intercellular adhesion molecule 1, and von Willebrand factor in patients with severe infection. *Am J Respir Crit Care Med.* (1998) 157:776–84. doi: 10.1164/ajrccm.157.3.9705034
15. Boldt J, Muller M, Kuhn D, Linke LC, Hempelmann G. Circulating adhesion molecules in the critically ill: a comparison between trauma and sepsis patients. *Intensive Care Med.* (1996) 22:122–8. doi: 10.1007/BF017 20718
16. Sessler CN, Windsor AC, Schwartz M, Watson L, Fisher BJ, Sugerman HJ, et al. Circulating ICAM-1 is increased in septic shock. *Am J Respir Crit Care Med.* (1995) 151:1420–7. doi: 10.1164/ajrccm.151.5.7735595
17. Tang H, Ivanciu L, Popescu N, Peer G, Hack E, Lupu C, et al. Sepsis-induced coagulation in the baboon lung is associated with decreased tissue factor pathway inhibitor. *Am J Pathol.* (2007) 171:1066–77. doi: 10.2353/ajpath.2007.070104
18. Faust SN, Levin M, Harrison OB, Goldin RD, Lockhart MS, Kondaveeti S, et al. Dysfunction of endothelial protein C activation in severe meningococcal sepsis. *N Engl J Med.* (2001) 345:408–16. doi: 10.1056/NEJM200108093450603
19. Mesters RM, Helterbrand J, Utterback BG, Yan B, Chao YB, Fernandez JA, et al. Prognostic value of protein C concentrations in neutropenic patients at high risk of severe septic complications. *Crit Care Med.* (2000) 28:2209–16. doi: 10.1097/00003246-200007000-00005
20. Levin EG, Marotti KR, Santell L. Protein kinase C and the stimulation of tissue plasminogen activator release from human endothelial cells. Dependence on the elevation of messenger. *RNA J Biol Chem.* (1989) 264:16030–6. doi: 10.1016/S0021-9258(18)71583-4
21. Echtenacher B, Weigl K, Lehn N, Männel DN. Tumor necrosis factor-dependent adhesions as a major protective mechanism early in septic peritonitis in mice. *Infect Immun.* (2001) 69:3550–5. doi: 10.1128/IAI.69.6.3550-3555.2001
22. Schlichting DE, Waxman AB, O'Brien LA, Wang T, Naum CC, et al. Circulating endothelial and endothelial progenitor cells in patients with severe sepsis. *Microvasc Res.* (2011) 81:216–21. doi: 10.1016/j.mvr.2010.11.011
23. Schmidt EP, Yang Y, Janssen WJ, Gandjeva A, Perez MJ, Barthel L, et al. The pulmonary endothelial glycocalyx regulates neutrophil adhesion and lung injury during experimental sepsis. *Nat Med.* (2012) 18:1217–23. doi: 10.1038/nm.2843
24. Cabrales P, Vázquez BYS, Tsai AG, Intaglietta M. Microvascular and capillary perfusion following glycocalyx degradation. *J Appl Physiol (1985).* (2007) 102:2251–2259. doi: 10.1152/japplphysiol.01155.2006
25. Anand D, Ray S, Srivastava LM, Bhargava S. Evolution of serum hyaluronan and syndecan levels in prognosis of sepsis patients. *Clin Biochem.* (2016) 49:768–76. doi: 10.1016/j.clinbiochem.2016.02.014
26. Lee DH, Dane MJC, van den Berg BM, Boels MGS, van Teeffelen JW, de Mutsert R, et al. Deeper penetration of erythrocytes into the endothelial glycocalyx is associated with impaired microvascular perfusion. *PLoS ONE.* (2014) 9:e96477. doi: 10.1371/journal.pone.0096477
27. Beurskens DM, Bol ME, Delhaas T, van de Poll MC, Reutelingsperger CP, Nicolaes GA, et al. Decreased endothelial glycocalyx thickness is an early predictor of mortality in sepsis. *Anaesth Intensive Care.* (2020) 48:221–8. doi: 10.1177/0310057X20916471
28. Leligdowicz A, Richard-Greenblatt M, Wright J, Crowley VM, Kain KC. Endothelial Activation: The Ang/Tie Axis in Sepsis. *Front Immunol.* (2018) 9:838. doi: 10.3389/fimmu.2018.00838
29. Rossaint J, Zarbock A. Tissue-specific neutrophil recruitment into the lung, liver, and kidney. *J Innate Immun.* (2013) 5:348–57. doi: 10.1159/000345943
30. De Backer D, Creteur J, Preiser J-C, Dubois M-J, Vincent J-L. Microvascular blood flow is altered in patients with sepsis. *Am J Respir Crit Care Med.* (2002) 166:98–104. doi: 10.1164/rccm.200109-016OC
31. Lu JL, Schmiege LM, Kuo L, Liao JC. Downregulation of endothelial constitutive nitric oxide synthase expression by lipopolysaccharide. *Biochem Biophys Res Commun.* (1996) 225:1–5. doi: 10.1006/bbrc.1996.1121
32. Zhou M, Wang P, Chaudry IH. Endothelial nitric oxide synthase is downregulated during hyperdynamic sepsis. *Biochim Biophys Acta.* (1997) 1335:182–90. doi: 10.1016/S0304-4165(96)00139-0
33. Preiser JC, Zhang H, Vray B, Hrabak A, Vincent JL. Time course of inducible nitric oxide synthase activity following endotoxin administration in dogs. *Nitric Oxide.* (2001) 5:208–11. doi: 10.1006/niox.2001.0342
34. Fujii T, Luethi N, Young PJ, Frei DR, Eastwood GM, French CJ, et al. Effect of Vitamin C, Hydrocortisone, and Thiamine vs. Hydrocortisone Alone on Time Alive and Free of Vasopressor Support Among Patients With Septic Shock: The VITAMINS Randomized Clinical Trial. *JAMA.* (2020) 323:423–31. doi: 10.1001/jama.2019.22176
35. López A, Lorente JA, Steingrub J, Bakker J, McLuckie A, Willatts S, et al. Multiple-center, randomized, placebo-controlled, double-blind study of the nitric oxide synthase inhibitor 546C88: effect on survival in patients with septic shock. *Crit Care Med.* (2004) 32:21–30. doi: 10.1097/01.CCM.0000105581.01815.C6
36. Trzeciak S, Glaspey LJ, Dellinger RP, Durflinger P, Anderson K, Dezfulian C, et al. Randomized controlled trial of inhaled nitric oxide for the treatment of microcirculatory dysfunction in patients with sepsis*. *Crit Care Med.* (2014) 42:2482–92. doi: 10.1097/CCM.0000000000000549
37. Boerma EC, Koopmans M, Konijn A, Kaiferova K, Bakker AJ, van Roon EN, et al. Effects of nitroglycerin on sublingual microcirculatory blood flow in patients with severe sepsis/septic shock after a strict resuscitation protocol: a double-blind randomized placebo controlled trial. *Crit Care Med.* (2010) 38:93–100. doi: 10.1097/CCM.0b013e3181b 02fc1
38. Luis-Silva F, Menegueti MG, Sepeda CDR, Petroski-Moraes BC, Sato L, Peres LM, et al. Effect of methylene blue on hemodynamic and metabolic response in septic shock patients. *Medicine (Baltimore).* (2022) 101:e28599. doi: 10.1097/MD.00000000000 28599
39. Ranieri VM, Thompson BT, Barie PS, Dhainaut J-F, Douglas IS, Finfer S, et al. Drotrecogin alfa (activated) in adults with septic shock. *N Engl J Med.* (2012) 366:2055–64. doi: 10.1056/NEJMoa1202290
40. Yasuda N, Goto K, Ohchi Y, Abe T, Koga H, Kitano T. The efficacy and safety of antithrombin and recombinant human thrombomodulin combination therapy in patients with severe sepsis and disseminated intravascular coagulation. *J Crit Care.* (2016) 36:29–34. doi: 10.1016/j.jcrc.2016. 06.008
41. Sies H. Oxidative stress: a concept in redox biology and medicine. *Redox Biol.* (2015) 4:180–3. doi: 10.1016/j.redox.2015.01.002

42. Victor VM, Rocha M. De la Fuente M. Immune cells: free radicals and antioxidants in sepsis. *Int Immunopharmacol.* (2004) 4:327–47. doi: 10.1016/j.intimp.2004.01.020
43. Cerwinka WH, Cooper D, Krieglstein CF, Ross CR, McCord JM, Granger DN. Superoxide mediates endotoxin-induced platelet-endothelial cell adhesion in intestinal venules. *Am J Physiol Heart Circ Physiol.* (2003) 284:H535–541. doi: 10.1152/ajpheart.00311.2002
44. Corda S, Laplace C, Vicaut E, Duranteau J. Rapid reactive oxygen species production by mitochondria in endothelial cells exposed to tumor necrosis factor-alpha is mediated by ceramide. *Am J Respir Cell Mol Biol.* (2001) 24:762–8. doi: 10.1165/ajrcmb.24.6.4228
45. Chung HY, Yokozawa T, Kim MS, Lee KH, Kim KW, Yang R, et al. The mechanism of nitric oxide and/or superoxide cytotoxicity in endothelial cells. *Exp Toxicol Pathol.* (2000) 52:227–33. doi: 10.1016/S0940-2993(00)80034-2
46. Vásquez-Vivar J, Kalyanaraman B, Martásek P. The role of tetrahydrobiopterin in superoxide generation from eNOS: enzymology and physiological implications. *Free Radic Res.* (2003) 37:121–7. doi: 10.1080/1071576021000040655
47. Szabó C, Módis K. Pathophysiological roles of peroxynitrite in circulatory shock. *Shock.* (2010) 34:4–14. doi: 10.1097/SHK.0b013e3181e7e9ba
48. Joffre J, Hellman J. Oxidative Stress and Endothelial Dysfunction in Sepsis and Acute Inflammation. *Antioxid Redox Signal.* (2021) 35:1291–307. doi: 10.1089/ars.2021.0027
49. Regoeczi E, Brain MC. Organ distribution of fibrin in disseminated intravascular coagulation. *Br J Haematol.* (1969) 17:73–81. doi: 10.1111/j.1365-2141.1969.tb05665.x
50. Levi M, van der Poll T, Schultz M. Systemic versus localized coagulation activation contributing to organ failure in critically ill patients. *Semin Immunopathol.* (2012) 34:167–79. doi: 10.1007/s00281-011-0283-7
51. Yang Q-P, Liu W-P, Guo L-X, Jiang Y, Li G-D, Bai Y-Q, et al. Autopsy report of four cases who died from Streptococcus suis infection, with a review of the literature. *Eur J Clin Microbiol Infect Dis.* (2009) 28:447–53. doi: 10.1007/s10096-008-0646-8
52. Dixon B. The role of microvascular thrombosis in sepsis. *Anaesth Intensive Care.* (2004) 32:619–29. doi: 10.1177/0310057X0403200502
53. Chang JC. Disseminated intravascular coagulation: new identity as endotheliopathy-associated vascular microthrombotic disease based on in vivo hemostasis and endothelial molecular pathogenesis. *Thromb J.* (2020) 18:25. doi: 10.1186/s12959-020-00231-0
54. de Stoppelaar SF. van 't Veer C, van der Poll T. The role of platelets in sepsis. *Thromb Haemost.* (2014) 112:666–77. doi: 10.1160/TH14-02-0126
55. Nguyen TC, Gushiken F, Correa JI, Dong J-F, Dasgupta SK, Thiagarajan P, et al. recombinant fragment of von Willebrand factor reduces fibrin-rich microthrombi formation in mice with endotoxemia. *Thromb Res.* (2015) 135:1025–30. doi: 10.1016/j.thromres.2015.02.033
56. De Backer D, Donadello K, Favory R. Link between coagulation abnormalities and microcirculatory dysfunction in critically ill patients. *Curr Opin Anaesthesiol.* (2009) 22:150–4. doi: 10.1097/ACO.0b013e328328d1a1
57. Secor D, Li F, Ellis CG, Sharpe MD, Gross PL, Wilson JX, et al. Impaired microvascular perfusion in sepsis requires activated coagulation and P-selectin-mediated platelet adhesion in capillaries. *Intensive Care Med.* (2010) 36:1928–34. doi: 10.1007/s00134-010-1969-3
58. Nieuwland R, Berckmans RJ, McGregor S, Böing AN, Romijn FP, Westendorp RG, et al. Cellular origin and procoagulant properties of microparticles in meningococcal sepsis. *Blood.* (2000) 95:930–5. doi: 10.1182/blood.V95.3.930.003k46_930_935
59. Wang J-G, Manly D, Kirchhofer D, Pawlinski R, Mackman N. Levels of microparticle tissue factor activity correlate with coagulation activation in endotoxemic mice. *J Thromb Haemost.* (2009) 7:1092–8. doi: 10.1111/j.1538-7836.2009.03448.x
60. Delabranche X, Boisramé-Helms J, Asfar P, Berger A, Mootien Y, Lavigne T, et al. Microparticles are new biomarkers of septic shock-induced disseminated intravascular coagulopathy. *Intensive Care Med.* (2013) 39:1695–703. doi: 10.1007/s00134-013-2993-x
61. Guven G, Hilty MP, Ince C. Microcirculation: Physiology, Pathophysiology, and Clinical Application. *Blood Purif.* (2020) 49:143–50. doi: 10.1159/000503775
62. Ince C. The microcirculation is the motor of sepsis. *Crit Care.* (2005) 9 Suppl 4:S13–9. doi: 10.1186/cc3753
63. Nakajima Y, Baudry N, Duranteau J, Vicaut E. Microcirculation in intestinal villi: a comparison between hemorrhagic and endotoxin shock. *Am J Respir Crit Care Med.* (2001) 164:1526–30. doi: 10.1164/ajrccm.164.8.2009065
64. Farquhar I, Martin CM, Lam C, Potter R, Ellis CG, Sibbald WJ. Decreased capillary density in vivo in bowel mucosa of rats with normotensive sepsis. *J Surg Res.* (1996) 61:190–6. doi: 10.1006/jsre.1996.0103
65. Taccone FS, Su F, De Deyne C, Abdellhai A, Pierrakos C, He X, et al. Sepsis is associated with altered cerebral microcirculation and tissue hypoxia in experimental peritonitis. *Crit Care Med.* (2014) 42:e114–122. doi: 10.1097/CCM.0b013e3182a641b8
66. Wester T, Hägglblad E, Awan ZA, Barratt-Due A, Kvernebo M, Halvorsen PS, et al. Assessments of skin and tongue microcirculation reveals major changes in porcine sepsis. *Clin Physiol Funct Imaging.* (2011) 31:151–8. doi: 10.1111/j.1475-097X.2010.00994.x
67. Hayes MA, Timmins AC, Yau EH, Palazzo M, Hinds CJ, Watson D. Elevation of systemic oxygen delivery in the treatment of critically ill patients. *N Engl J Med.* (1994) 330:1717–22. doi: 10.1056/NEJM199406163302404
68. Ellis CG, Bateman RM, Sharpe MD, Sibbald WJ, Gill R. Effect of a maldistribution of microvascular blood flow on capillary O(2) extraction in sepsis. *Am J Physiol Heart Circ Physiol.* (2002) 282:H156–164. doi: 10.1152/ajpheart.2002.282.1.H156
69. Humer MF, Phang PT, Friesen BP, Allard MF, Goddard CM, Walley KR. Heterogeneity of gut capillary transit times and impaired gut oxygen extraction in endotoxemic pigs. *J Appl Physiol (1985).* (1996) 81:895–904. doi: 10.1152/jappl.1996.81.2.895
70. Ince C, Sinaasappel M. Microcirculatory oxygenation and shunting in sepsis and shock. *Crit Care Med.* (1999) 27:1369–77. doi: 10.1097/00003246-199907000-00031
71. Østergaard L, Granfeldt A, Secher N, Tietze A, Iversen NK, Jensen MS, et al. Microcirculatory dysfunction and tissue oxygenation in critical illness. *Acta Anaesthesiol Scand.* (2015) 59:1246–59. doi: 10.1111/aas.12581
72. Walley KR. Heterogeneity of oxygen delivery impairs oxygen extraction by peripheral tissues: theory. *J Appl Physiol.* (1996) 81:885–94. doi: 10.1152/jappl.1996.81.2.885
73. Morin MJ, Unno N, Hodin RA, Fink MP. Differential expression of inducible nitric oxide synthase messenger RNA along the longitudinal and crypt-villus axes of the intestine in endotoxemic rats. *Crit Care Med.* (1998) 26:1258–64. doi: 10.1097/00003246-199807000-00031
74. Lange M, Hamahata A, Traber DL, Nakano Y, Traber LD, Enkhbaatar P. Heterogeneity of the effects of combined nitric oxide synthase inhibition on organ perfusion in ovine sepsis. *Burns.* (2013) 39:1565–70. doi: 10.1016/j.burns.2013.04.019
75. Bateman RM, Tokunaga C, Kareco T, Dorscheid DR, Walley KR. Myocardial hypoxia-inducible HIF-1alpha, VEGF, and GLUT1 gene expression is associated with microvascular and ICAM-1 heterogeneity during endotoxemia. *Am J Physiol Heart Circ Physiol.* (2007) 293:H448–456. doi: 10.1152/ajpheart.00035.2007
76. Ince C. Hemodynamic coherence and the rationale for monitoring the microcirculation. *Crit Care.* (2015) 19 Suppl 3:S8–S8. doi: 10.1186/cc14726
77. Santos AOMT, Furtado ES, Villela NR, Bouskela E. Microcirculatory effects of fluid therapy and dopamine, associated or not to fluid therapy, in endotoxemic hamsters. *Clin Hemorheol Microcirc.* (2011) 47:1–13. doi: 10.3233/CH-2010-1358
78. Zhang H, Li L, Wu J, Qu H-P, Tang Y-Q, Chen D-C. Time of dissociation between microcirculation, macrocirculation, and lactate levels in a rabbit model of early endotoxemic shock. *Chin Med J (Engl).* (2020) 133:2153–60. doi: 10.1097/CM9.0000000000000887
79. Trzeciak S, Dellinger RP, Parrillo JE, Guglielmi M, Bajaj J, Abate NL, et al. Early microcirculatory perfusion derangements in patients with severe sepsis and septic shock: relationship to hemodynamics, oxygen transport, and survival. *Ann Emerg Med.* (2007) 49:88–98, 98.e1–2. doi: 10.1016/j.annemergmed.2006.08.021
80. De Backer D, Donadello K, Sakr Y, Ospina-Tascon G, Salgado D, Scolletta S, et al. Microcirculatory alterations in patients with severe sepsis: impact of time of assessment and relationship with outcome. *Crit Care Med.* (2013) 41:791–9. doi: 10.1097/CCM.0b013e3182742e8b

81. Eun HC. Evaluation of skin blood flow by laser Doppler flowmetry. *Clin Dermatol.* (1995) 13:337–47. doi: 10.1016/0738-081X(95)00080-Y
82. Neviere R, Mathieu D, Chagnon JL, Lebleu N, Millien JP, Wattel F. Skeletal muscle microvascular blood flow and oxygen transport in patients with severe sepsis. *Am J Respir Crit Care Med.* (1996) 153:191–5. doi: 10.1164/ajrccm.153.1.8542115
83. Brunauer A, Koköfer A, Bataar O, Gradwohl-Matis I, Dankl D, Bakker J, et al. Changes in peripheral perfusion relate to visceral organ perfusion in early septic shock: A pilot study. *J Crit Care.* (2016) 35:105–9. doi: 10.1016/j.jcrc.2016.05.007
84. Freedlander SO, Lenhart CH. Clinical observations on the capillary circulation. *Arch Intern Med.* (1922) 29:12–32. doi: 10.1001/archinte.1922.00110010017002
85. Weinberg JR, Boyle P, Thomas K, Murphy K, Tooke JE, Guz A. Capillary blood cell velocity is reduced in fever without hypotension. *Int J Microcirc Clin Exp.* (1991) 10:13–9.
86. De Backer D. Dubois M-J. Assessment of the microcirculatory flow in patients in the intensive care unit. *Curr Opin Crit Care.* (2001) 7:200–3. doi: 10.1097/00075198-200106000-00010
87. Dilken O, Ergin B, Ince C. Assessment of sublingual microcirculation in critically ill patients: consensus and debate. *Ann Transl Med.* (2020) 8:793–793. doi: 10.21037/atm.2020.03.222
88. Sherman H, Klausner S, Cook WA. Incident dark-field illumination: a new method for microcirculatory study. *Angiology.* (1971) 22:295–303. doi: 10.1177/000331977102200507
89. Mancini DM, Bolinger L, Li H, Kendrick K, Chance B, Wilson JR. Validation of near-infrared spectroscopy in humans. *J Appl Physiol.* (1994) 77:2740–7. doi: 10.1152/jappl.1994.77.6.2740
90. Creteur J, Carollo T, Soldati G, Buchele G, De Backer D, Vincent J-L. The prognostic value of muscle StO2 in septic patients. *Intensive Care Med.* (2007) 33:1549–56. doi: 10.1007/s00134-007-0739-3
91. Vesterager P. Transcutaneous pO2 electrode. *Scand J Clin Lab Invest Suppl.* (1977) 146:27–30. doi: 10.3109/00365517709098929
92. Hernandez G, Luengo C, Bruhn A, Kattan E, Friedman G, Ospina-Tascon GA, et al. When to stop septic shock resuscitation: clues from a dynamic perfusion monitoring. *Ann Intensive Care.* (2014) 4:30. doi: 10.1186/s13613-014-0030-z
93. Kawaguchi R, Nakada T, Oshima T, Shinozaki M, Nakaguchi T, Haneishi H, et al. Optimal pressing strength and time for capillary refilling time. *Critical Care.* (2019) 23:4. doi: 10.1186/s13054-018-2295-3
94. Ebert RV, Stead EA. Circulatory failure in acute infections. *J Clin Invest.* (1941) 20:671–9. doi: 10.1172/JCI101260
95. Bourcier S, Pichereau C, Boelle P-Y, Nemlaghi S, Dubée V, Lejour G, et al. Toe-to-room temperature gradient correlates with tissue perfusion and predicts outcome in selected critically ill patients with severe infections. *Ann Intensive Care.* (2016) 6:63. doi: 10.1186/s13613-016-0164-2
96. Evans L, Rhodes A, Alhazzani W, Antonelli M, Coopersmith CM, French C, et al. Surviving sepsis campaign: international guidelines for management of sepsis and septic shock 2021. *Crit Care Med.* (2021) 49:e1063.
97. Duranteau J, Sitbon P, Teboul JL, Vicaut E, Anguel N, Richard C, et al. Effects of epinephrine, norepinephrine, or the combination of norepinephrine and dobutamine on gastric mucosa in septic shock. *Crit Care Med.* (1999) 27:893–900. doi: 10.1097/00003246-199905000-00021
98. Young JD, Cameron EM. Dynamics of skin blood flow in human sepsis. *Intensive Care Med.* (1995) 21:669–74. doi: 10.1007/BF01711546
99. Yura T, Yuasa S, Fukunaga M, Badr KF, Matsuo H. Role for Doppler ultrasound in the assessment of renal circulation: effects of dopamine and dobutamine on renal hemodynamics in humans. *Nephron.* (1995) 71:168–75. doi: 10.1159/000188707
100. Schneider AW, Kalk JF, Klein CP. Hepatic arterial pulsatility index in cirrhosis: correlation with portal pressure. *J Hepatol.* (1999) 30:876–81. doi: 10.1016/S0168-8278(99)80142-1
101. Macdonald SPJ, Kinnear FB, Arendts G, Ho KM, Fatovich DM. Near-infrared spectroscopy to predict organ failure and outcome in sepsis: the Assessing Risk in Sepsis using a Tissue Oxygen Saturation (ARISTOS) study. *Eur J Emerg Med.* (2019) 26:174–9. doi: 10.1097/MEJ.0000000000000535
102. De Backer D, Hollenberg S, Boerma C, Goedhart P, Büchele G, Ospina-Tascon G, et al. How to evaluate the microcirculation: report of a round table conference. *Crit Care.* (2007) 11:R101–R101. doi: 10.1186/cc6118
103. Verdant CL, De Backer D, Bruhn A, Clausi CM, Su F, Wang Z, et al. Evaluation of sublingual and gut mucosal microcirculation in sepsis: a quantitative analysis. *Crit Care Med.* (2009) 37:2875–81. doi: 10.1097/CCM.0b013e3181b029c1
104. Boerma EC, van der Voort PHJ, Spronk PE, Ince C. Relationship between sublingual and intestinal microcirculatory perfusion in patients with abdominal sepsis. *Crit Care Med.* (2007) 35:1055–60. doi: 10.1097/01.CCM.0000259527.89927.F9
105. Ince C, Boerma EC, Cecconi M, De Backer D, Shapiro NI, Duranteau J, et al. Second consensus on the assessment of sublingual microcirculation in critically ill patients: results from a task force of the European Society of Intensive Care Medicine. *Intensive Care Med.* (2018) 44:281–99. doi: 10.1007/s00134-018-5070-7
106. Aykut G, Veenstra G, Scorcella C, Ince C, Boerma C. Cytocam-IDF (incident dark field illumination) imaging for bedside monitoring of the microcirculation. *Intensive Care Med Exp.* (2015) 3:40. doi: 10.1186/s40635-015-0040-7
107. Gilbert-Kawai E, Coppel J, Bountziouka V, Ince C, Martin D. Caudwell Xtreme Everest and Xtreme Everest 2 Research Groups. A comparison of the quality of image acquisition between the incident dark field and sidestream dark field video-microscopes. *BMC Med Imaging.* (2016) 16:10. doi: 10.1186/s12880-015-0078-8
108. van Elteren HA, Ince C, Tibboel D, Reiss IKM, de Jonge RCJ. Cutaneous microcirculation in preterm neonates: comparison between sidestream dark field (SDF) and incident dark field (IDF) imaging. *J Clin Monit Comput.* (2015) 29:543–8. doi: 10.1007/s10877-015-9708-5
109. Ait-Oufella H, Bige N, Boelle PY, Pichereau C, Alves M, Bertinchamp R, et al. Capillary refill time exploration during septic shock. *Intensive Care Med.* (2014) 40:958–64. doi: 10.1007/s00134-014-3326-4
110. Lima A, Jansen TC, van Bommel J, Ince C. Bakker J. The prognostic value of the subjective assessment of peripheral perfusion in critically ill patients. *Crit Care Med.* (2009) 37:934–8. doi: 10.1097/CCM.0b013e31819869db
111. Hernández G, Ospina-Tascón GA, Damiani LP, Estenssoro E, Dubin A, Hurtado J, et al. Effect of a resuscitation strategy targeting peripheral perfusion status vs. serum lactate levels on 28-day mortality among patients with septic shock: the ANDROMEDA-SHOCK randomized clinical trial. *JAMA.* (2019) 321:654. doi: 10.1001/jama.2019.0071
112. Ait-Oufella H, Bourcier S, Alves M, Galbois A, Baudel J-L, Margetis D, et al. Alteration of skin perfusion in mottling area during septic shock. *Ann Intensive Care.* (2013) 3:31. doi: 10.1186/2110-5820-3-31
113. Ait-Oufella H, Lemoinne S, Boelle PY, Galbois A, Baudel JL, Lemant J, et al. Mottling score predicts survival in septic shock. *Intensive Care Med.* (2011) 37:801–7. doi: 10.1007/s00134-011-2163-y
114. Dumas G, Lavillegrand J-R, Joffre J, Bigé N. de-Moura EB, Baudel J-L, et al. Mottling score is a strong predictor of 14-day mortality in septic patients whatever vasopressor doses and other tissue perfusion parameters. *Crit Care.* (2019) 23:211. doi: 10.1186/s13054-019-2496-4
115. de Moura EB, Amorim FF, da Cruz Santana AN, Kanhouche G, de Souza Godoy LG, de Jesus Almeida L, et al. Skin mottling score as a predictor of 28-day mortality in patients with septic shock. *Intensive Care Med.* (2016) 42:479–80. doi: 10.1007/s00134-015-4184-4
116. Lavillegrand J-R, Dumas G, Bigé N, Zafimahazo D, Guidet B, Maury E, et al. Should we treat mild hypotension in septic patients in the absence of peripheral tissue hypoperfusion? *Intensive Care Med.* (2018) 44:1593–4. doi: 10.1007/s00134-018-5315-5
117. Legrand M, De Backer D, Dépret F, Ait-Oufella H. Recruiting the microcirculation in septic shock. *Ann Intensive Care.* (2019) 9:102, s13613-019-0577–9. doi: 10.1186/s13613-019-0577-9
118. Byrne L, Obonyo NG, Diab SD, Dunster KR, Passmore MR, Boon A-C, et al. Unintended Consequences: Fluid Resuscitation Worsens Shock in an Ovine Model of Endotoxemia. *Am J Respir Crit Care Med.* (2018) 198:1043–54. doi: 10.1164/rccm.201801-0064OC
119. Ospina-Tascon G, Neves AP, Occhipinti G, Donadello K, Büchele G, Simion D, et al. Effects of fluids on microvascular perfusion

in patients with severe sepsis. *Intensive Care Med.* (2010) 36:949–55. doi: 10.1007/s00134-010-1843-3
120. Hippensteel JA, Uchimido R, Tyler PD, Burke RC, Han X, Zhang F, et al. Intravenous fluid resuscitation is associated with septic endothelial glycocalyx degradation. *Crit Care.* (2019) 23:259. doi: 10.1186/s13054-019-2534-2
121. Hariri G, Joffre J, Deryckere S, Bigé N, Dumas G, Baudel J-L, et al. Albumin infusion improves endothelial function in septic shock patients: a pilot study. *Intensive Care Med.* (2018) 44:669–71. doi: 10.1007/s00134-018-5075-2
122. Boerma EC, Ince C. The role of vasoactive agents in the resuscitation of microvascular perfusion and tissue oxygenation in critically ill patients. *Intensive Care Med.* (2010) 36:2004–18. doi: 10.1007/s00134-010-1970-x
123. Secchi A, Ortanderl JM, Schmidt W, Walther A, Gebhard MM, Martin E, et al. Effects of dobutamine and dopexamine on hepatic micro- and macrocirculation during experimental endotoxemia: an intravital microscopic study in the rat. *Crit Care Med.* (2001) 29:597–600. doi: 10.1097/00003246-200103000-00023
124. Secchi A, Wellmann R, Martin E, Schmidt H. Dobutamine maintains intestinal villus blood flow during normotensive endotoxemia: an intravital microscopic study in the rat. *J Crit Care.* (1997) 12:137–41. doi: 10.1016/S0883-9441(97)90043-5
125. De Backer D, Zhang H, Manikis P, Vincent JL. Regional effects of dobutamine in endotoxic shock. *J Surg Res.* (1996) 65:93–100. doi: 10.1006/jsre.1996.0349
126. De Backer D, Creteur J, Dubois M-J, Sakr Y, Koch M, Verdant C. Vincent J-L. The effects of dobutamine on microcirculatory alterations in patients with septic shock are independent of its systemic effects*. *Crit Care Med.* (2006) 34:403–8. doi: 10.1097/01.CCM.0000198107.61493.5A
127. Hernandez G, Bruhn A, Luengo C, Regueira T, Kattan E, Fuentealba A, et al. Effects of dobutamine on systemic, regional and microcirculatory perfusion parameters in septic shock: a randomized, placebo-controlled, double-blind, crossover study. *Intensive Care Med.* (2013) 39:1435–43. doi: 10.1007/s00134-013-2982-0
128. Morelli A, Donati A, Ertmer C, Rehberg S, Lange M, Orecchioni A, et al. Levosimendan for resuscitating the microcirculation in patients with septic shock: a randomized controlled study. *Crit Care.* (2010) 14:R232. doi: 10.1186/cc9387
129. Zhang H, Smail N, Cabral A, Rogiers P, Vincent JL. Effects of norepinephrine on regional blood flow and oxygen extraction capabilities during endotoxic shock. *Am J Respir Crit Care Med.* (1997) 155:1965–71. doi: 10.1164/ajrccm.155.6.9196103
130. Bellomo R, Kellum JA, Wisniewski SR, Pinsky MR. Effects of norepinephrine on the renal vasculature in normal and endotoxemic dogs. *Am J Respir Crit Care Med.* (1999) 159:1186–92. doi: 10.1164/ajrccm.159.4.9802055
131. Regueira T, Bänziger B, Djafarzadeh S, Brandt S, Gorrasi J, Takala J, et al. Norepinephrine to increase blood pressure in endotoxaemic pigs is associated with improved hepatic mitochondrial respiration. *Crit Care.* (2008) 12:R88. doi: 10.1186/cc6956
132. Krouzecky A, Matejovic M, Radej J, Rokyta R, Novak I. Perfusion pressure manipulation in porcine sepsis: effects on intestinal hemodynamics. *Physiol Res.* (2006) 55:527–33. doi: 10.33549/physiolres.930821
133. Dubin A, Pozo MO, Casabella CA, Pálizas F, Murias G, Moseinco MC, et al. Increasing arterial blood pressure with norepinephrine does not improve microcirculatory blood flow: a prospective study. *Crit Care.* (2009) 13:R92. doi: 10.1186/cc7922
134. LeDoux D, Astiz ME, Carpati CM, Rackow EC. Effects of perfusion pressure on tissue perfusion in septic shock. *Crit Care Med.* (2000) 28:2729–32. doi: 10.1097/00003246-200008000-00007
135. Borrelli E, Roux-Lombard P, Grau GE, Girardin E, Ricou B, Dayer J-M, et al. Plasma concentrations of cytokines, their soluble receptors, and antioxidant vitamins can predict the development of multiple organ failure in patients at risk. *Crit Care Med.* (1996) 24:392–7. doi: 10.1097/00003246-199603000-00006
136. Medical Respiratory Intensive Care Unit Nursing, Fowler AA, Syed AA, Knowlson S, Sculthorpe R, Farthing D, et al. Phase I safety trial of intravenous ascorbic acid in patients with severe sepsis. *J Transl Med*. (2014) 12:32. doi: 10.1186/1479-5876-12-32
137. Na W, Shen H, Li Y, Qu D. Hydrocortisone, ascorbic acid, and thiamine (HAT) for sepsis and septic shock: a meta-analysis with sequential trial analysis. *J Intens Care.* (2021) 9:75. doi: 10.1186/s40560-021-00589-x
138. Lavillegrand J-R, Raia L, Urbina T, Hariri G, Gabarre P, Bonny V, et al. Vitamin C improves microvascular reactivity and peripheral tissue perfusion in septic shock patients. *Crit Care.* (2022) 26:25. doi: 10.1186/s13054-022-03891-8
139. Morelli A, Ertmer C, Westphal M, Rehberg S, Kampmeier T, Ligges S, et al. Effect of Heart Rate Control With Esmolol on Hemodynamic and Clinical Outcomes in Patients With Septic Shock: A Randomized Clinical Trial. *JAMA.* (2013) 310:1683. doi: 10.1001/jama.2013.278477
140. Morelli A, Donati A, Ertmer C, Rehberg S, Kampmeier T, Orecchioni A, et al. Microvascular Effects of Heart Rate Control With Esmolol in Patients With Septic Shock: A Pilot Study*. *Crit Care Med.* (2013) 41:2162–8. doi: 10.1097/CCM.0b013e31828a678d

Conflict of Interest: LZ has received a research grant from Jazz Pharmaceuticals, not related to this study.

The remaining author declares that the research was conducted in the absence of any commercial or financial relationships that could be construed as a potential conflict of interest.

Publisher's Note: All claims expressed in this article are solely those of the authors and do not necessarily represent those of their affiliated organizations, or those of the publisher, the editors and the reviewers. Any product that may be evaluated in this article, or claim that may be made by its manufacturer, is not guaranteed or endorsed by the publisher.

frontiers | Frontiers in Medicine

REVIEW
published: 08 July 2022
doi: 10.3389/fmed.2022.898592

Endothelial Glycocalyx Degradation in Critical Illness and Injury

Eric K. Patterson[1], *Gediminas Cepinskas*[1,2] *and Douglas D. Fraser*[1,3,4,5,6]*

[1] Centre for Critical Illness Research, Lawson Health Research Institute, London, ON, Canada, [2] Department of Medical Biophysics, Western University, London, ON, Canada, [3] Department of Pediatrics, Western University, London, ON, Canada, [4] Department of Physiology and Pharmacology, Western University, London, ON, Canada, [5] Department of Clinical Neurological Sciences, Western University, London, ON, Canada, [6] Children's Health Research Institute, Lawson Health Research Institute, London, ON, Canada

The endothelial glycocalyx is a gel-like layer on the luminal side of blood vessels that is composed of glycosaminoglycans and the proteins that tether them to the plasma membrane. Interest in its properties and function has grown, particularly in the last decade, as its importance to endothelial barrier function has come to light. Endothelial glycocalyx studies have revealed that many critical illnesses result in its degradation or removal, contributing to endothelial dysfunction and barrier break-down. Loss of the endothelial glycocalyx facilitates the direct access of immune cells and deleterious agents (e.g., proteases and reactive oxygen species) to the endothelium, that can then further endothelial cell injury and dysfunction leading to complications such as edema, and thrombosis. Here, we briefly describe the endothelial glycocalyx and the primary components thought to be directly responsible for its degradation. We review recent literature relevant to glycocalyx damage in several critical illnesses (sepsis, COVID-19, trauma and diabetes) that share inflammation as a common denominator with actions by several common agents (hyaluronidases, proteases, reactive oxygen species, etc.). Finally, we briefly cover strategies and therapies that show promise in protecting or helping to rebuild the endothelial glycocalyx such as steroids, protease inhibitors, anticoagulants and resuscitation strategies.

Keywords: glycocalyx, inflammation, sepsis, trauma, endothelium

OPEN ACCESS

Edited by:
W. Conrad Liles, University of Washington, United States

Reviewed by:
Takeshi Wada, Hokkaido University, Japan
Jeremie Joffre, University of California, San Francisco, United States

***Correspondence:**
Douglas D. Fraser
douglas.fraser@lhsc.on.ca

Specialty section:
This article was submitted to Intensive Care Medicine and Anesthesiology, a section of the journal Frontiers in Medicine

Received: *17 March 2022*
Accepted: *14 June 2022*
Published: *08 July 2022*

Citation:
Patterson EK, Cepinskas G and Fraser DD (2022) Endothelial Glycocalyx Degradation in Critical Illness and Injury. Front. Med. 9:898592. doi: 10.3389/fmed.2022.898592

GLYCOCALYX OVERVIEW

The glycocalyx is a complex, negatively charged, gel-like layer on the luminal side of endothelial cells (ECs), which is composed of glycosaminoglycans (GAGs) that are bound to membrane-spanning proteins that anchor the structure. It is a dynamic structure, with its various components consistently shed and replaced; in particular, hyaluronic acid (HA) is turned over rapidly (1). The structure of the glycocalyx depends on the organ and type of endothelium, for example: the endothelium can be continuous, fenestrated or sinusoid (2); the thickness of the glycocalyx varies with blood vessel size, ranging from approximately 0.5 μm thick in capillaries (3) to 2.5 μm in arteries (4); and the pulmonary endothelial glycocalyx can be more than 2 times thicker than in muscle (5).

The GAGs that constitute the glycocalyx are primarily heparan sulfate (HS), chondroitin sulfate (CS) and hyaluronic acid (also called hyaluronan or hyaluron). HS and CS are sulfated, and covalently bound to trans-membrane syndecans-1,4 or membrane-anchored glypican-1. HA is not sulfated, and is a much larger polymer than the former two, with a molecular weight often in the hundreds of kilodaltons to megadalton range. Additionally, hyaluronic acid is

non-covalently bound to multiple membrane-spanning CD44 molecules that are cell-surface glycoproteins involved in cell–cell interactions, cell adhesion, and migration (6) (**Figure 1**).

The glycocalyx has a net negative charge that helps determine interactions with proteins. In particular, it can adsorb positively charged regions of some plasma proteins and compliments endothelial barrier function by acting as the first barrier to plasma protein (which are mostly negatively charged, e.g., albumin) leakage into the interstitium. Further, by preventing protein leak from the vasculature, the glycocalyx helps to maintain osmotic pressure toward the blood vessel's lumen, thereby inhibiting water passage into tissues. Finally, the glycocalyx is anti-thrombotic/profibrinolytic, as well as anti-neutrophil/leukocyte attachment. These latter mechanisms are achieved through HS binding of positively charged regions on antithrombin (7, 8) and by burying cellular adhesion molecules within the depth of the intact glycocalyx (9). HS in the glycocalyx not only binds antithrombin, but also enhances its inhibition of thrombin and factors IXa, Xa (7) and XIa (10).

Exposure to inflammatory stimuli, including TNF-α (11) and endotoxin (12), as well as inflammatory states such as sepsis (13, 14), degrade the glycocalyx by triggering release or activity of various enzymes and/or reactive oxygen species (ROS) (**Figure 2**). Glycocalyx degradation exposes the underlying cell adhesion molecules, thereby promoting leukocyte (15) and platelet (16) adhesion and inducing a pro-thrombotic state. The barrier function of the endothelium is compromised by glycocalyx degradation, increasing its permeability to fluids and macromolecules, as well as leukocyte migration. Additionally, denuding the glycocalyx exacerbates EC exposure to proteases capable of degrading GAG-anchoring proteins, or cell junctions. A non-exhaustive list of agents which are thought to degrade various components of the endothelial glycocalyx in disease is provided in **Table 1**.

Hyaluronic Acid

The inflammatory mechanism(s) and enzyme(s) that are responsible for HA degradation in the vasculature are somewhat controversial. Hyaluronidase-1 was characterized from serum nearly 30 years ago (17), but its pH optimum of approximately 3.5 (17) suggests that it would be primarily active in lysosomes and would have limited activity in plasma. Indeed, data refutes hyaluronidase-1 as a sheddase in sepsis (18). Hyaluronidase-2 appears to have a membrane-tethered form (19), but again its pH optimum suggests limited activity in plasma, though platelet surface-bound hyaluronidase-2 degrades high molecular weight HA on the endothelial surface into pro-inflammatory fragments under neutral pH *in vitro* (20). Further, when hyaluronidase-2 and CD44 are co-expressed on HEK293 cells they extracellularly degrade HA with a pH optimum between 6.0 and 7.0 (21). The relatively low pH of inflamed and/or poorly perfused tissues could impart significant activity to these enzymes, especially hyaluronidase-2 since endothelial cells co-express CD44. More recently the protein transmembrane 2 (TMEM2) was shown to have significant hyaluronidase activity (22). TMEM2 is highly expressed in endothelial cells, at least of dermal, lymph or liver origin (22, 23) and functions to degrade free plasma HA in the liver (23). At present, it is unclear if TMEM2 instigates HA shedding or degradation during inflammation in non-liver blood vessels.

Changes in cell-surface HA during inflammation is not limited to degradation only. HA can form cable-like structures on the endothelial surface that serve as an attachment site for monocytes and platelets regardless of their inflammatory status (19). In addition to enzymatic cleavage, ROS such as hydroxyl radicals, hypochlorous acid, and peroxynitrite directly degrade HA (19, 24).

Heparan Sulfate

Heparanase-1 is expressed in platelets (25) and neutrophils (26), and it is located extracellularly as well as in lysosomes (27). It degrades HS at sites of inflammation or injury, thereby contributing to leukocyte attraction (27). Heparanase-1 activity is optimal at the acidic pH of approximately 6.4, and is somewhat active below pH 6.8 (28), suggesting it has activity in the relatively low pH environment of inflammation. Additionally, heparan sulfate is cleaved by connective tissue activating peptide-III (CTAP-III), an N-truncated version of CXCL7 with endoglycocidic heparinase activity (29). CTAP-III is expressed in both platelets and neutrophils at similar levels to heparanase-1 (27, 29). Despite the optimal pH of 5.8, CTAP-III has significant activity up to approximately pH 7.0 (29) suggesting it too has activity in inflammatory environments.

Chondroitin Sulfate

There are 3 known human hydrolases capable of degrading CS outside of lysosomes; SPAM1 (also called PH-20, located mostly in the sperm acrosome), hyaluronidase-1 (see above) and hyaluronidase-4 (30). Hyaluronidase-4, (also called CS hydrolase) has a membrane-bound form present in neutrophils that preferentially hydrolyze CS over HA (30).

Glycosaminoglycan-Related Effects

In addition to the direct mechanical and spatial effects, removing HA from the endothelial surface has other pro-inflammatory and pro-thrombotic effects, such as removing proteins bound or adsorbed to the glycocalyx. HA binds protease inhibitors such as the inter-alpha-trypsin inhibitors, and tumor necrosis factor-stimulated gene 6, which reduce neutrophil adhesion, ROS generation, hyaluronidase activity, complement activation and contributes to matrix metalloproteinase (MMP) inhibition (19, 31). Additionally, degraded HA fragments ($<$ 500 kDa) appear to have pro-inflammatory properties of their own (19). Tissue factor pathway inhibitor (TFPI) binds heparan sulfate molecules in the glycocalyx (32), helping it to maintain close proximity to the endothelium; as HS is removed, the pro and anti-thrombotic balance tilts toward complement activation and thrombus formation. Additionally, hyaluronidase treatment of primary human pulmonary vascular endothelial cells *in vitro* results in decreased NO production (33), which is necessary for platelet adhesion to the endothelial surface.

Glycosaminoglycan-Anchoring Proteins

Glycocalyx compromise is not only due to GAG degradation, but also *via* cleavage of the proteins that anchor the GAGs to the endothelial plasma membranes. Pre-treating tissues with the

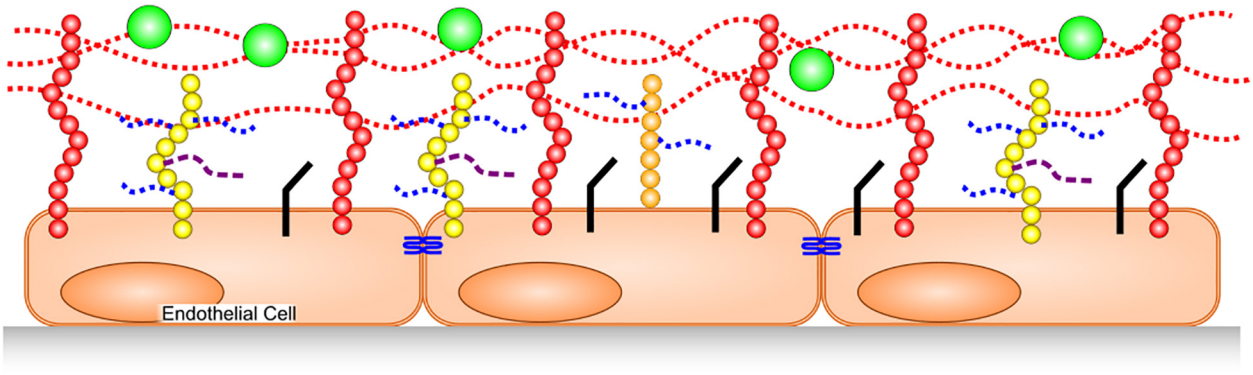

FIGURE 1 | Glycocalyx Structure. HA, dotted red lines, is bound to CD44 in membranes (red). HS (dotted blue) and CS (dashed purple) are covalently bound to syndecans (yellow) and glypican-1 (orange). Junctional proteins (blue), cellular adhesion molecules (black) adsorbed plasma proteins (green).

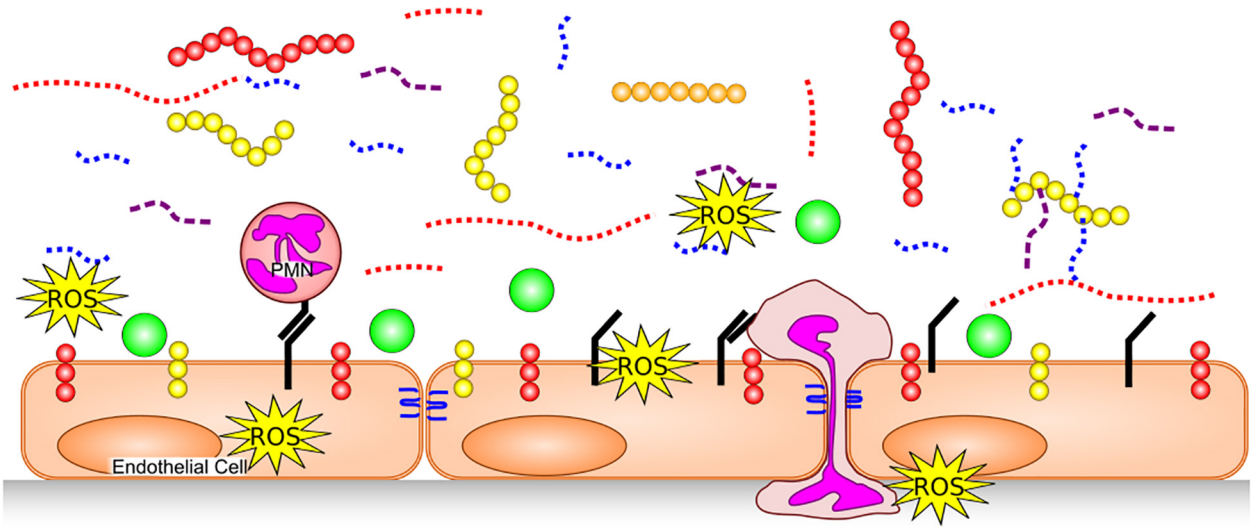

FIGURE 2 | Glycocalyx Degradation. The endothelial glycocalyx is degraded by proteases [which remove core proteins' ectodomains: syndecans (yellow), glipicans (orange) and CD44 (red)], GAG-degrading enzymes and ROS, leaving free fragments of HA (red dotted), HS (blue dotted) and CS (purple dashed). This exposes cellular adhesion molecules (black) on the endothelial surface, allowing easier binding of white blood cells [e.g., neutrophils (PMNs)] and platelets. Neutrophils can release additional proteases, further damaging core glycocalyx proteins, junctional proteins (blue) and produce additional ROS. With a degraded glycocalyx, blood flows closer to the endothelial cells and plasma proteins (green), can access the endothelial surface.

broad-spectrum MMP inhibitor doxycycline inhibited glycocalyx shedding and leukocyte adhesion in a murine inflammation model (34), demonstrating the crucial role for MMP-induced glycocalyx breakdown. More specifically, the membrane-bound MMP14 has been shown to cleave syndecan-1 (35) and CD44 (36). Additionally, syndecan-1 and syndecan-4 are cleaved by MMPs 2, 3, 7, 9, and 14, (37) as well as ADAM17 (38).

DISEASE-SPECIFIC GLYCOCALYX ALTERATIONS

Several major glycocalyx components have been used as biomarkers to distinguish sub-populations in critical illness and injury, as well as to prognosticate outcomes. A list of the literature cited herein, with the component studied, biochemical thresholds and/or statistical value is provided in **Table 2**.

Sepsis

Sepsis is defined as life-threatening organ dysfunction caused by a dysregulated host response to infection (39). Degradation of the glycocalyx encountered during sepsis conforms to the pattern seen in many severe inflammatory diseases. The systemic pro-inflammatory stimuli (e.g., cytokines, lipopolysaccharide, ROS) produced during sepsis are the initiating factors in a feed-forward cascade of inflammation and glycocalyx degradation (40, 41). The degraded glycocalyx allows the binding and extravasation of leukocytes, as well as platelet recruitment (40, 41), thereby resulting in further inflammation and greater risk of thrombosis. Further, glycocalyx loss leads to capillary leaking that contributes

TABLE 1 | Glycocalyx-degrading agents in critical illness.

Component	Degrading agent during critical illness	References
Hyaluronic acid	HYAL1, HYAL2, TMEM2, ROS	(17, 20–24)
Heparan sulfate	HYAL1, HEPase1, CTAP-III	(25–27, 29)
Chondroitin sulfate	HYAL4	(30)
Syndecan-1	MMP2,3,7,9, and 14, ADAM17	(35, 37, 38)
Syndecan-4	MMP2,3,7,9, and 14, ADAM17	(37, 38)
CD44	ADAM15, MMP14	(36, 126)

ADAM, a disintegrin and metalloproteinase; CTAP-III, connective tissue activating peptide-III; HEPase1, Heparanase-1; HYAL, hyaluronidase; MMP, matrix metalloproteinase; TMEM2, transmembrane 2; ROS, reactive oxygen species.

TABLE 2 | Glycocalyx components used as biomarkers.

Component	Threshold/ Value	Population, measure	References
PBR	AUC = 0.778	Sepsis, in-hospital mortality	(42)
	AUC = 0.75	COVID-19, 60-day mortality	(56)
Syndecan-1	OR = 1.850	Sepsis, in-hospital mortality	(14)
	AUC = 0.781	Sepsis, in-hospital mortality	(42)
	898 ng/mL, AUC = 0.801	Sepsis, 90-day mortality	(44)
	HR = 1.95	Septic shock, 90-day mortality	(46)
	813.8 ng/mL, AUC = 0.783	COVID-19, in-hospital mortality	(61)
	$p < 0.0001$	COVID-19, critical vs severe	(63)
	OR = 1.01, p = 0.043	Trauma, 30-day mortality	(74)
	40 ng/mL, AUC = 0.71, OR = 2.23	Trauma, 30-day mortality	(76)
	$p < 0.05$	T1D, nephropathy vs not	(95)
	$p < 0.0001$	T1D, microalbuminuria vs not	(96)
Hyaluronic acid	p = 0.006	Sepsis, 90-day mortality	(43)
	441 ng/mL, AUC = 0.827	Sepsis, 90-day mortality	(44)
	$p < 0.001$	COVID-19, ICU vs non-ICU	(60)
	$p < 0.05$	Trauma, coagulopathy vs not	(77)
	$p < 0.05$	T1D, microalbuminuria vs not	(90)
Heparan sulfate	p = 0.02	Sepsis, 90-day mortality	(43)
	$p < 0.05$	Sepsis, 28-day mortality	(45)
	$p < 0.05$	COVID-19, ICU vs non-ICU	(60)
	$p < 0.001$	COVID-19, critical vs moderate	(63)
	$p < 0.05$	Trauma, autoheparinization vs not	(71)

AUC, area under the curve for a receiver-operator characteristic; HR, hazard ratio; ICU, intensive care unit; OR, odds ratio; PBR, perfused boundary region, a measure of glycocalyx thickness; T1D, type-1 diabetes.

to systemic edema, hypovolemia, and along with thrombi, contribute to circulatory dysfunction (41). Ultimately, the above events result in hypoperfusion of tissues and organ damage that is a hallmark of sepsis (40, 41).

Measurements of the perfused boundary region in sublingual micro-vessels (a measurement of glycocalyx thickness), showed the glycocalyx is thinner in sepsis non-survivors than survivors, and admission perfused boundary region was associated with hospital mortality (AUC 0.778) (42).

On the day of intensive care unit (ICU) admission, sepsis patients showed a significantly higher median plasma concentration of HA and HS compared to controls, with those who died in the next 90 days displaying a significantly higher concentration within the sepsis population (43). In the same study, plasma HA and HS correlated with IL-6, IL-10, and sequential organ failure assessment (SOFA) score. A later study confirmed higher concentrations of HA, as well as syndecan-1, in sepsis patients at multiple time points of illness (44). HA and syndecan-1 concentrations were also higher for the first five ICU days in severe sepsis (sepsis with acute organ dysfunction) and septic shock (sepsis with refractory hypotension despite adequate fluid loading) patients, when compared to sepsis. Furthermore, HA and syndecan-1 were elevated for at least the first 3 days in septic shock vs. severe sepsis patients. More importantly, in survivors, the HA and syndecan-1 concentrations tended to decrease over the ICU stay, while they tended to slightly increase or stay the same in non-survivors. Both glycocalyx components were correlated with Acute Physiologic Assessment and Chronic Health Evaluation II (APACHE II) and SOFA scores; cutoff values of < 441 ng/mL HA on ICU day 7 or < 898 ng/mL syndecan-1 on ICU day 5 were found to predict 90 and 87% survival, respectively (44). Another study showed that plasma HA is increased in septic shock patients compared to healthy controls, but not pancreatitis patients (18). Interestingly, this same study showed that plasma hyaluronidase activity was actually lower in septic shock patients, compared to healthy controls. While plasma hyaluronidase measurements may prove to be interesting diagnostically or functionally, it's not clear if the plasma hyaluronidase (HYAL1), can act as a HA sheddase in either sepsis or other inflammatory diseases. HYAL2 is membrane-bound and has a pH optimum closer to that of inflamed tissues, though its activity would not be present in plasma tests due to its anchoring in the plasma membrane.

Patients with non-pulmonary sepsis, on mechanical ventilation and with an APACHE II $\geq$ 25, had higher plasma syndecan-1 concentrations on day 2 of ICU admission with levels that were significantly correlated with acute respiratory distress syndrome (ARDS), though this was not true of pulmonary sepsis patients (pneumonia or aspiration of gastric contents) (14). In those patients that developed ARDS, syndecan-1 levels were higher than in those that developed ARDS from non-pulmonary sepsis. Additionally, syndecan-1 levels were associated with vasopressor requirements, and circulatory, hepatic, renal, and coagulation failures (14). Moreover, higher syndecan-1 concentrations were independently predictive of in-hospital mortality. There was no correlation between syndecan-1 and plasma myeloperoxidase concentrations, used as a marker of neutrophil activation (a source of proteases).

While syndecan-1, HA and HS were significantly higher in septic shock patients compared to sepsis patients, and syndecan-1 was good at predicting progression to septic shock (81.8% sensitivity, 78.3% specificity), interestingly, it was not higher in non-survivors, vs. survivors (45). In contrast, the authors did identify significantly increased plasma concentrations of HS in non-survivors, compared to survivors (204.5 vs. 158.9 ng/mL). All three glycocalyx components measured had a weak

to moderate correlation with disease severity as assessed by either APACHE II or SOFA scores ($r \leq 0.5$) (45). Further, plasma syndecan-1 and HA concentrations were found to be significantly higher in a subset of patients with disseminated intravascular coagulation (DIC), and may be useful predictors of DIC, underscoring the importance of the anti-fibrinolytic actions attributed to the glycocalyx.

More recently, syndecan-1 plasma concentrations in septic shock patients were found to be more than double that of healthy volunteers on day 1 of ICU admission and were significantly associated with the general SOFA score and the coagulation SOFA subscale (46). Syndecan-1 concentrations were significantly associated with the need for renal replacement therapy, or slow dialysis provided to hemodynamically unstable patients, as well as the incidence of coagulation failure and 90-day mortality (46). Interestingly, many of these associations were found oppositely correlated with sphingosine 1-phosphate which protects syndecan-1 from shedding.

In sepsis cases, the coagulation system can become pathologically activated, resulting in DIC and thrombosis. Whole-blood measurements of coagulation in sepsis patients can reveal a hypo-, normal or hyper-coagulable state (47), while traditional lab tests may show the plasma is not hypercoagulable *per se* (48), leading to the hypothesis that endothelial dysfunction may be a major contributing factor to DIC. Indeed, glycocalyx degradation upsets the interplay between blood and the anti-coagulation/anti-thrombotic properties of the glycocalyx. In particular, removing HS will also remove the bound antithrombin from the endothelial surface, resulting in increased fibrin formation, thereby allowing thrombin easier access to membrane-spanning thrombomodulin to activate protein C. HS shedding and proteolysis also leads to decreased HS-bound TFPI in sepsis (49).

Monitoring the progression of glycocalyx damage markers (e.g., HA or syndecan-1) may prove to be useful to assess the progression of sepsis and predict survival. Currently, there is no single biomarker proven to predict sepsis progression or mortality, and considering the complexity of sepsis, a single biomarker is not likely to emerge. So far, the enzyme(s) responsible for HA shedding/degradation from the endothelium have not been positively identified. More work is required to positively identify the precise mechanism of HA shedding, whether it's enzymatic or chemically induced (e.g., ROS).

Coronavirus Disease 2019

While Coronavirus disease 2019 (COVID-19) is a newly emerged disease associated with SARS-CoV-2, multiple studies quickly identified microvascular injury and glycocalyx degradation as major pathophysiological disease mechanisms. Similar to bacterial sepsis, COVID-19 glycocalyx damage follows a familiar pattern and the glycocalyx degradation and endothelial damage seen in COVID-19 leads to a pro-thrombotic state (33, 50, 51) that in severe cases results in multi-organ thrombosis (50). Patient thrombosis has a negative effect on patient outcomes (52), with a thrombotic event being independently associated with mortality in COVID-19 patients (53, 54). Therapeutic doses of heparin reduce the likelihood of progression to intubation and death in non-critically ill hospitalized COVID-19 patients (52), highlighting the importance of thrombosis in COVID-19 disease.

Early in the pandemic, we investigated plasma from age- and sex-matched subjects, including COVID-19 ICU patients, non-COVID-19 ICU patients and healthy controls (33). Compared with healthy control subjects, COVID-19 positive patients had higher plasma von Willebrand factor, and glycocalyx-degradation products (chondroitin sulfate and syndecan-1). When compared with COVID-19 negative sepsis patients, COVID-19 positive patients had persistently higher soluble P-selectin, hyaluronic acid, and syndecan-1, particularly on ICU day 3 and thereafter. In fact, syndecan-1 continued to increase over the 7 days that COVID-19 patients were tested. Our data suggested that glycocalyx degradation was greater in COVID-19 patients, as opposed to age- and sex-matched non-COVID-19 ICU patients, perhaps explaining the greater risk of thrombosis in COVID-19 (33). As proof of principle, we removed surface hyaluronic acid from human pulmonary microvascular endothelial cells with hyaluronidase treatment resulting in depressed nitric oxide production, an instigating mechanism for platelet adhesion to the microvascular endothelium.

Additionally, we published a case report of a 15-year old female admitted to hospital with multi-system inflammatory syndrome associated with COVID-19 (MIS-C), and demonstrated that plasma HA was increased almost 7-fold over age and sex-matched healthy controls (55). Further, MMP7, which is known to cleave syndecans-1 and 4 (**Table 1**), was the most up-regulated analyte tested (over 15-fold) (55). These latter data were consistent with endothelial glycocalyx degradation following SARS-CoV-2 infection, albeit with a MIS-C presentation.

Measuring the perfused boundary region of sub-lingual blood vessels has become a useful bedside indicator of glycocalyx damage. Mechanically ventilated COVID-19 patients have been shown to have a thinner glycocalyx, compared to non-ventilated COVID-19 patients or healthy controls (56). The same study showed that plasma concentrations of HA were significantly higher in both non- and ventilated COVID-19 patients compared to controls, while syndecan-1 was higher in ventilated COVID patients compared to both non-ventilated COVID-19 patients and controls. Additionally syndecan-1 predicted development of moderate-to-severe ARDS (AUC 0.91), and a thinner glycocalyx was associated with 60-day mortality (56).

Subsequent studies have reported increased plasma syndecan-1 (57, 58) and HA (57, 59) in COVID-19 patients compared to healthy controls. One study showed plasma HA, HS, and CS were all increased in COVID-19 patients compared to healthy controls, but lower or similar to sepsis patients; though COVID-19 ICU patients had significantly higher concentrations of HA and HS compared to non-ICU COVID patients (60). Additionally, plasma hyaluronidase activity was higher in the ICU COVID-19 patients vs. the non-ICU patients, and plasma MMP2, MMP9 and cathepsin D activities (enzymes which may cleave GAG-anchoring proteins) were significantly increased in COVID-19 patients vs. healthy controls (60). Interestingly, COVID-19 patient plasma HA was also found to be low

molecular weight (pro-inflammatory) and bound with inter-alpha inhibitor protein, suggesting that free HA in COVID-19 plasma is a degradation product of ECs rather than increased HA release. HA and hyaluronidase plasma concentrations showed moderate correlations with SOFA score in COVID-19 patients. Studies utilizing cultured endothelial cells treated with COVID-19 patient plasma *in vitro* showed similar changes in HA, as well as hyaluronidase, MMP2, MMP9, and cathepsin activity (60).

Several studies suggest that blood markers of glycocalyx degradation are correlated with disease severity in COVID-19 patients. Serum syndecan-1 concentrations within the first day of ICU admission were significantly higher in non-surviving COVID-19 patients compared to survivors (61). The optimal cut-off value to distinguish survivors was 813.8 ng/mL, as determined by ROC analysis, and Kaplan-Meier analysis showed significantly worse outcomes in COVID-19 patients over the cut-off. Another study found that plasma heparanase activity and plasma heparan concentration were higher in COVID-19 patients compared to healthy controls, and that heparanase activity was significantly higher in ventilated ICU COVID patients vs. non-ICU COVID patients (62). Plasma syndecan-1 was significantly higher in COVID-19 patients classified as "critical" compared to those in the "severe" category; a difference that persisted for 14 days of ICU admission (63). A further study showed plasma HS concentrations were increased in COVID-19 patients compared to healthy controls (59, 64) and were associated with the severity of disease (64).

Even in convalescent COVID-19 patients who were never hospitalized, a persistent increase in serum syndecan-1 concentrations compared to healthy controls was found at a mean of 88 days post symptom onset, and was not significantly different from currently hospitalized COVID-19 patients (65). Another study found decreased glycocalyx thickness (using sublingual perfused boundary region) 4 months after COVID-19 infection (none required mechanical ventilation), which was similar to untreated hypertensive patients (66). While these studies contained relatively few subjects, they suggest glycocalyx degradation also occurs in mild cases of COVID-19, and elevated degradation products can persist for months after acute illness.

SARS-CoV-2 causes direct endothelial damage *via* ACE2 receptors, and ACE2 activation may be modulated by the health and thickness of the glycocalyx (67). In fact, the SARS-CoV-2 spike protein requires HS to aid ACE2 binding (68), a thick, healthy glycocalyx may act as a physical barrier, extending beyond the ACE2 receptor and preventing the virus from accessing the EC (67). However, by the time COVID-19 patients exhibit viremia, one would expect the disease to be advanced and the glycocalyx to be severely damaged *via* the inflammatory response.

Taken together, the published studies strongly suggest that the glycocalyx clearly undergoes a significant amount of degradation from COVID-19, likely contributing to platelet adhesion and increased risk of thrombosis seen in many cases of COVID-19. Thus, therapies to inhibit platelet adhesion (e.g., administration of nitric oxide *via* inhalation or by a donor) and to protect/restore the glycocalyx (e.g., sulodexide and/or sphingosine-1-phosphate) may be therapeutically indicated.

Trauma—Fluid Resuscitation

Similar to sepsis and COVID-19, trauma can lead to a hypercoagulative state due to the interplay of inflammation and vascular injury. Trauma-induced coagulopathy may begin with a hypercoagulative state that changes to hypcoagulation, or vice-versa, and can depend on several factors including the extent of trauma, the amount and rate of intravascular fluid administered, and the presence of excess fibrinolysis (69, 70). However, as seen below, trauma is consistently associated with glycocalyx degradation. Interestingly, in a subset of trauma patients, glycocalyx degradation, and the release of heparin-like GAGs, including HS, has been suggested to contribute to hypocoagulation, termed auto-heparinization (71). While trauma is known to increase the plasma concentrations of glycocalyx components such as HA, HS, CS, and syndecan-1 compared to healthy controls (72), it is less well known how the glycocalyx is affected by fluid resuscitation. Previous strategies to quickly resuscitate with large amounts of isotonic fluid may not be as beneficial as conservative strategies (73) and may lead indirectly to extra glycocalyx shedding.

Plasma syndecan-1 concentration in trauma patients upon arrival to the emergency department was an independent predictor of mortality after adjusting for age and injury severity (74). Patients above the median syndecan-1 concentration also showed increased markers of inflammation, endothelial activation/injury and fibrinolysis. Trauma patients with a lower plasma colloidal pressure, secondary to uncontrolled hemorrhage together with saline resuscitation, also had increased plasma HA and syndecan-1 compared to trauma patients with normal colloidal pressure (72). Blood syndecan-1 concentrations were elevated in trauma patients after admission to the emergency department, and those with above average syndecan-1 concentrations, had more indicators of microcirculatory dysfunction (75). While microcirculatory dysfunction improved over time and syndecan-1 concentrations decreased, syndecan-1 remained elevated for 30–50 h compared to healthy controls (75).

Trauma patients in the highest quartile of plasma syndecan-1 concentration upon admission to the emergency department had the highest rates of blood transfusion and 30-day in-hospital mortality (76). In fact, a blood concentration of 40 ng/mL syndecan-1 maximized sensitivity and specificity in predicting 24-h in-hospital mortality. Further, patients with plasma syndecan-1 $\geq$ 40 ng/mL were significantly more injured and had lower median systolic blood pressures and platelet counts (76). Higher plasma syndecan-1 levels translated into poorer outcomes, needing 4 times more blood products, having fewer hospital ventilator-free days and greater mortality.

Syndecan-1 seems to be the most well-studied glycocalyx degradation marker in trauma, however, a small study showed plasma HA concentrations are also significantly associated with acute traumatic coagulopathy and markers of coagulopathy (77).

While trauma itself degrades the glycocalyx, the choice of solution for intravenous resuscitation also contributes. When healthy subjects were administered 0.9% saline, Hartmann's

solution, 4% and 20% albumin in a double-blind crossover study, only the 0.9% saline produced evidence of glycocalyx degradation through increased plasma syndecan-1 (78). Though the fluid treatment was relatively mild in healthy subjects, it suggested that 0.9% saline, the most widely used resuscitation fluid globally, may be the harshest on the endothelial glycocalyx integrity. Indeed, normal saline was associated with poorer outcomes as compared to other crystalloids in critically ill adults (79), though glycocalyx integrity was not specifically investigated. Additionally, an *in vitro* study suggests hypernatremia, can be associated with normal saline infusion, damaging the endothelial glycocalyx, releasing HA and syndecan-1 (80).

Hemorrhagic shock patients showed significantly increased plasma syndecan-1 concentrations after their injury compared to healthy controls (81). After resuscitation with fresh frozen plasma, syndecan-1 significantly decreased, but it was still elevated over healthy controls (81). This latter response could be due, at least in part, to dilution by the administered fresh frozen plasma; however, *in vitro* studies suggest that fresh frozen plasma reduces endothelial permeability and aids syndecan-1 restoration (81). Indeed, administration of fresh frozen plasma to non-bleeding critically ill patients (45% sepsis patients) resulted in a significantly lower syndecan-1 plasma concentration when compared to plasma levels obtained before transfusion (565 vs. 675 pg/mL) (82). As cytokine/chemokine plasma concentrations were unaffected, and ADAMTS13 concentrations were increased, this latter data suggested that the reduced plasma syndecan-1 concentration was not dilutional. When patients with thoracic aortic dissection received an intravenous product made from pooled, solvent and detergent-treated plasma (OctaplasLG) during surgical repair, their plasma syndecan-1 levels were significantly reduced, indicating less glycocalyx injury (83).

The resuscitation of hemorrhagic trauma patients favors a saline-restricted approach, and emphasizes balanced transfusions that include fresh frozen plasma. While many studies have measured syndecan-1 concentrations after fluid resuscitation, most measured only a single time point after resuscitation and few monitored a time-course. Thus, the positive effects of fresh frozen plasma on the vascular glycocalyx requires further investigation.

Diabetes

Glycocalyx degradation in diabetes (e.g., hyperglycemia) or diabetes-associated complications [e.g., the systemic inflammatory response associated with diabetic ketoacidosis (84–87)] has not been studied as extensively as compared to other diseases with a severe inflammatory component. Nevertheless, the current knowledge indicates that the endothelial glycocalyx is degraded by acute hyperglycemia and that the endothelial glycocalyx thinning due to hyperglycemia contributes to impaired wound healing in diabetes patients (88).

In a small study of healthy males, acute hyperglycemia induced by a concentrated glucose infusion decreased systemic endothelial glycocalyx thickness, an observation that coincided with a rapid increase in circulating plasma levels of HA (89). This glycocalyx thinning was independent of rapid changes in osmolality, as the glycocalyx did not degrade in response to mannitol. Importantly, the glycocalyx thinning was ameliorated by co-infusion of the antioxidant N-acetyl cysteine, suggesting an important role for ROS. In another study, baseline systemic glycocalyx thickness was significantly decreased in type-1 diabetes patients, compared to controls; and there was a further decrease in type-1 diabetes patients with microalbuminuria (90). The measure of systemic glycocalyx thickness significantly correlated ($r = 0.73$, $p < 0.01$) with sublingual glycocalyx thickness measurements (90). Plasma HA concentrations were also increased in type 1 diabetes patients compared to controls, and again microalbuminuria increased this further (90). In contrast, another trial of 136 type-1 diabetes patients failed to show an association between glycocalyx thickness in sublingual micro-vessels and the level of albuminuria, although the diabetes patients did have a significantly decreased glycocalyx compared to controls (91).

Similar to type-1 diabetes, patients with type-2 diabetes showed a thinner baseline glycocalyx in sublingual and retinal vessels compared to normal controls; additionally these patients had increased plasma HA and hyaluronidase concentrations (92). First degree relatives of type-2 diabetes patients that are insulin resistant, and subjects with dysglycemia showed a lower baseline glycocalyx thickness in sublingual microvessels compared to normal controls (93). Furthermore, the glycocalyx acutely thinned in these subjects during oral glucose tolerance tests, while the thinning was not observed in healthy subjects (93).

While most glycocalyx studies in diabetes have focused on HA, plasma syndecan-1 levels are also significantly increased in type-2 diabetes patients compared to controls (94). Of the diabetes patients, mean fasting blood glucose was 10.32 mM and 29.3% had glucose in their urine. Another study of type-1 diabetes patients found significantly increased plasma concentrations of syndecan-1 in those with nephropathy compared to type-1 patients without (95). Again, the nephropathy patients' mean glycated hemoglobin was 9.18% vs. 7.58% for controls (normal 4–5.6%), suggesting the nephropathy patients blood glucose was not well controlled. Contrary to this, blood syndecan-1 levels in type-1 diabetic patients with microalbuminuria were increased as compared to patients without, and healthy controls, but no difference in glycated hemoglobin was found (96).

STRATEGIES/THERAPIES FOR PROTECTING/RESTORING GLYCOCALYX

Because of the extended time-course of glycocalyx recovery (97), and in light of the apparently long-lasting glycocalyx effects of COVID-19 (65, 66), therapies that protect the endothelial glycocalyx or support its replacement would be advantageous. Currently, there is limited data on trials or therapies in humans, likely due to the relatively brief time since the endothelial glycocalyx has gained prominence and the long timelines for clinical research. Many excellent basic science and pre-clinical models have emerged and have recently been reviewed elsewhere (98, 99) so here we will focus primarily on therapies which have human data.

Steroids

Glucocorticoids have a long history as anti-inflammatory agents; decreasing pro-inflammatory molecule release and reducing extravasation of white blood cells, making steroids an attractive agent for indirectly protecting the glycocalyx. A small trial showed pre-surgical administration of hydrocortisone to patients undergoing cardiac surgery with cardiopulmonary bypass significantly decreased plasma concentrations of heparan sulfate, but not syndecan-1, when compared post-operatively to untreated controls (100). Recently, a phase 2 study investigated the preoperative administration of dexamethasone on abdominal surgery patients with or without albumin, and found that there was no difference in post-operative day 1 plasma syndecan-1. However, the dexamethasone plus albumin group did have lower plasma heparan sulfate (101) concentrations. While this was a small trial with a total of 72 patients, and the improved glycocalyx markers were not substantial, the experimental treatment was well tolerated and there were fewer complications in the experimental group suggesting that the results may improve with different formulations. A single pre-operative dose of methylprednisolone was shown to cause a modest, but significant reduction in post-operative syndecan-1 concentrations compared to controls in patients undergoing total knee arthroplasty (102). As the studies examining the effects of steroids on the glycocalyx have focused on surgical outcomes, it is unclear if they would be effective in critical illness and prolonged inflammation. Critically ill COVID-19 patients respond well to steroid therapy, and glycocalyx degradation is a key pathophysiological mechanism in these patients, raising the possibility that the glycocalyx may be a potential steroid target (103).

Protease Inhibitors

A variety of proteases cleave syndecans and CD44 (see **Table 1**), making proteases an attractive target for reducing glycocalyx degradation and/or aiding the glycocalyx recovery. Tranexamic acid is a synthetic lysine derivative that inhibits plasminogen activation and its binding to fibrin, thereby inhibiting fibrinolysis (104). A recent study showed pre- and peri-operative administration of tranexamic acid in patients undergoing posterior lumbar fusion surgery significantly inhibited the 2 h postoperative increase in plasma syndecan-1 compared to untreated patients (105). A study of patients with moderate to severe traumatic brain injury showed a modest but significant decrease in plasma syndean-1 when tranexamic acid was administered within 2 h postinjury (106). While the exact mechanism of syndecan-1 preservation is unknown, it has been suggested from *in vivo* experiments that tranexamic acid additionally inhibits MMP activity (107) as well as fibrinolysis. Tranexamic acid's effect on the glycocalyx in critical illness has not been thoroughly studied, and although its effect limiting syndecan-1 shedding is promising, its action of inhibiting fibrinolysis (104) suggests it may be incompatible with conditions exhibiting DIC where it may stabilize pathological clots.

The relatively large number of MMPs which can cleave syndecans-1 and 4, and CD44 (**Table 1**) make MMPs an important target to rescue the glycocalyx. Despite musculoskeletal syndrome as a side effect of early broad-spectrum MMP inhibitors, several more selective MMP inhibitors, particularly those that inhibit MMP-2 or –9, have shown clinical benefit (108). These latter MMP inhibitors are protein-based, including antibodies and tissue inhibitors of MMPs (TIMPs), several of which are currently undergoing clinical trials (109), including an anti-MMP-9 antibody (110). Small peptide inhibitors of ADAM-17, which cleaves syndecan-1 and 4, have also been identified as potential therapeutics (109).

Due to the hypercoagulation that often accompanies critical illnesses, and because thrombin cleaves syndecan-4 (37) it is a rational a target for treatment. While direct thrombin inhibitors have not been specifically evaluated in trials of glycocalyx degradation, there are several compounds available for human use which may provide therapeutic benefit (111, 112).

Finally, the protease inhibitor Ulinastatin, which inhibits lipopolysaccharide-induced heparanase expression and activity, suppressed vascular permeability and HS degradation in mouse models (98).

Heparinoids/Glycosaminoglycans

Prophylactic administration of low molecular weight heparin lowered heparanase activity in non-ICU COVID-19 patients, though no differences in plasma HS were found, and it did not affect heparanase activity in ventilated COVID-19 patients (62). Other glycocalyx markers were not measured. Heparin can act to protect the glycocalyx *in vitro* and even help reconstitute it by mobilizing syndecan-1 (113).

Endogenous plasma hyaluronidase inhibitors increased during sepsis (18), suggesting exogenous inhibitor addition may be of benefit. The heparinoid Sulodexide is a heterogeneous mixture of sulfated glycosaminoglycans and acts as a heparinase inhibitor. Two months of Sulodexide treatment, increased sublingual, and retinal glycocalyx thickness in type-2 diabetes patients without increased plasma HA concentrations (92). A recent meta-analysis concluded that Sulodexide was reno-protective and decreased albumin excretion rate by 50% in patients with diabetic nephropathy (114). Since glycocalyx degradation in kidney endothelial cells was suspected to play a role in the pathogenesis of diabetic nephropathy (115), this latter finding suggested that Sulodexide may have restored the glycocalyx. Additionally, this data suggested that heparinoid therapy may be useful in the context of the long-term damage associated with COVID-19 (66, 67). Currently, heparin is often used as an anticoagulant in sepsis and COVID-19 patients; however, we are unaware of studies that have measured its effect on the glycocalyx in these diseases.

Resuscitation Strategies

Volume resuscitation with plasma or plasma products has recently gained attention. As discussed above (*Trauma—Fluid resuscitation*), administering fresh frozen plasma to non-hemorrhagic critically ill patients protected the glycocalyx (82); although plasma treatment for sepsis has been generally not recommended (116). Fluid resuscitation of septic shock patients with albumin-supplemented crystalloids did not affect plasma

syndecan-1 concentrations, although there was some possible endothelial protections (46). Moreover, a rodent hemorrhage model suggested albumin administration may partially restore the glycocalyx (117) and a pilot study in human septic shock patients indicated that an albumin infusion may restore endothelial function (118).

Sphingosine 1-phosphate has been shown to correlate with positive outcomes in septic shock (46), and the glycocalyx protective effects of plasma or its products may be a result of the sphingosine 1-phospate present in those products (99).

Although two recent clinical trials demonstrated early pre-hospital plasma administration to trauma patients conferred a significant survival benefit (119), there was no analysis of endothelial glycocalyx markers. Fresh frozen plasma was shown to help restore endothelial syndecan-1 *in vitro* (81), and another study showed early plasma resuscitation can restore the glycocalyx, as opposed to late plasma treatment that was ineffective (120). As discussed above, glycocalyx degradation was reduced by administration of OctaplasLG, as compared to fresh frozen plasma in patients undergoing emergency surgery for thoracic aorta dissection (83). Rodent studies of hemorrhagic shock indicated that plasma resuscitation (either fresh or fresh-frozen) protected or restored the endothelial glycocalyx, where lactated Ringer's or hydroxyethyl starch solution did not, and increased survival may have been dependent on syndecan-1 restoration [Reviewed in (121)].

Anti-inflammatory Therapies

Prophylactic administration of a TNF-α inhibitor ameliorated glycocalyx degradation in response to low-dose endotoxin in healthy volunteers (12), and a combination therapy of methotrexate and/or a TNF-α inhibitor in rheumatoid arthritis patients decreased syndecan-1 for greater than 6 weeks (122). However, whether TNF-α inhibition would be beneficial to the glycocalyx in the often more severe inflammation observed in critically ill patients is undetermined, although the history of TNF-α inhibition trials (123, 124) in sepsis would suggest not. Activation of the Tie2 receptor *in vitro* may promote recovery of the endothelial glycocalyx (125); in fact, the Tie2 agonist AV-001 is currently in a phase 2a trial for patients with severe COVID-19 (clinicaltrials.gov ID NCT05123755).

CONCLUDING REMARKS

Several major glycocalyx components have been used as biomarkers to distinguish sub-populations in critical illness or predict outcomes. Glycocalyx degradation occurs during critical illness/injury, but it is not the only pro-inflammatory and pro-thrombotic change to take place, and it must be viewed in context with other microvascular pathologies, endothelial dysfunction, leukocyte/platelet adhesion, and the release of inflammatory mediators, such as cytokines, proteases and ROS. Furthermore, glycocalyx degradation may not be a general response to inflammation; in fact, in some pathologies it may offer disease specific consequences (i.e., trauma-induced auto-heparinization vs. sepsis-induced DIC). Despite an abundance of basic and pre-clinical research into glycocalyx preserving and rebuilding strategies, there remains a lack of clinical trials in humans.

AUTHOR CONTRIBUTIONS

EP: data collection, data interpretation, and manuscript writing. GC and DF: concept, data interpretation, critical review of the manuscript, and submission. All authors contributed to the article and approved the submitted version.

FUNDING

EP's salary is supported by funding from the Heart and Stroke Foundation of Ontario (G-19-0026307) and the Natural Sciences and Engineering Research Council of Canada (RGPIN-2017-06336) to GC.

REFERENCES

1. Fallacara A, Baldini E, Manfredini S, Vertuani S. Hyaluronic acid in the third millennium. *Polymers (Basel).* (2018) 10:701. doi: 10.3390/polym10070701
2. Okada H, Takemura G, Suzuki K, Oda K, Takada C, Hotta Y, et al. Three-dimensional ultrastructure of capillary endothelial glycocalyx under normal and experimental endotoxemic conditions. *Crit Care.* (2017) 21:261. doi: 10.1186/s13054-017-1841-8
3. Vink H, Duling BR. Identification of distinct luminal domains for macromolecules, erythrocytes, and leukocytes within mammalian capillaries. *Circ Res.* (1996) 79:581–9. doi: 10.1161/01.RES.79.3.581
4. Reitsma S, oude Egbrink MGA, Vink H, van den Berg BM, Lima Passos V, Engels W, et al. Endothelial glycocalyx structure in the intact carotid artery: a two-photon laser scanning microscopy study. *J Vasc Res.* (2011) 48:297–306. doi: 10.1159/000322176
5. Yang Y, Schmidt EP. The endothelial glycocalyx. *Tissue Barriers.* (2013) 1:e23494. doi: 10.4161/tisb.23494
6. Lesley J, Hascall VC, Tammi M, Hyman R. Hyaluronan binding by cell surface cd44*. *J Biol Chem.* (2000) 275:26967–75. doi: 10.1016/S0021-9258(19)61467-5
7. Olson ST, Richard B, Izaguirre G, Schedin-Weiss S, Gettins PGW. Molecular mechanisms of antithrombin-heparin regulation of blood clotting proteinases. a paradigm for understanding proteinase regulation by serpin family protein proteinase inhibitors. *Biochimie.* (2010) 92:1587–96. doi: 10.1016/j.biochi.2010.05.011
8. Weitz JI. Heparan sulfate: antithrombotic or not? *J Clin Invest.* (2003) 111:952–4. doi: 10.1172/JCI200318234
9. Delgadillo LF, Marsh GA, Waugh RE. Endothelial glycocalyx layer properties and its ability to limit leukocyte adhesion. *Biophys J.* (2020) 118:1564–75. doi: 10.1016/j.bpj.2020.02.010
10. Wuillemin WA, Eldering E, Citarella F, de Ruig CP, ten Cate H, Hack CE. Modulation of contact system proteases by glycosaminoglycans: selective enhancement of the inhibition of factoR XIa*. *J Biol Chem.* (1996) 271:12913–8. doi: 10.1074/jbc.271.22.12913
11. Delgadillo LF, Lomakina EB, Kuebel J, Waugh RE. Changes in endothelial glycocalyx layer protective ability after inflammatory stimulus. *Am J Physiol Cell Physiol.* (2021) 320:C216–24. doi: 10.1152/ajpcell.00259.2020
12. Nieuwdorp M, Meuwese MC, Mooij HL, van Lieshout MHP, Hayden A, Levi M, et al. Tumor necrosis factor-α inhibition protects against endotoxin-induced endothelial glycocalyx perturbation. *Atherosclerosis.* (2009) 202:296–303. doi: 10.1016/j.atherosclerosis.2008.03.024

13. Belousoviene E, Kiudulaite I, Pilvinis V, Pranskunas A. Links between Endothelial Glycocalyx Changes and Microcirculatory Parameters in Septic Patients. *Life (Basel).* (2021) 11:790. doi: 10.3390/life11080790
14. Murphy LS, Wickersham N, McNeil JB, Shaver CM, May AK, Bastarache JA, et al. Endothelial glycocalyx degradation is more severe in patients with non-pulmonary sepsis compared to pulmonary sepsis and associates with risk of ARDS and other organ dysfunction. *Ann Intensive Care.* (2017) 7:102. doi: 10.1186/s13613-017-0325-y
15. Lipowsky HH. The endothelial glycocalyx as a barrier to leukocyte adhesion and its mediation by extracellular proteases. *Ann Biomed Eng.* (2012) 40:840–8. doi: 10.1007/s10439-011-0427-x
16. Chappell D, Brettner F, Doerfler N, Jacob M, Rehm M, Bruegger D, et al. Protection of glycocalyx decreases platelet adhesion after ischaemia/reperfusion: an animal study. *Eur J Anaesthesiol.* (2014) 31:474–81. doi: 10.1097/EJA.0000000000000085
17. Afify AM, Stern M, Guntenhoner M, Stern R. Purification and characterization of human serum hyaluronidase. *Arch Biochem Biophys.* (1993) 305:434–41. doi: 10.1006/abbi.1993.1443
18. van der Heijden J, Kolliopoulos C, Skorup P, Sallisalmi M, Heldin P, Hultström M, et al. Plasma hyaluronan, hyaluronidase activity and endogenous hyaluronidase inhibition in sepsis: an experimental and clinical cohort study. *Intensive Care Med Exp.* (2021) 9:53. doi: 10.1186/s40635-021-00418-3
19. Petrey A, de la Motte C. Hyaluronan, a crucial regulator of inflammation. *Front Immunol.* (2014) 5:101. doi: 10.3389/fimmu.2014.00101
20. de la Motte C, Nigro J, Vasanji A, Rho H, Kessler S, Bandyopadhyay S, et al. Platelet-derived hyaluronidase 2 cleaves hyaluronan into fragments that trigger monocyte-mediated production of proinflammatory cytokines. *Am J Pathol.* (2009) 174:2254–64. doi: 10.2353/ajpath.2009.080831
21. Harada H, Takahashi M. CD44-dependent intracellular and extracellular catabolism of hyaluronic acid by hyaluronidase-1 and –2*. *J Biol Chem.* (2007) 282:5597–607. doi: 10.1074/jbc.M608358200
22. Yamaguchi Y, Yamamoto H, Tobisawa Y, Irie F. TMEM2: a missing link in hyaluronan catabolism identified? *Matr Biol.* (2019) 78–79:139–46. doi: 10.1016/j.matbio.2018.03.020
23. Tobisawa Y, Fujita N, Yamamoto H, Ohyama C, Irie F, Yamaguchi Y. The cell surface hyaluronidase TMEM2 is essential for systemic hyaluronan catabolism and turnover. *J Biol Chem.* (2021) 297:101281. doi: 10.1016/j.jbc.2021.101281
24. Šoltés L, Mendichi R, Kogan G, Schiller J, Stankovská M, Arnhold J. Degradative action of reactive oxygen species on hyaluronan. *Biomacromolecules.* (2006) 7:659–68. doi: 10.1021/bm050867v
25. Yahalom J, Eldor A, Fuks Z, Vlodavsky I. Degradation of sulfated proteoglycans in the subendothelial extracellular matrix by human platelet heparitinase. *J Clin Invest.* (1984) 74:1842–9.
26. Matzner Y, Bar-Ner M, Yahalom J, Ishai-Michaeli R, Fuks Z, Vlodavsky I. Degradation of heparan sulfate in the subendothelial extracellular matrix by a readily released heparanase from human neutrophils. Possible role in invasion through basement membranes. *J Clin Invest.* (1985) 76:1306–13. doi: 10.1172/JCI112104
27. Griffin LS, Gloster TM. The enzymatic degradation of heparan sulfate. *Protein Pept Lett.* (2017) 24:710–22. doi: 10.2174/0929866524666170724113452
28. Gilat D, Hershkoviz R, Goldkorn I, Cahalon L, Korner G, Vlodavsky I, et al. Molecular behavior adapts to context: heparanase functions as an extracellular matrix-degrading enzyme or as a T cell adhesion molecule, depending on the local pH. *J Exp Med.* (1995) 181:1929–34. doi: 10.1084/jem.181.5.1929
29. Hoogewerf AJ, Leone JW, Reardon IM, Howe WJ, Asa D, Heinrikson RL, et al. Chemokines connective tissue activating peptide-III and neutrophil activating peptide-2 are heparin/heparan sulfate-degrading enzymes (*). *J Biol Chem.* (1995) 270:3268–77. doi: 10.1074/jbc.270.7.3268
30. Maciej-Hulme ML. New insights into human hyaluronidase 4/chondroitin sulphate hydrolase. *Front Cell Dev Biol.* (2021) 9:767924. doi: 10.3389/fcell.2021.767924
31. Lord MS, Melrose J, Day AJ, Whitelock JM. The inter-α-trypsin inhibitor family: versatile molecules in biology and pathology. *J Histochem Cytochem.* (2020) 68:907–27. doi: 10.1369/0022155420940067
32. Ho G, Broze GJ, Schwartz AL. Role of heparan sulfate proteoglycans in the uptake and degradation of tissue factor pathway inhibitor-coagulation factor Xa complexes*. *J Biol Chem.* (1997) 272:16838–44. doi: 10.1074/jbc.272.27.16838
33. Fraser DD, Patterson EK, Slessarev M, Gill SE, Martin C, Daley M, et al. Endothelial injury and glycocalyx degradation in critically Ill Coronavirus disease 2019 patients: implications for microvascular platelet aggregation. *Crit Care Explorat.* (2020) 2:e0194. doi: 10.1097/CCE.0000000000000194
34. Mulivor AW, Lipowsky HH. Inhibition of glycan shedding and leukocyte-endothelial adhesion in postcapillary venules by suppression of matrixmetalloprotease activity with doxycycline. *Microcirculation.* (2009) 16:657–66. doi: 10.3109/10739680903133714
35. Endo K, Takino T, Miyamori H, Kinsen H, Yoshizaki T, Furukawa M, et al. Cleavage of syndecan-1 by membrane type matrix metalloproteinase-1 stimulates cell migration *. *J Biol Chem.* (2003) 278:40764–70. doi: 10.1074/jbc.M306736200
36. Kajita M, Itoh Y, Chiba T, Mori H, Okada A, Kinoh H, et al. Membrane-type 1 matrix metalloproteinase cleaves Cd44 and promotes cell migration. *J Cell Biol.* (2001) 153:893–904.
37. Manon-Jensen T, Multhaupt HAB, Couchman JR. Mapping of matrix metalloproteinase cleavage sites on syndecan-1 and syndecan-4 ectodomains. *FEBS J.* (2013) 280:2320–31. doi: 10.1111/febs.12174
38. Pruessmeyer J, Martin C, Hess FM, Schwarz N, Schmidt S, Kogel T, et al. A Disintegrin and metalloproteinase 17 (ADAM17) mediates inflammation-induced shedding of syndecan-1 and –4 by lung epithelial cells. *J Biol Chem.* (2010) 285:555–64. doi: 10.1074/jbc.M109.059394
39. Singer M, Deutschman CS, Seymour CW, Shankar-Hari M, Annane D, Bauer M, et al. The third international consensus definitions for sepsis and septic shock (Sepsis-3). *JAMA.* (2016) 315:801–10. doi: 10.1001/jama.2016.0287
40. Uchimido R, Schmidt EP, Shapiro NI. The glycocalyx: a novel diagnostic and therapeutic target in sepsis. *Crit Care.* (2019) 23:16. doi: 10.1186/s13054-018-2292-6
41. Iba T, Levy JH. Derangement of the endothelial glycocalyx in sepsis. *J Thromb Haemost.* (2019) 17:283–94. doi: 10.1111/jth.14371
42. Beurskens DM, Bol ME, Delhaas T, van de Poll MC, Reutelingsperger CP, Nicolaes GA, et al. Decreased endothelial glycocalyx thickness is an early predictor of mortality in sepsis. *Anaesth Intensive Care.* (2020) 48:221–8. doi: 10.1177/0310057X20916471
43. Nelson A, Berkestedt I, Bodelsson M. Circulating glycosaminoglycan species in septic shock. *Acta Anaesth Scand.* (2014) 58:36–43. doi: 10.1111/aas.12223
44. Anand D, Ray S, Srivastava LM, Bhargava S. Evolution of serum hyaluronan and syndecan levels in prognosis of sepsis patients. *Clin Biochem.* (2016) 49:768–76. doi: 10.1016/j.clinbiochem.2016.02.014
45. Huang X, Hu H, Sun T, Zhu W, Tian H, Hao D, et al. Plasma endothelial glycocalyx components as a potential biomarker for predicting the development of disseminated intravascular coagulation in patients with sepsis. *J Intensive Care Med.* (2021) 36:1286–95. doi: 10.1177/0885066620949131
46. Piotti A, Novelli D, Meessen JMTA, Ferlicca D, Coppolecchia S, Marino A, et al. Endothelial damage in septic shock patients as evidenced by circulating syndecan-1, sphingosine-1-phosphate and soluble VE-cadherin: a substudy of ALBIOS. *Crit Care.* (2021) 25:113. doi: 10.1186/s13054-021-03545-1
47. Ostrowski SR, Windeløv NA, Ibsen M, Haase N, Perner A, Johansson PI. Consecutive thrombelastography clot strength profiles in patients with severe sepsis and their association with 28-day mortality: a prospective study. *J Crit Care.* (2013) 28:317.e1–11. doi: 10.1016/j.jcrc.2012.09.003
48. Simmons J, Pittet J-F. The coagulopathy of acute sepsis. *Curr Opin Anaesth.* (2015) 28:227–36. doi: 10.1097/ACO.0000000000000163
49. Lupu F, Kinasewitz G, Dormer K. The role of endothelial shear stress on haemodynamics, inflammation, coagulation and glycocalyx during sepsis. *J Cell Mol Med.* (2020) 24:12258–71. doi: 10.1111/jcmm.15895
50. Rapkiewicz AV, Mai X, Carsons SE, Pittaluga S, Kleiner DE, Berger JS, et al. Megakaryocytes and platelet-fibrin thrombi characterize multi-organ thrombosis at autopsy in COVID-19: a case series. *EClinicalMedicine.* (2020) 24:100434. doi: 10.1016/j.eclinm.2020.100434

51. Ortega-Paz L, Capodanno D, Montalescot G, Angiolillo DJ. Coronavirus disease 2019-associated thrombosis and coagulopathy: review of the pathophysiological characteristics and implications for antithrombotic management. *J Am Heart Assoc.* (2021) 10:e019650. doi: 10.1161/JAHA.120.019650
52. Bradbury CA, McQuilten Z. Anticoagulation in COVID-19. *Lancet.* (2022) 399:5–7. doi: 10.1016/S0140-6736(21)02503-4
53. Bilaloglu S, Aphinyanaphongs Y, Jones S, Iturrate E, Hochman J, Berger JS. Thrombosis in hospitalized patients with COVID-19 in a New York city health system. *JAMA.* (2020) 324:799–801. doi: 10.1001/jama.2020.13372
54. Malas MB, Naazie IN, Elsayed N, Mathlouthi A, Marmor R, Clary B. Thromboembolism risk of COVID-19 is high and associated with a higher risk of mortality: A systematic review and meta-analysis. *EClinicalMedicine.* (2020) 29:100639. doi: 10.1016/j.eclinm.2020.100639
55. Fraser DD, Patterson EK, Daley M, Cepinskas G. Case report: inflammation and endothelial injury profiling of COVID-19 pediatric multisystem inflammatory syndrome (MIS-C). *Front Pediatr.* (2021) 9:597926. doi: 10.3389/fped.2021.597926
56. Rovas A, Osiaevi I, Buscher K, Sackarnd J, Tepasse P-R, Fobker M, et al. Microvascular dysfunction in COVID-19: the MYSTIC study. *Angiogenesis.* (2021) 24:145–57. doi: 10.1007/s10456-020-09753-7
57. Goonewardena SN, Grushko OG, Wells J, Herty L, Rosenson RS, Haus JM, et al. Immune-mediated glycocalyx remodeling in hospitalized COVID-19 patients. *Cardiovasc Drugs Ther.* (2021) 1–7. doi: 10.1007/s10557-021-07288-7
58. Kim W-Y, Kweon OJ, Cha MJ, Baek MS, Choi S-H. Dexamethasone may improve severe COVID-19 *via* ameliorating endothelial injury and inflammation: A preliminary pilot study. *PLoS One.* (2021) 16:e0254167. doi: 10.1371/journal.pone.0254167
59. Potje SR, Costa TJ, Fraga-Silva TFC, Martins RB, Benatti MN, Almado CEL, et al. Heparin prevents in vitro glycocalyx shedding induced by plasma from COVID-19 patients. *Life Sci.* (2021) 276:119376. doi: 10.1016/j.lfs.2021.119376
60. Queisser KA, Mellema RA, Middleton EA, Portier I, Manne BK, Denorme F, et al. COVID-19 generates hyaluronan fragments that directly induce endothelial barrier dysfunction. *JCI Insight.* (2021) 6:e147472. doi: 10.1172/jci.insight.147472
61. Zhang D, Li L, Chen Y, Ma J, Yang Y, Aodeng S, et al. Syndecan-1, an indicator of endothelial glycocalyx degradation, predicts outcome of patients admitted to an ICU with COVID-19. *Mol Med.* (2021) 27:151. doi: 10.1186/s10020-021-00412-1
62. Buijsers B, Yanginlar C, de Nooijer A, Grondman I, Maciej-Hulme ML, Jonkman I, et al. Increased plasma heparanase activity in COVID-19 patients. *Front Immunol.* (2020) 11:2572. doi: 10.3389/fimmu.2020.575047
63. Ogawa F, Oi Y, Nakajima K, Matsumura R, Nakagawa T, Miyagawa T, et al. Temporal change in Syndecan-1 as a therapeutic target and a biomarker for the severity classification of COVID-19. *Thromb J.* (2021) 19:55. doi: 10.1186/s12959-021-00308-4
64. Fernández S, Moreno-Castaño AB, Palomo M, Martinez-Sanchez J, Torramadé-Moix S, Téllez A, et al. Distinctive biomarker features in the endotheliopathy of COVID-19 and septic syndromes. *Shock.* (2022) 57:95–105. doi: 10.1097/SHK.0000000000001823
65. Vollenberg R, Tepasse P-R, Ochs K, Floer M, Strauss M, Rennebaum F, et al. Indications of persistent glycocalyx damage in convalescent COVID-19 patients: a prospective multicenter study and hypothesis. *Viruses.* (2021) 13:2324. doi: 10.3390/v13112324
66. Lambadiari V, Mitrakou A, Kountouri A, Thymis J, Katogiannis K, Korakas E, et al. Association of COVID-19 with impaired endothelial glycocalyx, vascular function and myocardial deformation 4 months after infection. *Eur J Heart Fail.* (2021) 23:1916–26. doi: 10.1002/ejhf.2326
67. Targosz-Korecka M, Kubisiak A, Kloska D, Kopacz A, Grochot-Przeczek A, Szymonski M. Endothelial glycocalyx shields the interaction of SARS-CoV-2 spike protein with ACE2 receptors. *Sci Rep.* (2021) 11:12157. doi: 10.1038/s41598-021-91231-1
68. Yue J, Jin W, Yang H, Faulkner J, Song X, Qiu H, et al. Heparan sulfate facilitates spike protein-mediated SARS-CoV-2 host cell invasion and contributes to increased infection of SARS-CoV-2 G614 mutant and in lung cancer. *Front Mol Biosci.* (2021) 8:649575. doi: 10.3389/fmolb.2021.649575
69. Moore EE, Moore HB, Kornblith LZ, Neal MD, Hoffman M, Mutch NJ, et al. Trauma-induced coagulopathy. *Nat Rev Dis Primers.* (2021) 7:1–23. doi: 10.1038/s41572-021-00264-3
70. Hayakawa M. Pathophysiology of trauma-induced coagulopathy: disseminated intravascular coagulation with the fibrinolytic phenotype. *J Intensive Care.* (2017) 5:14. doi: 10.1186/s40560-016-0200-1
71. Ostrowski SR, Johansson PI. Endothelial glycocalyx degradation induces endogenous heparinization in patients with severe injury and early traumatic coagulopathy. *J Trauma Acute Care Surg.* (2012) 73:60–6. doi: 10.1097/TA.0b013e31825b5c10
72. Rahbar E, Cardenas JC, Baimukanova G, Usadi B, Bruhn R, Pati S, et al. Endothelial glycocalyx shedding and vascular permeability in severely injured trauma patients. *J Transl Med.* (2015) 13:117. doi: 10.1186/s12967-015-0481-5
73. Albreiki M, Voegeli D. Permissive hypotensive resuscitation in adult patients with traumatic haemorrhagic shock: a systematic review. *Eur J Trauma Emerg Surg.* (2018) 44:191–202. doi: 10.1007/s00068-017-0862-y
74. Johansson PI, Stensballe J, Rasmussen LS, Ostrowski SR. A high admission syndecan-1 level, a marker of endothelial glycocalyx degradation, is associated with inflammation, protein C depletion, fibrinolysis, and increased mortality in trauma patients. *Ann Surg.* (2011) 254:194–200. doi: 10.1097/SLA.0b013e318226113d
75. Naumann DN, Hazeldine J, Midwinter MJ, Hutchings SD, Harrison P. Poor microcirculatory flow dynamics are associated with endothelial cell damage and glycocalyx shedding after traumatic hemorrhagic shock. *J Trauma Acute Care Surg.* (2018) 84:81–8. doi: 10.1097/TA.0000000000001695
76. Gonzalez Rodriguez E, Ostrowski SR, Cardenas JC, Baer LA, Tomasek JS, Henriksen HH, et al. Syndecan-1: a quantitative marker for the endotheliopathy of trauma. *J Am Coll Surg.* (2017) 225:419–27. doi: 10.1016/j.jamcollsurg.2017.05.012
77. Walker SC, Richter RP, Zheng L, Ashtekar AR, Jansen JO, Kerby JD, et al. Increased plasma hyaluronan levels are associated with acute traumatic coagulopathy. *Shock.* (2022) 57:113–7. doi: 10.1097/SHK.0000000000001867
78. Bihari S, Wiersema UF, Perry R, Schembri D, Bouchier T, Dixon D, et al. Efficacy and safety of 20% albumin fluid loading in healthy subjects: a comparison of four resuscitation fluids. *J Appl Physiol.* (2019) 126:1646–60. doi: 10.1152/japplphysiol.01058.2018
79. Semler MW, Self WH, Wanderer JP, Ehrenfeld JM, Wang L, Byrne DW, et al. Balanced crystalloids versus saline in critically Ill adults. *N Engl J Med.* (2018) 378:829–39. doi: 10.1056/NEJMoa1711584
80. Martin JV, Liberati DM, Diebel LN. Excess sodium is deleterious on endothelial and glycocalyx barrier function: a microfluidic study. *J Trauma Acute Care Surg.* (2018) 85:128–34. doi: 10.1097/TA.0000000000001892
81. Haywood-Watson RJ, Holcomb JB, Gonzalez EA, Peng Z, Pati S, Park PW, et al. Modulation of syndecan-1 shedding after hemorrhagic shock and resuscitation. *PLoS One.* (2011) 6:e23530. doi: 10.1371/journal.pone.0023530
82. Straat M, Müller MC, Meijers JC, Arbous MS, Spoelstra-de Man AM, Beurskens CJ, et al. Effect of transfusion of fresh frozen plasma on parameters of endothelial condition and inflammatory status in non-bleeding critically ill patients: a prospective substudy of a randomized trial. *Crit Care.* (2015) 19:163. doi: 10.1186/s13054-015-0828-6
83. Stensballe J, Ulrich AG, Nilsson JC, Henriksen HH, Olsen PS, Ostrowski SR, et al. Resuscitation of endotheliopathy and bleeding in thoracic aortic dissections: the VIPER-OCTA randomized clinical pilot trial. *Anesth Analg.* (2018) 127:920–7. doi: 10.1213/ANE.0000000000003545
84. Close TE, Cepinskas G, Omatsu T, Rose KL, Summers K, Patterson EK, et al. Diabetic ketoacidosis elicits systemic inflammation associated with cerebrovascular endothelial cell dysfunction. *Microcirculation.* (2013) 20:534–43. doi: 10.1111/micc.12053
85. Woo MMH, Patterson EK, Clarson C, Cepinskas G, Bani-Yaghoub M, Stanimirovic DB, et al. Elevated leukocyte azurophilic enzymes in human diabetic ketoacidosis plasma degrade cerebrovascular endothelial

junctional proteins. *Crit Care Med.* (2016) 44:e846–53. doi: 10.1097/CCM.0000000000001720
86. Woo M, Patterson EK, Cepinskas G, Clarson C, Omatsu T, Fraser DD. Dynamic regulation of plasma matrix metalloproteinases in human diabetic ketoacidosis. *Pediatr Res.* (2016) 79:295–300. doi: 10.1038/pr.2015.215
87. Omatsu T, Cepinskas G, Clarson C, Patterson EK, Alharfi IM, Summers K, et al. CXCL1/CXCL8 (GROα/IL-8) in human diabetic ketoacidosis plasma facilitates leukocyte recruitment to cerebrovascular endothelium in vitro. *Am J Physiol Endocrinol Metab.* (2014) 306:E1077–84. doi: 10.1152/ajpendo.00659.2013
88. Shakya S, Wang Y, Mack JA, Maytin EV. Hyperglycemia-induced changes in hyaluronan contribute to impaired skin wound healing in diabetes: review and perspective. *Int J Cell Biol.* (2015) 2015:701738. doi: 10.1155/2015/701738
89. Nieuwdorp M, van Haeften TW, Gouverneur MCLG, Mooij HL, van Lieshout MHP, Levi M, et al. Loss of endothelial glycocalyx during acute hyperglycemia coincides with endothelial dysfunction and coagulation activation in vivo. *Diabetes.* (2006) 55:480–6. doi: 10.2337/diabetes.55.02.06.db05-1103
90. Nieuwdorp M, Mooij HL, Kroon J, Atasever B, Spaan JAE, Ince C, et al. Endothelial glycocalyx damage coincides with microalbuminuria in type 1 diabetes. *Diabetes.* (2006) 55:1127–32. doi: 10.2337/diabetes.55.04.06.db05-1619
91. Stougaard EB, Winther SA, Amadid H, Frimodt-Møller M, Persson F, Hansen TW, et al. Endothelial glycocalyx and cardio-renal risk factors in type 1 diabetes. *PLoS One.* (2021) 16:e0254859. doi: 10.1371/journal.pone.0254859
92. Broekhuizen LN, Lemkes BA, Mooij HL, Meuwese MC, Verberne H, Holleman F, et al. Effect of sulodexide on endothelial glycocalyx and vascular permeability in patients with type 2 diabetes mellitus. *Diabetologia.* (2010) 53:2646–55. doi: 10.1007/s00125-010-1910-x
93. Ikonomidis I, Pavlidis G, Lambadiari V, Kousathana F, Varoudi M, Spanoudi F, et al. Early detection of left ventricular dysfunction in first-degree relatives of diabetic patients by myocardial deformation imaging: the role of endothelial glycocalyx damage. *Int J Cardiol.* (2017) 233:105–12. doi: 10.1016/j.ijcard.2017.01.056
94. Wang J-B, Zhang Y-J, Zhang Y, Guan J, Chen L-Y, Fu C-H, et al. Negative correlation between serum syndecan-1 and apolipoprotein A1 in patients with type 2 diabetes mellitus. *Acta Diabetol.* (2013) 50:111–5. doi: 10.1007/s00592-010-0216-2
95. Kolseth IBM, Reine TM, Parker K, Sudworth A, Witczak BJ, Jenssen TG, et al. Increased levels of inflammatory mediators and proinflammatory monocytes in patients with type I diabetes mellitus and nephropathy. *J Diabet Complicat.* (2017) 31:245–52. doi: 10.1016/j.jdiacomp.2016.06.029
96. Svennevig K, Kolset SO, Bangstad H-J. Increased syndecan-1 in serum is related to early nephropathy in type 1 diabetes mellitus patients. *Diabetologia.* (2006) 49:2214–6. doi: 10.1007/s00125-006-0330-4
97. Potter DR, Jiang J, Damiano ER. The recovery time course of the endothelial-cell glycocalyx in vivo and its implications in vitro. *Circ Res.* (2009) 104:1318–25. doi: 10.1161/CIRCRESAHA.108.191585
98. Christina Drost C, Rovas A, Kümpers P. Protection and rebuilding of the endothelial glycocalyx in sepsis - science or fiction? *Matrix Biology Plus.* (2021) 12:100091. doi: 10.1016/j.mbplus.2021.100091
99. Milford EM, Reade MC. Resuscitation fluid choices to preserve the endothelial glycocalyx. *Crit Care.* (2019) 23:77. doi: 10.1186/s13054-019-2369-x
100. Brettner F, Chappell D, Nebelsiek T, Hauer D, Schelling G, Becker BF, et al. Preinterventional hydrocortisone sustains the endothelial glycocalyx in cardiac surgery. *Clin Hemorheol Microcirc.* (2019) 71:59–70. doi: 10.3233/CH-180384
101. Yanase F, Tosif SH, Churilov L, Yee K, Bellomo R, Gunn K, et al. A randomized, multicenter, open-label, blinded end point, phase 2, feasibility, efficacy, and safety trial of preoperative microvascular protection in patients undergoing major abdominal surgery. *Anesth Analg.* (2021) 133:1036–47. doi: 10.1213/ANE.0000000000005667
102. Lindberg-Larsen V, Ostrowski SR, Lindberg-Larsen M, Rovsing ML, Johansson PI, Kehlet H. The effect of pre-operative methylprednisolone on early endothelial damage after total knee arthroplasty: a randomised, double-blind, placebo-controlled trial. *Anaesthesia.* (2017) 72:1217–24. doi: 10.1111/anae.13983
103. Sterne JAC, Murthy S, Diaz JV, Slutsky AS, Villar J, Angus DC, et al. Association between administration of systemic corticosteroids and mortality among critically Ill patients with COVID-19. *JAMA.* (2020) 324:1–13. doi: 10.1001/jama.2020.17023
104. McCormack PL. Tranexamic acid. *Drugs.* (2012) 72:585–617. doi: 10.2165/11209070-000000000-00000
105. Kim HJ, Lee B, Lee BH, Kim SY, Jun B, Choi YS. The effect of tranexamic acid administration on early endothelial damage following posterior lumbar fusion surgery. *J Clin Med.* (2021) 10:1415. doi: 10.3390/jcm10071415
106. Anderson TN, Hinson HE, Dewey EN, Rick EA, Schreiber MA, Rowell SE. early tranexamic acid administration after traumatic brain injury is associated with reduced syndecan-1 and angiopoietin-2 in patients with traumatic intracranial hemorrhage. *J Head Trauma Rehabil.* (2020) 35:317–23. doi: 10.1097/HTR.0000000000000619
107. Diebel ME, Martin JV, Liberati DM, Diebel LN. The temporal response and mechanism of action of tranexamic acid in endothelial glycocalyx degradation. *J Trauma Acute Care Surg.* (2018) 84:75–80. doi: 10.1097/TA.0000000000001726
108. Fields GB. The rebirth of matrix metalloproteinase inhibitors: moving beyond the dogma. *Cells.* (2019) 8:984. doi: 10.3390/cells8090984
109. Pluda S, Mazzocato Y, Angelini A. Peptide-based inhibitors of ADAM and ADAMTS metalloproteinases. *Front Mol Biosci.* (2021) 8:703715. doi: 10.3389/fmolb.2021.703715
110. Santamaria S, de Groot R. Monoclonal antibodies against metzincin targets. *Br J Pharmacol.* (2019) 176:52–66. doi: 10.1111/bph.14186
111. Arsenault KA, Hirsh J, Whitlock RP, Eikelboom JW. Direct thrombin inhibitors in cardiovascular disease. *Nat Rev Cardiol.* (2012) 9:402–14. doi: 10.1038/nrcardio.2012.61
112. Lee CJ, Ansell JE. Direct thrombin inhibitors. *Br J Clin Pharmacol.* (2011) 72:581–92. doi: 10.1111/j.1365-2125.2011.03916.x
113. Li X, Ma X. The role of heparin in sepsis: much more than just an anticoagulant. *Br J Haematol.* (2017) 179:389–98. doi: 10.1111/bjh.14885
114. Li R, Xing J, Mu X, Wang H, Zhang L, Zhao Y, et al. Sulodexide therapy for the treatment of diabetic nephropathy, a meta-analysis and literature review. *Drug Des Devel Ther.* (2015) 9:6275–83. doi: 10.2147/DDDT.S87973
115. Dogné S, Flamion B, Caron N. Endothelial glycocalyx as a shield against diabetic vascular complications. *Arterioscler Thromb Vasc Biol.* (2018) 38:1427–39. doi: 10.1161/ATVBAHA.118.310839
116. Rimmer E, Houston BL, Kumar A, Abou-Setta AM, Friesen C, Marshall JC, et al. The efficacy and safety of plasma exchange in patients with sepsis and septic shock: a systematic review and meta-analysis. *Crit Care.* (2014) 18:699. doi: 10.1186/s13054-014-0699-2
117. Torres LN, Chung KK, Salgado CL, Dubick MA, Torres Filho IP. Low-volume resuscitation with normal saline is associated with microvascular endothelial dysfunction after hemorrhage in rats, compared to colloids and balanced crystalloids. *Crit Care.* (2017) 21:160. doi: 10.1186/s13054-017-1745-7
118. Hariri G, Joffre J, Deryckere S, Bigé N, Dumas G, Baudel J-L, et al. Albumin infusion improves endothelial function in septic shock patients: a pilot study. *Intensive Care Med.* (2018) 44:669–71. doi: 10.1007/s00134-018-5075-2
119. Pusateri AE, Moore EE, Moore HB, Le TD, Guyette FX, Chapman MP, et al. Association of prehospital plasma transfusion with survival in trauma patients with hemorrhagic shock when transport times are longer than 20 minutes. *JAMA Surg.* (2020) 155:e195085. doi: 10.1001/jamasurg.2019.5085
120. Diebel LN, Martin JV, Liberati DM. Microfluidics: a high-throughput system for the assessment of the endotheliopathy of trauma and the effect of timing of plasma administration on ameliorating shock-associated endothelial dysfunction. *J Trauma Acute Care Surg.* (2018) 84:575–82. doi: 10.1097/TA.0000000000001791
121. Barelli S, Alberio L. The role of plasma transfusion in massive bleeding: protecting the endothelial glycocalyx? *Front Med.* (2018) 5:91. doi: 10.3389/fmed.2018.00091

122. Deyab G, Reine TM, Vuong TT, Jenssen T, Hjeltnes G, Agewall S, et al. Antirheumatic treatment is associated with reduced serum Syndecan-1 in Rheumatoid Arthritis. *PLoS One.* (2021) 16:e0253247. doi: 10.1371/journal.pone.0253247
123. Abraham E, Wunderink R, Silverman H, Perl TM, Nasraway S, Levy H, et al. Efficacy and safety of monoclonal antibody to human tumor necrosis factor alpha in patients with sepsis syndrome. A randomized, controlled, double-blind, multicenter clinical trial. TNF-alpha MAb Sepsis Study Group. *JAMA.* (1995) 273:934–41.
124. Fisher CJ, Agosti JM, Opal SM, Lowry SF, Balk RA, Sadoff JC, et al. Treatment of septic shock with the tumor necrosis factor receptor:Fc fusion protein. The soluble TNF receptor sepsis study group. *N Engl J Med.* (1996) 334:1697–702. doi: 10.1056/NEJM199606273342603
125. Drost CC, Rovas A, Kusche-Vihrog K, Slyke PV, Kim H, Hoang VC, et al. Tie2 activation promotes protection and reconstitution of the endothelial glycocalyx in human sepsis. *Thromb Haemost.* (2019) 119:1827–38. doi: 10.1055/s-0039-1695768
126. Yang X, Meegan JE, Jannaway M, Coleman DC, Yuan SY. A disintegrin and metalloproteinase 15-mediated glycocalyx shedding contributes to vascular leakage during inflammation. *Cardiovasc Res.* (2018) 114:1752–63.

Conflict of Interest: The authors declare that the research was conducted in the absence of any commercial or financial relationships that could be construed as a potential conflict of interest.

Publisher's Note: All claims expressed in this article are solely those of the authors and do not necessarily represent those of their affiliated organizations, or those of the publisher, the editors and the reviewers. Any product that may be evaluated in this article, or claim that may be made by its manufacturer, is not guaranteed or endorsed by the publisher.

frontiers | Frontiers in Medicine

TYPE Original Research
PUBLISHED 28 July 2022
DOI 10.3389/fmed.2022.880657

OPEN ACCESS

EDITED BY
Roberta Russo,
University of Naples Federico II, Italy

REVIEWED BY
Artem N. Kuzovlev,
Research Institute General Resuscitation im.V.A.Negovskogo, Russia
Aurora Hernandez-Machado,
University of Barcelona, Spain
Giovanna Tomaiuolo,
University of Naples Federico II, Italy

*CORRESPONDENCE
Michaël Piagnerelli
michael.piagnerelli@chu-charleroi.be

SPECIALTY SECTION
This article was submitted to Intensive Care Medicine and Anesthesiology, a section of the journal Frontiers in Medicine

RECEIVED 21 February 2022
ACCEPTED 27 June 2022
PUBLISHED 28 July 2022

CITATION
Vanderelst J, Rousseau A, Selvais N, Biston P, Zouaoui Boudjeltia K and Piagnerelli M (2022) Evolution of red blood cell membrane complement regulatory proteins and rheology in septic patients: An exploratory study. *Front. Med.* 9:880657. doi: 10.3389/fmed.2022.880657

Evolution of red blood cell membrane complement regulatory proteins and rheology in septic patients: An exploratory study

Julie Vanderelst[1], Alexandre Rousseau[2], Nicolas Selvais[1], Patrick Biston[1], Karim Zouaoui Boudjeltia[2] and Michaël Piagnerelli[1,2]*

[1]Intensive Care, CHU-Charleroi Marie-Curie, Université libre de Bruxelles, Charleroi, Belgium, [2]Experimental Medicine Laboratory, CHU-Charleroi Vésale, ULB 222 Unit, Université libre de Bruxelles, Montigny-le-Tilleul, Belgium

Background: During sepsis, red blood cell (RBC) deformability is altered. Persistence of these alterations is associated with poor outcome. Activation of the complement system is enhanced during sepsis and RBCs are protected by membrane surface proteins like CD35, CD55 and CD59. In malaria characterized by severe anemia, a study reported links between the modifications of the expression of these RBCs membrane proteins and erythrophagocytosis. We studied the evolution of RBCs deformability and the expression of RBC membrane surface IgG and regulatory proteins in septic patients.

Methods: By flow cytometry technics, we measured at ICU admission and at day 3–5, the RBC membrane expression of IgG and complement proteins (CD35, 55, 59) in septic patients compared to RBCs from healthy volunteers. Results were expressed in percentage of RBCs positive for the protein. RBC shape was assessed using Pearson's second coefficient of dissymmetry (PCD) on the histogram obtained with a flow cytometer technique. A null value represents a perfect spherical shape. RBC deformability was determined using ektacytometry by the elongation index in relation to the shear stress (0.3–50 Pa) applied to the RBC membrane. A higher elongation index indicates greater RBC deformability.

Results: RBCs from 11 septic patients were compared to RBCs from 21 volunteers. At ICU admission, RBCs from septic patients were significantly more spherical and RBC deformability was significantly lower in septic patients for all shear stress $\geq$1.93 Pa. These alterations of shape and deformability persists at day 3–5. We observed a significant decrease at ICU admission only in CD35 expression on RBCs from septic patients. This low expression remained at day 3–5.

Conclusions: We observed in RBCs from septic patients a rapid decrease expression of CD35 membrane protein protecting against complement

activation. These modifications associated with altered RBC deformability and shape could facilitate erythrophagocytosis, contributing to anemia observed in sepsis. Other studies with a large number of patients and assessment of erythrophagocytosis were needed to confirm these preliminary data.

KEYWORDS

sepsis, red blood cell, complement, deformability, rheology, erythrophagocytosis

Introduction

Alterations of the microcirculation and the cellular metabolism cause multiple organ failure, the final evolution of septic shock leading to death (1–3). In sepsis, alterations of the microcirculation, where the oxygen (O_2) exchange between blood and cells was performed, and especially their persistence, are associated with morbidity and mortality (2, 4).

Red blood cells (RBCs), as the O_2 transporters and sensors of local hypoxia, are key elements of the microcirculation (5). These important physiologic functions are related to the RBC membrane integrity which allows the cell to deform and pass through capillaries. Using flow cytometry and ektacytometry, we previously observed altered RBC shape and deformability in septic patients (6–8) and reported that persistence of these alterations was associated with poor outcome (7). We also showed that a more spherical RBC shape in septic patients was associated with decreased sialic acid (SA) content in the RBC membrane (6, 9). These modifications of SA content and sphericity stimulated anaerobic glycolysis as demonstrated by increased intra-erythrocytic concentrations of 2,3 diphosphoglycerate and lactate (9). These results suggest links between the membrane, where glycolytic enzymes are anchored (10), and an enhanced ability of the altered RBCs to produce and liberate ATP by glycolysis (11). Although RBC SA content was decreased, the membrane proteins were not modified (12), in contrast to the lipid part of the RBC membrane in patients with bacterial sepsis (13).

Sepsis is a complex physiopathological model where circulating erythrocytes are vulnerable due, among other things, oxidative injuries occurring under the imbalance of redox homeostasis (14, 15) and activation of the innate immune response with increased complement proteins (16, 17).

RBCs are directly in contact with these complement regulatory proteins and are protected by membrane receptors against membrane damage: CD35, also name Complement Receptor type 1 - CR1, which inhibits complement activation (18) and carries immune complexes or cell fragments to spleen or liver for their clearance from the blood (19). Other RBC complement regulatory proteins included: CD55 (Decay Accelerating Factor - DAF) and CD59 (MembraneAttack Complex Inhibitory Factor – MACIF); both protecting RBCs against hemolysis by activated complement (18). RBC clearance was also enhanced by membrane antibody binding by immunoglobin G (IgG).

Various studies (19, 20) have established a relationship between the modification of the expression of these membrane proteins and the increase in erythrophagocytosis, leading to anemia in various pathologies such as beta-thalassemia and malaria. Nevertheless, none of these studies were performed in sepsis where the complement was also stimulated. In this study, we want to investigate the RBC rheology (shape and deformability) and the expression of different complement regulatory proteins (potential markers of erythrophagocytosis or hemolysis) on the membrane of RBCs from septic patients compared to healthy volunteers.

Methods

This prospective study was conducted medico -surgical ICU in the CHU-Charleroi, Belgium during 9 months after approval by the local and central ethical committees (ISPPC 008 and CHU-Erasme, Brussels). An informed consent was required for blood analysis.

We enrolled a group of patients with sepsis. Sepsis was diagnosed on the basis of the Third International Consensus Definitions for Sepsis and Septic Shock (21) with a proven bacterial or viral infection.

Patients were enrolled at ICU admission and during days 3–5 if they stayed in the ICU.

Finally, we enrolled a group of healthy hospital employees as controls. Patients and healthy volunteers with RBC pathologies, i.e., sickle cell disease, thalassemia, microcytosis and macrocytosis, were not included in the study.

Patients

Demographic data were collected from septic patients and volunteers: age, sex, origin of infections, treatment with vasopressors, length of ICU stay and mortality.

For ICU patients, we calculated the Simplified acute physiology score (SAPS 3) (22) and the Sequential organ failure assessment (SOFA) score on day 1 of the ICU admission (23).

We also recorded the following laboratory data: RBC count, hemoglobin (Hb) concentration, hematocrit, erythrocyte count, mean corpuscular volume, leukocyte and platelet counts and lactate and C-reactive protein (CRP) concentrations.

Flow cytometry and expression of membrane regulatory proteins

The experiments were performed using a flow cytometer: MACSQuant 10 from MiltenyiBiotec®.

RBCs (10^6/mm^3) were first diluted 500× in Hanks'Balanced Salt Solution (HBSS). The antibodies (Ab), CD35, CD55, CD59, IgG, were added in the quantities recommended by the supplier BD Pharmigen®.

After 15 min of incubation, in the dark and at room temperature, the solution containing the Ab was then washed with 400 µl of HBSS (300 × g for 5 min at room temperature) and then re-suspended in 500 µl of HBSS.

After addition of 1 ml of CD235a to identify RBCs, incubation for 10 min at 4–10°C was performed. For each Ab, we proceeded to the passage of a corresponding iso-typical counting a minimum of 15,000 events.

A compensation matrix was applied to each sample, in order to compensate for the overlapping fluorescence emission spectra of some fluorochromes present on the Ab. Finally, we recorded the percentage of cells expressing fluorescence of the labeled Ab by setting our positivity threshold with the corresponding iso-typical.

Measurements of RBC Shape

As change in RBC shape is time dependent, analyzes were completed in a maximum of 90 min. Measurement techniques have been described elsewhere (6, 24). Data were collected on a MacsQuant® Analyzer 10 flow cytometer (Miltenyi Biotec BV, ZZ Leiden, Netherlands). The forward light scatter channels (FSCs) were set on a linear scale. Cell size is the principal component of the FSC signal. For estimation of RBC shape, we used the second coefficient of dissymmetry of Pearson (PCD), applying low shear stresses (12 µl/min RBC flow rate) to allow the RBCs to rotate in the flow without deformation (25). In this technique, we did not add fluorescently labeled agglutinins that can alter RBC shape.

Whole blood (2 µl) was mixed with isotonic (286 mOsm) phosphate-buffer saline at 25°C. This study was limited to 30,000 events and lasted for 15 s. In healthy volunteers, after positioning of the obscuration bar, the cytometer viewed the flow of ellipsoid, biconcave RBCs as essentially two populations of cells, and the FSC histograms showed a typically bimodal distribution of RBCs.

We calculated the PCD = [3 × (mean – median)/ SD] on the histogram as an estimation of the sphericity of the RBCs (6, 24). In general, the PCD values of RBCs in healthy volunteers are around −0.6 and a PCD value of 0 represents a perfect spherical shape.

Measurements of RBC deformability

RBC deformability was assessed using ektacytometry (LORRCA; Mechatronics Instruments BV, AN Zwaag, Netherlands). We used the same analytical method as that used by Donadello et al. (7): a suspension of RBCs was mixed with polyvinylpyrrolidone 360 solution, an isotonic viscous medium (PVP, 4%; MW 360 kDa; viscosity 30 ± 2 mPa·s), to obtain a final solution with a constant hematocrit of 0.2%. Using a Couette system composed of a glass cup and a precisely fitting bob, with a gap of 0.36 mm between the cylinders, the liquid solution was sheared and illuminated by a laser beam in order to obtain a diffraction pattern produced by the deformed cells. This diffraction was analyzed by a computer, which also controls the cup rotational speed and the predetermined shear stresses. The elongation index (EI) is calculated as: $EI = (L - W)/(L + W)$, where L and W are the length and width of the diffraction pattern, respectively. The geometry of the diffraction pattern is elliptical. For a given shear stress, the greater the RBC deformability, the higher the EI. At 37°C, we assessed the EI curves for 12 consecutive shear stress values, because human RBC deformability reaches a plateau at 50 Pa: 0.3, 0.48, 0.76, 1.21, 1.93, 3.07, 4.89, 7.78, 12.3, 19.7, 31 and 50 Pa. Interassay variabilities for each shear stress were: 51, 8.2, 3.9, 2.4, 1.7,1.6, 1.1, 1.3, 1.7, 1.2, 1.4 and 1.2%, respectively.

From the shear stress-response curves of shape change, we calculated the maximal RBC elongation (EI max) and curves are presented in logarithmic scales (26).

Statistical analysis

The laboratory results were anonymized and entered into an Excel spreadsheet. The program used to perform the statistical analysis was SigmaStat version 12.0 (Systat Software Ins, San Jose, California). Results are presented as median values [interquartile range 25%−75%] or percentages and were compared by Mann–Whitney Rank Sum test. Comparisons of EI for SS used the ANOVA test.

The change in PCD or EI over time was evaluated using a Friedman repeat measures analysis of variance with Bonferroni *post-hoc* adjustments. A p value <0.05 was considered as statistically significant.

10.3389/fmed.2022.880657

TABLE 1 Subject demographics, biological characteristics, and outcomes.

	Healthy volunteers ($n = 21$)	Septic patients ($n = 19$)	p-Value
Age (years)	50 [23–57]	65 [55–70]	0.002
Sex (M/F)	10/11	14/5	0.1
SAPS 3	ND	56 [53–69]	
SOFA at day 1	ND	8 [4–10]	
Hemoglobin (g/dl)	14.3 [13.7–16.1]	11.2 [9.3–14.6]	0.017
Hematocrit (%)	43.6 [40.1–47.0]	34.4 [28.3–42.7]	0.012
RBC (10^9/mm^3)	4910 [4322–5380]	3700 [3170–4380]	0.004
MCV (mm^3)	90.9 [88.1–93.6]	94.6 [89.3–96.6]	0.2
WBC ($\times 10^3$/mm^3)	6.0 [5.2–6.8]	16.2 [10.3–23.7]	< 0.001
Platelets ($\times 10^3$/mm^3)	249 [194–308]	258 [234–325]	0.66
Urea (mg/dl)	34 [31–42]	46 [38–42]	0.04
Creatinine (mg/dl)	0.85 [0.78–0.94]	1.23 [0.85–1.75]	0.03
Na^+ (mEq/L)	141 [140–142]	139 [137–141]	0.03
Bilirubin (mg/dl)	0.7 [0.5–0.9]	0.7 [0.4–1.3]	0.8
Glycemia (mg/dl)	82 [77–89]	155 [119–226]	< 0.001
CRP (mg/dl)	1 [0.5–4.0]	140 [65–226]	< 0.001
Lactate (mmol/L)	ND	1.6 [1.3–2.1]	
pH	ND	7.41 [7.38–7.44]	
PaO_2/FiO_2	ND	203 [151–290]	
Vasopressor dosesmcg/kg h ($n = 9$)	ND	0.17 [0.09–0.23]	
ICU length of stay (days)	ND	5 [4–6]	
ICU Mortality (%)	ND	6 (32)	

Results are presented as median [25th−75th] percentiles and compared by Mann–Whitney test. NR, non-relevant; SAPS III, Simplified acute physiology score 3; and SOFA, sequential organ failure assessment; RBC, red blood cell; MCV, mean corpuscular volume; WBC, white blood cell; CRP, C-reactive protein.

TABLE 2 Comparisons of membrane receptor proteins and Ig G at ICU admission.

	Healthy volunteers ($n = 21$)	Septic patients ($n = 19$)	p-Value
CD 35	23.04 [11.39–32.57]	12.30 [9.02–22.92]	0.042
CD 55	95.82 [94.93–97.96]	95.40 [94.30–96.20]	0.78
CD 59	92.34 [86.40–93.61]	91.31 [80.22–94.88]	0.11
Ig G	1.55 [0.90–2.35]	1.29 [1.03–2.18]	0.87

Results

Patients

Nineteen septic ICU patients within 24 h of admission were included and 21 healthy volunteers. Eleveen of the 19 (58%) septic patients were studied during 3–5 days. Clinical characteristics are shown in Table 1. The volunteers were younger than septic patients (53 [34–59] vs. 66 [55–71] years; $p = 0.01$). Fifteen of the 19 (79%) patients with sepsis were in shock at the moment of inclusion.

Sepsis was due to peritonitis in eight patients (42%); pneumonia in four (21%); urinary tract infection in two (10%); meningitidis in two (10%) and osteitis in one (5%). Three of these patients (16%) also had a positive blood culture at day 1. ICU mortality was 32%.

Biological data

ICU patients at admission were significantly more anemic than volunteers (RBC count for septic patients: $3{,}700{\cdot}10^6$/mm^3 vs. for healthy volunteers: $4{,}910{\cdot}10^6$/mm^3; $p = 0.004$; Table 1). As expected, inflammation suggested by WBC count and CRP concentrations were significantly higher in septic patients (WBC count for septic: $16.2.10^3$/mm^3 vs. for healthy volunteers: $6.0.10^6$/mm^3; $p < 0.001$). There was also more acute kidney failure in septic patients (creatinine for septic patients: 1.23 [0.85–1.75] vs. 0.85 [0.78–0.94] mg/dl for healthy volunteers, $p = 0.032$; Table 1).

Flow cytometry and expression of membrane regulatory proteins

At ICU admission, we noted a significant decrease only in the expression of CD35 on the RBC membrane surface in septic patients compared to volunteers (Table 2). In the 11 septic patients studied for 3–5 days, no significant changes

in membrane protein expression over time were observed (Table 3).

RBC shape

At ICU admission, the PCD was significantly lower in septic patients than in healthy volunteers suggesting a more spherical shape (−0.399 [−0.563; −0.180] vs. −0.538 [−0.657; −0.491]; $p = 0.026$; Figure 1). The PCD remained lower on day 3–5 in 11 septic patients: for ICU admission −0.398 [−0.560; −0.075] vs. −0.404 [−0.516; −0.129] on day 3–5; $p = 0.21$.

RBC deformability

At ICU admission, deformability was significantly impaired in RBCs from septic patients compared to RBCs from healthy volunteers for shear stress ≥1.93 Pa (Figure 2). The EI max for septic patients was 0.577 ± 0.032 compared to 0.612 ± 0.010 for healthy volunteers; $p < 0.001$.

TABLE 3 Evolution of the receptor membrane receptor proteins and Ig G in septic patients at day 1 and 3–5 ($n = 11$).

	Day 1 ($n = 11$)	Day 3–5 ($n = 11$)	p-Value
CD 35	11.30 [7.80–25.00]	15.60 [8.50–20.30]	0.56
CD 55	94.97 [93.15–96.12]	94.35 [91.65–95.28]	0.46
CD 59	82.43 [69.95–93.45]	92.62 [83.21–93.34]	0.11
Ig G	1.69 [1.28–2.48]	1.76 [1.11–6.2]	0.64

We followed 11 septic patients until day 3–5. The EI max on day 1 (0.576 ± 0.041) was similar to day 3–5 (0.586 ± 0.02); $p = 0.25$.

Discussion

Sepsis is a complex disease characterized by inflammation, altered microcirculation and mitochondrial dysfunction (1, 2). Enhanced activation of the complement contributes to the inflammation and leads to cells lysis and phagocytosis by the reticuloendothelial cells (16, 17).

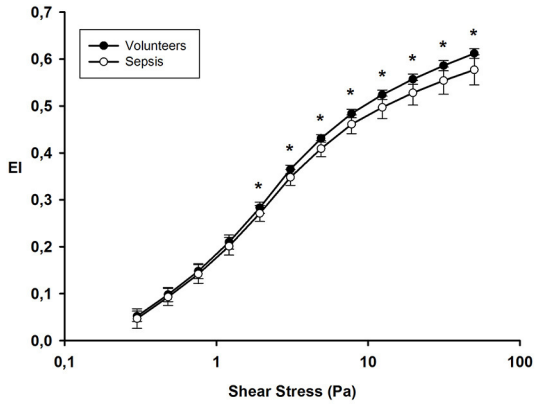

FIGURE 2
Elongation index at different shear stress values on day 1 in healthy volunteers and septic patients. *p value < 0.05.

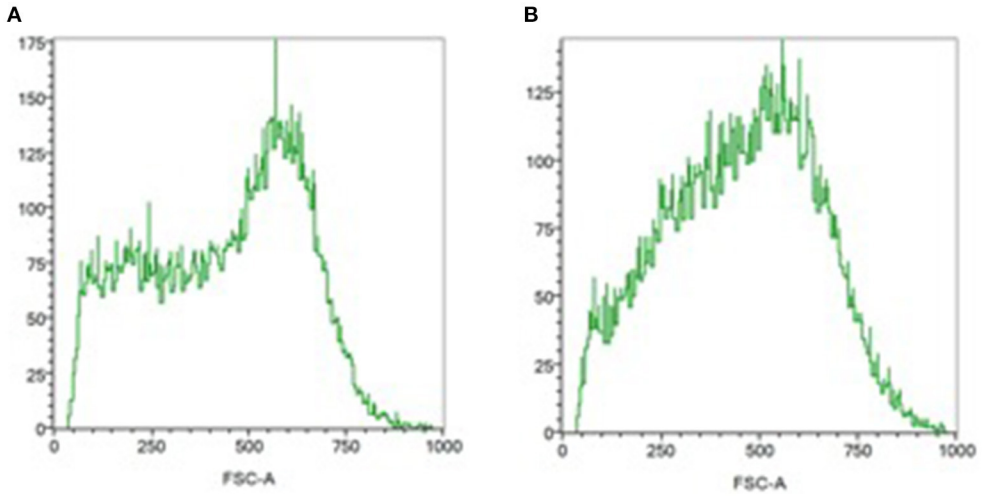

FIGURE 1
Assessment of the RBC shape by flow cytometry. RBC distribution histograms relating number of events and forward light scatter (FSC) distribution (size estimation). **(A)** In normal biconcave, ellipsoid red blood cells, the FSC distribution (size estimation) is bimodal. **(B)** Monomodal distribution is observed in septic patient, suggesting a more spherical shape.

RBCs, as the oxygen transporters and sensors of local hypoxia are in contact with the complement proteins and are protects by several complement regulatory proteins. RBC membrane is the key element of deformability (5) and it's modifications could alter the RBC shape and rheology.

In this study, we observed a more RBC spherical shape and altered deformability in septic patients already at ICU admission. These alterations persisted at day 3–5. On these RBCs from septic patients, only membrane CD35 expression significantly decreased during the first 5 days.

Previously, we observed altered RBC shape using flow cytometry and RBC deformability using ektacytometry in septic patients (6, 8, 27) and reported that persistence of these alterations was associated with poor outcome (7). In this work, we confirmed these results on the shape and deformability of RBCs. These alterations may be secondary to changes in the membrane, which is the key element in the RBC deformability (6). For example, we showed that a more spherical RBC shape in septic patients was associated with decreased sialic acid content – a carbohydrate- on the RBC membrane (9) and we observed an increased neuraminidase activity, an enzyme that cleaves sialic acid on the RBC membrane in these septic patients (9).

The complement system represents the first line of defense that is involved in the clearance of pathogens, dying cells and immune complexes via opsonization, induction of an inflammatory response and the formation of a lytic pore. RBCs, as a circulating blood cells, are in contact with enhanced complement proteins observed in sepsis and expresses membrane complement regulatory proteins to limit complement activation. Decreased expression of the membrane regulatory proteins may result in complement activation and accelerated removal of these modified RBCs.

CD 35 also called CR1, is a surface protein that binds C3b in circulating immune complexes, making these complexes available for uptake by macrophages of the reticuloendothelial system (18).

Complement proteins deposits were already observed in RBCs from ICU patients. Indeed, Muroya et al. observed significantly higher amounts of C4d on the RBCs surface from 40 trauma patients compared to RBCs from 17 healthy volunteers (28). *Ex-vivo* addition of RBCs from universal donors with sera from trauma patients promotes C4d depositions and limited their deformability assessed by microchannel arrays. Modifications of band 3 phosphorylation, accelerated calcium influx and enhanced nitric oxide production could be the origin of altered deformability (29).

Recently, Lam et al. (30) compared complement (C3b and C4b) deposition on RBCs in COVID-19 patients compared to non-COVID-19 septic patients and healthy volunteers. These authors observed on 11 septic patients an increase of RBCs with bound C3b/iC3b/C3dg and C4d but also in COVID-19 patients compared with healthy volunteers. These results agreed with our results and suggested complement activation products were present on the RBC membrane from septic patients. Kisserli et al. (31) also observed an acquired decrease of RBC CR1 density from COVID-19 patients. They observed a relationship between decrease RBC CR1 density and severity of hypoxemia and in 32 patients with a longitudinal study, they observed a decrease of RBC CR1 density at day 10. These results were difficult to extrapolate in septic non-COVID 19 patients due to particular pathophysiology of the SARS-CoV 2 disease (32). Moreover, Kisserli et al. (31) compared these results to RBCs from healthy volunteers but not septic patients.

Waitumbi et al. (19) observed deficiencies in CR1 but also in CD 55 and an increase in CD 59 in RBCs from patients with severe anemia due to *Plasmodium falciparum*. These results suggested an increase in erythrophagocytosis in this pathology. We found the same results in our septic patients but only for CD35 and not for the other complement regulatory proteins like CD 55 and CD 59, no IgG deposit on the RBC membrane. The difference with our results may be explained by the number of patients studied and difference in the characteristics of the included patients (children with anemia due to malaria in the study of Waitumbi et al. without sepsis and adult ICU septic in our study). Age of the subjects studied was probably important. Indeed, Waitumbi et al. (33) observed a lower RBC complement regulatory protein in young children and increased into adulthood. In contrast, we included only adult patients in our study. Moreover, CD 55 and CD 59 protects RBCs against hemolysis by the complement and this phenomenon was not frequently observed in sepsis.

Mechanisms by macrophages of the reticuloendothelial system recognize senescent RBCs for clearance include enzymatic dysfunctions, neoantigens on RBC surface, exposure phosphatidylserine and decreased deformability due to membrane damage (34).

Our study suggests that a decrease in CD35 expression on the RBC surface may be part of the accelerated aging process and erythrophagocytosis in RBCs from septic patients as well as an increase in RBC sphericity. Blocking complement activation could therefore be an interesting therapy to limit the development of anemia in these patients, and possibly tissue damage related to complement proteins activation, as suggested in COVID-19 patients (19, 35). Moreover, a selective inhibition of one complement protein rather than the whole complement activation pathway would be more interesting in terms of morbidity, especially against the increased risk nosocomial infections (36). Nevertheless, further studies on a large number of non-COVID-19 sepsis or septic shock patients are needed to confirm this hypothesis.

There are several limitations to our study. First, the number of subjects included in the study is limited. Due to ICU

discharges or deaths, our sample has been further reduced over time. Therefore, a study with a larger population and longer than 5 days is needed to confirm the results obtained.

Second, we have voluntarily limited ourselves to the observation of the expression of three membrane proteins (CD 35, CD 55, CD 59) and IgG. It would also be interesting to study the expression of RBC membrane CD 47 because it plays a role in the phagocytosis process (37). This could reinforce our hypothesis of accelerated RBC aging in sepsis. Third, we observed a decrease of RBC membrane regulatory proteins but we have not measured blood complement proteins to confirm enhancement due to sepsis. Four, we did not included a group of non-septic ICU patients. Those patients with moderate inflammation may also have alterations on RBC membrane complement regulatory proteins. Indeed, we have previously observed an altered RBC shape in these patients (6).

In conclusion, our results show that the RBCs of septic patients have an increased sphericity as well as decreased deformability, and this pattern did not change over 3–5 days. In addition, we observed a decrease in the expression of membrane complement regulatory protein CD 35. These shape, deformability and membrane changes observed on the RBCs of septic patients could promote erythrophagocytosis.

Data availability statement

The raw data supporting the conclusions of this article will be made available by the authors, without undue reservation.

Ethics statement

The studies involving human participants were reviewed and approved by ISPPC 008 and CHU-Erasme, Brussels. The patients/participants provided their written informed consent to participate in this study.

Author contributions

JV, NS, KZ, and MP designed the study. JV, AR, NS, PB, KZ, and MP performed the research. JV, KZ, and MP wrote the paper. All authors revised the paper critically and approved the final version.

Conflict of interest

The authors declare that the research was conducted in the absence of any commercial or financial relationships that could be construed as a potential conflict of interest.

Publisher's note

All claims expressed in this article are solely those of the authors and do not necessarily represent those of their affiliated organizations, or those of the publisher, the editors and the reviewers. Any product that may be evaluated in this article, or claim that may be made by its manufacturer, is not guaranteed or endorsed by the publisher.

References

1. Bakker J, Kattan E, Annane D, Castro R, Cecconi M, De Backer D, et al. Current practice and evolving concepts in septic shock resuscitation. *Intens Care Med.* (2022) 48:148–63. doi: 10.1007/s00134-021-06595-9

2. De Backer D, Ricottilli F, Ospina-Tascon GA. Septic shock: a microcirculation disease. *Curr Opin Anaestesiol.* (2021) 34:85–91. doi: 10.1097/ACO.0000000000000957

3. Preau S, Vodovar D, Jung B, Lancel S, Zafrani L, Flatres A, et al. Energetic dysfunction in sepsis: a narrative review. *Ann Intensive Care.* (2021) 11:104. doi: 10.1186/s13613-021-00893-7

4. Yajnik V, Maarouf R. *Sepsis and the* microcirculation: the impact on outcomes. *Curr Opin Anaesthesiol.* (2022) 35:230–5. doi: 10.1097/ACO.0000000000001098

5. Piagnerelli M, Zouaoui Boudjeltia K, Vanhaeverbeek M, Vincent J-L. Red blood cell rheology in sepsis. *Intensive Care Med.* (2003) 29:1052–61. doi: 10.1007/s00134-003-1783-2

6. Piagnerelli M, Zouaoui Boudjeltia K, Brohee D, Piro P, Carlier E, Vincent JL, et al. Alterations of red blood cell shape and sialic acid membrane content in septic patients. *Crit Care Med.* (2003) 31:2156–62. doi: 10.1097/01.CCM.0000079608.00875.14

7. Donadello K, Piagnerelli M, Reggiori G, Gottin L, Scolletta S, Occhipinti G, et al. Reduced red blood cell deformability over time is associated with a poor outcome in septic patients. *Microvasc Res.* (2015) 101:8–14. doi: 10.1016/j.mvr.2015.05.001

8. Reggiori G, Occhipinti G, De Gasperi A, Vincent JL, Piagnerelli M. Early alterations of red blood cell rheology in critically ill patients. *Crit Care Med.* (2009) 37:3041–6. doi: 10.1097/CCM.0b013e3181b02b3f

9. Piagnerelli M, Boujeltia KZ, Rapotec A, Richard T, Brohée D, Babar S, et al. Neuraminidase alters red blood cells in sepsis. *Crit Care Med.* (2009) 37:1244–50. doi: 10.1097/CCM.0b013e31819cebbe

10. Campanella ME, Chu H, Low PS. Assembly and regulation of a glycolytic enzyme complex on the human erythrocyte membrane. *Proc Natl Acad Sci USA.* (2005) 102:2402–7. doi: 10.1073/pnas.0409741102

11. McMahon TJ, Darrow CC, Hoehn BA, Zhu H. Generation and export of red blood cell ATP in health and disease. *Front Physiol.* (2021) 12:754638. doi: 10.3389/fphys.2021.754638

12. Piagnerelli M, Cotton F, Van Nuffelen M, Vincent JL, Gulbis B. Modifications in erythrocyte membrane protein content are not responsible for the alterations in rheology in sepsis. *Shock.* (2012) 37:17–21. doi: 10.1097/SHK.0b013e318237d55a

13. Kempe DS, Akel A, Lang PA, Hermle T, Biswas R, Muresanu J, et al. Suicidal erythrocyte death in sepsis. *J Mol Med.* (2007) 85:273–81. doi: 10.1007/s00109-006-0123-8

14. Bateman RN, Sharpe MD, Singer M, Ellis CG. The effect of sepsis on the erythrocyte. *Int J Mol Sci.* (2017) 18:1932. doi: 10.3390/ijms18091932

15. Maruyama T, Hieda M, Mawatari S, Fujino T. Rheological abnormalities in human erythrocytes subjected to oxidative inflammation. *Front Physiol.* (2022) 13:837926. doi: 10.3389/fphys.2022.837926

16. Markiewski MM, DeAngelis RA, Lambris JD. Complexity of complement activation in sepsis. *J Cell Mol Med*. (2008) 12 (6A):2245–54. doi: 10.1111/j.1582-4934.2008.00504.x

17. Mannes M, Schmidt CQ, Nilsson B, Ekdahl KN, Huber-Lang M. Complement as driver of systemic inflammation and organ failure in trauma, burn, and sepsis. *Semin Immunopathol*. (2021) 43:773–88. doi: 10.1007/s00281-021-00872-x

18. Thielen AJF, Zeerleder S, Wouters D. Consequences of dysregulated complement regulators on red blood cells. *Blood Rev*. (2018) 32:280–8. doi: 10.1016/j.blre.2018.01.003

19. Waitumbi JN, Opollo MO, Muga RO, Misore AO, Soute JA. Red cell surface changes and erythrophagocytosis in children with severe *Plasmodium falciparum* anemia. *Blood*. (2000) 95:1481–6. doi: 10.1182/blood.V95.4.1481.004k15_1481_1486

20. Kurtogllu AU, Koçtekin B, Kurtoglu E, Yildiz M, Bozkurt S. Expression of CD55, CD59, and CD35 on red blood cells of β-thalassaemia patients. *Centr Eur J Immunol*. (2017) 42:78–84. doi: 10.5114/ceji.2017.67321

21. Singer M, Deutschman CS, Seymour CW, Shankar-Hari M, Annane D, Bauer M, et al. The third international consensus definitions for sepsis and septic shock (Sepsis-3). *JAMA*. (2016) 315:801–10. doi: 10.1001/jama.2016.0287

22. Moreno RP, Metnitz PGH, Almeida E, Jordan B, Bauer P, Abizanda Campos R, et al. SAPS 3- From evaluation of the patient to evaluation of the intensive care unit. *Intens Care Med*. (2005) 31:1345–55. doi: 10.1007/s00134-005-2763-5

23. Vincent JL, Moreno R, Takala J, Willatts S, De Mendoça A, Bruining H, et al. The SOFA (Sepsis-related organ failure assessment score to describe organ dysfunction/failure). *Intens Care Med*. (1996) 22:707–10. doi: 10.1007/BF01709751

24. Piagnerelli M, Zouaoui Boudjeltia K, Brohee D, Vereestraten A, Piro P, Vincent JL, et al. Assessment of erythrocyte shape by flow cytometry techniques. *J Clin Pathol*. (2007) 60:549–54. doi: 10.1136/jcp.2006.037523

25. Bitbol M. Red blood cell orientation in orbit C=0. *Biophys J*. (1986) 49:1055–68. doi: 10.1016/S0006-3495(86)83734-1

26. Condon RM, Kim JE, Deitch EA, Machiedo GW, Spolarics Z. Appearance of an erythrocyte population with decreased deformability and hemoglobin content following sepsis. *Am J Physiol Heart Circ Physiol*. (2003) 284:H2177–84. doi: 10.1152/ajpheart.01069.2002

27. Piagnerelli M, Vanderelst J, Rousseau A, Monteyne D, Perez-Morga D, Biston P, et al. Red blood cell shape and deformability in patients with COVID-19 acute respiratory distress syndrome. *Front Physiol*. (2022) 13:849910. doi: 10.3389/fphys.2022.849910

28. Muroya T, Kannan L, Ghiran IC, Shevkoplyas SS, Paz Z, Tsokos M, et al. C4d deposits on the surface of RBCs in trauma patients and interferes with their function. *Crit Care Med*. (2014) 42:e364–72. doi: 10.1097/CCM.0000000000000231

29. Remigante A, Morabito R, Marino A. Band 3 protein function and oxidative stress in erythrocytes. *J Cell Physiol*. (2021) 236:6225–34. doi: 10.1002/jcp.30322

30. Lam LKM, Reilly JP, Rux AH, Murphy SJ, Kuri-Cervantes L, Weisman AR, et al. Erythrocytes identify complement activation in patients with COVID-19. *Am J Physiol Lung Cell Mol Physiol*. (2021) 321:L485–9. doi: 10.1152/ajplung.00231.2021

31. Kisserli A, Schneider N, Audonnet S, Tabary T, Goury A, Cousson J, et al. Acquired decrease of the C3b/C4b receptor (CR1, CD35.) and increased C4d deposits on erythrocytes from ICU COVID-19 patients. *Immunobiology*. (2021) 226:152093. doi: 10.1016/j.imbio.2021.152093

32. Azoulay E, Fartoukh M, Darmon M, Géri G, Voiriot G, Dupont T, et al. Increased mortality in patients with severe SARS-CoV-2 infection admitted within seven days of disease onset. *Intens Care Med*. (2020) 46:1714–22. doi: 10.1007/s00134-020-06202-3

33. Waitumbi JN, Donvito B, Kisserli A, Cohen JH, Soute JA. Age-related changes in red blood cell complement regulatory proteins and susceptibility to severe malaria. *J Infect Dis*. (2004) 190:1183–91. doi: 10.1086/423140

34. Thiagarajan P, Parker CJ, Prchal JT. How do red blood cells die? *Front Physiol*. (2021) 12:655393. doi: 10.3389/fphys.2021.655393

35. Vlaar APJ, de Bruin S, Busch M, Timmermans SAMEG, van Zeggeren IE, Koning R, et al. Anti-C5a antibody IFX-1(vilobelimab) treatment versus best supportive care for patients with severe COVID-19 (PANAMO): an exploratory, open-label, phase 2 randomised controlled trial. *Lancet Rheumatol*. (2020) 2:e764–73. doi: 10.1016/S2665-9913(20)30341-6

36. Afzali B, Noris M, Lambrecht BN, Kemper C. The state of complement in COVID-19. *Nat Rev Immunol*. (2022) 22:77–84. doi: 10.1038/s41577-021-00665-1

37. Burger P, Hilarius-Stockman P, de Korte D, van den Berg TK, van Bruggen R. CD47 functions as a molecular switch for erythrocyte phagocytosis. *Blood*. (2012) 119:5512–21. doi: 10.1182/blood-2011-10-386805

frontiers | Frontiers in Physiology

TYPE Original Research
PUBLISHED 20 September 2022
DOI 10.3389/fphys.2022.980460

OPEN ACCESS

EDITED BY
Giuseppe Paglia,
University of Milano Bicocca, Italy

REVIEWED BY
Charles E. McCall,
Wake Forest Baptist Medical Center, United States
Nara Liessi,
Italian Institute of Technology (IIT), Italy

*CORRESPONDENCE
David A. Ford,
david.ford@health.slu.edu

SPECIALTY SECTION
This article was submitted to Lipid and Fatty Acid Research, a section of the journal Frontiers in Physiology

RECEIVED 29 June 2022
ACCEPTED 30 August 2022
PUBLISHED 20 September 2022

CITATION
Amunugama K, Pike DP and Ford DA (2022), E. coli strain-dependent lipid alterations in cocultures with endothelial cells and neutrophils modeling sepsis.
Front. Physiol. 13:980460.
doi: 10.3389/fphys.2022.980460

E. coli strain-dependent lipid alterations in cocultures with endothelial cells and neutrophils modeling sepsis

Kaushalya Amunugama[1,2], Daniel P. Pike[1,2] and David A. Ford[1,2]*

[1]Edward A. Doisy Department of Biochemistry and Molecular Biology, Saint Louis University School of Medicine, St. Louis, MO, United States, [2]Center for Cardiovascular Research, Saint Louis University School of Medicine, St. Louis, MO, United States

Dysregulated lipid metabolism is common in infection and inflammation and is a part of the complex milieu underlying the pathophysiological sequelae of disease. Sepsis is a major cause of mortality and morbidity in the world and is characterized by an exaggerated host response to an infection. Metabolic changes, including alterations in lipid metabolism, likely are important in sepsis pathophysiology. Here, we designed an *in vitro* cell culture model using endothelial cells, *E. coli*, and neutrophils to mimic sepsis in a simplified cell model. Lipid alterations were studied in the presence of the pathogenic *E. coli* strain CFT073 and non-pathogenic *E. coli* strain JM109. We employed untargeted lipidomics to first identify lipid changes and then targeted lipidomics to confirm changes. Both unique and shared lipid signatures were identified in cocultures with these *E. coli* strains. In the absence of neutrophils, the CFT073 strain elicited alterations in lysophosphatidylcholine and diglyceride molecular species during coculture while both strains led to increases in phosphatidylglycerols. Lipid alterations in these cocultures changed with the addition of neutrophils. In the presence of neutrophils with *E. coli* and endothelial cells, triglyceride increases were a unique response to the CFT073 strain while phosphatidylglycerol and diglyceride increases occurred in response to both strains. Phosphatidylethanolamine also increased in neutrophils, *E. coli* and endothelial cells cocultures, and this response was greater in the presence of the CFT073 strain. We further evaluated changes in phosphatidylethanolamine in a rat model of sepsis, which showed multiple plasma phosphatidylethanolamine molecular species were elevated shortly after the induction of sepsis. Collectively, these findings demonstrate unique lipid responses by co-cultures of *E. coli* with endothelial cells which are dependent on the *E. coli* strain as well as the presence of neutrophils. Furthermore, increases in phosphatidylethanolamine levels in CFT073 urosepsis *E. coli*, endothelial cell, neutrophil cocultures were similarly observed in the plasma of septic rats.

KEYWORDS

sepsis, *E. coli*, lipids, neutrophils, endothelial cells, infection, lipidomics

Introduction

Lipids play essential roles in physiological and pathological processes. They are crucial components of cell membranes and signaling mechanisms, and they serve as energy sources. Dysregulated lipid metabolism and activation of lipid-mediated signaling pathways are observed in various disease conditions, including sepsis and COVID-19 (Gijon et al., 1995; Bruegel et al., 2012; Rival et al., 2013; Ahmad et al., 2020; Amunugama et al., 2021a; Snider et al., 2021). Plasma lipidome changes during COVID-19 have been attributed to secretory phospholipase A_2 activity (Snider et al., 2021). Sepsis is a life-threatening organ dysfunction caused by an exaggerated immune response to an infection (Rudd et al., 2020). Sepsis disease heterogeneities, including bacterial (or viral, including SARS-CoV-2) speciation of the initial infection, may lead to specific mechanisms mediating the pathophysiological sequelae of the disease and specific biomarkers.

Systemic neutrophil activation and endothelial barrier dysfunction are common in sepsis. Neutrophils are the major white blood cells that are activated in the early stages of sepsis and are vital for microbial killing. The role of neutrophils in the pathogenesis of sepsis is complex and not completely understood. Several studies show impaired neutrophil migration to the site of inflammation, declined chemotactic responses, and decreased endothelial-leukocyte interactions during sepsis (Alves-Filho et al., 2008; Kovach and Standiford, 2012; Sae-Khow et al., 2020). Alternatively, neutrophil hyperactivation and enhanced neutrophil recruitment have been shown to improve pathogen clearance and sepsis survival (Liaw et al., 2005; Craciun et al., 2010). Additionally, due to continuous inflammatory stimuli and endotoxin exposure during sepsis, the endothelium becomes activated to promote a pro-adhesive and pro-thrombotic surface (Cepinskas and Wilson, 2008). The activated endothelium destabilizes the gap junctions and tight junctions leading to loss of the endothelial barrier (Li et al., 2020). Endothelial hyperpermeability may result in interstitial edema, which subsequently increases interstitial pressure and organ damage in sepsis (Ait-Oufella et al., 2010). Pro-thrombotic endothelium triggers platelet-leukocyte aggregates blocking the microcirculation (Joffre et al., 2020).

Although the blood-endothelial interface has an important pathophysiological role in sepsis, little is known regarding lipids at this interface in the presences of bacteria. Here we designed a simplified *in vitro* cell culture-based model to investigate lipid signatures altered under conditions mimicking sepsis. The human endothelial cell line EA.hy926 (EA) was exposed to either uroseptic CFT073 or non-pathogenic JM109 *E. coli* strains in the presence and absence of neutrophils. Untargeted and targeted lipidomics were performed to identify altered lipid profiles. These studies revealed significant changes in multiple lipid classes and lipid molecular species under the different coculture conditions tested. Furthermore, coculture of endothelial cells, neutrophils and uroseptic CFT073 *E. coli* led to increased phosphatidylethanolamine levels, which were also elevated in the plasma during an early stage of rat sepsis.

Materials and methods

Neutrophil preparation

Neutrophils were isolated from whole blood of healthy human donors as previously described with approval by the Saint Louis University Institutional Review Board (Amunugama et al., 2021b). Briefly, whole blood was centrifuged over a density gradient. After centrifugation, the polymorphonuclear cell band was isolated and washed with Hanks's balanced salt solution (HBSS). The red blood cells were lysed and neutrophils were washed twice with HBSS before preparing relevant neutrophil concentrations in HBSS.

Bacteria strains

CFT073 and JM109 *E. coli* strains were used as pathogenic and non-pathogenic strains, respectively. Overnight pre-cultured bacteria were sub-cultured in Luria-Bertani (LB) broth shaking at 260 rpm at 37°C until they reached the exponential growth phase. Bacteria cell number was calculated using pre-drawn growth curves. Bacteria were washed in HBSS and appropriate concentrations were prepared in HBSS.

Coculture sample preparation for lipidomics

Endothelial-*E. coli* cocultures were prepared as follows. Endothelial EA.hy926 (EA) cells were plated on 6 well plates and grown to 100% confluency in Dulbecco's Modified Eagle medium with 10% FBS. Plates were rinsed with HBSS and 20×10^6/ml of CFT073 *E. coli* or JM109 *E. coli* were added in HBSS and incubated 1 or 2 h at 37°C. The EA: *E. coli* cell ratio was 1:20. Control samples were prepared by culturing EA and bacteria separately and combining them at the end of incubation. Experiments were performed using 3 biological replicates each having 3 experimental replicates. Endothelial-*E. coli*-neutrophil cocultures were prepared as follows, EA.hy926 cells were plated on 6 well plates and were rinsed with HBSS prior to the addition of 20×10^6/ml CFT073 or JM109 *E. coli* in HBSS. Cultures were incubated for 1 h at 37°C. Subsequently, 2×10^6 human neutrophils in 0.5 ml HBSS were added into each well, keeping the ratio of neutrophils: bacteria at 1:10 in the coculture. The EA: *E. coli*: neutrophil ratio was 1:20:2. The cultures were further incubated an additional hour at 37°C. In parallel to these coculture experiments, control experiments were

performed by incubating *E. coli*, neutrophils, and EA cells separately at 37°C. Following incubation, coculture samples were rapidly scraped into glass tubes and methanol was added prior to rapid freezing on dry ice. The control samples were treated under identical conditions to coculture conditions. Coculture and control samples were stored at −80°C until lipid extraction. During the lipid extraction step, the control EA, *E. coli*, and neutrophil samples were combined to generate a single control sample. To account for the neutrophil donor variability, untargeted lipidomics samples were performed using 5 biological replicates with different neutrophil donors each having 3 experimental replicates. Targeted lipidomics experiments were performed using 3 biological replicates each having 3 experimental replicates.

Lipid extraction for untargeted and targeted lipidomics

Lipids were extracted using a modified Bligh Dyer extraction method as previously described (Bligh and Dyer, 1959). Samples were spiked with 100 µl of internal lipid standard mix that consists of 1.5 µg phosphatidylcholine (PC) (20:0/20:0, where x:y/x:y indicates x number of carbons and y number of double bonds in *sn*-1 and *sn*-2 fatty acids esterified to the glycerol backbone), 0.3 µg phosphatidylethanolamine PE (14:0/14:0), 0.2 µg sphingomyelin (d18:1/17:0, where d indicates dihydro aliphatic group in the sphingosine backbone), 0.15 µg cholesteryl ester (17:0), 0.1 µg fatty acid (17:0), 15 ng ceramide (Cer) (17:0), 0.15 µg lysophosphatidylcholine (LPC) (17:0), 0.1 µg phosphatidylserine (PS) (14:0/14:0), 0.15 µg triglyceride (TG) (17:0/17:0/17:0), 0.2 µg phosphatidylglycerol (PG) (14:0/14:0) and 0.05 µg diglyceride (DG) (20:0/20:0). Lipid extracts were dried under nitrogen and were dissolved in methanol: isopropanol (1:1) for lipidomic analysis.

LC conditions

Reverse-phase HPLC was performed using an Accucore C18 column (2.1 mm × 150 mm) at 35°C. Mobile phase A was comprised of 60% acetonitrile, 40% water, 10 mM ammonium formate and 0.1% formic acid. Mobile phase B was comprised of 90% isopropanol, 10% acetonitrile with 2 mM ammonium formate, and 0.02% formic acid. The HPLC gradient started at 30% B, which was held for 3 min, followed by a discontinuous gradient as follows: 1) 30% B to 60% B over 4 min; 2) 60% B to 85% B over 8 min; 3) 85% B to 100% B over 9 min; and 4) 100% B continued for 3 min. The autosampler temperature was kept at 10°C. This HPLC method was employed for both untargeted and targeted parallel reaction monitoring (PRM) analyses.

MS conditions for untargeted and targeted lipidomics

Untargeted lipidomics and targeted PRM lipidomics were performed using a Q-Exactive mass spectrometer (Thermo Scientific). For untargeted lipidomics data-dependent mass spectrometry-mass spectrometry ($ddMS^2$), the top 10 most abundant peaks from a full MS1 scan were acquired in both positive and negative ion modes. Full scan MS1 was performed with chromatogram peak width set at 7 s, scan range 200–1,200 m/z, AGC target 1×10^6, resolution 70,000, and maximum injection time 246 ms. For $ddMS^2$ negative ion analyses, parameters were resolution 17,500, maximum injection time 54 ms; AGC target 2×10^5; isolation window 1.0 m/z; normalized collision energy (NCE) 20, 30, and 40; and dynamic exclusion at 10 s. Similar parameters were used for positive ion mode $ddMS^2$ analyses, except NCE was set to 20 and 40. Ions present in blank injections were excluded.

For two-cell and three-cell coculture systems, targeted lipidomics was performed by PRM using Q-Exactive MS/MS. TG, and DG were analyzed in positive ion mode while PE and PG species were detected by negative ion mode. PC species were quantified by positive ion while negative ion mode PRM was also performed to confirm the respective fatty acids. Fatty acid composition of complex lipids was determined by MS/MS of fatty acids and fatty acid loss in negative and positive ion mode, respectively. The *m/z* of parent ion and product ion fragments used for species confirmation are given in the (Supplementary Table S1). Quantification of each lipid species was performed based on the lipid standards and normalized to the EA cells (1×10^6 cells in a well) that were scraped and extracted in coculture and control samples.

MS data processing for untargeted lipidomics

MS data were analyzed using Xcalibur Qual Browser (Thermo Scientific). Untargeted LC-MS data were processed using LipidSearch 4.1 (Thermo Scientific) (Breitkopf et al., 2017; Contrepois et al., 2018). Both positive and negative MSdd.raw (data-dependent) files were used for lipid identification. Peak areas were normalized to internal lipid standards for each lipid class. Only the lipid classes that were normalized to internal standards were selected for further analysis. Each identified lipid was manually validated by investigating MS/MS fragmentation, the compatible retention time for lipid class, and acceptable peak shape. The fragmentation pattern for each lipid class was further confirmed by running a standard mix alone. The normalized, main ion data were transferred to MetaboAnalyst 5.0 for data analysis (Chong and Xia, 2020). Data scaling was set to autoscaling (mean-centered and divided by the standard

deviation of each variable). The significant species were selected using the cut-off of 1.5-fold change and p-value < 0.05. Following volcano plot analysis, the top-ranked lipid species were selected for targeted lipidomics using PRM.

Bacterial survival assay

Bacterial survival in coculture conditions was assessed by first adding 100 U/ml of DNAse to eliminate cell aggregates. Then, 50 µl of the sample was diluted in pH 11 water and incubated at room temperature for 5 min to lyse cells as previously described (Parker et al., 2014). Subsequently, samples were serially diluted in HBSS and plated on LB agar plates. Following overnight incubation, colony-forming units were calculated. The bacterial survival was calculated as a percentage of the starting bacteria number.

Lactate dehydrogenase assay

The cell viability of EA cells following bacteria exposure was determined by lactate dehydrogenase (LDH) release. After incubation with bacteria, cell media was collected and the amount of LDH was measured using an LDH kinetic assay as previously described (Freyer and Harms, 2017). The assay was performed in 96 clear well plates and the absorbance was measured at 530 nm using a multimode plate reader (Enspire). The percentage of LDH release was expressed as the proportion of LDH release in cells treated with 0.1% Triton X-100.

Rat cecal slurry studies and plasma lipid analyses

All animal experiments were conducted with the approval of the Institutional Animal Care and Use Committee at Saint Louis University. Young adult male Sprague-Dawley (Harlan–Indianapolis, IN, United States) weighing between 270–330 g were maintained in a temperature and humidity-controlled room with a 12 h light/dark cycle and unrestricted access to chow and water. Cecal slurry (CS) was prepared from donor male Sprague-Dawley rats (Pike et al., 2020). Rats were ip administered either CS (15 ml/kg) or 15% glycerol vehicle control in a total volume of 20 ml/kg, with the remaining 5 ml/kg being sterile saline (B Braun Medical, Bethlehem, PA, United States). At the time of CS administration, animals were administered a concurrent 30 ml/kg dose of subcutaneous sterile saline. Four and 8 h following CS injection, rats were euthanized, and blood was collected *via* cardiac puncture. An additional cohort of CS septic rats were treated 8 h following CS injection with both 25 mg/kg ceftriaxone (Hospira) in sterile saline (im) and a subcutaneous 30 ml/kg dose of sterile saline. In this cohort at 12 h following CS injection, rats were euthanized, and blood was collected *via* cardiac puncture. This model of sepsis has previously been shown to have an approximately 25% survival rate following 3 days (Pike et al., 2020). Without ceftriaxone and supplemental fluids at 8 h, less than 10% survival is observed following 20 h of CS injection. Plasma was immediately prepared and then stored at −80°C within 45 min of blood collection. To minimize freeze thaw cycles to two times or less, plasma was stored in aliquots. Rats were euthanized by injecting 0.5 ml Somnasol (390 mg/ml sodium pentobarbital and 50 mg/ml phenytoin sodium), ip followed by thoracotomy.

Plasma lipids were extracted in the presence of internal standards as described for coculture analyses. PC and PE molecular species were detected by selected reaction monitoring with an Altis TSQ mass spectrometer equipped with a Vanquish UHPLC System (Thermo Scientific). Lipids were separated on an Accucore C30 column 2.1 mm × 150 mm (Thermo Scientific) with mobile phase A comprised of 60% acetonitrile, 40% water, 10 mM ammonium formate, and 0.1% formic acid and mobile phase B comprised of 90% isopropanol, 10% acetonitrile with 2 mM ammonium formate, and 0.02% formic acid. Initial conditions were 30% B with a discontinuous gradient to 100% B at a flow rate of 0.260 ml/min.

Data analysis and statistics

Student's t-test was used to compare two groups while one-way analysis of variance with Tukey's post hoc analysis and Dunnett's post hoc test were used to compare three or more multiple comparisons. All data were represented as mean with standard deviation with averages of 3 biological replicates unless otherwise indicated. Following untargeted data processing by LipidSearch 4.1, data was transferred to MetaboAnalyst 5.0 to perform additional statistical analyses. GraphPad Prism was used for all other statistical analyses.

Results

Untargeted lipidomics reveal both unique and shared lipidomic signatures following endothelial exposure to CFT073 and JM109 *E. coli*

Initial studies examined changes in the endothelial lipidome in response to bacteria exposure with cocultures of either CFT073 or JM109 *E. coli* strains with EA.hy926 cells as illustrated in Figure 1A. Untargeted lipidomics was performed to study the array of lipidome changes and was followed by targeted lipidomics to confirm the identities and quantify lipids. Untargeted lipidomics analyses revealed the CFT073 *E. coli* strain

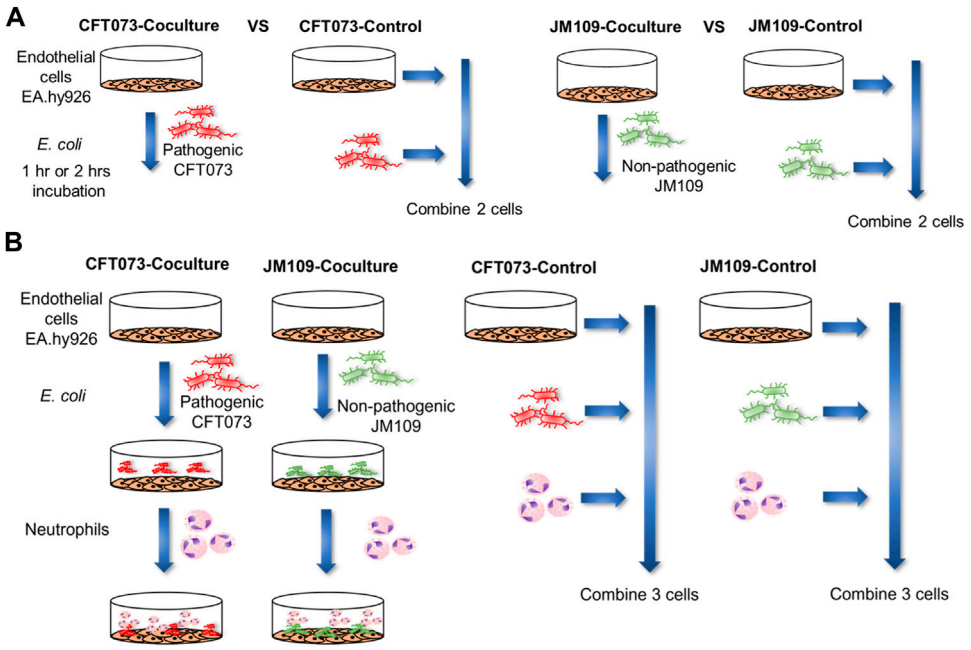

FIGURE 1
Schematic illustration of the workflow for coculture lipidomics. **(A)** 2 cell system: EA hy.926 cells (EA) were exposed to 20 × 10^6 of either CFT073 or JM109 *E. coli* for 1 or 2 h at 37°C. The cell ratio of EA:*E. coli* was 1:20. Control samples for this system were prepared by combining *E. coli*, and EA cells that were incubated separately. **(B)** 3-cell system: EA cells were exposed to 20 × 10^6 of either CFT073 or JM109 *E. coli* for 1 h at 37°C. Subsequently, 2 × 10^6 neutrophils were added and further incubated for 1 h at 37°C. The cell number ratio of EA:*E. coli*:neutrophils was 1:20:2. Control samples were prepared by combining *E. coli*, neutrophils and EA cells that were incubated separately. At the end of incubation, cells and media were collected for lipidomic studies.

induces more lipid changes compared to the JM109 strain following both 1 and 2 h exposures (Figures 2A–D). Exposure to CFT073 for 1 h resulted in increased levels of 14 lipid molecular species (Figure 2A) while 2 h exposures led to increased levels of 67 lipid molecular species (Figure 2B). In contrast, at both 1 and 2 h exposures the JM109 strain led to increases in 5 and 8 lipid molecular species, respectively (Figures 2C,D).

To characterize lipids that differ between CFT073 and JM109 exposure, the significantly increased and decreased lipids were compared between the two *E. coli* strains (Figures 2E,F; Supplementary Tables S2, S3). There were four lipids increased in all coculture conditions (common intersection in Figure 2E), which were all PG molecular species including PG 16:0/16:1, PG 16:0/18:1, PG 16:1/18:1, and PG 18:1/18:1. Fifty-five unique lipid species were identified in the CFT073 2 h coculture condition. These lipids included TG (6 species), DG (16 species), Cer (15 species), PE (11 species), and PC (6 species). However, there were few common lipid molecular species that decreased under these four coculture conditions. Several DG and PE molecular species were decreased in CFT073 strain and JM109 strain exposures to EA cells (Figure 2F).

Cer increases following 2 h coculture suggested cell death under these conditions. Accordingly, we investigated cell death under these conditions. Figure 3 shows CFT073 causes ~9 % and ~45% cytotoxicity at 1 and 2 h, respectively. JM109 did not cause cell death (below 1% cytotoxicity) at either incubation time (Figure 3). Accordingly, we selected 1 h coculture conditions for further targeted lipidomic analysis of lipid classes identified by untargeted analysis to detect lipid changes prior to cell death.

Increased or decreased lipids identified in untargeted analysis were subjected to targeted lipidomics using PRM. Targeted analysis confirmed DG 16:0/18:1 and DG 16:0/16:0 levels have a significant increase in CFT073 coculture while several other DG species trended toward decreasing (Figure 4A). DG species in this targeted analysis were unchanged in JM109 cocultures. Most of the PG species were significantly increased in JM109 cocultures compared to the control condition (Figure 4B). Overall, PG levels were lower in CFT073 cocultures compared to JM109 cell cocultures. However, the magnitude of increases in 16:1/18:1 and 18:1/18:1 PG levels in response to coculture conditions with CFT073 in respect to control culture conditions was much greater compared to that in JM109. Additionally, LPC 16:0 and LPC 18:0 levels were elevated only in CFT073 coculture (Figure 4C). Interestingly although significant changes in PE were suggested by untargeted lipidomics, changes in PE species were not confirmed during both of the coculture conditions using targeted analyses (Figure 4D).

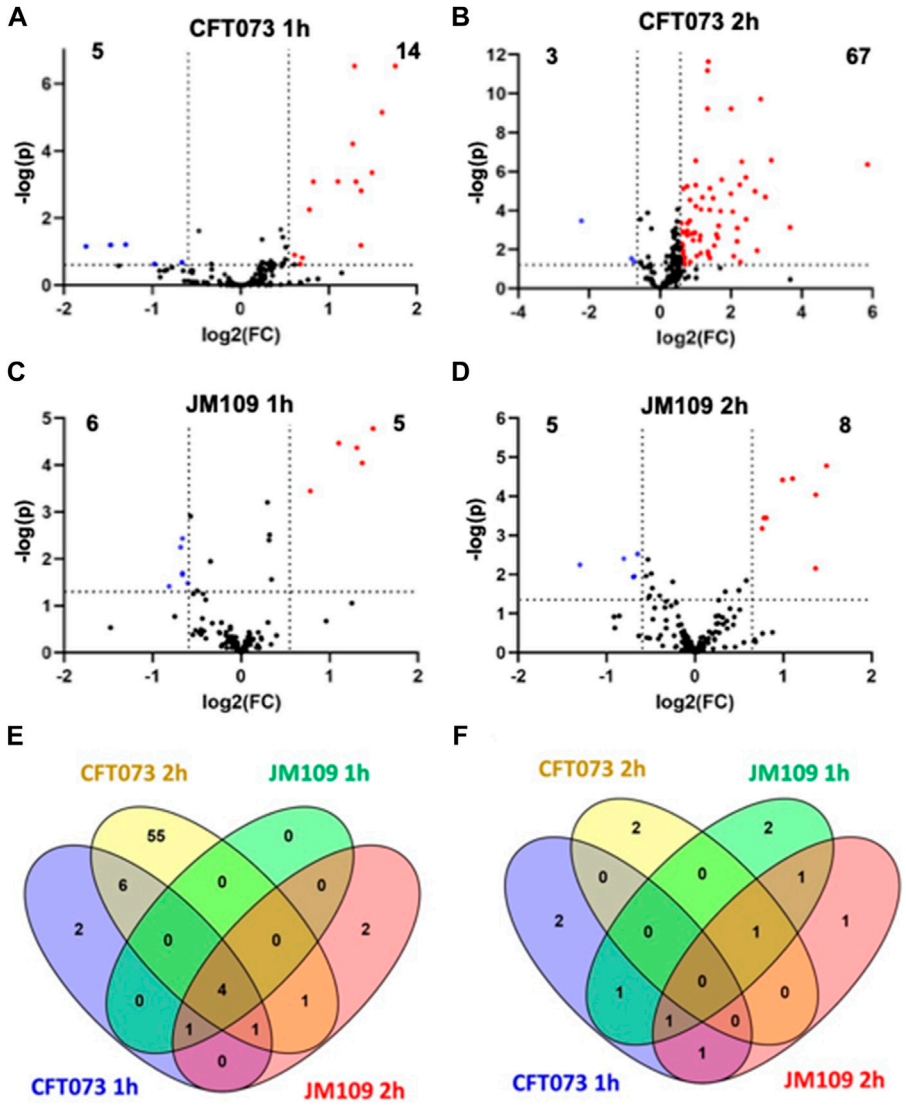

FIGURE 2
Untargeted lipidomics reveal changes in lipidomes during bacteria endothelial coculture (2-cell system). Volcano plots are shown comparing coculture conditions to the respective combined control cultures. CFT073 cocultures were compared to CFT073 combined control at 1 h **(A)** and 2 h **(B)** coculture intervals. JM109 cocultures were compared to JM109 combined control at 1 h **(C)** and 2 h **(D)** coculture intervals. Statistical significance for A, B, C and D were evaluated by *t*-test (p-value < 0.05) and fold change (FC) threshold at 1.5 **(E)** Venn diagram representing increased lipid molecular species in CFT073 coculture and JM109 coculture at 1 and 2 h. **(F)** Venn diagram representing decreased lipid molecular species in CFT073 coculture and JM109 coculture at 1 and 2 h.

Bacteria species-dependent lipidomic alterations in the presence of neutrophils

To characterize the coculture lipidome in the presence of neutrophils following initial bacteria coculture with endothelial cells we designed a 3-cell system as illustrated in Figure 1B. As in our studies with EA cells and *E. coli,* we first analyzed changes in the lipidome using untargeted approaches followed by targeted methods. The untargeted lipidomic analysis identified a total of 270 annotated lipid species across 11 lipid classes in both CFT073 and JM109 coculture conditions. Eighty lipid species were significantly elevated in CFT073 coculture compared to the CFT073 combined control (Figure 5A). In contrast, JM109 coculture condition resulted in only 25 significantly elevated lipid species (Figure 5B). However, JM coculture showed a higher number of decreased lipid species (22 lipids) while CFT073 coculture showed only 10 decreased lipid species (Figures 5A,B).

To determine unique and shared lipid signatures due to bacteria strain-specific cocultures, we then compared

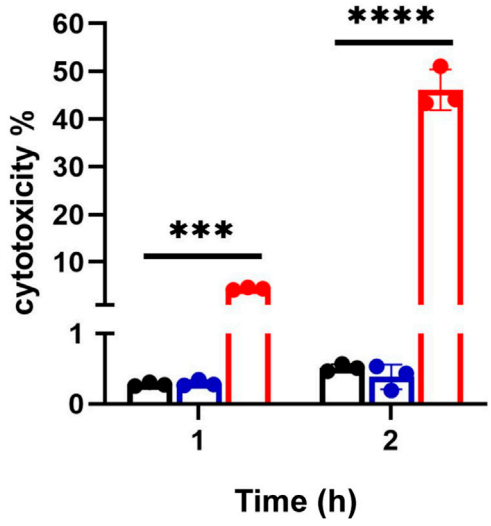

FIGURE 3
Bacteria mediated endothelial cell death. EA cells were exposed to either CFT073 (red) or JM109 (blue) at EA:*E. coli* cell ratio of 1:20 for indicated times at 37°C. At the end of incubation, media were collected and LDH assay was performed as described in "*Materials and Methods*". Statistics were performed using one way ANOVA, $n = 3$, p value: ****$p < 0.0001$, ***$p < 0.001$.

increased lipid species in CFT073 and JM109 cocultures (Figure 5C). Fifteen lipid species were commonly increased in CFT073 and JM109 cocultures. These common increased lipid species exclusively consist of DG and PG species (Supplementary Table S4). In contrast, there were no common decreased lipid species in comparisons between CFT073 and JM109 coculture conditions (Figure 5D; Supplementary Table S5). We then classified significantly altered lipids into lipid classes. Lipid species that were elevated in CFT073 coculture were distributed among TG, DG, PG, PC, and PE (Figure 5E). Most of the elevated lipids belong to TG and DG classes. The decreased lipids included additional lipid classes such as LPC, PS, and Cer. Interestingly, PC, Cer, and LPC were decreased in JM109 coculture while PS was decreased in CFT073 coculture (Figure 5F).

Next, targeted lipidomics using PRM was performed to confirm and quantify top-ranked lipids identified in untargeted lipidomics from the 3-cell systems. Except for TG 18:0/18:1/22:5, TG targets containing polyunsaturated fatty acids were significantly increased in the CFT073 coculture system (Figure 6A). TG species were elevated approximately 5-fold compared to controls and were 4-fold higher than that of the JM109 coculture system. Consistent with untargeted analysis, none of the TG species were significantly increased in JM109 coculture. In general, multiple DG species were increased in both CFT073 and JM109 cocultures compared to their controls (Figure 6B). DG 18:0/22:6 was increased in both CFT073 and JM109 cocultures while some DG species were uniquely increased in either the CFT073 or JM109 coculture condition. Overall, CFT073 cocultures showed a higher levels of DG species compared to JM109 cocultures. In cocultures with either CFT073 or JM109, PGs were significantly increased (Figure 6C) compared to controls, which confirmed untargeted lipidomic analyses. Among ten PG species tested, PG 16:0/18:1, PG18:1/18:1, PG 16:0/16:1, and PG 16:1/18:1 showed an approximately 2-fold increase in both CFT073 and JM109 cocultures compared to controls. Targeted lipidomic analysis of CFT073 cocultures demonstrated significant increases in all PE species tested except PE 17:1/16:0 (Figure 6D). PE 16:1/18:1 and PE 16:0/16:1 were significantly elevated in JM109 cocultures. Although untargeted analyses indicated several PC species were increased in CFT073 and JM109 cocultures, targeted analyses did not confirm changes in levels of these PC species (Figure 6E). Additionally, the differences in strain response with and without neutrophils were assessed at the 1 and 2 h time points (Figures 7A–D; Supplementary Tables S6–S9). These data highlight that more lipid species were increased or decreased when neutrophils were added to either CFT073 or JM109 cultured with EA cells.

Bacterial survival in coculture conditions

To explore the potential cause of the disparity of lipidomic profiles in these coculture systems including neutrophils, bacterial survival was assessed. Previous studies have shown that CFT073 *E. coli* is capable of adhesion, invasion, and colonization in epithelial cells and resistance to neutrophil killing mechanisms (Li et al., 2019) (Amunugama et al., 2021b). Thus, we tested the hypothesis that CFT073 *E. coli* survival is greater in the presence of neutrophils compared to that of JM109 *E. coli*. Figure 8 shows CFT073 *E. coli* survived in the presence of EA cells and neutrophils. In contrast, JM109 *E. coli* did not proliferate in the presence of EA cells and had reduced survival with the addition of neutrophils.

Plasma phosphatidylethanolamine and phosphatidylcholine levels in septic rats

Since targeted analyses showed PE levels were increased while PC levels did not change in the 3-cell coculture system we examined changes in these lipids in the more complex *in vivo* setting of rat sepsis. Four hours following sepsis induction by ip injection of cecal slurry, multiple rat plasma PE molecular species levels were increased compared to vehicle

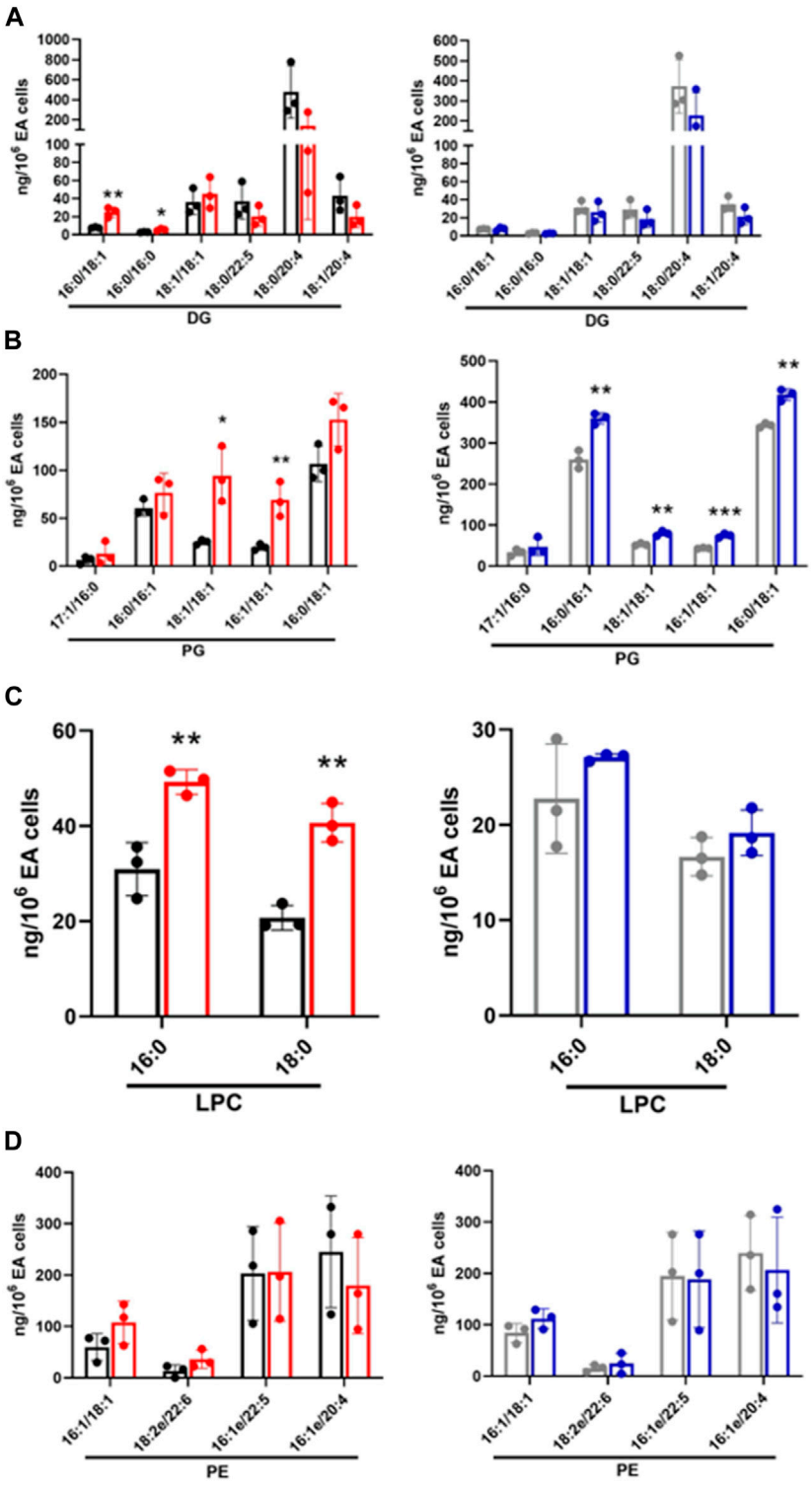

FIGURE 4
Targeted lipidomics of endothelial and *E. coli* coculture following a 1 h incubation. Following untargeted lipidomic analysis, significantly altered lipids detected between cocultures and control conditions following a 1 h incubation were selected for targeted lipidomics. Lipid species were analyzed by PRM using Q Exactive MS/MS. DG **(A)**, PG **(B)**, and LPC **(C)**, and PE **(D)** were measured in CFT073 coculture (red), CFT073 combined control (black), JM109 coculture (blue) and JM109 combined control samples (gray). Statistics were performed using unpaired *t*-test, $n = 3$ for average of 3 biological replicates, p value: $^{***}p < 0.001$, $^{**}p < 0.01$, $^{*}p < 0.05$.

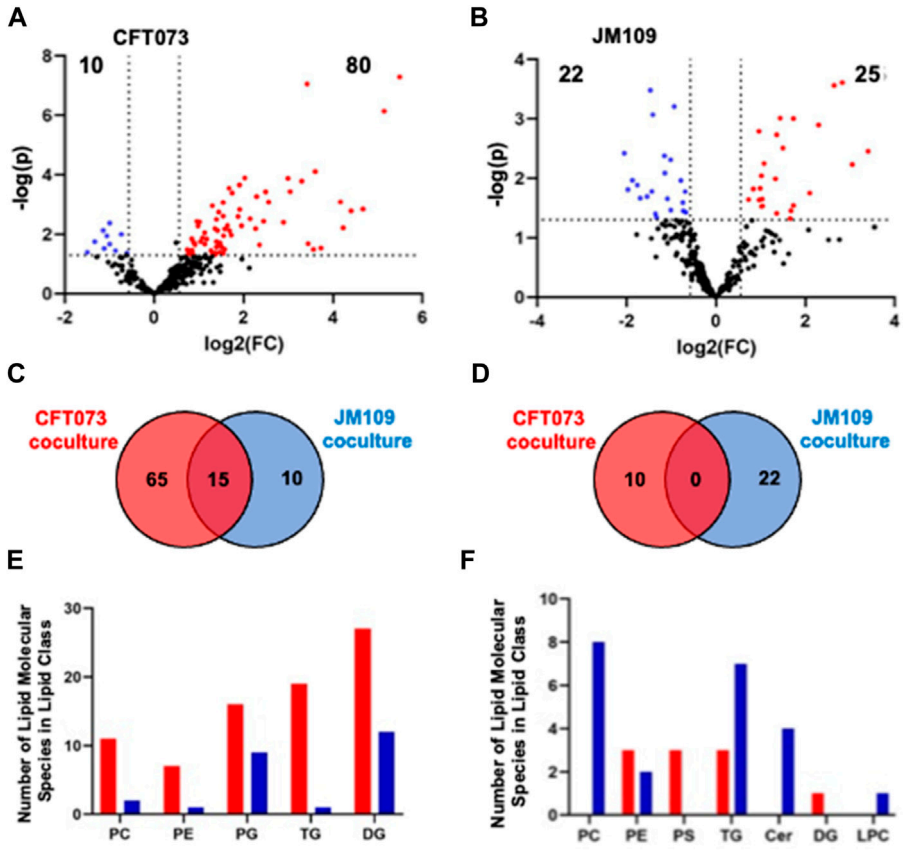

FIGURE 5
Untargeted lipidomics reveal altered lipid levels during bacteria coculture with endothelial cells and neutrophils. **(A)** Volcano plot comparing CFT073 coculture with CFT073 combined control. **(B)** Volcano plot of JM109 coculture compared to JM109 combined control. Statistical significance was evaluated by *t*-test (p-value < 0.05) and fold change (FC) threshold at 1.5. The number of increased and decreased lipids are shown in their respective quadrants. **(C)** Venn diagram representing increased lipid molecular species for comparisons between CFT073 coculture and JM109 coculture. **(D)** Decreased lipid species for comparisons between CFT073 and JM109 cocultures. **(E)** Increased lipid molecular species by lipid class from either CFT073 (red) and JM109 (blue) cocultures. **(F)** Decreased lipid molecular species by lipid class from either CFT073 or JM109 cocultures.

treated rats (Figure 9A). In contrast multiple PC molecular species levels decreased in septic animals (Figure 9A). In our analyses we were unable to detect appreciable amounts of PG in the plasma, and thus we were unable to followup on this target which was observed to change in the 3-cell coculture studies. We further assessed changes in PE and PC at 8 and 12 h following cecal slurry injection. The trend of an increase in plasma PE observed at 4 h continued at 8 and 12 h post cecal slurry injection (Figures 9B,C). One difference over time was that plasma PC levels were no longer elevated 12 h post cecal slurry injection.

Discussion

Understanding changes in lipid levels elicited by the complex interaction of neutrophils with endothelium in the presence of bacteria have the potential to provide new insights into complex metabolic changes during bacterial challenge as well as potentially lead to the discovery of lipid biomarkers for sepsis and infection. The use of 2-cell and 3-cell coculture systems allowed us to identify lipid changes caused by bacteria interaction with host cells in the presence and absence of neutrophils. Our cell model was designed considering *in vivo* infection events, where bacteria first interact with endothelial cells and later neutrophils reach the site of inflammation for the clearance of bacteria. Unique and shared lipidomic signatures were observed during CFT073 and JM109 exposure to EA cells in the presence and absence of neutrophils. However, the CFT073 urosepsis *E. coli* strain caused more lipid changes compared to JM109 non-pathogenic *E. coli* in the presence of both EA cells and neutrophils. Most of the increased lipids are in the TG, DG, PG, and PE lipid classes. Further studies in an *in vivo* rat sepsis

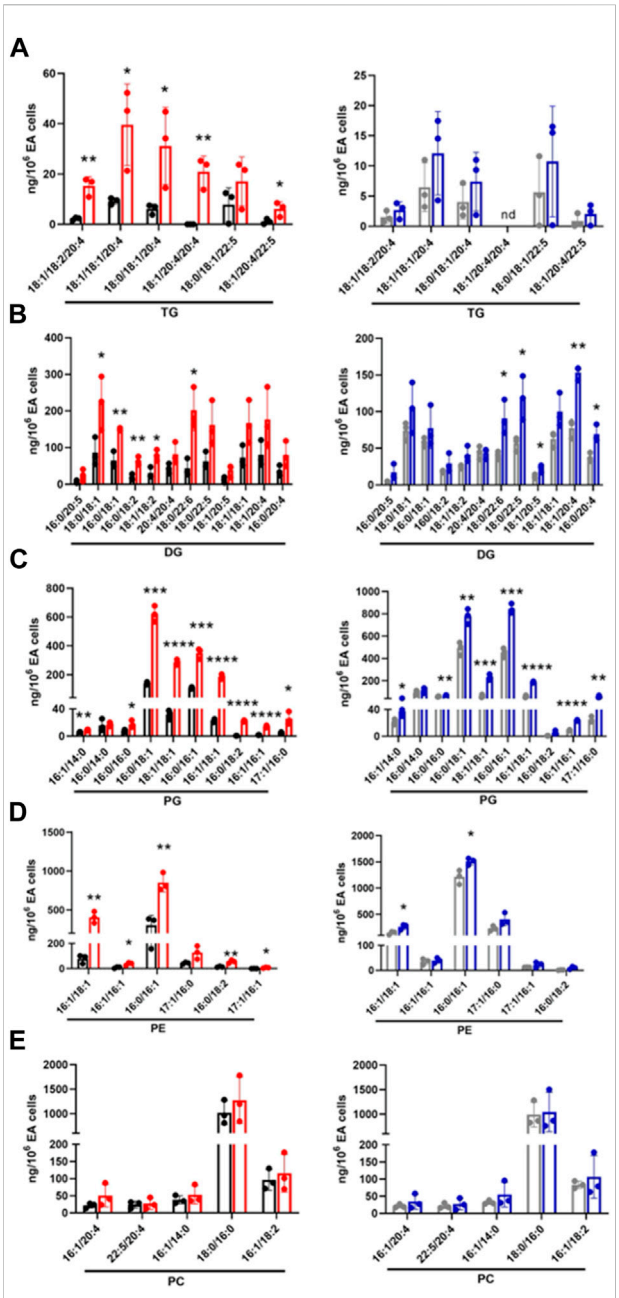

FIGURE 6
Targeted analyses based on targets identified in unbiased analyses of endothelial, *E. coli* and neutrophil coculture (3-cell system). Lipid molecular species identified following untargeted lipidomics of endothelial, *E. coli* and neutrophil cocultures (3-cell system) were quantified using PRM. TG **(A)**, DG **(B)**, PG **(C)**, PE **(D)**, and PC **(E)** were measured in CFT073 coculture (red), CFT073 combined control (black), JM109 coculture (blue) and JM109 combined control samples (gray). Statistics were performed using unpaired *t*-test, $n = 3$ for average of 3 biological replicates, p value: ****$p < 0.0001$, ***$p < 0.001$, **$p < 0.01$, *$p < 0.05$.

model also showed increases in PE levels in the plasma 4–12 h after the induction of sepsis.

Circulating lipid levels are dysregulated during infections including sepsis (Kitchens et al., 2003; Khovidhunkit et al., 2004; Tam, 2013; Amunugama et al., 2021a). For instance, Lee et al. (2015) showed sepsis-non survivors had decreased serum TG concentrations compared to sepsis survivors, and the TG levels were associated with sepsis mortality. Early studies have shown that gram-negative bacteria resulted in marked increases in serum TG concentrations (Gallin et al., 1969). Similarly, the 3-cell coculture system with the uroseptic CFT073 *E. coli* strain led to increased TG levels. These changes in TG levels were not observed in the 3-cell coculture system with the non-pathogenic JM109 *E. coli* strain. Several studies demonstrated that elevated TG level is linked with endothelial dysfunction, oxidative stress, apoptosis, and inflammation (Eiselein et al., 2007; Kajikawa and Higashi, 2019; Gorzelak-Pabiś et al., 2020). Moreover, TG-rich lipoproteins induce neutrophil activation (Alipour et al., 2008). Several DGs were significantly elevated in both CFT073 and JM109 cocultures. DGs increased with CFT073 incubated with EA cells in the absence of neutrophils. DG levels increased to much greater levels when neutrophils were added to either CFT073 or JM109 cocultures with EA cells.

Significant changes in phospholipids were revealed under coculture conditions, including PG and PE lipid classes. Importantly, we found plasma levels of multiple PE molecular species to be elevated in early stages of rat sepsis. This may be an important new finding since there is limited information on the role of PE in inflammation. For example, one report indicates PE facilitates the binding of *E. coli* to the cell membranes and induces apoptosis (Barnett Foster et al., 2000). Further studies need to be conducted to understand the role of PE in bacteria-endothelial-neutrophil interactions. Using our lipid analytical platform, we did not detect appreciable levels of plasma PG, which make it difficult to accurately determine whether plasma PG levels are altered in our rat sepsis model.

Our strategy in these studies was to first perform untargeted lipidomics in a cell model of sepsis followed by confirmation by targeted analyses and subsequent evaluation of targets in a rat model of sepsis (Figure 10). While most candidate lipids detected using untargeted approaches were confirmed by targeted approaches, the increases in PC levels detected by untargeted lipidomics could not be confirmed by targeted lipidomics. MS-based targeted or untargeted lipidomics approaches have their distinct advantages and limitations (Cajka and Fiehn, 2016). We took advantage of untargeted lipidomics to efficiently and robustly identifying a

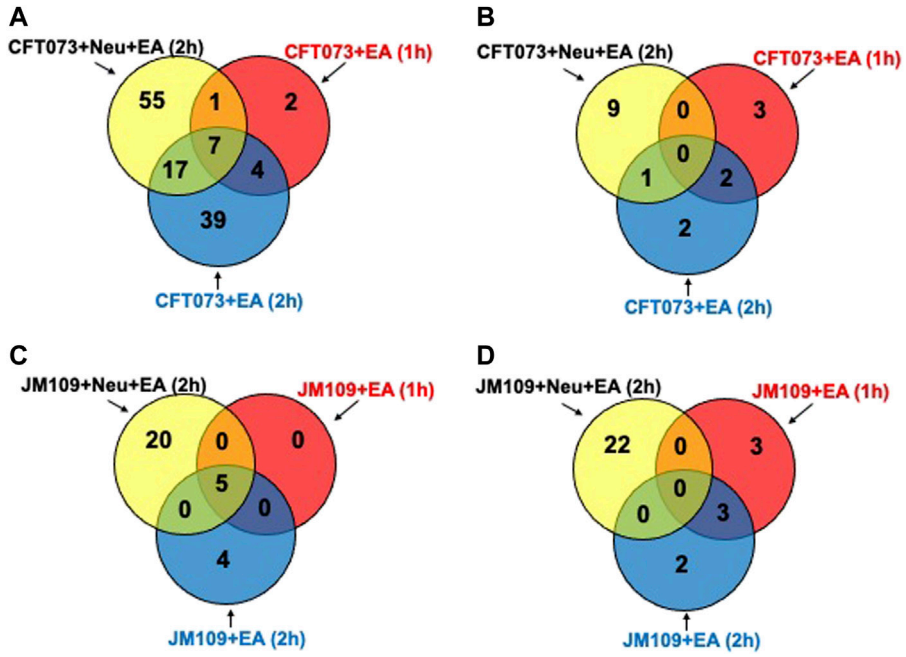

FIGURE 7
Differences in bacterial strain response with and without neutrophils at early and late time. Venn diagram representing increased **(A)** or decreased **(B)** lipid molecular species for comparisons between CFT073 cultured with EA cells with or without neutrophils at early and late time. Venn diagram representing increased **(C)** or decreased **(D)** lipid molecular species for comparisons between JM109 cultured with EA cells with or without neutrophils at early and late time.

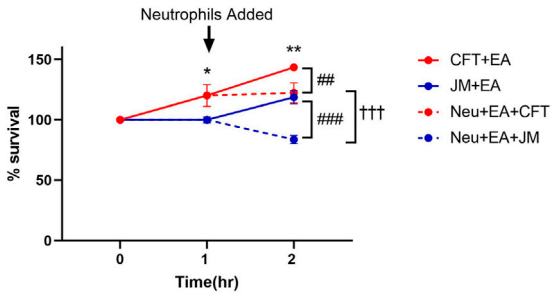

FIGURE 8
Bacterial survival during coculture conditions. Growth of CFT073 and JM109 bacteria in coculture conditions were analyzed by plating on LB agar plates as described in *"Materials and Methods"*. Bacteria survival % was calculated compared to the starting bacteria in the cultures. Data represent average of 3 biological replicates. Statistics were performed using unpaired *t*-test and one way ANOVA. *p* value: $^{**}p < 0.01$, $^{*}p < 0.05$ indicate CFT073 cocultured with endothelial cells (EA) compared to JM109 cocultured with EA cells. *p* value: $^{\#\#\#}p < 0.001$ $^{\#\#}p < 0.01$ indicate CFT073 or JM109 cocultured with EA cells compared to neutrophils added in the cocultures. *p* value: $^{\dagger\dagger\dagger}p < 0.001$ indicate coculture of CFT073, EA cells with neutrophils compared to coculture of JM109, EA cells with neutrophils.

large array of lipid species, then used targeted lipidomics to confirm and quantify candidate lipids (Telenga et al., 2014; Contrepois et al., 2018). Studies have shown that untargeted lipidomics approaches may have potential false positive and negative predictions caused by data processing tools and in-source fragmentation (Xu et al., 2018). Overall, these findings demonstrate the advantage of performing untargeted lipidomics to identify candidate targets but highlight the need to confirm lipid species by subsequent targeted approaches.

There are hundreds to thousands of lipid species that can be altered depending on physiological, pathophysiological and environmental conditions. Identifying these lipids is a daunting task using biased approaches. The evolution of high-resolution mass spectrometry and the development of lipid cloud mass spectrometry libraries has led to the ability to perform untargeted lipidomics to discover changes in lipid composition under different parameters and perhaps discover lipids that are important in biological processes or serve as biomarkers. As shown in this study confirming these candidates by subsequent targeted lipidomics approaches is important to verify these candidates. We applied these

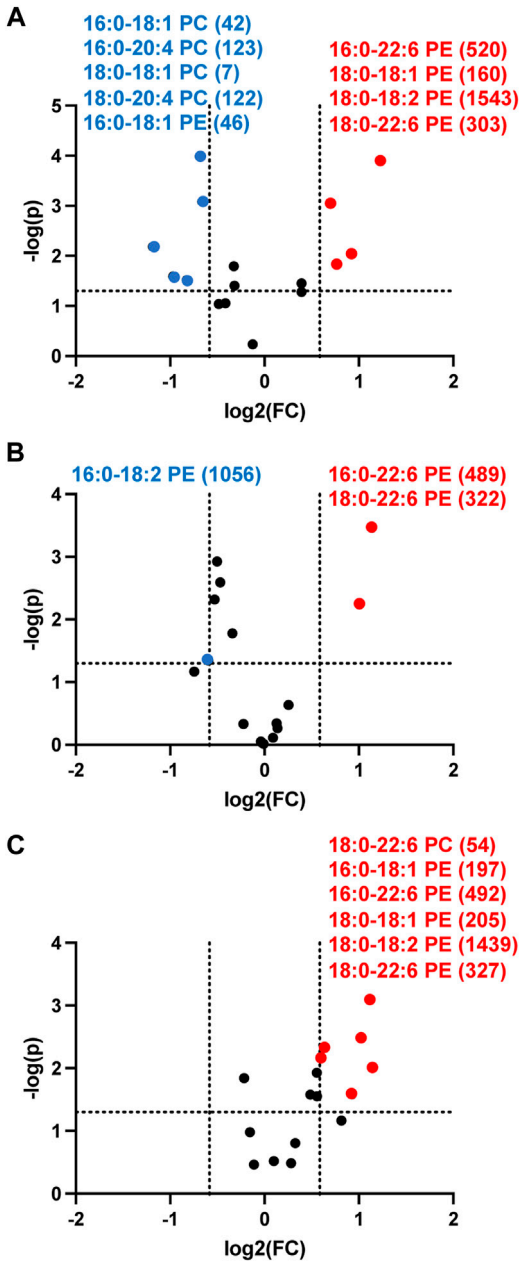

FIGURE 9
Volcano plot showing disparate changes in plasma phosphatidylethanolamine and phosphatidylcholine in septic rats. Rats were injected with cecal slurry (n = 5) to elicit sepsis or vehicle (n = 6) as described in "*Materials and Methods*". Plasma was collected 4 h **(A)**, 8 h **(B)**, and 12 h **(C)** following cecal slurry treatment, and lipids were extracted and subjected to targeted analyses for PE and PC levels. Statistical significance was evaluated by t-test (p-value < 0.05) and fold change (FC) threshold at 1.5. (x following indicated molecular species) indicates mean value for cecal slurry treatment rat plasma levels in either nM or μM for indicated PE or PC molecular species, respectively. Blue and red data points represent molecular species that significantly decrease and increase, respectively and meet the FC criteria of 1.5.

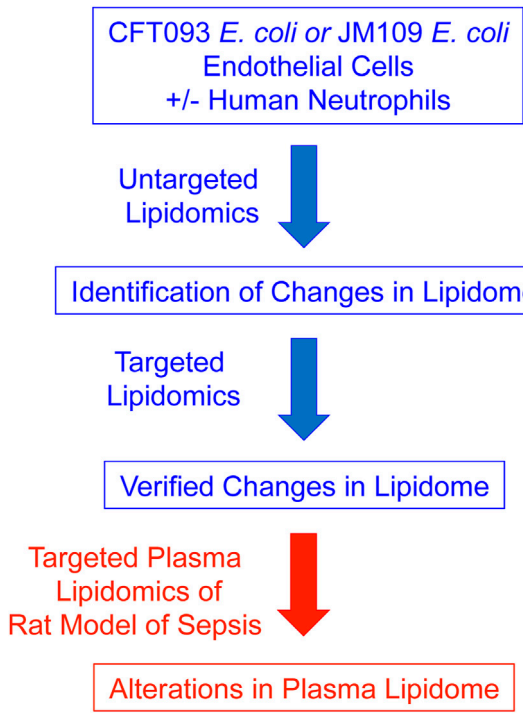

FIGURE 10
Schematic of Strategy for the Identification of Lipidomic Changes during Sepsis. The cell culture models depicted in Figure 1 were used to determine lipidomic changes first by untargeted lipidomics and subsequent verification of lipid changes by targeted lipidomics. The PC and PE molecular species targets were then examined in the plasma of septic rats.

principles to find unique lipid species, which accumulate in cocultures of endothelial cells with two different strains of *E. coli* leading to the production of unique lipids. Pathogenic CFT073 *E. coli*, compared to non-pathogenic JM109 *E. coli*, led to the most profound changes in lipids. Neutrophils enhanced the increased production of lipid species in cocultures. The *E. coli*, endothelial cell, neutrophil coculture system was designed to model changes that could occur during sepsis. The role of lipid species identified in cocultures need to be further examined as mediators or protectants of endothelial cell death and neutrophil-mediated bacterial killing. While we recognize this coculture system lacks the complexity of *in vivo* responses during sepsis, many of the lipid changes observed in the coculture model have been observed in plasma during sepsis by others as discussed above. Furthermore, the observation of increased PE levels in CFT073 *E. coli*, neutrophil, endothelial cell cocultures led to our finding that plasma PE levels, but not PC levels, were elevated 4 h after the induction of rat sepsis. The pathophysiological significance of the increase of PE during sepsis needs to be

further examined. Furthermore, the mechanisms leading to increased plasma PE levels in contrast to decreased plasma PC levels need to be investigated. Finally, the possibility that plasma PE levels are associated with sepsis outcomes needs to be examined in future studies.

Data availability statement

The raw data supporting the conclusion of this article will be made available by the authors, without undue reservation.

Ethics statement

The studies involving human participants were reviewed and approved by Saint Louis University Institutional Review Board. The patients/participants provided their written informed consent to participate in this study. The animal study was reviewed and approved by Institutional Animal Care and Use Committee at Saint Louis University.

Author contributions

KA performed experimental studies, data analyses, statistical analysis, and prepared the manuscript. DP performed experimental studies, data analyses, statistical analysis. DF was responsible for oversight of all aspects of studies, manuscript preparation, and final manuscript.

Funding

This study was supported (in part) by research funding from the National Institutes of Health R01 GM-115553 and S10OD025246 to DF, and National Institutes of Health F30 HL-142193 to DP.

Conflict of interest

The authors declare that the research was conducted in the absence of any commercial or financial relationships that could be construed as a potential conflict of interest.

Publisher's note

All claims expressed in this article are solely those of the authors and do not necessarily represent those of their affiliated organizations, or those of the publisher, the editors and the reviewers. Any product that may be evaluated in this article, or claim that may be made by its manufacturer, is not guaranteed or endorsed by the publisher.

Supplementary material

The Supplementary Material for this article can be found online at: https://www.frontiersin.org/articles/10.3389/fphys.2022.980460/full#supplementary-material

References

Agwu, D. E., McPhail, L. C., Chabot, M. C., Daniel, L. W., Wykle, R. L., and McCall, C. E. (1989). Choline-linked phosphoglycerides. *J. Biol. Chem.* 264 (3), 1405–1413. doi:10.1016/s0021-9258(18)94202-x

Ahmad, N. S., Tan, T. L., Arifin, K. T., Ngah, W. Z. W., and Yusof, Y. A. M. (2020). High sPLA2-IIA level is associated with eicosanoid metabolism in patients with bacterial sepsis syndrome. *PLoS One* 15 (3), e0230285. doi:10.1371/journal.pone.0230285

Ait-Oufella, H., Maury, E., Lehoux, S., Guidet, B., and Offenstadt, G. (2010). The endothelium: Physiological functions and role in microcirculatory failure during severe sepsis. *Intensive Care Med.* 36 (8), 1286–1298. doi:10.1007/s00134-010-1893-6

Alipour, A., van Oostrom, A. J., Izraeljan, A., Verseyden, C., Collins, J. M., Frayn, K. N., et al. (2008). Leukocyte activation by triglyceride-rich lipoproteins. *Arterioscler. Thromb. Vasc. Biol.* 28 (4), 792–797. doi:10.1161/ATVBAHA.107.159749

Alves-Filho, J. C., de Freitas, A., Spiller, F., Souto, F. O., and Cunha, F. Q. (2008). The role of neutrophils in severe sepsis. *Shock* 30 (1), 3–9. doi:10.1097/SHK.0b013e3181818466

Amunugama, K., Kolar, G. R., and Ford, D. A. (2021). Neutrophil myeloperoxidase derived chlorolipid production during bacteria exposure. *Front. Immunol.* 12 (3219), 701227. doi:10.3389/fimmu.2021.701227

Amunugama, K., Pike, D. P., and Ford, D. A. (2021). The lipid biology of sepsis. *J. Lipid Res.* 62, 100090. doi:10.1016/j.jlr.2021.100090

Barnett Foster, D., Abul-Milh, M., Huesca, M., and Lingwood, C. A. (2000). Enterohemorrhagic *Escherichia coli* induces apoptosis which augments bacterial binding and phosphatidylethanolamine exposure on the plasma membrane outer leaflet. *Infect. Immun.* 68 (6), 3108–3115. doi:10.1128/iai.68.6.3108-3115.2000

Bligh, E. G., and Dyer, W. J. (1959). A rapid method of total lipid extraction and purification. *Can. J. Biochem. Physiol.* 37 (8), 911–917. doi:10.1139/o59-099

Breitkopf, S. B., Ricoult, S. J. H., Yuan, M., Xu, Y., Peake, D. A., Manning, B. D., et al. (2017). A relative quantitative positive/negative ion switching method for untargeted lipidomics via high resolution LC-MS/MS from any biological source. *Metabolomics.* 13 (3), 30. doi:10.1007/s11306-016-1157-8

Bruegel, M., Ludwig, U., Kleinhempel, A., Petros, S., Kortz, L., Ceglarek, U., et al. (2012). Sepsis-associated changes of the arachidonic acid metabolism and their diagnostic potential in septic patients. *Crit. Care Med.* 40 (5), 1478–1486. doi:10.1097/CCM.0b013e3182416f05

Cajka, T., and Fiehn, O. (2016). Toward merging untargeted and targeted methods in mass spectrometry-based metabolomics and lipidomics. *Anal. Chem.* 88 (1), 524–545. doi:10.1021/acs.analchem.5b04491

Cepinskas, G., and Wilson, J. X. (2008). Inflammatory response in microvascular endothelium in sepsis: Role of oxidants. *J. Clin. Biochem. Nutr.* 42 (3), 175–184. doi:10.3164/jcbn.2008026

Chong, J., and Xia, J. (2020). Using MetaboAnalyst 4.0 for metabolomics data analysis, interpretation, and integration with other omics data. *Methods Mol. Biol.* 2104, 337–360. doi:10.1007/978-1-0716-0239-3_17

Contrepois, K., Mahmoudi, S., Ubhi, B. K., Papsdorf, K., Hornburg, D., Brunet, A., et al. (2018). Cross-platform comparison of untargeted and targeted lipidomics approaches on aging mouse plasma. *Sci. Rep.* 8 (1), 17747. doi:10.1038/s41598-018-35807-4

Craciun, F. L., Schuller, E. R., and Remick, D. G. (2010). Early enhanced local neutrophil recruitment in peritonitis-induced sepsis improves bacterial clearance and survival. *J. Immunol.* 185 (11), 6930–6938. doi:10.4049/jimmunol.1002300

Eiselein, L., Wilson, D. W., Lamé, M. W., and Rutledge, J. C. (2007). Lipolysis products from triglyceride-rich lipoproteins increase endothelial permeability, perturb zonula occludens-1 and F-actin, and induce apoptosis. *Am. J. Physiol. Heart Circ. Physiol.* 292 (6), H2745–H2753. doi:10.1152/ajpheart.00686.2006

Freyer, D., and Harms, C. (2017). Kinetic lactate dehydrogenase assay for detection of cell damage in primary neuronal cell cultures. *Bio. Protoc.* 7 (11), e2308–e. doi:10.21769/BioProtoc.2308

Gallin, J. I., Kaye, D., and O'Leary, W. M. (1969). Serum lipids in infection. *N. Engl. J. Med.* 281 (20), 1081–1086. doi:10.1056/NEJM196911132812001

Gijon, M. A., Perez, C., Mendez, E., and Sanchez Crespo, M. (1995). Phospholipase A2 from plasma of patients with septic shock is associated with high-density lipoproteins and C3 anaphylatoxin: Some implications for its functional role. *Biochem. J.* 306 (1), 167–175. doi:10.1042/bj3060167

Gorzelak-Pabiś, P., Wozniak, E., Wojdan, K., Chalubinski, M., and Broncel, M. (2020). Single triglyceride-rich meal destabilizes barrier functions and initiates inflammatory processes of endothelial cells. *J. Interferon Cytokine Res.* 40 (1), 43–53. doi:10.1089/jir.2018.0173

Gray, M. J., Wholey, W. Y., and Jakob, U. (2013). Bacterial responses to reactive chlorine species. *Annu. Rev. Microbiol.* 67, 141–160. doi:10.1146/annurev-micro-102912-142520

Joffre, J., Hellman, J., Ince, C., and Ait-Oufella, H. (2020). Endothelial responses in sepsis. *Am. J. Respir. Crit. Care Med.* 202 (3), 361–370. doi:10.1164/rccm.201910-1911TR

Kajikawa, M., and Higashi, Y. (2019). Triglycerides and endothelial function: Molecular biology to clinical perspective. *Curr. Opin. Lipidol.* 30 (5), 364–369. doi:10.1097/MOL.0000000000000630

Khovidhunkit, W., Kim, M. S., Memon, R. A., Shigenaga, J. K., Moser, A. H., Feingold, K. R., et al. (2004). Effects of infection and inflammation on lipid and lipoprotein metabolism: Mechanisms and consequences to the host. *J. Lipid Res.* 45 (7), 1169–1196. doi:10.1194/jlr.R300019-JLR200

Kitchens, R. L., Thompson, P. A., Munford, R. S., and O'Keefe, G. E. (2003). Acute inflammation and infection maintain circulating phospholipid levels and enhance lipopolysaccharide binding to plasma lipoproteins. *J. Lipid Res.* 44 (12), 2339–2348. doi:10.1194/jlr.M300228-JLR200

Kovach, M. A., and Standiford, T. J. (2012). The function of neutrophils in sepsis. *Curr. Opin. Infect. Dis.* 25 (3), 321–327. doi:10.1097/QCO.0b013e3283528c9b

Lee, S. H., Park, M. S., Park, B. H., Jung, W. J., Lee, I. S., Kim, S. Y., et al. (2015). Prognostic implications of serum lipid metabolism over time during sepsis. *Biomed. Res. Int.* 2015, 789298. doi:10.1155/2015/789298

Li, X., Pei, G., Zhang, L., Cao, Y., Wang, J., Yu, L., et al. (2019). Compounds targeting YadC of uropathogenic *Escherichia coli* and its host receptor annexin A2 decrease bacterial colonization in bladder. *EBioMedicine* 50, 23–33. doi:10.1016/j.ebiom.2019.11.014

Li, Z., Yin, M., Zhang, H., Ni, W., Pierce, R. W., Zhou, H. J., et al. (2020). BMX represses thrombin-PAR1-mediated endothelial permeability and vascular leakage during early sepsis. *Circ. Res.* 126 (4), 471–485. doi:10.1161/CIRCRESAHA.119.315769

Liaw, W. J., Chen, T. H., Lai, Z. Z., Chen, S. J., Chen, A., Tzao, C., et al. (2005). Effects of a membrane-permeable radical scavenger, Tempol, on intraperitoneal sepsis-induced organ injury in rats. *Shock* 23 (1), 88–96. doi:10.1097/01.shk.0000145937.70085.89

Parker, H. A., Magon, N. J., Green, J. N., Hampton, M. B., and Winterbourn, C. C. (2014). "Analysis of neutrophil bactericidal activity," in *Neutrophil methods and protocols*. Editors M. T. Quinn and F. R. DeLeo (Totowa, NJ: Humana Press), 291–306.

Pike, D. P., Vogel, M. J., McHowat, J., Mikuzis, P. A., Schulte, K. A., and Ford, D. A. (2020). 2-Chlorofatty acids are biomarkers of sepsis mortality and mediators of barrier dysfunction in rats. *J. Lipid Res.* 61 (7), 1115–1127. doi:10.1194/jlr.RA120000829

Rival, T., Cinq-Frais, C., Silva-Sifontes, S., Garcia, J., Riu, B., Salvayre, R., et al. (2013). Alteration of plasma phospholipid fatty acid profile in patients with septic shock. *Biochimie* 95 (11), 2177–2181. doi:10.1016/j.biochi.2013.08.006

Rudd, K. E., Johnson, S. C., Agesa, K. M., Shackelford, K. A., Tsoi, D., Kievlan, D. R., et al. (2020). Global, regional, and national sepsis incidence and mortality, 1990-2017: Analysis for the global burden of disease study. *Lancet (London, Engl.* 395 (10219), 200–211. doi:10.1016/S0140-6736(19)32989-7

Sae-Khow, K., Tachaboon, S., Wright, H. L., Edwards, S. W., Srisawat, N., Leelahavanichkul, A., et al. (2020). Defective neutrophil function in patients with sepsis is mostly restored by *ex vivo* ascorbate incubation. *J. Inflamm. Res.* 13, 263–274. doi:10.2147/JIR.S252433

Snider, J. M., You, J. K., Wang, X., Snider, A. J., Hallmark, B., Zec, M. M., et al. (2021). Group IIA secreted phospholipase A2 is associated with the pathobiology leading to COVID-19 mortality. *J. Clin. Invest.* 131 (19), e149236. doi:10.1172/JCI149236

Tam, V. C. (2013). Lipidomic profiling of bioactive lipids by mass spectrometry during microbial infections. *Semin. Immunol.* 25 (3), 240–248. doi:10.1016/j.smim.2013.08.006

Telenga, E. D., Hoffmann, R. F., Ruben, K., Hoonhorst, S. J., Willemse, B. W., van Oosterhout, A. J., et al. (2014). Untargeted lipidomic analysis in chronic obstructive pulmonary disease. Uncovering sphingolipids. *Am. J. Respir. Crit. Care Med.* 190 (2), 155–164. doi:10.1164/rccm.201312-2210OC

Xu, L., Wang, X., Jiao, Y., and Liu, X. (2018). Assessment of potential false positives via orbitrap-based untargeted lipidomics from rat tissues. *Talanta* 178, 287–293. doi:10.1016/j.talanta.2017.09.046

frontiers | Frontiers in Medicine

TYPE Original Research
PUBLISHED 27 September 2022
DOI 10.3389/fmed.2022.985955

OPEN ACCESS

EDITED BY
W. Conrad Liles,
University of Washington,
United States

REVIEWED BY
Tobias Piegeler,
University Hospital Leipzig, Germany
Gabriela Porto Petraki,
Universidade de Pernambuco, Brazil
Robert Hahn,
Karolinska Institutet (KI), Sweden

*CORRESPONDENCE
Akio Suzuki
akio@gifu-u.ac.jp
Hideshi Okada
hideshi@gifu-u.ac.jp

†These authors have contributed equally to this work

RECEIVED 04 July 2022
ACCEPTED 29 August 2022
PUBLISHED 27 September 2022

CITATION
Suzuki K, Okada H, Sumi K, Tomita H, Kobayashi R, Ishihara T, Mizuno Y, Yamaji F, Kamidani R, Miura T, Yasuda R, Kitagawa Y, Fukuta T, Suzuki K, Miyake T, Kanda N, Doi T, Yoshida T, Yoshida S, Tetsuka N, Ogura S and Suzuki A (2022) Syndecan-1 as a severity biomarker for patients with trauma.
Front. Med. 9:985955.
doi: 10.3389/fmed.2022.985955

Syndecan-1 as a severity biomarker for patients with trauma

Keiko Suzuki[1,2†], Hideshi Okada[3*†], Kazuyuki Sumi[2], Hiroyuki Tomita[4], Ryo Kobayashi[2,5], Takuma Ishihara[6], Yosuke Mizuno[3], Fuminori Yamaji[3], Ryo Kamidani[3], Tomotaka Miura[1,3], Ryu Yasuda[3], Yuichiro Kitagawa[3], Tetsuya Fukuta[3], Kodai Suzuki[3], Takahito Miyake[3], Norihide Kanda[3], Tomoaki Doi[3], Takahiro Yoshida[3], Shozo Yoshida[3,7], Nobuyuki Tetsuka[1], Shinji Ogura[3] and Akio Suzuki[2,5*]

[1]Department of Infection Control, Gifu University Graduate School of Medicine, Gifu, Japan, [2]Department of Pharmacy, Gifu University Hospital, Gifu, Japan, [3]Department of Emergency and Disaster Medicine, Gifu University Graduate School of Medicine, Gifu, Japan, [4]Department of Tumor Pathology, Gifu University Graduate School of Medicine, Gifu, Japan, [5]Laboratory of Advanced Medical Pharmacy, Gifu Pharmaceutical University, Gifu, Japan, [6]Innovative and Clinical Research Promotion Center, Gifu University Hospital, Gifu, Japan, [7]Department of Abuse Prevention Emergency Medicine, Gifu University Graduate School of Medicine, Gifu, Japan

Tissue injury and hemorrhage induced by trauma lead to degradation of the endothelial glycocalyx, causing syndecan-1 (SDC-1) to be shed into the blood. In this study, we investigated whether serum SDC-1 is useful for evaluating trauma severity in patients. A single-center, retrospective, observational study was conducted at Gifu University Hospital. Patients transported to the emergency room for trauma and subsequently admitted to the intensive care unit from January 2019 to December 2021 were enrolled. A linear regression model was constructed to evaluate the association of serum SDC-1 with injury severity score (ISS) and probability of survival (Ps). A total of 76 trauma patients (54 men and 22 women) were analyzed. ISS was significantly associated with serum SDC-1 level in trauma patients. Among the six body regions defined in the AIS used to calculate the ISS score, "chest" and "abdominal or pelvic contents" were significantly associated with serum SDC-1 level, and "extremities or pelvic girdle" also tended to show an association with serum SDC-1 level. Moreover, increasing serum SDC-1 level was significantly correlated with decreasing Ps. Serum SDC-1 may be a useful biomarker for monitoring the severity of trauma in patients. Further large-scale studies are warranted to verify these results.

KEYWORDS

trauma, syndecan-1, injury severity score, glycocalyx, probability of survival

Introduction

Trauma is a global phenomenon and one of the main causes of death worldwide (1). The major causes of trauma-related death within the first 24 h are hemorrhage and brain injury, and respiratory distress, organ failure, and infection in the period thereafter (2). Because trauma has a wide range of presentations, both in injury type and the location and effect of individual wounds, the ability to measure injury severity is particularly important for comparison of disparate types of trauma. The Injury Severity Score (ISS) is an anatomical scoring system that provides an overall score for patients with multiple injuries, in which each injury is assigned an Abbreviated Injury Scale (AIS) score (3, 4). While the ISS is regarded as the gold standard for grading trauma severity (5, 6), it is important to note that trauma severity measured using the ISS is anatomically based, and reveals no information on disease pathophysiology. However, the systemic response induced by tissue injury and hemorrhage, which includes the release of damage-associated molecular patterns (DAMPs), hypoperfusion and reperfusion, inflammatory responses, and activation of endocrine and neurological systems, leads to endothelial cell activation, resulting in cellular and organ dysfunction (6). Thus, although the pathophysiology of trauma is characterized by endothelial injury, this is not considered by the ISS.

The endothelial glycocalyx, a gel-like layer of glycoproteins that covers the luminal surface of the capillary endothelium, is thought to maintain organ and vascular homeostasis (7). Syndecan-1 (SDC-1), the core protein in heparan sulfate proteoglycan, is found in the endothelial glycocalyx and shed into the blood in various systemic inflammatory conditions, including trauma (7, 8), sepsis (9), acute respiratory distress syndrome (10), acute kidney injury (11) and cardiovascular disease (12, 13). Additionally, several studies have demonstrated an association between serum SDC-1 level and mortality in trauma patients (14, 15). A prospective cohort study of 75 trauma patients reported that serum SDC-1 level $\geq$ 63 ng/ml was an independent factor for 30-day mortality after adjusting for age and ISS (15). Similarly, a prospective observational study of 410 trauma patients revealed that serum SDC-1 level $\geq$ 40 ng/ml was a significant factor for 30-day in-hospital mortality using multivariable logistic analysis adjusted for age, ISS, arrival systolic blood pressure, and base excess (14). However, it is unclear whether serum SDC-1 is a useful marker of severity in patients with trauma.

The aim of this study was to investigate the relationship between ISS and serum SDC-1 levels on admission to the emergency room in trauma patients.

Methods

Patients

This single-center retrospective observational study was conducted at Gifu University Hospital, which is affiliated with Gifu University (Gifu, Japan). Patients transported to the emergency room (ER) for trauma and admitted to the intensive care unit at Gifu University from January 2019 to December 2021 were included. Patients were excluded from the present analysis if they were transported to hospital 24 h or more after the onset of injury, had an unclear onset time of injury, were diagnosed with an AIS of <3, received cardiopulmonary resuscitation or fluid resuscitation during transport, were undergoing maintenance dialysis, or were aged under 20 years.

Data collection and study design

Upon transport to the ER, blood was sampled from eligible patients. Data derived from these blood samples were used in the present analysis. All laboratory data, except serum SDC-1, and patient demographics were extracted from the hospital's electronic medical records.

AIS was scored by physicians using AIS2008 (16). To calculate the ISS score, we used the six body regions defined in the AIS: 1. Head and neck, 2. Face, 3. Chest, 4. Abdomen, 5. Extremities pelvis, 6. Surface. The ISS score was calculated from the three most severely injured of the six body regions using the equation: $\mathrm{ISS} = (\mathrm{AIS}_1)^2 \pm (\mathrm{AIS}_2)^2 \pm (\mathrm{AIS}_3)^2$.

The probability of survival (Ps) is a commonly used parameter in the field of trauma care. It can be calculated from the AIS, ISS and Trauma and Injury Severity Score (TRISS) as follows:

$$\begin{aligned} Ps &= 1/(1 \pm e^{-b}) \\ e &= 2.718282 \text{ (base of natural logarithm)} \\ b &= b_0 \pm b_1(\mathrm{RTS}) \pm b_2(\mathrm{ISS}) \pm b_3(\text{Age Index}) \end{aligned}$$

where RTS is the revised trauma score and b_0, b_1, b_2, b_3 are coefficients. The coefficients b0–b3 are derived from multiple-regression analysis of the Major Trauma Outcome Study database (17). For patients under 55 years old, the age index is 0, while for patients > 55 years old, the age index is 1. These coefficients change depending on whether subjects are pediatric patients or have blunt trauma. RTS can be calculated from the following three physiological parameters:

$$\mathrm{RTS} = 0.9368\ (\mathrm{GCS}) \pm 0.7326\ (\mathrm{SBP}) \pm 0.2908\ (\mathrm{RR})$$

where GCS is the Glasgow Coma Scale, SBP is systolic blood pressure (mmHg), and RR is respiratory rate (/min). Serum SDC-1 concentrations were measured using an enzyme-linked immunosorbent assay (950.640.192; Diaclone, Besancon, Cedex, France). These data were retrospectively analyzed.

Statistical analysis

Patients' baseline characteristics are presented as median and interquartile range (IQR) for continuous variables, and frequency and proportion for categorical variables. To evaluate the association between ISS and serum SDC-1, we performed multivariable regression analysis adjusted for covariates we defined a priori based on factors previously shown to be strongly associated with serum SDC-1 and ISS. For serum SDC-1, these were age (18, 19), gender (20, 21), previous treatment with transfusion and/or angiography at another hospital before being transported to our hospital (22). For ISS, these were: medication history of antiplatelet use and/or anticoagulant use (23, 24). Because the distribution of serum SDC-1 was skewed, natural log transformation was used in the regression model and the results are presented with back-transformation.

To evaluate which of the six body regions defined in the AIS used to calculate the ISS score was associated with serum SDC-1, a similar analysis was performed by replacing the ISS with the body region-specific score. The association between Ps and serum SDC-1 was also evaluated using a multivariable linear regression model. A two-sided P-value < 0.05 was considered significant. All analyses were performed using R 4.1.1 (The R Project for Statistical Computing).

Ethics statement

The investigation conformed with the principles outlined in the Declaration of Helsinki. Ethics approval was obtained from the medical ethics committee of Gifu University Graduate School of Medicine, Gifu, Japan (Institutional review board approval No. 2021-B097). In view of the retrospective nature of the study, subject informed consent was not required.

Results

Patient characteristics

The disposition of the enrolled patients is shown in Figure 1. A total of 447 patients with trauma were transferred to our ER during the study period. Of these, 228 patients

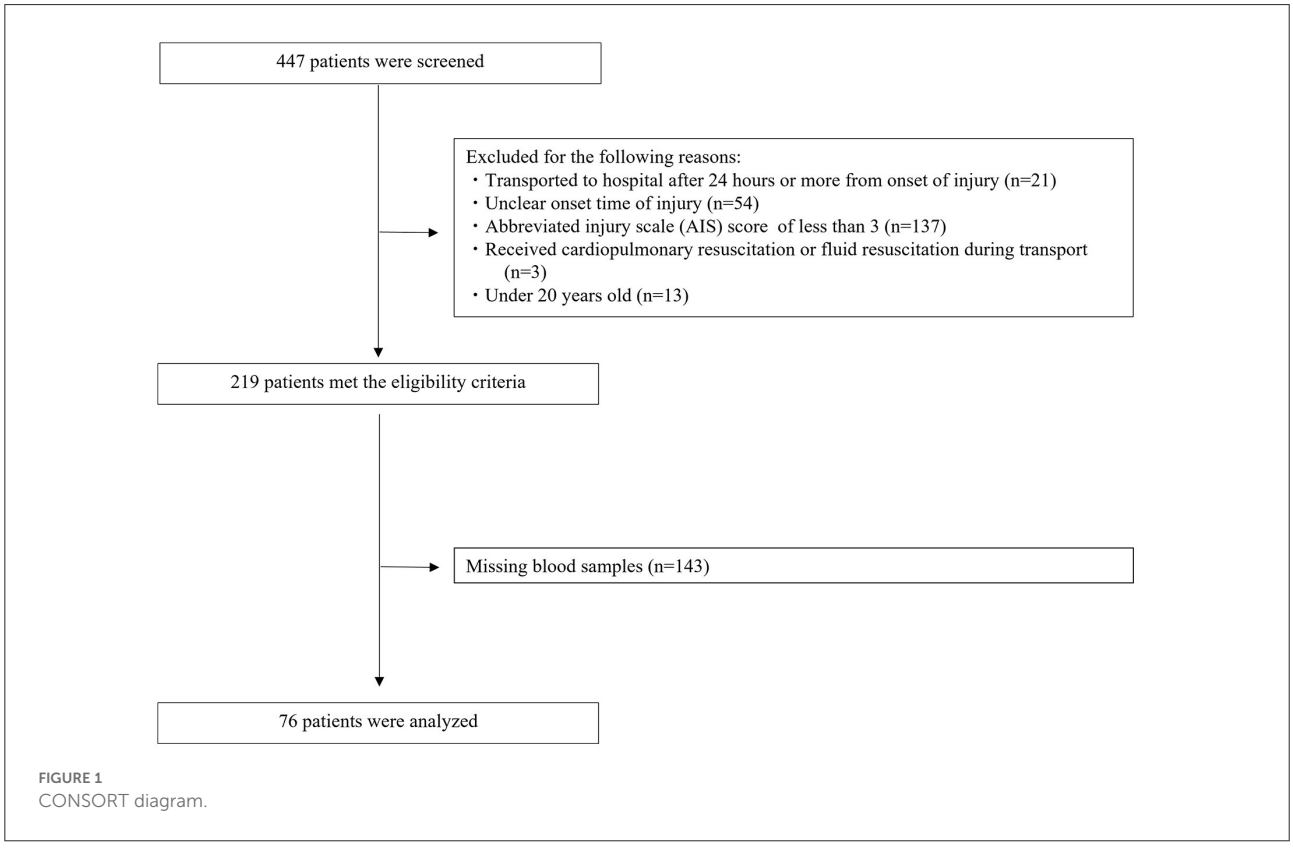

FIGURE 1
CONSORT diagram.

were excluded for the following reasons: AIS < 3 (n = 137), unclear onset time of injury (n = 54), transported to hospital 24 h or more after onset of injury (n = 21), under 20 years old (n = 13), and received cardiopulmonary resuscitation or fluid resuscitation during transport (n = 3). A total of 219 patients met the eligibility criteria. However, 143 of these patients had missing blood samples, which meant we could not determine their serum SDC-1 levels. Thus, the remaining 76 patients (54 men and 22 women) were analyzed in this study.

Patient demographics are shown in Table 1. Median age was 66.0 years (IQR, 47.0–78.0) and median duration of hospital stay was 29.0 days (IQR, 20.0–48.8). The most common cause of trauma was falling from a height (n = 35, 46.0%), followed by motor vehicle accident (n = 33, 43.4%) and others (n = 8, 10.5%). A total of 3 (3.9%) and 5 (6.6%) patients had received transfusion and angiography at another hospital before being transported to our hospital, respectively. Further, 6 (7.9%) and 3 (3.9%) patients were taking antiplatelet agents and anticoagulants, respectively.

TABLE 1 Patient demographics.

Age, years, median (IQR)	66.0 (47.0–78.0)
Sex, male/female, *n* (%)	54 (71.1)/22 (28.9)
Treatment by previous doctor, *n* (%)	
Transfusion	3 (3.9)
Angiography	5 (6.6)
Medication	
Antiplatelet agents	6 (7.9)
Anticoagulants	3 (3.9)
Reasons for injury, *n* (%)	
Falling accident	35 (46.0)
Traffic accident	33 (43.4)
Other	8 (10.5)
Length of hospital stay, days, median (IQR)	29.0 (20.0–48.8)
Laboratory data on arrival at ER	
Alb	3.7 (3.3–4.1)
AST	43.0 (28.8–77.0)
ALT	30.5 (20.8–50.5)
CRE	0.9 (0.7–1.1)
BUN	17.9 (13.8–21.6)
WBC	13.0 (8.2–16.9)
HGB	12.4 (10.3–13.9)
PLT	210.5 (161.5–255.0)
FIB	216.0 (187.5–279.8)
FDP	95.2 (29.5–226.9)
D-dimer	37.4 (12.1–75.7)

All data indicate median, 25–75th percentile unless otherwise indicated.
IQR, interquartile range; ER, emergency room; Alb, albumin; AST, aspartate aminotransferase; ALT, alanine aminotransferase; CRE, creatinine; BUN, blood urea nitrogen; WBC, white blood cells; HGB, hemoglobin, PLT; platelets, FIB; fibrinogen, FDP; fibrin degradation product.

Relationship between ISS and serum SDC-1 levels on admission to the emergency room

The median time from onset of trauma to blood collection in the ER was 62.5 min (IQR, 39.75–150.25). The median serum SDC-1 level was 34.6 ng/mL (IQR, 27.1–67.8), and the median ISS score was 20 (IQR 13.8–29.0). The results of the multivariable linear regression model adjusted for age, gender, treatment history (transfusion and angiography) and medication history (antiplatelet agents and anticoagulants) are shown in Table 2 and Figure 2. ISS was significantly associated with serum SDC-1 level in trauma patients with AIS ≥3 [Exp (β) = 1.046, 95% confidence interval (CI) = 1.020–1.072, P = 0.001, R^2 = 0.23].

We subsequently used a multivariable linear regression model adjusted for age, gender, treatment history (transfusion and angiography) and medication history (antiplatelet agents and anticoagulants) to determine whether the ISS score for each of the six body regions defined in the AIS was associated with serum SDC-1 level. As shown in Table 3 and Figure 3, the body region-specific score for "chest" and "abdominal or pelvic contents" were significantly associated with serum SDC-1 level in trauma patients (chest: Exp (β) = 1.273, 95%CI = 1.076–1.506, P = 0.006, R^2 = 0.18; abdominal or pelvic contents: Exp (β) = 1.326, 95%CI = 1.090–1.614, P = 0.005, R^2 = 0.18), and the score for "extremities or pelvic girdle" also tended to show an association with serum SDC-1 level (Exp (β) = 1.178, 95%CI = 0.982–1.412, P = 0.077, R^2 = 0.12).

TABLE 2 Linear regression between serum SDC-1 and ISS in trauma patients at arrival at the ER.

Factor	Exp (β)	95%LCI	95%UCI	*P*-value	R^2
ISS	1.046	1.02	1.072	0.001	0.23

Exp (β), exponentiation of the β coefficient; R^2, coefficient of determination; IQR, interquartile range; LCI, lower confidence interval; UCI, upper confidence interval; ISS, injury severity score; ER, emergency room.
Adjusted for age, gender, previous treatment, and medication history (antiplatelets or anticoagulants).

Relationship between probability of survival and serum SDC-1 level on admission to the emergency room

The median Ps was 0.9225 (IQR 0.8134–0.9655). The multivariable linear regression model showed that increasing serum SDC-1 level was significantly correlated with decreasing Ps after adjustment for age, gender, treatment history

(transfusion and angiography) and medication history (antiplatelet agents and anticoagulants) (Exp (β) = 0.973, 95%CI = 0.96–0.986, $P < 0.001$, $R^2 = 0.26$, Table 4; Figure 4).

Discussion

We demonstrated that serum SDC-1 level measured on admission to the emergency room in patients with trauma was significantly associated with ISS. Among the six body regions defined in the AIS used to calculate the ISS score, "chest" and "abdominal or pelvic contents" were significantly associated with serum SDC-1 level in trauma patients, and "extremities or pelvic girdle" tended to show an association with serum SDC-1 level. Moreover, increasing serum SDC-1 level was significantly correlated with decreasing Ps.

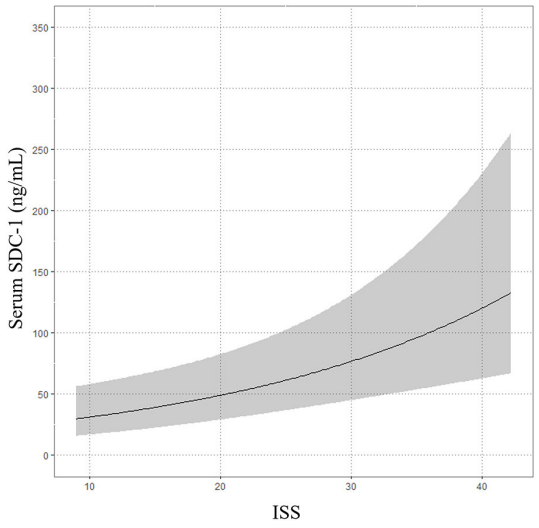

FIGURE 2
Association between serum SDC-1 and injury severity score (ISS).

The composition and function of the endothelial glycocalyx are related to the pathophysiology of trauma (8), with the shedding of SDC-1 from the endothelial glycocalyx into serum having been shown to be associated with several inflammatory cytokines and chemical mediators related to the pathophysiology of trauma (14, 15, 25). The ISS is correlated with adrenaline, interleukin (IL)-6, histone-complexed DNA fragments, high-mobility group box 1 (HMGB1), soluble thrombomodulin (sTM) and protein C in trauma patients with high serum SDC-1 levels ($\geq$ 63 ng/ml) but not in those with low SDC-1 levels ($<$ 63 ng/ml) (15). Patients with serum SDC-1 $\geq$ 40 ng/ml suffering from blunt or penetrating trauma have nearly 1.5-fold higher sTM levels in the initial 24 h after the trauma than patients with serum SDC-1 $<$ 40 ng/ml (14). Serum SDC-1 levels in severely injured patients experiencing hemorrhagic shock are positively correlated with interleukin-10 and inversely correlated with interferon (IF)-γ, fractalkine and IL-1β (25). These findings suggest that serum SDC-1 may reflect the pathophysiology of trauma.

Two clinical studies in trauma patients have also reported relationships between serum SDC-1 and ISS. In an observational study of 80 trauma patients, Johansson et al. showed that those with acute coagulopathy of trauma shock (ACoTS), defined as activated partial thromboplastin time or international normalized ratio above the normal reference level, had significantly higher median ISS values and serum SDC-1 levels than non-ACoTS patients [ISS: 34 (IQR 30–43) vs. 17 (IQR 10–25), $P < 0.001$; SDC-1: 62 (IQR 34–107) *vs* 31 (IQR 18–48), $P = 0.013$] (26). The same group also reported in a prospective cohort study of 75 trauma patients that the ISS did not significantly differ between a high serum SDC-1 group and low serum SDC-1 group (15). However, it is important to note that the median ISS was higher in the high serum SDC-1 group than in the low serum SDC-1 group [23 (IQR 14–37) vs. 17 (IQR 14–28)]. Additionally, neither of the two studies described above used continuous values to analyze the relationship between SDC-1 level and ISS, nor did they discuss the validity of grouping by the median value. In fact, the median serum SDC-1 level and

TABLE 3 Linear regression between serum SDC-1 and six body regions defined in the AIS used to calculate the ISS score in trauma patients on arrival at the ER.

Body region	Exp (β)	95%LCI	95%UCI	*P*-value	R^2
Head or neck	1.061	0.909	1.239	0.445	0.09
Face	1.073	0.736	1.566	0.71	0.08
Chest	1.273	1.076	1.506	0.006	0.18
Abdominal or pelvic contents	1.326	1.09	1.614	0.005	0.18
Extremities or pelvic girdle	1.178	0.982	1.412	0.077	0.12
External	0.876	0.467	1.643	0.676	0.08

Exp (β), exponentiation of the β coefficient, R^2, coefficient of determination; IQR, interquartile range; LCI, lower confidence interval; UCI, upper confidence interval; ISS, injury severity score; ER, emergency room.
Adjusted for age, gender, previous treatment, and medication history (antiplatelets or anticoagulants).

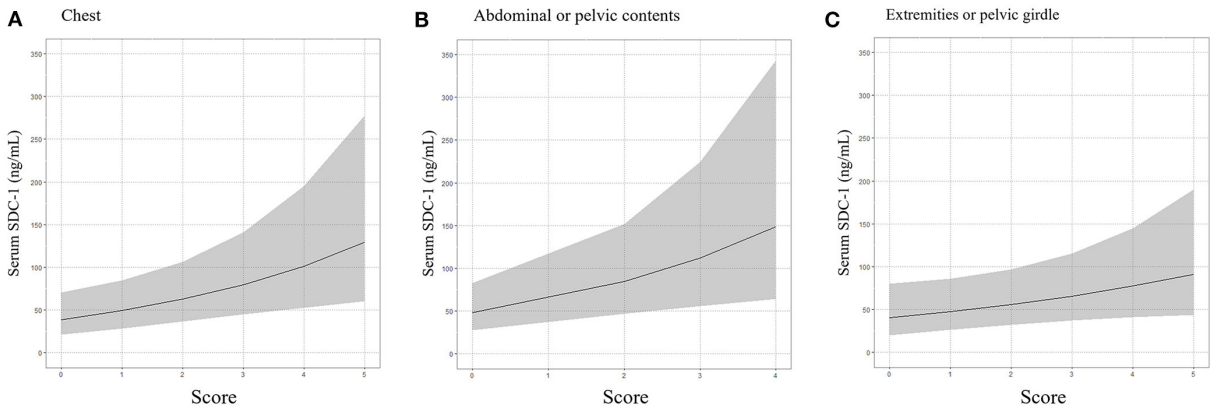

FIGURE 3
Association between serum SDC-1 and chest **(A)**, abdominal or pelvic contents **(B)** and extremities or pelvic girdle **(C)**, body regions defined by the AIS used to calculate ISS score.

TABLE 4 Linear regression between serum SDC-1 and probability of survival in trauma patients at arrival at the ER.

Factor	Exp (β) *	95%LCI	95%UCI	*P*-value	R^2
Ps (/0.01)	0.973	0.96	0.986	<0.001	0.26

Exp (β), exponentiation of the β coefficient; R^2, coefficient of determination; IQR, interquartile range; LCI, lower confidence interval; UCI, upper confidence interval; Ps, probability of survival; ER, emergency room.
Adjusted for age, gender, previous treatment, and medication history (antiplatelets or anticoagulants).
*The value for increments of 0.01 in Ps.

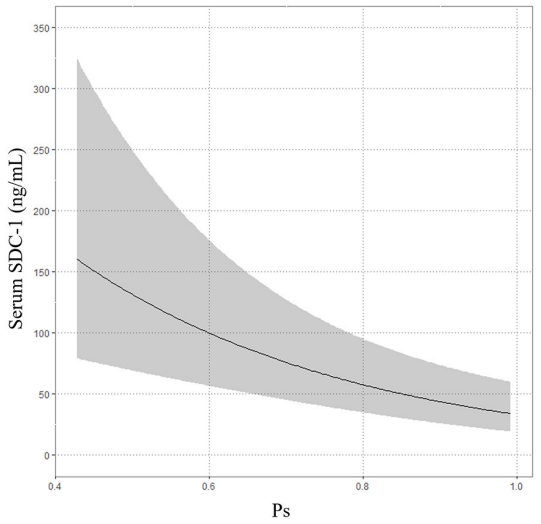

FIGURE 4
Association between serum SDC-1 and probability of survival (Ps).

ISS score in the present study was different to those of the prior studies. In the present study, multivariable regression analysis adjusted for age, gender, previous treatment, and medication history demonstrated that serum SDC-1 level measured on admission to the emergency room in trauma patients was significantly associated with ISS. This result indicates that serum SDC-1 may be a useful biomarker of severity in patients with trauma.

Moreover, we showed that among the six body regions defined in the AIS used to calculate the ISS score, "chest" and "abdominal or pelvic contents" were significantly associated with serum SDC-1 level, and that "extremities or pelvic girdle" tended to be associated with serum SDC-1 level. In contrast, "head or neck," "face" and "external" regions were not associated with serum SDC-1 level. The reason for the difference in association between serum SDC-1 and the ISS score for each body region defined by the AIS is unclear. However, we speculate that the total surface area of the endothelium in each region may differentially influence the amount of serum SDC-1. For example, the "head and neck," "face" and "external" regions, mainly categorized as ectodermic tissue, have a small surface area of endothelium, whereas "chest" and "abdominal or pelvic contents" and "extremities or pelvic girdle," mainly categorized as endodermic or mesodermic tissue, have a greater surface area of endothelium. Reports from surgeries of the abdominal, cardiac and thoracic regions have indicated elevated levels of serum SDC-1, which is consistent with the present results (27–29). Additionally, the structure and components of the endothelial glycocalyx differ among organs, as does its susceptibility to injury (7, 30). The endothelial glycocalyx in

the capillaries of the brain, for example, unlike that in the capillaries of the heart and lungs, is extremely thick. As a result, lipopolysaccharide-induced vascular injury completely eliminates the endothelial glycocalyx in cardiac and pulmonary capillaries but leaves much of it in the cerebral capillaries intact (30). These factors may explain the difference in correlation between SDC-1 and the ISS score for some body regions defined by the AIS but not others.

In the present study, we used probability of survival to evaluate the association between serum SDC-1 level and mortality in trauma patients because mortality was only 3.947% (3/76). In the multivariable linear regression model, increasing serum SDC-1 level was significantly correlated with decreasing Ps, a result that is consistent with those of previous reports (15, 25).

This study has several limitations. First, we were unable to evaluate the extent of endothelium injury and serum inflammatory cytokine and chemical mediator levels (e.g., IL-6, histone-complexed DNA fragments, HMGB1, sTM, protein C) related to the pathophysiology of trauma. Second, in addition to the endothelial glycocalyx, SDC-1 is also expressed in other organs. However, we did not evaluate SDC-1 expression in different organs in this study. Third, we evaluated the Ps but not mortality in this study. Fourth, due to the retrospective nature of this study, a large number of patients ($n = 143$) who met the eligibility criteria were excluded because of missing blood samples, as this prevented us from determining their serum SDC-1 levels. Moreover, potentially relevant confounding factors may have been missed. Finally, the sample size was small and data were obtained from a single institution.

In conclusion, serum SDC-1 may be a useful biomarker for evaluating severity in trauma patients, especially trauma in the "chest," "abdominal or pelvic contents" and "extremities or pelvic girdle" regions. Additionally, elevated serum SDC-1 levels may be an important risk factor for mortality in patients with trauma. Further large-scale studies are warranted to verify the usefulness of serum SDC-1 as a marker of severity in trauma patients.

Data availability statement

The raw data supporting the conclusions of this article will be made available by the authors, without undue reservation.

Ethics statement

The studies involving human participants were reviewed and approved by ethics approval was obtained from the Medical Ethics Committee of the Gifu University Graduate School of Medicine, Gifu, Japan (record no: 2021-B097). Written informed consent for participation was not required for this study in accordance with the national legislation and the institutional requirements.

Author contributions

KeS and AS wrote the manuscript. KeS, KaS, YM, FY, RKo, TMiu, RY, YK, TF, KoS, TMiy, and NK collected the blood samples. KeS, KaS, and RKo measured the syndecan-1 concentration using ELISA. KeS and RY created the database. TI performed the statistical analysis. YM, FY, RKa, TMiu, RY, YK, TF, KoS, TMiy, NK, TD, TY, and SY treated the patients. HT, SY, NT, and SO supervised the study. HO and AS revised and edited the manuscript. All authors contributed to the article and approved the submitted version.

Acknowledgments

We would like to thank DMC Corp. (www.dmed.co.jp) for providing English language editing of this paper.

Conflict of interest

The authors declare that the research was conducted in the absence of any commercial or financial relationships that could be construed as a potential conflict of interest.

Publisher's note

All claims expressed in this article are solely those of the authors and do not necessarily represent those of their affiliated organizations, or those of the publisher, the editors and the reviewers. Any product that may be evaluated in this article, or claim that may be made by its manufacturer, is not guaranteed or endorsed by the publisher.

References

1. Sakran JV, Greer SE, Werlin E, McCunn M. Care of the injured worldwide: trauma still the neglected disease of modern society. *Scand J Trauma Resusc Emerg Med.* (2012) 20:64. doi: 10.1186/1757-7241-20-64

2. Holcomb JB. del Junco DJ, Fox EE, Wade CE, Cohen MJ, Schreiber MA, et al. The prospective, observational, multicenter, major trauma transfusion (PROMMTT) study: comparative effectiveness of a time-varying treatment with competing risks. *JAMA Surg.* (2013) 148:127–36. doi: 10.1001/2013.jamasurg.387

3. Baker SP, O'Neill B, Haddon W Jr. Long WB The injury severity score: a method for describing patients with multiple injuries and evaluating emergency care. *J Trauma.* (1974) 14:187–96. doi: 10.1097/00005373-197403000-00001

4. Baker SP, O'Neill B. The injury severity score: an update. *J Trauma.* (1976) 16:882–5. doi: 10.1097/00005373-197611000-00006

5. Lavoie A, Moore L, LeSage N, Liberman M, Sampalis JS. The injury severity score or the new injury severity score for predicting intensive care unit admission and hospital length of stay? *Injury.* (2005) 36:477–83. doi: 10.1016/j.injury.2004.09.039

6. Lord JM, Midwinter MJ, Chen YF, Belli A, Brohi K, Kovacs EJ, et al. The systemic immune response to trauma: an overview of pathophysiology and treatment. *Lancet.* (2014) 384:1455–65. doi: 10.1016/S0140-6736(14)60687-5

7. Suzuki A, Tomita H, Okada H. Form follows function: the endothelial glycocalyx. *Transl Res.* (2022). doi: 10.1016/j.trsl.2022.03.014

8. Chignalia AZ, Yetimakman F, Christiaans SC, Unal S, Bayrakci B, Wagener BM, et al. The glycocalyx and trauma: a review. *Shock.* (2016) 45:338–48. doi: 10.1097/SHK.0000000000000513

9. Uchimido R, Schmidt EP, Shapiro NI. The glycocalyx: a novel diagnostic and therapeutic target in sepsis. *Crit Care.* (2019) 23:16. doi: 10.1186/s13054-018-2292-6

10. Schmidt EP, Overdier KH, Sun X, Lin L, Liu X, Yang Y, et al. Urinary glycosaminoglycans predict outcomes in septic shock and acute respiratory distress syndrome. *Am J Respir Crit Care Med.* (2016) 194:439–49. doi: 10.1164/rccm.201511-2281OC

11. Libório AB, Braz MB, Seguro AC, Meneses GC, Neves FM, Pedrosa DC, et al. Endothelial glycocalyx damage is associated with leptospirosis acute kidney injury. *Am J Trop Med Hyg.* (2015) 92:611–6. doi: 10.4269/ajtmh.14-0232

12. Padberg JS, Wiesinger A, di Marco GS, Reuter S, Grabner A, Kentrup D, et al. Damage of the endothelial glycocalyx in chronic kidney disease. *Atherosclerosis.* (2014) 234:335–43. doi: 10.1016/j.atherosclerosis.2014.03.016

13. Kitagawa Y, Kawamura I, Suzuki K, Okada H, Ishihara T, Tomita H, et al. Serum syndecan-1 concentration in hospitalized patients with heart failure may predict readmission-free survival. *PLoS ONE.* (2021) 16:e0260350. doi: 10.1371/journal.pone.0260350

14. Gonzalez Rodriguez E, Ostrowski SR, Cardenas JC, Baer LA, Tomasek JS, Henriksen HH, et al. Syndecan-1: a quantitative marker for the endotheliopathy of trauma. *J Am Coll Surg.* (2017) 225:419–27. doi: 10.1016/j.jamcollsurg.2017.05.012

15. Johansson PI, Stensballe J, Rasmussen LS, Ostrowski SR, A. high admission syndecan-1 level, a marker of endothelial glycocalyx degradation, is associated with inflammation, protein C depletion, fibrinolysis, and increased mortality in trauma patients. *Ann Surg.* (2011) 254:194–200. doi: 10.1097/SLA.0b013e318226113d

16. Gennarelli TAWEAftAoAM. *Abbreviated Injury Scale 2005: Update 2008.* Barrington, Ill: Association for the Advancement of Automative Medicine (2008).

17. Boyd CR, Tolson MA, Copes WS. Evaluating trauma care: the TRISS method. Trauma score and the injury severity score. *J Trauma.* (1987) 27:370–8. doi: 10.1097/00005373-198704000-00005

18. Oda K, Okada H, Suzuki A, Tomita H, Kobayashi R, Sumi K, et al. Factors Enhancing Serum Syndecan-1 Concentrations: A Large-Scale Comprehensive Medical Examination. J Clin Med. 2019;8(9). doi: 10.3390/jcm8091320

19. Bruijns SR, Guly HR, Bouamra O, Lecky F, Lee WA. The value of traditional vital signs, shock index, and age-based markers in predicting trauma mortality. *J Trauma Acute Care Surg.* (2013) 74:1432–7. doi: 10.1097/TA.0b013e31829246c7

20. van Teeffelen J, Jansen C, Spaan J, Vink H. Gender difference in systemic glycocalyx volume in mice. *FASEB J.* (2007) 21:A491. doi: 10.1096/fasebj.21.5.A491-a

21. Magnotti LJ, Fischer PE, Zarzaur BL, Fabian TC, Croce MA. Impact of gender on outcomes after blunt injury: a definitive analysis of more than 36,000 trauma patients. *J Am Coll Surg.* (2008) 206:984–91. doi: 10.1016/j.jamcollsurg.2007.12.038

22. Chappell D, Bruegger D, Potzel J, Jacob M, Brettner F, Vogeser M, et al. Hypervolemia increases release of atrial natriuretic peptide and shedding of the endothelial glycocalyx. *Crit Care.* (2014) 18:538. doi: 10.1186/s13054-014-0538-5

23. Francesco V, Roberto B, Giulia C, Piero CS, Michele A, Andrea S, et al. All elderly are fragile, but some are more fragile than others: an epidemiological study from one of the busiest trauma centers in Italy. *Updates Surg.* (2022). doi: 10.1007/s13304-022-01337-y

24. Kerschbaum M, Lang S, Henssler L, Ernstberger A, Alt V, Pfeifer C, et al. Influence of oral anticoagulation and antiplatelet drugs on outcome of elderly severely injured patients. *J Clin Med.* (2021) 10:1649 doi: 10.3390/jcm10081649

25. Haywood-Watson RJ, Holcomb JB, Gonzalez EA, Peng Z, Pati S, Park PW, et al. Modulation of syndecan-1 shedding after hemorrhagic shock and resuscitation. *PLoS One.* (2011) 6:e23530. doi: 10.1371/journal.pone.0023530

26. Johansson PI, Sørensen AM, Perner A, Welling KL, Wanscher M, Larsen CF, et al. Disseminated intravascular coagulation or acute coagulopathy of trauma shock early after trauma? An observational study. *Crit Care.* (2011) 15:R272. doi: 10.1186/cc10553

27. Pesonen E, Passov A, Andersson S, Suojaranta R, Niemi T, Raivio P, et al. Glycocalyx degradation and inflammation in cardiac surgery. *J Cardiothorac Vasc Anesth.* (2019) 33:341–5. doi: 10.1053/j.jvca.2018.04.007

28. Pustetto M, Goldsztejn N, Touihri K, Engelman E, Ickx B, Van Obbergh L. Intravenous lidocaine to prevent endothelial dysfunction after major abdominal surgery: a randomized controlled pilot trial. *BMC Anesthesiol.* (2020) 20:155. doi: 10.1186/s12871-020-01075-x

29. Arthur A, McCall PJ, Jolly L, Kinsella J, Kirk A, Shelley BG. Endothelial glycocalyx layer shedding following lung resection. *Biomark Med.* (2016) 10:1033–8. doi: 10.2217/bmm-2016-0163

30. Ando Y, Okada H, Takemura G, Suzuki K, Takada C, Tomita H, et al. Brain-specific ultrastructure of capillary endothelial glycocalyx and its possible contribution for blood brain barrier. *Sci Rep.* (2018) 8:17523. doi: 10.1038/s41598-018-35976-2

frontiers | Frontiers in Medicine

TYPE Original Research
PUBLISHED 29 November 2022
DOI 10.3389/fmed.2022.1045728

OPEN ACCESS

EDITED BY
W. Conrad Liles,
University of Washington, United States

REVIEWED BY
Coen Maas,
University Medical Center Utrecht, Netherlands
Alexander Vonk,
Amsterdam University Medical Center, Netherlands

*CORRESPONDENCE
Martine E. Bol
martine.bol@mumc.nl

SPECIALTY SECTION
This article was submitted to Intensive Care Medicine and Anesthesiology, a section of the journal Frontiers in Medicine

RECEIVED 15 September 2022
ACCEPTED 02 November 2022
PUBLISHED 29 November 2022

CITATION
Bol ME, Huckriede JB, van de Pas KGH, Delhaas T, Lorusso R, Nicolaes GAF, Sels JEM and van de Poll MCG (2022) Multimodal measurement of glycocalyx degradation during coronary artery bypass grafting. *Front. Med.* 9:1045728. doi: 10.3389/fmed.2022.1045728

Multimodal measurement of glycocalyx degradation during coronary artery bypass grafting

Martine E. Bol[1,2]*, J. B. Huckriede[3], K. G. H. van de Pas[1], T. Delhaas[4], R. Lorusso[2,5], G. A. F. Nicolaes[3], J. E. M. Sels[1,4,6] and M. C. G. van de Poll[1,2,7]

[1]Department of Intensive Care Medicine, Maastricht University Medical Center (MUMC+), Maastricht, Netherlands, [2]School of Nutrition and Translational Research in Metabolism (NUTRIM), Maastricht University, Maastricht, Netherlands, [3]Department of Biochemistry, Cardiovascular Research Institute Maastricht (CARIM), Maastricht University, Maastricht, Netherlands, [4]Department of Biomedical Engineering, Cardiovascular Research Institute Maastricht (CARIM), Maastricht University, Maastricht, Netherlands, [5]Department of Cardio-Thoracic Surgery, Maastricht University Medical Center (MUMC+), Maastricht, Netherlands, [6]Department of Cardiology, Maastricht University Medical Center (MUMC+), Maastricht, Netherlands, [7]Department of Surgery, Maastricht University Medical Center (MUMC+), Maastricht, Netherlands

Background: Glycocalyx shedding and subsequent endothelial dysfunction occur in many conditions, such as in sepsis, in critical illness, and during major surgery such as in coronary artery bypass grafting (CABG) where it has been shown to associate with organ dysfunction. Hitherto, there is no consensus about the golden standard in measuring glycocalyx properties in humans. The objective of this study was to compare different indices of glycocalyx shedding and dysfunction. To this end, we studied patients undergoing elective CABG surgery, which is a known cause of glycocalyx shedding.

Materials and methods: Sublingual glycocalyx thickness was measured in 23 patients by: 1) determining the perfused boundary region (PBR)—an inverse measure of glycocalyx thickness—by means of sidestream dark field imaging technique. This is stated double, 2) measuring plasma levels of the glycocalyx shedding products syndecan-1, hyaluronan, and heparan sulfate and 3) measuring plasma markers of impaired glycocalyx function and endothelial activation (Ang-2, Tie-2, E-selectin, and thrombomodulin). Measurements were performed directly after induction, directly after onset of cardiopulmonary bypass (CPB), and directly after cessation of CPB. We assessed changes over time as well as correlations between the various markers.

Results: The PBR increased from 1.81 ± 0.21 μm after induction of anesthesia to 2.27 ± 0.25 μm ($p < 0.0001$) directly after CPB was initiated and did not change further during CPB. A similar pattern was seen for syndecan-1, hyaluronan, heparan sulfate, Ang-2, Tie-2, and thrombomodulin. E-selectin levels also increased between induction and the start of CPB and increased further during CPB. The PBR correlated moderately with heparan sulfate, E-selectin, and thrombomodulin and weakly with Syndecan-1, hyaluronan, and Tie-2. Shedding markers syndecan-1 and hyaluronan correlated with all

functional markers. Shedding marker heparan sulfate only correlated with Tie-2, thrombomodulin, and E-selectin. Thrombomodulin correlated with all shedding markers.

Conclusion: Our results show that glycocalyx thinning, illustrated by increased sublingual PBR and increased levels of shedding markers, is paralleled with impaired glycocalyx function and increased endothelial activation in CABG surgery with CPB. As correlations between different markers were limited, no single marker could be identified to represent the glycocalyx in its full complexity.

KEYWORDS

glycocalyx, microcirculation, CABG, cardiopulmonary bypass, endothelial activation

Introduction

The microcirculation is compromised during numerous disease states, such as sepsis, shock, critical illness, and major surgery (1–5). Microcirculatory dysfunction may include increased flow heterogeneity and decreased vascular density (6). A known cause of microcirculatory dysfunction is coronary artery bypass graft (CABG) surgery in which microcirculatory dysfunction has been linked to postoperative increased lactate levels and elevated acute organ injury scores (7–11). In patients undergoing major abdominal surgery, as well as in septic patients and shock patients, microcirculatory derangements have been associated with impaired organ function and impaired outcomes (3, 5, 12–14). As such, protection and restoration of the microcirculation shows great promise to reduce complications and improve outcomes (15).

A key component of the microcirculation that is affected is the glycocalyx (16, 17). The glycocalyx is a gel-like layer lining the luminal side of vascular endothelial cells. It is a network of proteoglycans, glycosaminoglycans, and glycoproteins with non-covalently linked endothelium- and plasma-derived molecules therein (18, 19). The glycocalyx forms a primary barrier between blood constituents and vascular endothelium, thereby preventing leakage of plasma components, inhibiting platelet activation, regulating signaling molecules, and regulating leukocyte adhesion (18, 20).

Despite the importance of the glycocalyx in (patho)physiology and its potential as a target in the prevention of end-organ damage, there is no golden standard for its assessment (21). Generally, one of the following methods is used for glycocalyx measurements: (1) measurement of the sublingual glycocalyx dimensions using a video microscope, (2) measurement of degradation markers (glycocalyx constituents) in plasma, and (3) measurement of functional aspects of the glycocalyx/endothelial activation such as markers of vessel wall permeability. Different studies, among which some were performed during CABG surgery, reported different subsets of variables (16, 17, 22–24). This complicates comparisons between studies and the establishment of associations between different markers.

In this study, we evaluated glycocalyx dynamics through all three measurement methods simultaneously to gain more insights into glycocalyx (patho)physiology and how the different measurement methods relate to each other. We studied patients undergoing CABG surgery with extracorporeal circulation and induced cardiac ischemia as they form a predictable, *in vivo* model of endothelial glycocalyx dysfunction.

Materials and methods

A representative sample of adult patients (≥18 years) that undergo elective CABG surgery with the use of cardiopulmonary bypass (CPB) were considered eligible for inclusion. Patients were included if an observer and equipment were available for performing measurements. The only exclusion criteria that were applied were related to the technical feasibility of sublingual SDF imaging (i.e., no oral injuries or infections). The study protocol was approved by the medical ethics committee of the Maastricht University Medical Center (MUMC+) and written informed consent was obtained from all participants before inclusion. To obtain a complete dataset during CABG surgery, patients were excluded from the study in case not all measurements could be performed.

Measurements

Anesthesia was induced and maintained with propofol, midazolam, sufentanil, and rocuronium, after which the

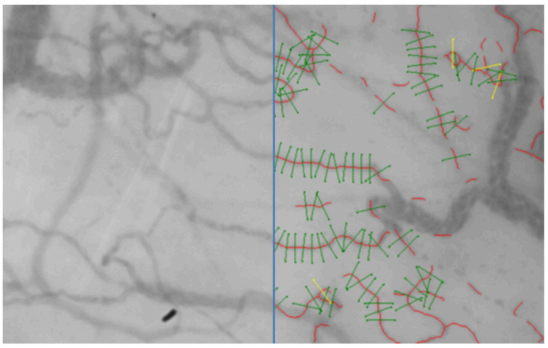

FIGURE 1
A frame recorded with an SDF camera with on the right an overlay of the vessels (red) with valid measurement points (green) that were detected and analyzed by the GlycoCheck software.

sternum was opened and vessels (generally the left internal thoracic artery and the great saphenous vein) were prepared for coronary grafting. Cardiac arrest was established after aortic cross-clamping by administration of a potassium-rich cardioplegia solution either added to a crystalloid solution (St. Thomas cardioplegia) or blood (blood cardioplegia) according to the surgeon's preference. A heart-lung machine with a roller pump and a heater-cooler device (Sorin Stockert S5, Livanova, Mirandola, Italy) was used to conduct CPB with heparin-coated circuits. Heparin was administered prior to the start of CPB to achieve an activated clotting time (ACT) of at least 400 s. After cessation of the CPB, the effect of heparin was reversed with protamine sulfate (1 mg of protamine for every 100 units of heparin). Shed blood, collected during both the heparinized and non-heparinized phase of surgery and buffered in a cell saver reservoir, was transfused into the patient at the end of surgery. Additionally, cardiotomy suction was performed. Normothermia was maintained during surgery. After surgery, patients were admitted to the intensive care unit (ICU).

Data were collected at four points in time: (1) directly after induction of anesthesia (baseline), (2) directly after start of CPB, (3) directly after cessation of CPB, and (4) 2 h after surgery at

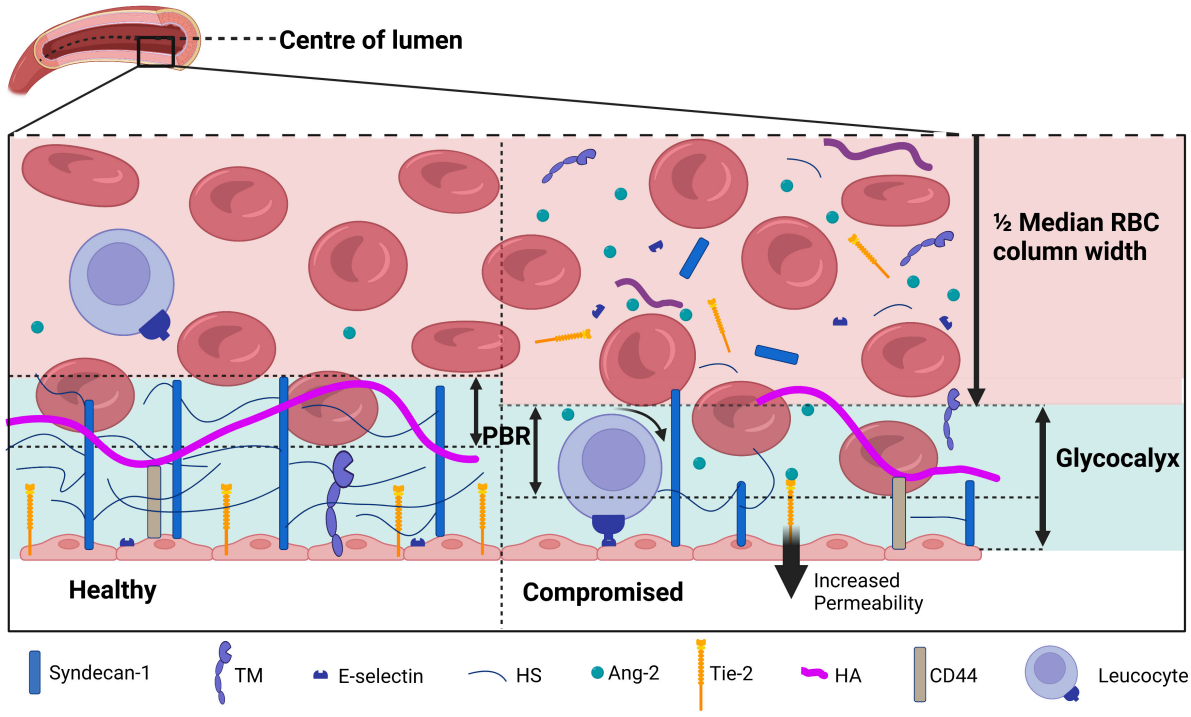

FIGURE 2
A schematic overview of the glycocalyx under physiological **(left)** and diseased **(right)** conditions covering the endothelial cells in the lumen of a blood vessel. The perfused boundary region (PBR) is defined as the distance between the median red blood cell (RBC) column width and the limit where erythrocytes can be found. During physiological conditions, the glycocalyx is composed of syndecan-1 and glycosaminoglycans including heparan sulfate (HS) and hyaluronan (HA). Receptors such as thrombomodulin (TM), Tie-2, and E-selectin are present on the endothelial membrane. During disease, the glycocalyx is damaged and components are shed to the plasma, which causes an increase in the PBR as erythrocytes are able to penetrate deeper in the glycocalyx layer. Activation of endothelial cells causes both activation and release of surface receptors TM, Tie-2, and E-selectin. E-selectin activation increases leukocyte rolling, increased Ang-2 levels binding to Tie-2 increases vessel permeability. Figure created with www.biorender.com.

the ICU. Study measurements did not alter standard surgical procedures as performed in our center.

Sublingual glycocalyx measurements

At all four time points, multiple sublingual microcirculation movies of 1 s (23 frames) were acquired with an SDF camera (CapiScope HVCS, KK Technology, Honiton, UK) fitted with GlycoCheck software (Microvascular Health Solutions Inc., Salt Lake City, UT, USA) to obtain a single measurement for each time point. At each time point, three consecutive measurements were performed with the GlycoCheck as previous research by us and others indicated this to be crucial to achieve reliable results (25, 26).

Analysis of the sublingual movies per time point was performed with GlycoCheck software. GlycoCheck's measurement method is described by Lee et al. (27). In brief, measurement points are defined at 10 μm intervals on automatically detected vessels with a diameter between 5 and 25 μm (**Figure 1**). A single measurement was complete when at least 3,000 measurement points had been acquired. Sublingual glycocalyx thickness is calculated based on the assumption that the glycocalyx can roughly be divided into two sublayers: an inner layer that is penetrable to red blood cells—the so-called perfused boundary region (PBR)—and an outer layer that is impenetrable to red blood cells. As an intact glycocalyx is less penetrable to red blood cells compared to a damaged glycocalyx, the PBR can be used as an inverse measure of glycocalyx thickness (**Figure 2**). The measurement time was limited to 15 min at each time point; if measurements were not completed at that time, they were registered as missing data. Reasons for prolonged sublingual measurements include large amounts of saliva or debris in the mouth and excess lingual movement.

Glycocalyx markers

Directly after induction of anesthesia, directly after onset of CPB and directly after CPB was ceased, blood samples were collected from a radial, arterial line in citrate tubes and centrifuged twice at 4,000 RPM for 12 min at room temperature. Plasma was stored at −80°C and later analyzed to determine glycocalyx shedding products and markers that indicate glycocalyx function and endothelial activation. To determine glycocalyx shedding products, commercial enzyme-linked immunosorbent assays (ELISAs) were used according to the manufacturer's instructions for Syndecan-1 (DuoSet ELISA, R&D systems, Bio-Techne, Minneapolis, USA), hyaluronan (DuoSet ELISA, R&D systems, Bio-Techne, Minneapolis, USA) and heparan sulfate (Elabscience Biotechnology Inc., Houston, Texas, USA). To determine glycocalyx function and endothelial activation, Angiopoietin-2 [a marker that reflects vascular permeability (28)], Tie-2 [a marker that reflects vascular instability, including endothelial barrier function and inflammation (29)], E-selectin [a marker expressed on activated endothelium to mediate rolling leukocyte adhesion (30)], and thrombomodulin [an anticoagulant mediator expressed by endothelial cells that can bind to the glycocalyx (31)] were measured with commercial ELISAs from R&D systems (DuoSet ELISA, Bio-Techne, Minneapolis, USA). Plasma samples were diluted 1:10 for R&D systems and 1:100 for Elabscience in 1% BSA reagent diluent. All plasma measurements were performed in triplicate, averaged, and corrected for plasma dilution during surgery with respect to the levels measured directly after induction by correcting for hemoglobin levels.

Statistical analysis

Data analysis was performed using GraphPad Prism (Version 9.2.0; GraphPad Software, San Diego, CA, USA). Normality was assessed using the Kolmogorov-Smirnov test for normality. Data are presented as mean ± standard deviation (SD) for normally distributed data and as median [25th–75th percentile] for non-normally distributed data. Outliers were identified based on the Tukey method. Differences between time points were tested using the repeated measures ANOVA or the Friedman test as appropriate. *Post-hoc* testing was performed using a paired t-test or Wilcoxon signed-rank test with Bonferroni correction. Correlations between variables were calculated using Spearman rank correlation tests. A Spearman's rho below 0.2 was considered negligible, between 0.2 and 0.4 was considered weak, between 0.4 and 0.6 was considered moderate, between 0.6 and 0.8 was considered strong and above 0.8 was considered very strong. P-values < 0.05 were considered statistically significant.

Results

Study population

Of the 35 patients measured, 12 were excluded from the study for not having a full set of measurements. Baseline characteristics of the 23 included patients are shown in **Table 1**. The included population shows classical characteristics for patients that undergo elective CABG surgery, meaning 35% of patients were diabetic, 87% had hypertension and the mean BMI was 28.2 ± 4.9 (32). Hemoglobin levels dropped from 8.0 ± 0.9 mmol/L directly after induction to 5.3 ± 1.1 mmol/L at the start of the CPB and 5.3 ± 0.8 mmol/L when CPB was stopped.

Sublingual SDF video camera measurements

The PBR increased from 1.81 ± 0.21 μm at baseline to 2.27 ± 0.25 μm directly after CPB was started ($p < 0.0001$).

TABLE 1 patient characteristics of the 23 patients.

Characteristic	Value
Age (years)	68.0 ± 6.4
Female; *N* (%)	3 (13%)
Height (cm)	172.4 ± 7.6
Weight (kg)	84 ± 15
BMI (kg/m^2)	28.2 ± 4.9
Hypertension; *N* (%)	20 (87%)
Diabetes; *N* (%)	8 (35%)
Aortic clamp time (minutes)	52 ± 19
Number of grafts	3 (2–4)
Length of ICU stay (days)	2 (2–3)
Length of hospital stay (days)	8 (7–9)
SOFA score the day after surgery	4.4 ± 2.4

BMI, Body Mass Index; ICU, Intensive Care Unit, SOFA, Sequential Organ Failure Assessment.

There was no significant change in PBR between the beginning and the end of CPB (PBR = 2.23 ± 0.19 μm). Two hours after arrival at the ICU the PBR was, compared to its value directly after onset of CPB, significantly decreased to 1.98 ± 0.19 μm, but still statistically significantly higher than the PBR at baseline (Figure 3A).

Glycocalyx shedding markers

Syndecan-1 was, compared to its value at baseline, statistically significantly increased directly after CPB was started. Syndecan-1 levels at the end of CPB did not differ significantly from the levels measured at the start of extracorporeal circulation (Figure 3B). One patient had an increased level of syndecan-1 at baseline that increased even further during surgery (top outlier of Figure 3B). At the start of CPB, heparan sulfate had increased from baseline. No statistically significant change in heparan sulfate concentrations was observed between the start and end of CPB (Figure 3C). Directly after CPB was started, hyaluronan plasma concentrations increased significantly with respect to baseline. No significant change was observed during CPB (Figure 3D).

Markers indicating glycocalyx function and endothelial activation

At the start of CPB, Ang-2 concentrations were increased from baseline. No significant change in Ang-2 concentrations was observed between the start and end of CPB (Figure 3E). A single patient showed high levels of Ang-2 at baseline that increased further during surgery (outliers of Figure 3E); this was not the same patient that showed relatively high syndecan-1 levels. At the onset of CPB, Tie-2 concentrations were significantly increased with respect to baseline. Concentrations of Tie-2 at the start and end of CPB did not differ significantly (Figure 3F). Directly after onset of CPB, E-selectin concentrations were increased significantly from baseline. During CPB the E-selectin concentrations significantly increased further (Figure 3G). Directly after CPB was started, the concentrations of thrombomodulin were increased was started with respect to baseline (Figure 3H). There was no statistically significant change between the start and end of CPB.

Correlations within measurement methods

Table 2 shows the Spearman rank correlation coefficients within and between the different measurement methods. Shedding marker hyaluronan correlated strongly with syndecan-1 and only weakly with heparan sulfate. Syndecan-1 and heparan sulfate did not correlate significantly with each other. Functional markers Ang-2 correlated moderately with Tie-2 and weakly with E-selectin. Thrombomodulin correlated moderately with E-selectin and weakly with Tie-2.

Correlation between measurement methods

The PBR correlated moderately with the shedding marker heparan sulfate and the functional markers E-selection and Thrombomodulin. A weak correlation was observed between PBR and syndecan-1, hyaluronan, and Tie-2. Thrombomodulin correlated strongly with shedding marker Syndecan-1 and moderately with the other shedding markers hyaluronan and heparan sulfate. Shedding marker syndecan-1 was moderately correlated with functional marker E-selectin. Other correlations between markers of glycocalyx dysfunction and glycocalyx shedding were weak or absent (Ang-2 vs. heparan sulfate) (Table 2). Thrombomodulin and E-selectin were the only markers that correlated with any marker of a different aspect of glycocalyx injury.

Discussion

In this paper we investigated glycocalyx damage during CABG surgery with CPB through three measurement methods simultaneously: indirect visualization using a video microscope, glycocalyx shedding product concentrations, and markers indicating glycocalyx function and endothelial activation. The aim of our study was to investigate how these different measurements relate to each other during CABG surgery as this is a well-known cause of glycocalyx damage. A pattern of early damage was present directly after the onset of CPB and neither further damage nor recovery was observed for all three measurement methods. Only the systemic inflammation

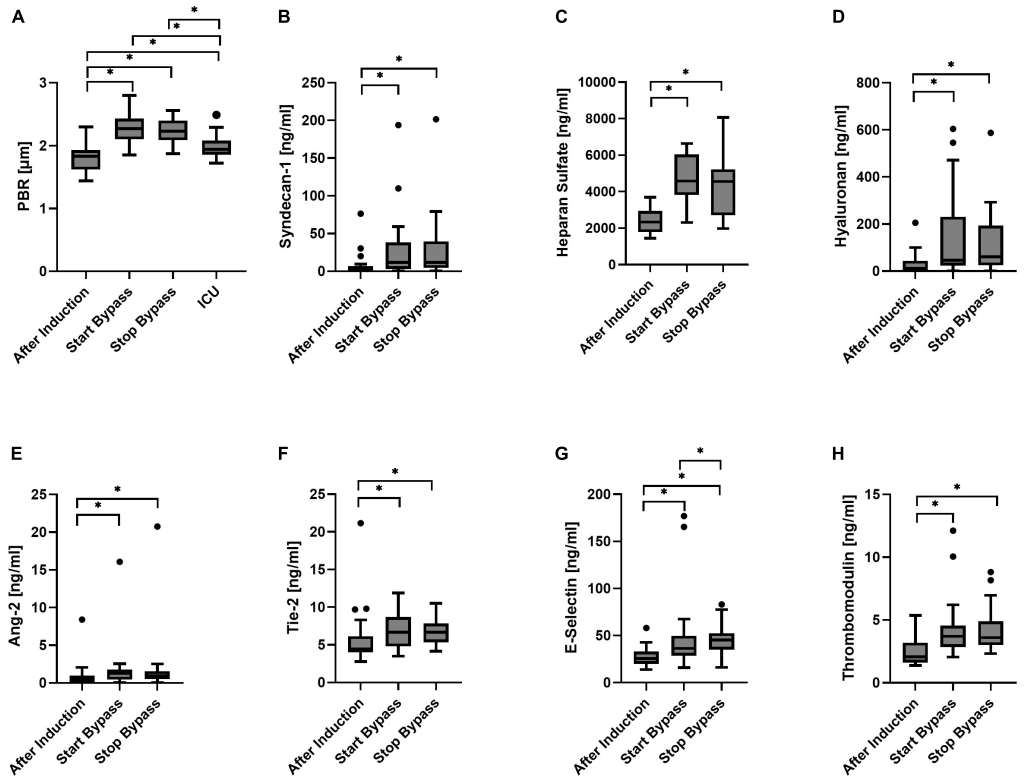

FIGURE 3
Boxplot of the perfused boundary region [PBR; **(A)**], Syndecan-1 **(B)**, heparan sulfate **(C)**, hyaluronan **(D)**, Angiopoietin-2 [Ang-2, **(E)**], Tie-2 **(F)**, E-selectin **(G)**, and thrombomodulin **(H)** for all time points. $N = 23$ during surgery; $N = 19$ at ICU. $^*p < 0.05$.

marker E-selectin (33, 34), an adhesion receptor that mediates leukocyte rolling on the endothelium showed an additional increase during CPB.

Our study shows that an increase in PBR and glycocalyx shedding product levels was paralleled with impaired glycocalyx/endothelial function and increased endothelial activation. This suggests a close relationship between glycocalyx thickness and vascular endothelial function during CABG surgery with CPB. This is in line with the perception that the endothelial glycocalyx serves as a key factor in maintaining homeostasis of the vascular endothelium (35, 36). Even though a causal relationship cannot be established from our data, some evidence suggests that glycocalyx damage at least precedes impaired endothelial function as Richter et al. showed that in septic children and in mouse models of sepsis, heparan sulfate levels peak prior to Ang-2 levels (37). Elevated Ang-2 concentrations have been associated with increased albuminuria which is associated with impaired pulmonary and renal function (38, 39). Additionally, endothelial dysfunction as reflected by increased thrombomodulin concentrations was associated with increased duration and severity of acute kidney injury following severe trauma (40). As such, preservation of glycocalyx integrity may reduce peri- and post-operative organ dysfunction and complications.

Our data further shows glycocalyx damage, as reflected by all three measurement methods, to be present directly after the onset of CPB and to persist, but not worsen, during CPB. Potential sources of glycocalyx damage between post-induction of anesthesia and the first minutes of CPB flow include surgical trauma, large amount of fluid administration (including CPB priming fluid), and initiation of CPB (including contact blood activation) (9). The timeframe of our measurements does not allow us to identify which of these aspects contribute to the observed glycocalyx degradation and dysfunction. Our study aim, however, was not to determine factors that damage the glycocalyx, but to compare different measurement methods. For this aim we needed glycocalyx shedding to take place between our measurement points, which it did according to our data. As such the chosen time points were in line with our aim.

A strength of our study is the fact that we performed simultaneous measurements allowing for a comparison between the different outcome measures (9). As surgical techniques and anesthesiologic procedures vary between medical centers, it is not evident that markers can be compared between different studies. Factors, such as whether pulsatile CPB flow was used

TABLE 2 Spearman rho correlation coefficients (top number) and their respective *p*-values (bottom number) for the correlations between measurements.

		SDF camera	Shedding markers			Functional/endothelial activation markers			
		PBR	Syndecan-1	Hyaluronan	Heparan Sulfate	Ang-2	Tie-2	E-selectin	Thrombo-modulin
SDF camera	PBR		0.38 0.0012	0.29 0.016	0.42 3.9×10^{-4}	0.11 0.37; NS	0.35 0.0036	0.44 1.4×10^{-4}	0.41 4.7×10^{-4}
Shedding markers	Syndecan-1	0.38 0.0012		0.60 6.13×10^{-8}	0.19 0.11; NS	0.35 0.0034	0.36 0.0023	0.40 0.00058	0.66 7.69×10^{-10}
	Hyaluronan	0.29 0.016	0.60 6.13×10^{-8}		0.30 0.013	0.28 0.019	0.28 0.020	0.27 0.0024	0.48 2.61×10^{-5}
	Heparan Sulfate	0.42 3.9×10^{-4}	0.19 0.11; NS	0.30 0.013		0.085 0.49; NS	0.34 0.0043	0.28 0.0020	0.48 3.28×10^{-5}
Functional/ endothelial activation markers	Ang-2	0.11 0.37; NS	0.35 0.0034	0.28 0.019	0.085 0.49; NS		0.53 2.9×10^{-6}	0.37 0.0017	0.23 0.054; NS
	Tie-2	0.35 0.0036	0.36 0.0023	0.28 0.020	0.34 0.0043	0.53 2.9×10^{-6}		0.52 4.12×10^{-6}	0.29 0.015
	E-selectin	0.44 1.4×10^{-4}	0.40 0.00058	0.27 0.0024	0.28 0.0020	0.37 0.0017	0.52 4.12×10^{-6}		0.48 2.45×10^{-5}
	Thrombo-modulin	0.41 4.7×10^{-4}	0.66 7.69×10^{-10}	0.48 2.61×10^{-5}	0.48 3.28×10^{-5}	0.23 0.054; NS	0.29 0.015	0.48 2.45×10^{-5}	

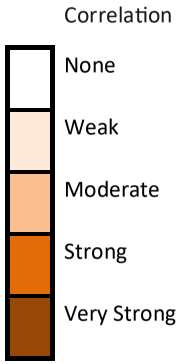

10.3389/fmed.2022.1045728

or not, have been shown to potentially influence glycocalyx dynamics (7, 16).

Most measurements correlated only weakly with each other implying no single measurement could suffice to comprehensively describe glycocalyx dynamics. Thrombomodulin, a marker that indicates impaired glycocalyx/endothelial activation, showed the best overall correlations with all shedding markers and the PBR. This implies that it should be chosen if only a single measurement is to be used. Classically, thrombomodulin is considered to be a cofactor for thrombin binding mediating protein C activation and inhibiting thrombin activity and hence, thereby functioning as an anticoagulant (41). In recent years, thrombomodulin is increasingly acknowledged to exhibit more properties such as an anti-inflammatory function (42, 43). Recent studies have shown thrombomodulin levels to be of specific interest as it proves to be a valuable prognostic marker associated with increased mortality rate and disease progression (44).

Syndecan-1, the most widely reported marker representing glycocalyx integrity (45), proved to be the shedding marker showing the highest correlations with the functional aspects of endothelial glycocalyx. PBR correlated moderately at most with all three shedding markers and with all functional markers but Ang-2. This implies that both syndecan-1 and thrombomodulin levels result in a better overview of glycocalyx integrity. PBR, however, is a non-invasive point-of-care measurement that can provide bed-side glycocalyx monitoring. Due to its ease of use and rapid results it may still be regarded as a valuable glycocalyx measurement method.

A limitation of our study is that we did not also perform measurements before anesthesia. However, Dekker et al. showed that PBR, syndecan-1, and heparan sulfate did not differ before and after induction of anesthesia (16) and additionally our measured PBR and marker concentrations reflect levels consistent with no or very limited elevation (46). Another limitation of our study is the fact that we compared circulating plasma markers with the PBR measured sublingually with an SDF camera. It cannot be guaranteed that measurements performed sublingually correctly reflect systemic changes in glycocalyx integrity although evidence suggests that in case of systemic changes in glycocalyx dimensions, the sublingual glycocalyx dimensions change accordingly (47–49). As the sublingual region is easily accessible, providing a non-invasive measurement, it is widely used to study microcirculatory parameters such as the glycocalyx (50, 51). The PBR is not based on direct visualization of the glycocalyx thickness, but based on the assumption that impaired glycocalyx is more permeable when damaged (52). Despite the mentioned limitations of the PBR, its potential value has been underlined by studies that link increased PBR with increased disease severity and worse clinical outcomes such as organ damage and mortality in different populations (12, 53).

To our knowledge, we are the first to simultaneously evaluate glycocalyx integrity through sublingual video microscopy, different shedding markers, and multiple functional markers. Our results show glycocalyx thinning to be paralleled with impaired glycocalyx function and increased endothelial activation in CABG surgery with CPB. As correlations between different markers were limited, no single marker could be identified to represent the glycocalyx in its full complexity. It is important to realize in future research that different markers represent different aspects of glycocalyx injury and are to be used complementary.

Data availability statement

The raw data supporting the conclusions of this article will be made available by the authors upon request, without undue reservation.

Ethics statement

The studies involving human participants were reviewed and approved by the Medical Ethics Committee of the Maastricht University Medical Center (MUMC+). The patients/participants provided their written informed consent to participate in this study.

Author contributions

MB and JH performed the data acquisition and analysis. KP performed data acquisition. All authors contributed to designing the study, drafting the manuscript, and substantially revising the manuscript.

Funding

This study was funded by “Stichting Hartsvrienden Rescar” (Grant No. 080317).

Acknowledgments

Financial support of “Stichting Hartsvrienden Rescar” was gratefully acknowledged.

Conflict of interest

The authors declare that the research was conducted in the absence of any commercial or financial relationships that could be construed as a potential conflict of interest.

Publisher's note

References

1. Ashruf JF, Bruining HA, Ince C. New insights into the pathophysiology of cardiogenic shock: the role of the microcirculation. *Curr Opin Crit Care.* (2013) 19:381–6. doi: 10.1097/MCC.0b013e328364d7c8

2. Colbert JF, Schmidt EP. Endothelial and microcirculatory function and dysfunction in sepsis. *Clin Chest Med.* (2016) 37:263–75. doi: 10.1016/j.ccm.2016.01.009

3. De Backer D, Creteur J, Dubois MJ, Sakr Y, Vincent JL. Microvascular alterations in patients with acute severe heart failure and cardiogenic shock. *Am Heart J.* (2004) 147:91–9. doi: 10.1016/j.ahj.2003.07.006

4. De Backer D, Creteur J, Preiser JC, Dubois MJ, Vincent JL. Microvascular blood flow is altered in patients with sepsis. *Am J Respir Crit Care Med.* (2002) 166:98–104. doi: 10.1164/rccm.200109-016OC

5. Jhanji S, Lee C, Watson D, Hinds C, Pearse RM. Microvascular flow and tissue oxygenation after major abdominal surgery: association with post-operative complications. *Intensive Care Med.* (2009) 35:671–7. doi: 10.1007/s00134-008-1325-z

6. De Backer D, Donadello K, Taccone FS, Ospina-Tascon G, Salgado D, Vincent JL. Microcirculatory alterations: potential mechanisms and implications for therapy. *Ann Intensive Care.* (2011) 1:27. doi: 10.1186/2110-5820-1-27

7. Koning NJ, Vonk AB, Vink H, Boer C. Side-by-side alterations in glycocalyx thickness and perfused microvascular density during acute microcirculatory alterations in cardiac surgery. *Microcirculation.* (2016) 23:69–74. doi: 10.1111/micc.12260

8. Koning NJ, Vonk AB, Meesters MI, Oomens T, Verkaik M, Jansen EK, et al. Microcirculatory perfusion is preserved during off-pump but not on-pump cardiac surgery. *J Cardiothorac Vasc Anesth.* (2014) 28:336–41. doi: 10.1053/j.jvca.2013.05.026

9. den Os MM, van den Brom CE, van Leeuwen ALI, Dekker NAM. Microcirculatory perfusion disturbances following cardiopulmonary bypass: a systematic review. *Crit Care.* (2020) 24:218. doi: 10.1186/s13054-020-02948-w

10. Greenwood JC, Jang DH, Hallisey SD, Gutsche JT, Horak J, Acker MA, et al. Severe impairment of microcirculatory perfused vessel density is associated with postoperative lactate and acute organ injury after cardiac surgery. *J Cardiothorac Vasc Anesth.* (2021) 35:106–15. doi: 10.1053/j.jvca.2020.04.045

11. De Backer D, Dubois MJ, Schmartz D, Koch M, Ducart A, Barvais L, et al. Microcirculatory alterations in cardiac surgery: effects of cardiopulmonary bypass and anesthesia. *Ann Thorac Surg.* (2009) 88:1396–403. doi: 10.1016/j.athoracsur.2009.07.002

12. Beurskens DM, Bol MM. E. Bol Decreased endothelial glycocalyx thickness is an early predictor of mortality in sepsis. *Anaesth Intensive Care.* (2020) 48:221–8. doi: 10.1177/0310057X20916471

13. Trzeciak S, Dellinger RP, Parrillo JE, Guglielmi M, Bajaj J, Abate NL, et al. Early microcirculatory perfusion derangements in patients with severe sepsis and septic shock: relationship to hemodynamics, oxygen transport, and survival. *Ann Emerg Med.* (2007) 49:88–98. doi: 10.1016/j.annemergmed.2006.08.021

14. den Uil CA, Lagrand WK, van der Ent M, Jewbali LS, Cheng JM, Spronk PE, et al. Impaired microcirculation predicts poor outcome of patients with acute myocardial infarction complicated by cardiogenic shock. *Eur Heart J.* (2010) 31:3032–9. doi: 10.1093/eurheartj/ehq324

15. Koning NJ, K.H.G. van M.C.G. van de Poll Pas Lange F, van Meurs M, Jongman RM, Ahmed Y, Schwarte LA, et al. Reduction of vascular leakage by imatinib is associated with preserved microcirculatory perfusion and reduced renal injury markers in a rat model of cardiopulmonary bypass. *Br J Anaesth.* (2018) 120:1165–75. doi: 10.1016/j.bja.2017.11.095

16. Dekker NAM, Veerhoek D, Koning NJ, van Leeuwen ALI, Elbers PWG, van den Brom CE, et al. Postoperative microcirculatory perfusion and endothelial glycocalyx shedding following cardiac surgery with cardiopulmonary bypass. *Anaesthesia.* (2019) 74:609–18. doi: 10.1111/anae.14577

17. Dekker NAM, Veerhoek D, van Leeuwen ALI, Vonk ABA, van den Brom CE, Boer C. Microvascular alterations during cardiac surgery using a heparin or phosphorylcholine-coated circuit. *J Cardiothorac Vasc Anesth.* (2020) 34:912–9.

18. Reitsma S, Slaaf DW, Vink H, van Zandvoort MA, oude Egbrink MG. The endothelial glycocalyx: composition, functions, and visualization. *Pflugers Arch.* (2007) 454:345–59.

19. Dane M, van den Berg B, Lee DH, Boels M, Tiemeier G, Avramut C, et al. A microscopic view on the renal endothelial glycocalyx. *Am J Physiol Renal Physiol.* (2015) 308:F956–66. doi: 10.1152/ajprenal.00532.2014

20. Zeng Y. Endothelial glycocalyx as a critical signalling platform integrating the extracellular haemodynamic forces and chemical signalling. *J Cell Mol Med.* (2017) 21:1457–62. doi: 10.1111/jcmm.13081

21. Banerjee S, Mwangi JG, Stanley TK, Mitra R, Ebong EE. Regeneration and assessment of the endothelial glycocalyx to address cardiovascular disease. *Indust Eng Chem Res.* (2021) 60:17328–47. doi: 10.1016/j.jss.2019.03.018

22. Bruegger, D, Rehm M, Abicht J, Paul JO, Stoeckelhuber M, Pfirrmann M, et al. Shedding of the endothelial glycocalyx during cardiac surgery: on-pump versus off-pump coronary artery bypass graft surgery. *J Thorac Cardiovasc Surg.* (2009) 138:1445–7.

23. Robich M, Ryzhov S, Kacer D, Palmeri M, Peterson SM, Quinn RD, et al. Prolonged cardiopulmonary bypass is associated with endothelial glycocalyx degradation. *J Surg Res.* (2020) 251:287–95.

24. Nussbaum C, Haberer A, Tiefenthaller A, Januszewska K, Chappell D, Brettner F, et al. Perturbation of the microvascular glycocalyx and perfusion in infants after cardiopulmonary bypass. *J Thorac Cardiovasc Surg.* (2015) 150:1474–81.e1. doi: 10.1016/j.jtcvs.2015.08.050

25. Bol ME, Beurskens DMH, Delnoij TSR, Roekaerts P, Reutelingsperger CPM, Delhaas T, et al. Variability of microcirculatory measurements in critically Ill patients. *Shock.* (2020) 54:9–14.

26. Eickhoff MK, Winther SA, Hansen TW, Diaz LJ, Persson F, Rossing P, et al. Assessment of the sublingual microcirculation with the GlycoCheck system: reproducibility and examination conditions. *PLoS One.* (2020) 15:e0243737. doi: 10.1371/journal.pone.0243737

27. Lee DH, Dane MJC, van den Berg BM, Boels MGS, van Teeffelen JW, de Mutsert R, et al. Deeper penetration of erythrocytes into the endothelial glycocalyx is associated with impaired microvascular perfusion. *PLoS One.* (2014) 9:e96477. doi: 10.1371/journal.pone.0096477

28. Akwii RG, Sajib MS. Role of angiopoietin-2 in vascular physiology and pathophysiology. *Cells.* (2019) 8:471.

29. Leligdowicz A, Richard-Greenblatt M, Wright J, Crowley VM, Kain KC. Endothelial activation: the Ang/Tie axis in sepsis. *Front Immunol.* (2018) 9:838. doi: 10.3389/fimmu.2018.00838

30. Ley K, Allietta M, Bullard DC, Morgan S. Importance of E-selectin for firm leukocyte adhesion in vivo. *Circ Res.* (1998) 83:287–94. doi: 10.1161/01.res.83.3.287

31. Boffa MC, Karmochkine M. Thrombomodulin: an overview and potential implications in vascular disorders. *Lupus.* (1998) 7(Suppl 2):S120–5. doi: 10.1177/096120339800700227

32. Cornwell LD, Omer S, Rosengart T, Holman WL, Bakaeen FG. Changes over time in risk profiles of patients who undergo coronary artery bypass graft surgery: the veterans affairs surgical quality improvement program (VASQIP). *JAMA Surg.* (2015) 150:308–15. doi: 10.1001/jamasurg.2014.1700

33. Smith CW. Potential significance of circulating E-selectin. *Circulation.* (1997) 95:1986–8.

34. Polfus LM, Raffield LM, Wheeler MM, Tracy RP, Lange LA, Lettre G, et al. Whole genome sequence association with E-selectin levels reveals loss-of-function variant in African Americans. *Hum Mol Genet.* (2019) 28:515–23. doi: 10.1093/hmg/ddy360

35. Uchimido R, Schmidt E, Shapiro N. The glycocalyx: a novel diagnostic and therapeutic target in sepsis. *Crit Care.* (2019) 23:16.

36. Ince C, Mayeux PR, Nguyen T, Gomez H, Kellum JA, Ospina-Tascon GA, et al. The endothelium in sepsis. *Shock.* (2016) 45:259–70.

37. Richter RP, Ashtekar AR, Zheng L, Pretorius D, Kaushlendra T, Sanderson RD, et al. Glycocalyx heparan sulfate cleavage promotes endothelial cell angiopoietin-2 expression by impairing shear stress–related AMPK/FoxO1 signaling. *JCI Insight.* (2022) 7:e155010. doi: 10.1172/jci.insight.155010

38. Chang FC, Lai TS, Chiang CK, Chen YM, Wu MS, Chu TS, et al. Angiopoietin-2 is associated with albuminuria and microinflammation in chronic kidney disease. *PLoS One.* (2013) 8:e54668. doi: 10.1371/journal.pone.0054668

39. Brudney CS, Gosling P, Manji M. Pulmonary and renal function following cardiopulmonary bypass is associated with systemic capillary leak. *J Cardiothorac Vasc Anesth.* (2005) 19:188–92.

40. Hatton GE, Isbell KD, Henriksen HH, Stensballe J, Brummerstedt M, Johansson PI, et al. Endothelial dysfunction is associated with increased incidence, worsened severity, and prolonged duration of acute kidney injury after severe trauma. *Shock.* (2021) 55:311–5. doi: 10.1097/SHK.0000000000001638

41. Li YH, Kuo CH, Shi GY, Wu HL. The role of thrombomodulin lectin-like domain in inflammation. *J Biomed Sci.* (2012) 19:34.

42. Loghmani H, Conway EM. Exploring traditional and nontraditional roles for thrombomodulin. *Blood.* (2018) 132:148–58. doi: 10.1182/blood-2017-12-768994

43. Watanabe-Kusunoki K, Nakazawa D, Ishizu A, Atsumi T. Thrombomodulin as a physiological modulator of intravascular injury. *Front Immunol.* (2020) 11:575890. doi: 10.3389/fimmu.2020.575890

44. Califano F, Giovanniello T, Pantone P, Campana E, Parlapiano C, Alegiani F, et al. Clinical importance of thrombomodulin serum levels. *Eur Rev Med Pharmacol Sci.* (2000) 4:59–66.

45. Yanase F, Naorungroj T, Bellomo R. Glycocalyx damage biomarkers in healthy controls, abdominal surgery, and sepsis: a scoping review. *Biomarkers.* (2020) 25:425–35. doi: 10.1080/1354750X.2020.1787518

46. Astapenko D, Turek Z, Dostal P, Hyspler R, Ticha A, Kaska M, et al. Effect of short-term administration of lipid emulsion on endothelial glycocalyx integrity in ICU patients - A microvascular and biochemical pilot study. *Clin Hemorheol Microcirc.* (2019) 73:329–39. doi: 10.3233/CH-190564

47. Broekhuizen LN, Lemkes BA, Mooij HL, Meuwese MC, Verberne H, Holleman F, et al. Effect of sulodexide on endothelial glycocalyx and vascular permeability in patients with type 2 diabetes mellitus. *Diabetologia.* (2010) 53:2646–55. doi: 10.1007/s00125-010-1910-x

48. Qian J, Yang Z, Cahoon J, Xu J, Zhu C, Yang M, et al. Post-resuscitation intestinal microcirculation: its relationship with sublingual microcirculation and the severity of post-resuscitation syndrome. *Resuscitation.* (2014) 85:833–9. doi: 10.1016/j.resuscitation.2014.02.019

49. Nieuwdorp M, Meuwese MC, Mooij HL, Ince C, Broekhuizen LN, Kastelein JJP, et al. Measuring endothelial glycocalyx dimensions in humans: a potential novel tool to monitor vascular vulnerability. *J Appl Physiol.* (2008) 104:845–52. doi: 10.1152/japplphysiol.00440.2007

50. Hahn RG, Patel V, Dull RO. Human glycocalyx shedding: systematic review and critical appraisal. *Acta Anaesthesiol Scand.* (2021) 65:590–606. doi: 10.1111/aas.13797

51. De Backer D, Hollenberg S, Boerma C, Goedhart P, Buchele G, Ospina-Tascon G, et al. How to evaluate the microcirculation: report of a round table conference. *Crit Care.* (2007) 11:R101. doi: 10.1186/cc6118

52. Dane MJ, Khairoun M, Lee DH, van den Berg BM, Eskens BJ, Boels MG, et al. Association of kidney function with changes in the endothelial surface layer. *Clin J Am Soc Nephrol.* (2014) 9:698–704.

53. Vlahu CA, Lemkes BA, Struijk DG, Koopman MG, Krediet RT, Vink H. Damage of the endothelial glycocalyx in dialysis patients. *J Am Soc Nephrol.* (2012) 23:1900–8.

frontiers | Frontiers in Medicine

TYPE Original Research
PUBLISHED 01 December 2022
DOI 10.3389/fmed.2022.1058235

OPEN ACCESS

EDITED BY
W. Conrad Liles,
University of Washington, United States

REVIEWED BY
Maxime Nguyen,
Centre Hospitalier Regional Universitaire De Dijon, France
Feng Shen,
Affiliated Hospital of Guizhou Medical University, China

*CORRESPONDENCE
Peter Pickkers
peter.pickkers@radboudumc.nl

†These authors have contributed equally to this work and share senior authorship

SPECIALTY SECTION
This article was submitted to Intensive Care Medicine and Anesthesiology, a section of the journal Frontiers in Medicine

RECEIVED 30 September 2022
ACCEPTED 07 November 2022
PUBLISHED 01 December 2022

CITATION
van Lier D, Picod A, Marx G, Laterre P-F, Hartmann O, Knothe C, Azibani F, Struck J, Santos K, Zimmerman J, Bergmann A, Mebazaa A and Pickkers P (2022) Effects of enrichment strategies on outcome of adrecizumab treatment in septic shock: *Post-hoc* analyses of the phase II adrenomedullin and outcome in septic shock 2 trial. *Front. Med.* 9:1058235. doi: 10.3389/fmed.2022.1058235

Effects of enrichment strategies on outcome of adrecizumab treatment in septic shock: *Post-hoc* analyses of the phase II adrenomedullin and outcome in septic shock 2 trial

Dirk van Lier[1], Adrien Picod[2], Gernot Marx[3], Pierre-François Laterre[4], Oliver Hartmann[5], Claudia Knothe[6], Feriel Azibani[2], Joachim Struck[6], Karine Santos[7], Jens Zimmerman[6], Andreas Bergmann[5,6], Alexandre Mebazaa[2,8†] and Peter Pickkers[1*†] on behalf of AdrenOSS-2 study participants

[1]Department of Intensive Care Medicine and Radboud Center for Infectious Diseases (RCI), Radboud University Medical Center, Nijmegen, Netherlands, [2]Anesthésie-Réanimation, Hôpital Lariboisière, AP–HP, Paris, France, [3]Klinik fur Operative Intensivmedizin und Intermediate Care, Universitätsklinikum Aachen, Aachen, Germany, [4]Unité de Soins Intensifs, Cliniques Universitaires Saint-Luc (UCL Bruxelles), Brussels, Belgium, [5]Sphingotec GmbH, Hennigsdorf, Germany, [6]Adrenomed AG, Hennigsdorf, Germany, [7]4TEEN4 Pharmaceuticals GmbH, Hennigsdorf, Germany, [8]Université de Paris, U942 Inserm, MASCOT, APHP, Fédération Hospitalo-Universitaire PROMICE, Hôpitaux Universitaires Saint-Louis-Lariboisière, Paris, France

Purpose: Adrecizumab, a non-neutralizing antibody of adrenomedullin (ADM) was recently investigated regarding its potential to restore endothelial barrier function in septic shock patients with high plasma ADM levels. Circulating dipeptidyl peptidase 3 (cDPP3), a protease involved in the degradation of several cardiovascular mediators, represents another biological pathway strongly associated with outcome in septic shock, although unrelated to ADM. Therefore, the prognosis of patients with elevated cDPP3 may not be influenced by Adrecizumab. Also, time until initiation of treatment may influence efficacy.

Objective: To evaluate effects of cDPP3-based enrichment on treatment efficacy of Adrecizumab.

Materials and Methods: *Post-hoc* analysis of AdrenOSS-2, a phase-II, double-blind, randomized, placebo-controlled biomarker-guided trial of Adrecizumab.

Results: Compared to the total study cohort [HR for 28-day mortality of 0.84 (95% CI 0.53;1.31), p = 0.439], therapeutic benefit of Adrecizumab tended to be more pronounced in the subgroup of 249 patients with low cDPP3 (<50 ng/mL); [HR of 0.61 (95% CI 0.34;1.08), p = 0.085]. Median duration

to study drug infusion was 8.5 h. In the subgroup of 129 patients with cDPP3 <50 ng/mL and an early start of treatment (<8.5 h after septic shock diagnosis) HR for 28-day mortality vs. placebo was 0.49 (95% CI 0.21–1.18), p = 0.105. In multivariate interaction analyses corrected for baseline disease severity, both cDPP3, as well as the cDPP3 * treatment interaction term were associated with a reduced HR for 28-day mortality in the Adrecizumab treated group; p = 0.015 for cDPP3 in univariate analysis, p = 0.025 for the interaction term between cDPP3 and treatment group. In contrast, treatment timing was not significantly associated with 28-day mortality in multivariate interaction analyses.

Discussion: In septic shock patients with high ADM levels, a further *post-hoc* enrichment strategy based on cDPP3 may indicate (with all the caveats to be considered for *post-hoc* subgroup analyses) that therapeutic efficacy is most pronounced in patients with lower cDPP3 levels.

KEYWORDS

sepsis, septic shock, adrenomedullin, dipeptidyl peptidase 3, AdrenOSS-2, Adrecizumab

Introduction

Sepsis is defined as an inflammatory disorder, during which a dysregulated host response to infection results in life threatening organ dysfunction, leading to substantial patient mortality (1). During sepsis, both vascular tone and vascular integrity are compromised, ultimately contributing to the development of septic shock (2). Septic shock is characterized by increased blood lactate levels, as well as the necessity for vasopressor therapy to maintain mean arterial pressure despite adequate fluid resuscitation (1, 3). Although knowledge on the molecular mechanisms associated with sepsis development has vastly increased, treatment strategies remain virtually unchanged, consisting of supporting therapies including adequate and timely antimicrobial therapy, control of infection, fluid resuscitation and vasopressor therapy to maintain vascular tone (4).

Adrenomedullin (ADM) is a hormone essential for regulation of endothelial barrier function (5). During sepsis, multiple processes stimulate ADM release (6, 7) and increased ADM levels are associated with sepsis severity, development of organ dysfunction, including vasopressor/inotrope dependency (8–10), as well as mortality. In preclinical sepsis models, Adrecizumab, a non-neutralizing monoclonal anti-ADM antibody, improved endothelial barrier function and reduced organ failure, as well as mortality (11–13). Following the results of these preclinical studies, dose-finding, as well as a proof-of-mechanism in healthy volunteers (14), the proof-of-concept phase-2 trial AdrenOSS-2 was performed to evaluate the safety, tolerability and efficacy of Adrecizumab in septic shock patients (10, 15).

An increasing body of evidence demonstrates that multiple signaling pathways are altered during sepsis (16), reinforcing the notion that sepsis represents a highly heterologous syndrome (17). In AdrenOSS-2 the baseline concentration of the molecular biomarker "biologically active Adrenomedullin" (bio-ADM) was implemented as an enrichment strategy, aimed at reducing patient-heterogeneity by selecting patients with a higher mortality risk and (based on the mechanism of action) improved chances of treatment benefit. While this enrichment strategy represents one of the first examples of personalized medicine in sepsis trial design, significant further reductions in patient heterogeneity might be achieved by combining multiple biomarkers for patient selection.

Dipeptidyl peptidase 3 (DPP3) is an ubiquitous catalytic enzyme only present at low plasma concentration in healthy subjects, where it is involved in the degradation of several important regulators of vascular tone (18, 19). During septic shock, high concentrations of circulating DPP3 (cDPP3 for circulating DPP3) are associated with impaired outcome (20). Putatively, high concentrations of cDPP3 are the result of increased release of DPP3 caused by cellular injury (19). Interestingly, preclinical animal studies demonstrated that intravenous injection of DPP3 in healthy rodents caused impairment of cardiac function, while cDPP3 inhibition with a specific monoclonal antibody restored cardiac function in a rodent sepsis model (21). Based on these findings, DPP3 appears to represent a distinct molecular pathway in septic shock (19). This pathway is most likely contributing to the outcome of septic shock in a way not directly related to adrenomedullin.

We hypothesize that a subset of septic shock patients with high bio-ADM levels also presents with high cDPP3 levels. Moreover, we hypothesize that patients with high cDPP3 levels

have worse outcome, as well as a less pronounced therapeutic benefit when treated with Adrecizumab, since increased cDPP3 represents an independent risk factor of death in septic shock that is not targeted by Adrecizumab. Also, as it is generally recognized that early initiation of treatment may improve clinical outcome in septic shock patients, subgroup analyses based on time between diagnosis of septic shock and start of treatment were also conducted, both with and without stratification based on cDPP3 levels.

Materials and methods

Study design

The AdrenOSS-2 (Adrenomedullin and Outcome in Septic Shock 2) trial was a double-blind, placebo-controlled, randomized, multicenter, proof-of-concept, biomarker-guided and dose-finding phase II trial (clinicaltrials.gov identifier NCT 02338843) (15). In brief, adults (≥18 years) in the early phase of septic shock could be enrolled. As this was a biomarker-guided trial, one inclusion criterion was an elevated bio-ADM plasma concentration at baseline (>70 pg/mL), a cut-off value based on the increased risk of impaired outcome found in previous studies in sepsis and septic shock patients (8–10, 22–24). Patients also needed to be in the early phase of septic shock, defined as start of vasopressor therapy <12 h before study inclusion.

Patients were randomly assigned in a 1:1:2 ratio to either Adrecizumab (HAM 8101) 2 mg/kg, 4 mg/kg bodyweight or placebo. Patients received the assigned trial medication as a single intravenous infusion, administered over approximately 1 h. Dose selection was based on the phase-I study results (14), that showed a relevant Adrecizumab-induced elevation of plasma bio-ADM (over the bio-ADM concentrations present in the absence of Adrecizumab) for a time period of ∼7 days, the clinically most relevant phase in septic shock. Since Adrecizumab was given in molar excess of several hundred-fold above the concentration of bio-ADM in both treatment arms (2 mg/kg and 4 mg/kg), both dosage groups were pooled for the current *post-hoc* analysis.

Measurements

Ethylenediaminetetraacetic acid (EDTA)-anticoagulated blood samples for determination of bio-ADM were obtained prior to randomization. As bio-ADM cut-offs served as one of the main inclusion criteria in the original AdrenOSS-2 protocol, a rapid measurement assay was used (8). For determination of cDPP3, EDTA-anticoagulated blood samples were taken immediately before start of administration of the investigational product. Blood was centrifuged for 10 min at 4°C, after which plasma was stored at −80°C until blinded analysis using a cDPP3 luminescence immunoassays (4TEEN4 Pharmaceuticals GmbH, Berlin, Germany). The details and design principles of this assay are provided elsewhere (25).

Outcome evaluation

The main objective of this *post-hoc* analysis was to assess the interplay between cDPP3 concentrations and the therapeutic efficacy of Adrecizumab, as determined by changes in hazard ratios for 28-day mortality based on cDPP3 stratification. Secondly, we investigated the influence of cohort stratification based on time from diagnosis of septic shock to initiation of the study drug on 28-day mortality hazard ratios. Lastly, we assessed the influence of cohort stratification combining cDPP3 assessment and time until initiation of treatment on 28-day mortality hazard ratios. Secondary objectives of these *post-hoc* analyses included changes in SOFA score after 24 h of treatment, based on the aforementioned cohort stratification approaches. Safety endpoints included adverse event report rates in groups stratified by cDPP3 levels.

Statistics

Continuous variables are presented as median [interquartile range (IQR)], whereas categorical variables are presented as counts and percentages. All reported outcomes are calculated for subgroups of the original intention to treat (ITT) study population. High cDPP3 levels were defined as ≥ 50 ng/mL for this *post-hoc* analysis. This cut-off signifies a concentration of cDPP3 well above the median of the AdrenOSS-2 ITT study, is outside the range of normal values determined for cDPP3 in earlier studies (19, 20, 25) and does not exclude a major subset of patients. For the comparison of "early" and "late" start of Adrecizumab treatment, cohorts were dichotomized at the median time from diagnosis of septic shock until start of treatment.

All-cause mortality for 28-day follow-up was evaluated and Kaplan–Meier plots were generated comparing Adrecizumab (combined doses) vs. placebo. The log-rank test was chosen for showing differences in mortality rates among treatment groups. In order to further investigate the interplay between cDPP3 concentration, treatment timing and therapeutic efficacy of Adrecizumab, we performed an interaction analysis between Adrecizumab treatment and baseline cDPP3 concentration, i.e., a Cox regression was performed that included cDPP3, treatment status and the interaction term. The same analysis was performed for time from diagnosis of septic shock until start of treatment instead of cDPP3. Both models also included baseline

SOFA scores as a correction for baseline disease severity. For these interaction analyses, continuous variables were log-transformed. Proportional hazard assumptions of the generated models were tested by calculating the Schoenfeld residuals for all relevant covariates. We did not apply model adjustment for additional covariates (e.g., other candidate biomarkers), as the studies sample size was not sufficient, and thus underpowered to allow for the performance of multivariate regression analyses of this complexity.

For comparison of patient characteristics, the Kruskal–Wallis test was applied to continuous variables. Categorical variables are summarized category-wise with numbers and percentages and compared using the Chi^2 test for contingency tables. Student's *t*-tests were applied for comparisons (combined doses of Adrecizumab vs. placebo) of change in SOFA scores from baseline after 24 h of treatment. The primary aim of these *post-hoc* analyses is to determine the effect size for Adrecizumab employing further enrichment criteria. These analyses are exploratory, and smaller sample sizes of subgroups defined by further enrichment criteria need to be taken into account in the interpretation of the results. Based on decreasing sample size, it is anticipated that results of subgroups may not differ significantly, but may indicate trends of treatment effects. No correction for multiple testing was performed and a two-sided *p*-value of <0.05 is considered to indicate statistical significance. All analyses were performed using SAS version 9.3, and R version 3.4.3.[1]

Results

Study population and *post-hoc* subgroup analyses

A total of 459 patients were screened of which 301 were randomized to either placebo (n = 152) or Adrecizumab (n = 149) (15). The full list of inclusion and exclusion criteria can be found in the AdrenOSS-2 study protocol (15). Of all patients originally studied in AdrenOSS-2, plasma samples suitable for analysis of cDPP3 were missing in 3 patients, these patients were excluded from further analyses. Correspondingly, a total of 298 patients were available for these *post-hoc* analyses.

Median [IQR] age of the patients was 71.0 [61; 77] years, 61.1% of patients were male, median [IQR] APACHE-II score was 32 [29; 36], while the SOFA score was 10 [8; 12]. Sources of infection were predominantly abdomen (21.6%), lung (20.9%) or urinary tract (17.9%).

1 http://www.r-project.org

Circulating dipeptidyl peptidase 3 levels and associations with admission characteristics and mortality (intention to treat population)

Baseline median [IQR] cDPP3 of the total cohort was 22.8 [14.6; 39.8] ng/mL. A total of 49 (16%) patients presented with cDPP3 levels above the specified cut-off of >50 ng/mL. The 28-day mortality rate of patients with a cDPP3 level >50 ng/mL was 51.0% (all treatment groups, n = 49) compared to 20.5% in the low cDPP3 group (n = 249). A more detailed analysis for subgroups with a cut-off level of cDPP3 of 50 ng/mL was applied. The patient subgroups split by this cut-off level exhibited important differences in sepsis severity at baseline, with SOFA score, inflammation related parameters like IL-6 and PCT, lactate concentrations, fluid input and norepinephrine dose requirements that were markedly higher in patients with a cDPP3 concentration of >50 ng/mL at baseline (**Table 1**). In both the low and high cDPP3 subgroups, no significant differences in baseline characteristics were observed between the Adrecizumab and placebo group, suggesting that randomization remained intact in these subgroups (**Supplementary Table 1**).

Adrecizumab therapeutic efficacy by baseline circulating dipeptidyl peptidase 3 levels

In the original intention to treat (ITT) analysis (n = 301), the hazard ratio (HR) for 28-day mortality associated with Adrecizumab treatment was 0.84 (95% CI 0.53–1.31; p = 0.439; (**Figure 1A**). Corresponding incidence of 28-day mortality was 23 vs. 28%, p = 0.410 for the Adrecizumab and placebo groups, respectively. The significant interaction between cDPP3 concentration and Adrecizumab therapeutic efficacy was first illustrated by employing a cDPP3 level of 50 ng/mL as a cut-off. In patients with cDPP3 levels <50 ng/mL (n = 249) the HR for mortality associated with Adrecizumab tended to improve to 0.61 (95% CI 0.34–1.08; p = 0.085) (**Figure 1B**). The corresponding incidence of 28-day mortality was 16% in the Adrecizumab group, vs. 25%, in the placebo group, p = 0.080 for difference.

To further assess the interplay between stratification based on cDPP3 and 28-day mortality, multivariable Cox proportional hazard modeling was performed. This multivariate model included cDPP3 (as a continuous variable), treatment group (Adrecizumab or Placebo), as well as the interaction term of both these variables. The model also included baseline SOFA scores as a correction for baseline disease severity. In this model, cDPP3, treatment and the cDPP3 * treatment

TABLE 1 Demographics and baseline characteristics.

	cDPP3 < 50 ng/mL (n = 249)	cDPP3 > 50 ng/mL (n = 49)	*P*-value
Demographics			
Age (years)	71 [62–78]	68 [61–75]	0.164
BMI (kg/m2)	25.8 [23.4–30.2]	26.0 [23.9–28.1]	0.674
Gender, female, *n* (%)	98 (39.4)	19 (38.8)	0.939
Severity scores			
SOFA (points)	9 [8–11]	11 [9–14]	<0.001
APACHE II (points)	32 [29–36]	32 [27–36]	0.594
Hospital admission characteristics			
Temperature (°C)	37.0 [36.4–37.6]	36.9 [36.4–37.4]	0.759
HR (bpm)	97 [83–111]	101 [88–121]	0.098
MAP (mmHg)	72 [66–79]	71 [65–77]	0.424
Norepinephrine requirement (mcg/kg/min)	0.411 [0.205–0.779]	0.760 [0.357–1.400]	<0.001
Mechanical ventilation, *n* (%)	131 (52.3)	32 (65.3)	0.103
IL-6 (pg/mL)	2016 [480–11112]	12055 [2657–53060]	<0.001
PCT (ng/mL)	37.88 [8.26–87.10]	62.72 [27.92–129.80]	0.005
eGFR, MDRD (ml/min*1.73 m^2)	37.4 [22.7–58.0]	30.7 [21.4–38.0]	0.025
Lactate (mmol/L)	2.8 [1.6–4.6]	5.0 [3.7–8.3]	<0.001
PaO2/FiO2 (mmHg/%)	245 [176–343]	213 [136–343]	0.329
Fluid Input, first 24 h (mL)	2592 [1588–4274]	4044 [2894–4890]	<0.001
Time from septic shock to trt start (h)	8.4 [5.8–10.8]	9.5 [6.1–11.2]	0.224
Origin of sepsis			0.010
Lung, *n* (%)	53 (21.3)	9 (18.4)	
Peritonitis, *n* (%)	58 (23.3)	7 (14.3)	
Skin and soft tissue, *n* (%)	20 (8.0)	3 (6.1)	
Urinary tract, *n* (%)	49 (19.7)	4 (8.2)	
Other, *n* (%)	69 (27.8)	26 (53.1)	

Differences in continuous variables were assessed with Kruskal–Wallis tests, while differences in categorical variables were assessed using Chi^2 tests.
cDPP3, circulating dipeptidyl peptidase 3; BMI, body mass index; SOFA, sequential organ failure assessment; APACHE, acute physiology and chronic health evaluation; HR, heart rate; MAP, mean arterial pressure; PCT, procalcitonin; eGFR, estimated glomerular filtration rate.

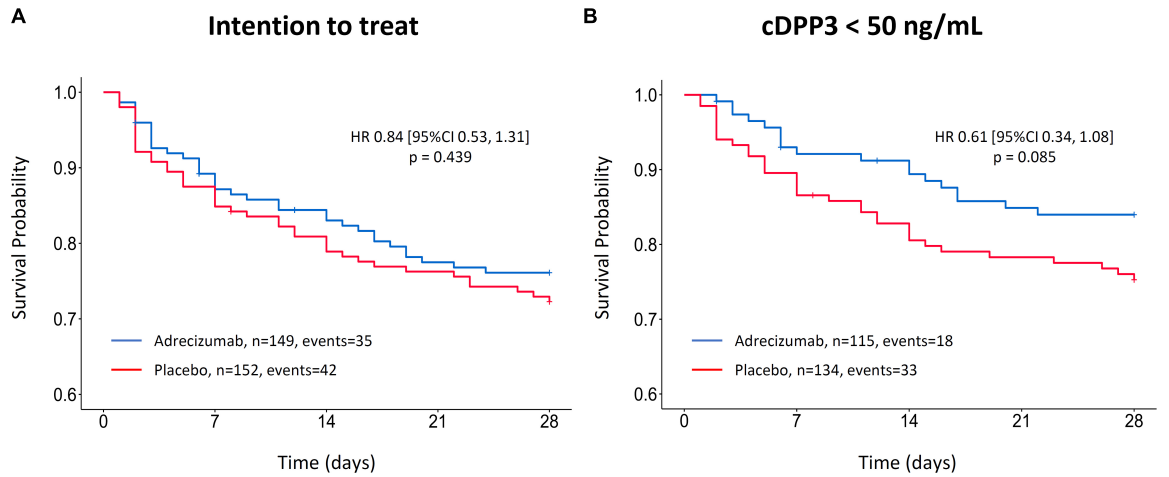

FIGURE 1
Kaplan–Meier of 28-day mortality after Adrecizumab/placebo infusion, based on circulating dipeptidyl peptidase 3 (cDPP3) stratification. Data is displayed for the original intention to treat (ITT) analysis (15) **(A)** and the cDPP3 <50 ng/mL subgroup **(B)**. Both Adrecizumab dosing groups were combined. Crosses represent censored patients.

TABLE 2 Multivariate risk models of treatment interaction with circulating dipeptidyl peptidase 3 (cDPP3) (model 1) and time until start of treatment (model 2).

Variable	*n*	events	HR	95% CI	*P*-value
Multivariate model 1					
cDPP3	252	67	1.44	1.07–1.92	0.015
Treatment (Adrecizumab)	252	67	0.10	0.02–0.67	0.017
Baseline SOFA-score	252	67	3.51	1.30–9.49	0.014
cDPP3 * treatment (Adrecizumab)	252	67	1.72	1.07–2.77	0.025
Multivariate model 2					
TTT	254	67	0.97	0.46–2.04	0.932
Treatment (Adrecizumab)	254	67	0.37	0.04–3.71	0.397
Baseline SOFA-score	254	67	7.35	2.83–19.1	<0.001
TTT * treatment (Adrecizumab)	254	67	1.41	0.47–4.24	0.544

TTT, Time from diagnosis of septic shock until initiation of treatment ("Time till treatment"). * signifies the interaction term between two variables. Continuous variables [circulating dipeptidyl peptidase 3 (cDPP3), sequential organ failure assessment (SOFA)-scores, TTT] were log-transformed.

interaction term were significantly associated with 28-day mortality; $p = 0.015$ for cDPP3, $p = 0.017$ for treatment group and $p = 0.025$ for the interaction term between cDPP3 and treatment group. An overview of the model's associated hazard ratios and 95% CI's is presented in Table 2. The hazard ratio of Adrecizumab treatment varying on cDPP3 level is displayed in Figure 2.

Adrecizumab therapeutic efficacy by time to treatment after diagnosis of septic shock

For the comparison of "early" and "late" start of Adrecizumab treatment, cohorts were first dichotomized at the median time from diagnosis of septic shock until start of treatment. Median [IQR] time from septic shock diagnosis to start of Adrecizumab treatment was 8.5 [5.9; 11.0] h. A total of 151 patients received treatment early after septic shock diagnosis (<8.5 h). The hazard ratio for 28-day mortality was not significantly lower for patients that were treated early (within 8.5 h) after septic shock diagnosis (HR 0.71 (95% CI 0.36–1.39) $p = 0.322$, $n = 151$, Figure 3A), compared to patients that started treatment later [HR 0.95 (95% CI 0.52–1.75) $p = 0.868$, $n = 150$, Figure 3B]. The corresponding incidence of 28-day mortality in the early treatment group was 20 vs. 26%, $p = 0.342$ for the Adrecizumab and placebo groups respectively, compared to 27 vs. 29%, $p = 0.759$ in the late treatment group. Next, a multivariable Cox proportional hazard model was generated, which included treatment timing (as a continuous variable), treatment group (Adrecizumab or Placebo) as well as the interaction term. This model also included baseline SOFA scores as a correction for baseline disease severity. In this model, both treatment timing and the interaction term were not significantly associated with 28-day mortality (Table 2).

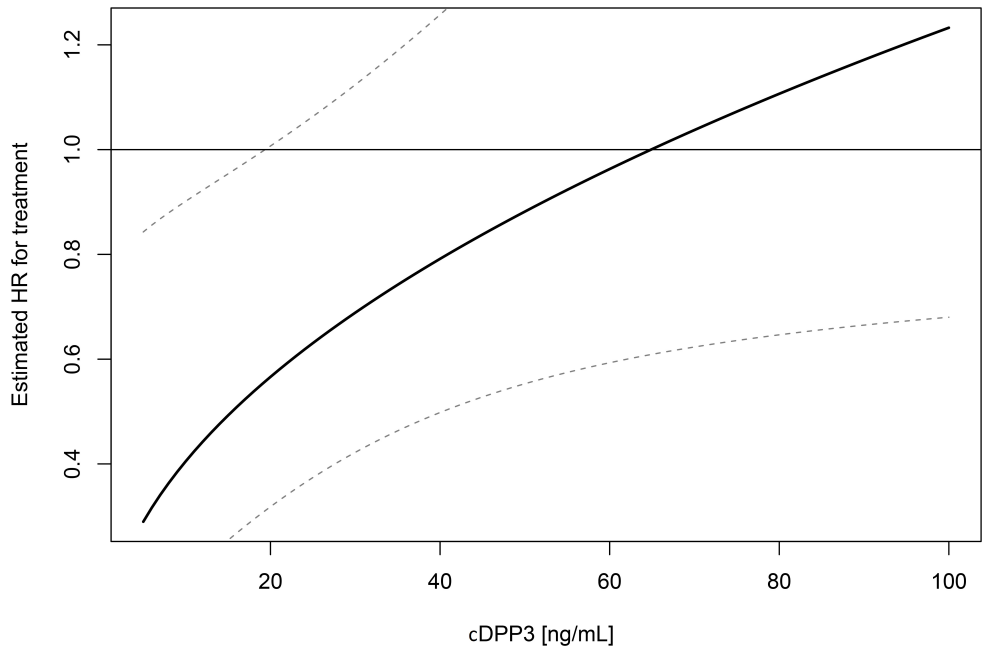

FIGURE 2
Hazard ratio (HR) of Adrecizumab treatment varying on circulating dipeptidyl peptidase 3 (cDPP3) level. Reported results are from an interaction analysis between Adrecizumab treatment and baseline cDPP3 concentration, i.e., a Cox regression was performed that included cDPP3, treatment status and the interaction term. HR and associated 95% CI compared to the placebo group are displayed.

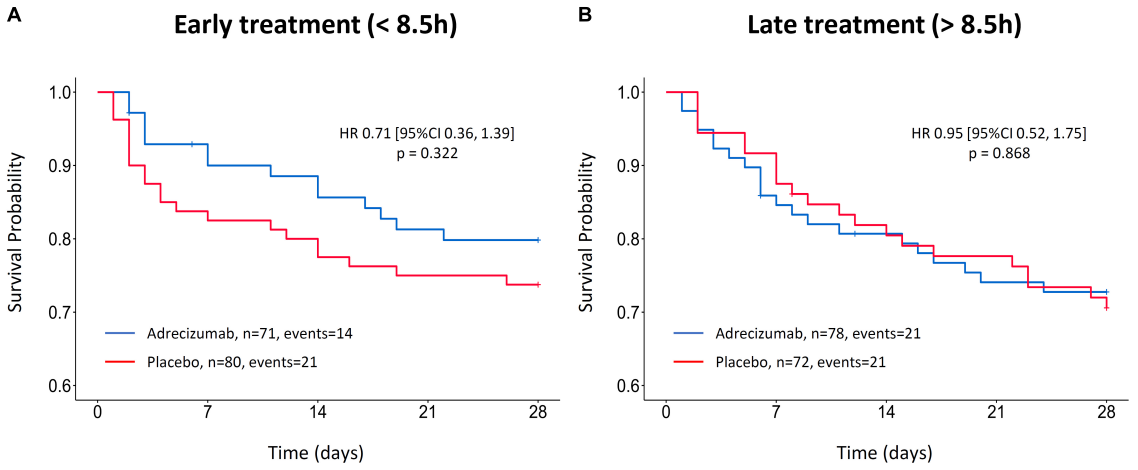

FIGURE 3
Kaplan–Meier of 28-day mortality after Adrecizumab/placebo infusion, based on treatment timing stratification. **(A)** Kaplan–Meier of patients treated <8.5 h after septic shock diagnoses. **(B)** Kaplan–Meier of patients treated >8.5 h after septic shock diagnosis. Both Adrecizumab dosing groups were combined. Crosses represent censored patients.

Adrecizumab therapeutic efficacy by circulating dipeptidyl peptidase 3 levels and treatment timing combined

The hazard ratio of 28-day mortality in a total of 129 patients with baseline cDPP3 levels <50 ng/mL and an early initiation of Adrecizumab treatment compared to patients that received placebo was HR 0.49 (95% CI 0.20–1.18), $p = 0.094$, (Figure 4). The corresponding 28-day mortality in this group was 13% for patients treated with Adrecizumab vs. 24% for patients treated with placebo, $p = 0.099$ for difference.

Multivariable Cox proportional hazard analysis through a model including both cDPP3, treatment timing and the respective interaction terms was not performed, as the interaction term associated with treatment timing was already not significantly associated with 28-day mortality.

Associations between circulating dipeptidyl peptidase 3, treatment timing and sequential organ failure assessment score improvement after 24 h of treatment

Change from baseline SOFA score 24 h after initiation of treatment (Δ-SOFA score) based on the different subgroup stratifications was investigated as an exploratory secondary outcome. In the ITT population, the Δ-SOFA score was more beneficial for the Adrecizumab group; being 0.01 point (95% CI −0.56; 0.58), vs. a further increase of 1.02 point (95% CI 0.35; 1.68) for the placebo group, $p = 0.045$ for difference (Figure 5A). When patients with a high baseline cDPP3 level (>50 ng/mL) were excluded, differences in Δ-SOFA scores became more pronounced, represented by a decrease of 0.55 point (95% CI −1.07; −0.03) vs. an increase of 0.81 point (95% CI 0.12; 1.50) in the placebo group, $p = 0.007$ for difference (Figure 5B). In contrast, patients treated with Adrecizumab with an earlier start of treatment (<8.5 h) did not display significantly more pronounced improvements in SOFA score after 24 h of treatment (Figure 5C). Correspondingly, a stratification approach combining cDPP3 and early treatment did not appear of more benefit compared to a stratification approach based on cDPP3 alone; SOFA score improvement of 0.93 point (95% CI −1.82; −0.05) in the Adrecizumab group vs. a deterioration trend of 0.70 point (95% CI −0.43; 1.82) in the placebo group, $p = 0.048$ for difference (Figure 5D).

Adrecizumab safety by baseline circulating dipeptidyl peptidase 3 levels

No treatment related differences in adverse events (AE) and treatment emergent adverse event (TEAE) occurrence were found in the low cDPP3 subgroup; 96.5% AEs for Adrecizumab (combined dosage groups) vs. 94.0% AEs for placebo, $p = 0.368$ and 94.8% TEAEs for Adrecizumab (combined dosage groups) vs. 93.3% for placebo, $p = 0.632$.

Discussion

In this *post-hoc* analysis of the AdrenOSS-2 trial, we demonstrated a significant interaction between cDPP3 levels

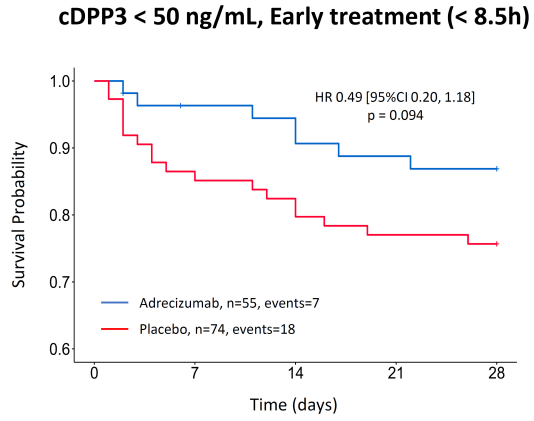

FIGURE 4
Kaplan–Meier of 28-day mortality after Adrecizumab/placebo infusion, based on a combined stratification approach implementing a cDPP3 <50 ng/mL as well as a treatment time <8.5 h after diagnosis of shock. Both Adrecizumab dosing groups were combined. Crosses represent censored patients.

and the therapeutic efficacy of Adrecizumab. In addition, we show that a shorter time to treatment initiation was not significantly associated with therapeutic efficacy. These results make it plausible that further enrichment of septic shock patient groups based on cDPPP3 concentration may increase chances of demonstrating therapeutic efficacy of Adrecizumab in future clinical trials, while a strategy aimed at further shortening time to initiation of treatment shows less promise.

Determining the cut-off of cDPP3 that allows for an optimal benefit-risk ratio for Adrecizumab treatment and, on the other hand, does not exclude an extensive group of sepsis patients that could still experience relevant benefit, goes beyond the data presented in this *post-hoc* analysis. Additional risk-benefit analyses performed during interim analysis of the phase-3 study of Adrecizumab should focus mainly on the impact of an imbalanced distributions of risks (demographics, critical parameters at baseline) on the results in subgroups of (even) smaller sample sizes that are no longer supported by randomized allocation.

Interestingly, in an observational study in septic shock patients, it was described that patients with high levels of both cDPP3 and bio-ADM had a substantially increased 28-day mortality compared to patients with high levels of only one of them (19). Although observational, this study first provided the first suggestion that bio-ADM and DPP3 might represent two distinct and partly independent pathophysiological mechanisms involved in the development of organ dysfunction during sepsis. In other words, an increased bio-ADM could be used to identify patients that may benefit from Adrecizumab therapy, whereas increased cDPP3 concentrations could be used to identify patients that may have lower chances of benefit, as they have an impaired prognosis based on another pathophysiological process that is hypothetically not influenced by Adrecizumab therapy.

The observed benefits of population enrichment with cDPP3 might be explained by the molecular pathways involved in the release of both bio-ADM and DPP3. DPP3 is a cytosolic enzyme, putatively reaching higher concentrations

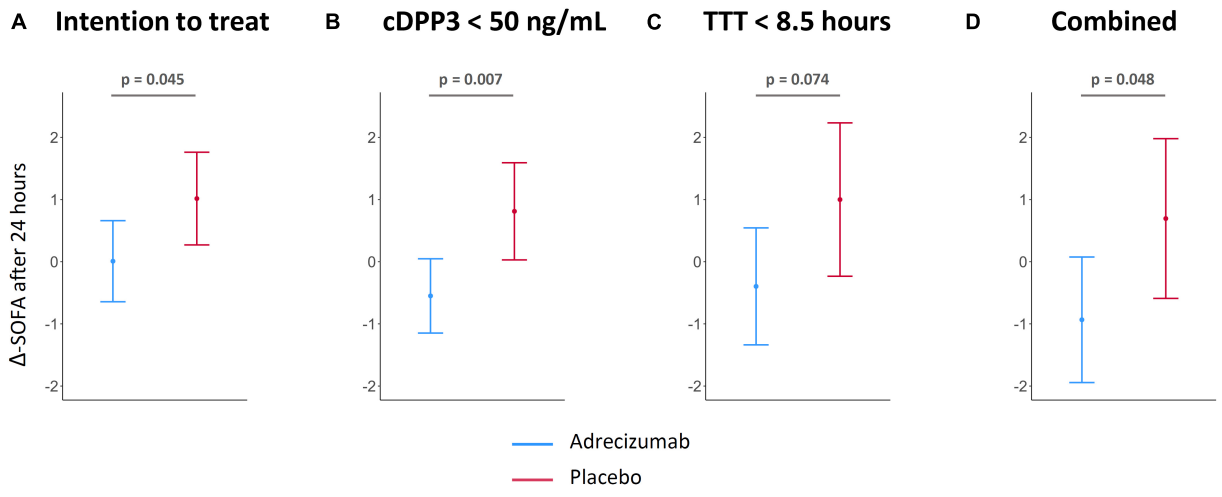

FIGURE 5
Change of sequential organ failure assessment (SOFA) score after Adrecizumab/placebo infusion, based on circulating dipeptidyl peptidase 3 (cDPP3) stratification. Data is displayed for the original intention to treat (ITT) analysis (15) **(A)**, the cDPP3 <50 ng/mL subgroup **(B)**, the early treatment (<8.5 h) subgroup **(C)** and the subgroup combining cDPP3 and treatment timing stratification **(D)**. The SOFA score was determined immediately prior to dosing and 24 h after start of treatment. The difference between the SOFA score pre-dosing and the SOFA score after 24 h of treatment was calculated for each patient, and the means ± 95% CI from the resulting values are represented in the Figure. For patients who died within 24 h of treatment, the SOFA was set to 24.

in the circulation in case of extensive cell injury (19, 26). During sepsis, this cell injury is likely caused by a profound impairment of microcirculatory tissue perfusion despite treatment. In animal studies, administration of exogeneous DPP3 provoked a rapid deterioration of left ventricular systolic function, putatively linked to reduced concentration of positive inotropic DPP3 substrates and/or increased concentration of negative inotropic products of DPP3 cleavage (27). In accordance with this finding, in preclinical models of sepsis and cardiogenic shock, inhibition of cDPP3 resulted in improved cardiac function index, as well as improved survival (21, 27). Interestingly, a cDPP3 blocking antibody is currently in preclinical stages of development (19, 27). During shock, upregulation of the renin angiotensin aldosterone system (RAAS) is a potentially life-saving response aimed at maintaining hemodynamic stability and adequate tissue perfusion (28). The degradation of compensatory RAAS response related mediators, e.g., angiotensin 2, caused by the uncontrolled release of DPP3 might be significantly contributing to the hemodynamic compromise in septic shock patients. As these mechanisms act independently of the ADM pathway, a more pronounced effect of Adrecizumab in patients without elevated cDPP3 levels appears plausible. Supporting this hypothesis, we demonstrated a significant interaction of cDPP3 levels with Adrecizumab treatment efficacy in a multivariate interaction analysis that was corrected for baseline disease severity.

The release of bio-ADM during sepsis represents a compensatory response aimed at restoring endothelial barrier function, a mechanism that falls short during refractory shock (5, 19). Observational studies have found a strong association of bio-ADM (at admission to ICU) with clinical outcomes in severe sepsis and septic shock (8–10). Additional studies showed that an even better prediction of outcome was provided by bio-ADM kinetics following the first 24 h of ICU treatment (10, 23, 24). Patients with high admission bio-ADM concentrations, that subsequently normalized after 24 h of treatment, demonstrated markedly improved chances of surviving (9.5% 28-day mortality), while patients in which bio-ADM concentrations remained high, or increased after 24 h, had a 28-day mortality of 38.1% (10). These results imply that adequate control of bio-ADM responses during the early hours of treatment of septic shock may relevantly impact outcome. In contrast, we found no significant associations between an early initiation of Adrecizumab treatment and Adrecizumab efficacy. Of note, the original AdrenOSS-2 study protocol already emphasized an early start of treatment after shock diagnosis, as only patients that could start study therapy within 12 h after start of vasopressors were eligible for study participation. Based on our results, it appears that this inclusion window of <12 h after shock diagnosis was already adequate to account for the early changes in bio-ADM responses mentioned above.

Our results have several research relevant implications. First, an upper limit of cDPP3 concentrations at baseline may serve as an additional patient enrichment criterion, allowing for the identification of a major subset of septic shock patients (with high bio-ADM levels but no elevated cDPP3 concentrations) that are more likely to benefit from Adrecizumab treatment. Second, while a timely start of Adrecizumab treatment after onset of septic shock might be of importance to improve chances of therapeutic benefit, our data do not support the necessity for an even earlier start of treatment than was achieved in the phase-2 trial. These findings emphasize the need for future sepsis trials to embrace enrichment strategies and, thereby, improve chances of detecting clinically relevant treatment effects in patient subsets that would otherwise be "diluted" in an unselected population. The upcoming phase III trial of the Adrecizumab program, called ENCOURAGE-1, aims to implement both strategies investigated in this *post-hoc* analysis, starting therapy early after initiation of vasopressor therapy as well as selecting patients based on rapid bedside assessment of relevant biomarkers. Based on our results, this trial will use a high concentration of bio-ADM as an inclusion criterium, while a high concentration of cDPP3 will serve as an exclusion criterium.

Despite the limitations of *post-hoc* analyses, the data presented here can provide relevant guidance for patient enrolment in future trials (e.g., the ENCOURAGE-1 trial). Further selection of subgroups results in smaller sample sizes, leading to limited statistical power. As the original study was a phase-2 safety and tolerability study, not powered to demonstrate beneficial effects on survival or other clinical endpoints, it is not surprising that several treatment differences in subgroups do not reach statistical significance. As for any *post-hoc* analysis, the results should be viewed as explorative and hypothesis-generating. Also, because cardiac function assessment, as well as measurements of hypoperfusion related parameters were not performed during the AdrenOSS-2 trial, the proposed pathophysiological mechanisms explaining the associations of cDPP3 with outcome remain largely speculative.

Conclusion

Our results illustrate that a subset of septic shock patients with high bio-ADM levels also display high levels of cDPP3. We show that there is an interaction between cDPP3 concentrations and the therapeutic efficacy of Adrecizumab. This implies that increased efficacy of Adrecizumab may be present in the subgroup of patients with lower cDPP3 levels. Patient enrichment strategies implementing assessment of cDPP3 thus appear to identify a major subgroup of septic shock patients that may have an more pronounced benefit from treatment with Adrecizumab. The pathophysiological mechanism related to increased cDPP3 concentrations is putatively not related to

bio-ADM and can, therefore, not be targeted by the treatment with Adrecizumab. These results reinforce the notion that from a pathophysiological point of view, sepsis should be viewed as a heterologous syndrome, rather than a single disease entity. To improve the chance of finding clinically relevant treatment effects, future sepsis trials should account for this heterogeneity by incorporating population enrichment strategies, preferably related to the mechanism of action of the therapy under investigation and/or exclusion of patients that show evidence of dysregulated processes that cannot be addressed by the intervention. These results warrant confirmation, which may be provided by ENCOURAGE-1, the phase III trial of Adrecizumab in septic shock patients, which will include cDPP3 assessment as well as early initiation of treatment as additional eligibility criteria.

Data availability statement

The raw data supporting the conclusions of this article will be made available by the authors, without undue reservation.

Ethics statement

The trial procedures and the informed consent form (ICF) process were approved by the respective independent ethics committee (IEC) following international standards and national requirements of each participating country. The AdrenOSS-2 trial was registered at https://clinicaltrials.gov/ (NCT03085758). The patients/participants provided their written informed consent to participate in this study.

AdrenOSS-2 study participants

Lila-Fariza Abeud, Pierre Asfar, Ludmila Baudrillart, Michael Bauer, Albertus Beishuizen, Caroline Berghe, Laure Berton, Paul Bourzeix, Diego Castanares, Kamile Cerlinskaite, Coralie Chalot, Benjamin Chousterman, Raphaël Clere-Jehl, Christine Collienne, Damien Contou, Thomas Daix, Julien Demiselle, Arnaud Desachy, Nicolas Deye, Tom Dormans, Anne-Aurore Duchambon, Thierry Dugernier, Marie-France Dujardin, Jacques Duranteau, Perrine Engels, Bruno Evrard, Anne-Laure Fedou, Marie-Celine Fournier, Bruno François, Alexandra Gay, Ludovic Gèrards, Leslie Gielens, Thomas Godet, Marine Goudelin, Tassadit Hadjam, Phillipe Hantson, Julie Helms, Isabelle Herafa, Oscar Hoiting, Alexa Hollinger, Vincent Huberlant, Tuija Javanainen, Philippe Jorens, Clement Jourdaine, Mahir Karakas, Stefan Kluge, Jean-Claude Lacherade, Jean-Baptiste Lascarrou, Matthieu Legrand, Badr Louadah, Martin Maëlle, Emmanuelle Mercier, Hamid Merdji, Ferhat Meziani, Alexandra Monnier, Virginie Montiel. Arthur Neuschwander, Haikel Oueslati, Gaëtan Plantefève, Julien Pottecher, Céline Prevost, Suzanne Renard, Tobias Schuerholz, Wytze Vermeijden, Philippe Vignon, Constance Vuillard, Emmanuel Weiss, Xavier Wittebole, Arthur van Zanten, and Alexander Zarbock.

Author contributions

GM, P-FL, AM, and PP conceptualized the study. DL and AP drafted the manuscript. DL and OH performed the data analysis. KS performed the cDPP3 sample analyses and measurement quality control. All authors critically revised the manuscript and read and approved the final manuscript.

Funding

This study received funding from Adrenomed AG. The funder was not involved in the study design, data collection, the writing of this article or the decision to submit it for publication.

Acknowledgments

We thank Steffen Stürzebecher for his review, scientific input, and substantial support to this manuscript.

Conflict of interest

Authors DL, AP, and FA were invited to a meeting in Berlin by 4TEEN4 Pharmaceuticals GmbH. Author GM received travel and consultancy reimbursements from Adrenomed, 4TEEN4, and Sphingotec. Author P-FL received fees as a coordinator of the original trial's clinical coordinating center. He also reports travel and consultancy reimbursements from Adrenomed, 4TEEN4, and Sphingotec. Author OH was employed by Sphingotec GmbH, the company holding patent rights for the bio-ADM assay and a license to commercialize the cDPP3 assay. Authors CK, JS, and JZ were employed by Adrenomed AG, the company holding patent rights for the Adrecizumab compound. Author KS was employed by 4TEEN4 Pharmaceuticals, the company holding patent rights for the cDPP3 assay. Author AB was the managing director of Sphingotec GmbH and holds shares in it. Author AM reports personal fees from Orion, Sanof, Adrenomed, Epygon, and Fire 1 and grants and personal fees from 4TEEN4, Abbott, Roche, and SphingoTec.

Author PP received travel and consultancy reimbursement from Adrenomed, SphingoTec, 4TEEN4, AM-Pharma, Baxter, and EBI.

Publisher's note

Supplementary material

The Supplementary Material for this article can be found online at: https://www.frontiersin.org/articles/10.3389/fmed.2022.1058235/full#supplementary-material

References

1. Singer M, Deutschman CS, Seymour CW, Shankar-Hari M, Annane D, Bauer M, et al. The third international consensus definitions for sepsis and septic shock (Sepsis-3). *JAMA*. (2016) 315:801–10. doi: 10.1001/jama.2016.0287

2. Joffre J, Hellman J, Ince C, Ait-Oufella H. Endothelial responses in sepsis. *Am J Respir Crit Care Med.* (2020) 202:361–70. doi: 10.1164/rccm.201910-1911TR

3. Angus DC, van der Poll T. Severe sepsis and septic shock. *New Engl J Med.* (2013) 369:2063. doi: 10.1056/NEJMc1312359

4. Gotts JE, Matthay MA. Sepsis: pathophysiology and clinical management. *BMJ.* (2016) 353:i1585. doi: 10.1136/bmj.i1585

5. Geven C, Bergmann A, Kox M, Pickkers P. Vascular effects of adrenomedullin and the anti-adrenomedullin antibody adrecizumab in sepsis. *Shock.* (2018) 50:132–40. doi: 10.1097/SHK.0000000000001103

6. Hofbauer KH, Jensen BL, Kurtz A, Sandner P. Tissue hypoxygenation activates the adrenomedullin system in vivo. *Am J Physiol Regul Integr Comp Physiol.* (2000) 278:R513–9. doi: 10.1152/ajpregu.2000.278.2.R513

7. Hofbauer KH, Schoof E, Kurtz A, Sandner P. Inflammatory cytokines stimulate adrenomedullin expression through nitric oxide-dependent and -independent pathways. *Hypertension.* (2002) 39:161–7. doi: 10.1161/hy1201.097201

8. Marino R, Struck J, Maisel AS, Magrini L, Bergmann A, Di Somma S. Plasma adrenomedullin is associated with short-term mortality and vasopressor requirement in patients admitted with sepsis. *Crit Care.* (2014) 18:R34. doi: 10.1186/cc13731

9. Caironi P, Latini R, Struck J, Hartmann O, Bergmann A, Maggio G, et al. Circulating biologically active adrenomedullin (bio-ADM) predicts hemodynamic support requirement and mortality during sepsis. *Chest.* (2017) 152:312–20. doi: 10.1016/j.chest.2017.03.035

10. Mebazaa A, Geven C, Hollinger A, Wittebole X, Chousterman BG, Blet A, et al. Circulating adrenomedullin estimates survival and reversibility of organ failure in sepsis: the prospective observational multinational Adrenomedullin and Outcome in Sepsis and Septic Shock-1 (AdrenOSS-1) study. *Crit Care.* (2018) 22:354. doi: 10.1186/s13054-018-2243-2

11. Geven C, Peters E, Schroedter M, Struck J, Bergmann A, McCook O, et al. Effects of the humanized anti-adrenomedullin antibody adrecizumab (HAM8101) on vascular barrier function and survival in rodent models of systemic inflammation and sepsis. *Shock.* (2018) 50:648–54. doi: 10.1097/SHK.0000000000001102

12. Blet A, Deniau B, Geven C, Sadoune M, Caillard A, Kounde PR, et al. Adrecizumab, a non-neutralizing anti-adrenomedullin antibody, improves haemodynamics and attenuates myocardial oxidative stress in septic rats. *Intensive Care Med Exp.* (2019) 7:25. doi: 10.1186/s40635-019-0255-0

13. Wagner K, Wachter U, Vogt JA, Scheuerle A, McCook O, Weber S, et al. Adrenomedullin binding improves catecholamine responsiveness and kidney function in resuscitated murine septic shock. *Intensive Care Med Exp.* (2013) 1:21. doi: 10.1186/2197-425X-1-2

14. Geven C, van Lier D, Blet A, Peelen R, Ten Elzen B, Mebazaa A, et al. Safety, tolerability and pharmacokinetics/pharmacodynamics of the adrenomedullin antibody adrecizumab in a first-in-human study and during experimental human endotoxaemia in healthy subjects. *Br J Clin Pharmacol.* (2018) 84:2129–41. doi: 10.1111/bcp.13655

15. Laterre PF, Pickkers P, Marx G, Wittebole X, Meziani F, Dugernier T, et al. Safety and tolerability of non-neutralizing adrenomedullin antibody adrecizumab (HAM8101) in septic shock patients: the AdrenOSS-2 phase 2a biomarker-guided trial. *Intensive Care Med.* (2021) 47:1284–94. doi: 10.1007/s00134-021-06537-5

16. Reddy K, Sinha P, O'Kane CM, Gordon AC, Calfee CS, McAuley DF. Subphenotypes in critical care: translation into clinical practice. *Lancet Respir Med.* (2020) 8:631–43. doi: 10.1016/S2213-2600(20)30124-7

17. van Lier D, Pickkers P. Circulating biomarkers to assess cardiovascular function in critically ill. *Curr Opin Crit Care.* (2021) 27:261–8.

18. Prajapati SC, Chauhan SS. Dipeptidyl peptidase III: a multifaceted oligopeptide N-end cutter. *FEBS J.* (2011) 278:3256–76. doi: 10.1111/j.1742-4658.2011.08275.x

19. van Lier D, Kox M, Pickkers P. Promotion of vascular integrity in sepsis through modulation of bioactive adrenomedullin and dipeptidyl peptidase 3. *J Intern Med.* (2020) 289:792–806. doi: 10.1111/joim.13220

20. Blet A, Deniau B, Santos K, van Lier DPT, Azibani F, Wittebole X, et al. Monitoring circulating dipeptidyl peptidase 3 (DPP3) predicts improvement of organ failure and survival in sepsis: a prospective observational multinational study. *Crit Care.* (2021) 25:61. doi: 10.1186/s13054-021-03471-2

21. Deniau B, Blet A, Santos K, Vaittinada Ayar P, Genest M, Kastorf M, et al. Inhibition of circulating dipeptidyl-peptidase 3 restores cardiac function in a sepsis-induced model in rats: A proof of concept study. *PLoS One.* (2020) 15:e0238039. doi: 10.1371/journal.pone.0238039

22. Kim H, Hur M, Struck J, Bergmann A, Di Somma S. Circulating biologically active adrenomedullin predicts organ failure and mortality in sepsis. *Ann Lab Med.* (2019) 39:454–63.

23. Lundberg OHM, Lengquist M, Spangfors M, Annborn M, Bergmann D, Schulte J, et al. Circulating bioactive adrenomedullin as a marker of sepsis, septic shock and critical illness. *Crit Care.* (2020) 24:636. doi: 10.1186/s13054-020-03351-1

24. Lemasle L, Blet A, Geven C, Cherifa M, Deniau B, Hollinger A, et al. Bioactive adrenomedullin, organ support therapies, and survival in the critically ill: results from the french and european outcome registry in ICU Study. *Crit Care Med.* (2020) 48:49–55. doi: 10.1097/CCM.0000000000004044

25. Rehfeld L, Funk E, Jha S, Macheroux P, Melander O, Bergmann A. Novel methods for the quantification of dipeptidyl peptidase 3 (DPP3) concentration and activity in human blood samples. *J Appl Lab Med.* (2019) 3:943–53. doi: 10.1373/jalm.2018.027995

26. Takagi K, Blet A, Levy B, Deniau B, Azibani F, Feliot E, et al. Circulating dipeptidyl peptidase 3 and alteration in haemodynamics in cardiogenic shock: results from the OptimaCC trial. *Eur J Heart Fail.* (2019) 22:279–86. doi: 10.1002/ejhf.1600

27. Deniau B, Rehfeld L, Santos K, Dienelt A, Azibani F, Sadoune M, et al. Circulating dipeptidyl peptidase 3 is a myocardial depressant factor: dipeptidyl peptidase 3 inhibition rapidly and sustainably improves haemodynamics. *Eur J Heart Fail.* (2019) 22:290–9. doi: 10.1002/ejhf.1601

28. Bitker L, Burrell LM. Classic and nonclassic renin-angiotensin systems in the critically Ill. *Crit Care Clin.* (2019) 35:213–27.

Frontiers in Medicine

Translating medical research and innovation into improved patient care

A multidisciplinary journal which advances our medical knowledge. It supports the translation of scientific advances into new therapies and diagnostic tools that will improve patient care.

Discover the latest Research Topics

See more →

Frontiers

Avenue du Tribunal-Fédéral 34
1005 Lausanne, Switzerland
frontiersin.org

Contact us

+41 (0)21 510 17 00
frontiersin.org/about/contact